Electroweak Precision Observables and Effective Four-Fermion Interactions in Warped Extra Dimensions

Dissertation
zur Erlangung des Grades
"Doktor der Naturwissenschaften"
am Fachbereich Physik, Mathematik und Informatik
der Johannes Gutenberg-Universität in Mainz

Torsten Pfoh
geboren in Mainz

Mainz, September 2011

Datum der mündlichen Prüfung: 12.09.2011

Dissertation an der Universität Mainz (D77)

Abstract

In this thesis, we study the phenomenology of selected observables in the context of the Randall-Sundrum scenario of a compactified warped extra dimension. Gauge and matter fields are assumed to live in the whole five-dimensional space-time, while the Higgs sector is localized on the infrared boundary. An effective four-dimensional description is obtained via Kaluza-Klein decomposition of the five dimensional quantum fields. The symmetry breaking effects due to the Higgs sector are treated exactly, and the decomposition of the theory is performed in a covariant way. We develop a formalism, which allows for a straight-forward generalization to scenarios with an extended gauge group compared to the Standard Model of elementary particle physics. As an application, we study the so-called custodial Randall-Sundrum model and compare the results to that of the original formulation. We present predictions for electroweak precision observables, the Higgs production cross section at the LHC, the forward-backward asymmetry in top-antitop production at the Tevatron, as well as the width difference, the CP-violating phase, and the semileptonic CP asymmetry in B_s decays.

Zusammenfassung

In dieser Arbeit studieren wir die Phänomenologie einiger ausgesuchter Observablen im Kontext des Randall-Sundrum Szenarios einer kompaktifizierten gekrümmten Extradimension. Es wird angenommen, dass Eich- und Materiefelder in der gesamten fünfdimensionalen Raumzeit leben, während der Higgs-Sektor auf der sogenannten Infrarot-Brane lokalisiert ist. Eine effektive vierdimensionale Beschreibung wird mittels einer Kaluza-Klein Zerlegung der fünfdimensionalen Quantenfelder erreicht. Die durch den Higgs-Sektor verursachten symmetriebrechenden Effekte werden hierbei exakt behandelt, und die Zerlegung der Theorie wird in kovarianter Weise vollzogen. Wir entwickeln einen Formalismus, der eine direkte Verallgemeinerung auf Szenarien mit einer erweiterten Eichgruppe im Vergleich zum Standardmodell der Elementarteilchenphysik erlaubt. Als Anwendung studieren wir das sogenannte custodial Randall-Sundrum Modell, und vergleichen die Resultate mit denen der ursprünglichen Formulierung. Wir machen Vorhersagen für elektroschwache Präzisionsobservalen, den Wirkungsquerschnitt für die Higgs-Produktion am LHC, die Vorwärts-Rückwärts Asymmetrie in der Top-Antitop Produktion am Tevatron, sowie die Zerfallsbreitendifferenz, die CP-verletzende Phase und die semileptonische CP-Asymmetrie in B_s-Zerfällen.

Contents

1 Introduction

In this thesis, we want to study electroweak precision observables, as well as some selected topics of flavor physics, which are of special interest within the search for new physics at the Large Hadron Collider and the Tevatron. The calculations will be performed in the context of the Randall-Sundrum scenario, which is perhaps one of the most discussed extensions to the Standard model of elementary particle physics. As it is explained in detail later, the Randall-Sundrum model involves one additional compactified spacial dimension, but preserves ordinary four dimensional Poincaré invariance. Nevertheless, one has to understand how matter and gauge fields are described in a five dimensional space-time. As a further complication, we will generalize our studies to an extended gauge sector, which fits that one of the Standard model at low energies. The gauge fixing will be treated in a covariant way. Therefore, one has to extend the class of R_ξ gauges in two ways: First, the effects of the compactified space-time have to be taken into account, second, the new heavy gauge fields have to be included. Furthermore, the mechanism of electroweak symmetry breaking plays a major role in all our considerations.

In order to get started, we will provide the reader with a discussion of all the above issues in the Standard model. Of course, such an introduction can not be complete. It should rather catch up the basic ideas, and give the formulas which need to be generalized within the context of an extra dimension or an extended gauge group. More detailed elaborations can be found in [1], [2], and [3] for instance, which we will use as foundation for our discussions. We are not going to provide an introduction to quantum field theory in general, which is far beyond the scope of this thesis. However, we want spend some time on discussing the concept of effective field theories, which is a powerful approach for the study of multi-scale problems. The experienced reader may directly jump to subsection 1.7. There, we will give some theoretical and empirical reasons, why we are expecting to find new physics at current collider experiments. Furthermore, a detailed outline of all topics treated in this thesis will be provided at the end of the introduction.

1.1 About symmetries and field quantization

When one asks a theoretical particle physicist about the most general purpose of collider experiments at highest energies, he may answer with a short question: What is the Lagrange density $\mathcal{L}(x)$ of the observable nature and to what energy does it hold?

The Lagrange density is a formal object, which is used to define a quantum field theory (QFT). The purpose of the following pages is to discuss its ingredients. First of all, there are many similarities between QFTs and classical field theories, such as the Maxwell theory.

Here, the electric potential $\phi(x)$ and the vector potential $\vec{A}(x)$ of the magnetic field are combined to four components of a Lorentz vector $A^\mu(x)$, where x denotes the coordinate of the four dimensional space-time. The current $j^\mu(x)$ is defined as the electric charge times the four-velocity of a moving charged particle, which serves as a source. The Lagrange density is a Lorentz-invariant object, which consists of a kinetic term for $A^\mu(x)$, and a source term, which couples the potential to the current

$$\mathcal{L}_{\text{Maxwell}}(x) = -\frac{1}{4}\, F_{\mu\nu}(x)F^{\mu\nu}(x) + j_\mu(x)A^\mu(x)\,. \tag{1.1}$$

Here, $F_{\mu\nu}(x) = \partial_\mu A_\nu(x) - \partial_\nu A_\mu(x)$ is the field-strength tensor with $\partial^\mu \equiv \partial/\partial x_\mu$, and we use natural units featuring $\hbar = c = 1$ throughout the article. Apart from Lorentz symmetry, the Lagrange density possesses a local gauge symmetry, which reflects the fact that potentials themselves are not observable, but rather the field strengths obtained from derivatives of the potentials. Indeed, the shift of the vector potential $A^\mu(x) \to A^\mu(x) - \partial^\mu\chi(x)$ leaves the Lagrange density invariant, if in addition the continuity equation $\partial^\mu j_\mu(x) = 0$ holds. Here, $\chi(x)$ denotes an arbitrary scalar potential. On the other hand, the continuity equation is nothing more than the statement, that the electric charge is conserved. We see that already at the classical level nature seems to be controlled by simple symmetry and conservation laws. Note that a term $\propto A_\mu(x)A^\mu(x)$ would violate the local gauge invariance of the theory. The physical interpretation of such a term will be discussed below.

The action S is defined as the space-time integral over $\mathcal{L}$, where the integration boundaries are sent to infinity. We write

$$S = \int dx^4 \mathcal{L}(x)\,. \tag{1.2}$$

If we insert the Lagrange density (1.1) and apply the famous variational principle, we obtain Maxwell's equations. When we go to a QFT, the formal expression for the action does not change. All symmetries that are present in the classical (free) theory are kept. However, within the canonical quantization procedure, the potential $A^\mu(x)$ has to be reinterpreted as a single, relativistic quantum mechanical particle, which we call a field. Technically, the classical potential has to be replaced by a field operator. If the operator acts on the ground state of the theory (which we call the vacuum), it produces a single quantum field. For the Maxwell theory, this field is the photon, and the field operator is given by

$$A^\mu(x) = \frac{1}{(2\pi)^{3/2}} \int \frac{d^3k}{2\omega_k} \sum_{\lambda=0}^{3} \left[\epsilon^\mu_\lambda(k)\, c_\lambda(k)\, e^{-ikx} + \epsilon^{\mu\,*}_\lambda(k)\, c^\dagger_\lambda(k)\, e^{ikx}\right]\,. \tag{1.3}$$

Here, k and ω_k are the photon momentum and the energy, and ϵ^μ is its polarization vector. The creation and annihilation operators $c^\dagger_\lambda(k)$ and $c_\lambda(k)$ are defined in momentum space and satisfy commutation relations. Setting the current $j^\mu(x)$ to zero, Maxwell's equations are now understood as the equations of motion (EOMs) of the free photon field, which satisfies the dispersion relation $p^2 = \omega^2$. In other words, the EOMs describe the on-shell propagation. A different approach to field quantization is the path integral formalism, invented by *Richard Feynman* back in the six-tees. Here, the field serves as integration variable within the path integral, which enters the generating functional of the theory. Without going into further details here, we note that the different components of a quantum field correspond to the degrees of freedom of the respective particle. For the photon field however, something seems to be wrong at the first sight. As light is observed as a transversal wave, the photon has two helicity states. One the other hand, a Lorentz vector has four components. Only two of them (or certain linear combinations) can therefore correspond to physical degrees of freedom. The additional components arise due to the gauge freedom we already observe at the classical level. Indeed, this gauge freedom leads to difficulties in the field quantization. Within the functional appoach for instance, the path integral diverges, as one integrates over an infinite set of gauge-equivalent configurations. Here, a gauge fixing is used to pick out one (arbitrary) representative, thus giving a meaning to the path integral. Within the canonical procedure, there is no canonical conjugate momentum for the zero component $A^0(x)$, unless one adds an additional term to the action by choosing a specific gauge. On the other hand, a naive gauge fixing would spoil the gauge invariance of the theory. A solution has been given by *L.D. Faddeev* and *V.N. Popov* [4], where the path integral is augmentend by a unity expression consisting of a functional integral over a gauge-fixing condition times a functional determinant. The latter gives rise to so-called ghost fields, which so to say keep the gauge freedom within the theory, but are non observable as physical particles, as they have the wrong combination of spin and statistics.[1]

Coming back to classical field theories, we note that quantum fields are classified in representations of the Lorentz group. The Maxwell field lives in the vector representation and transforms via

$$A^\mu(x) \to A'^\mu(x) = \Lambda^\mu_\nu A^\nu(x)\,, \tag{1.4}$$

where Λ^μ_ν is the component (μ,ν) of a Lorentz transformation. The most simple representation consists of scalar fields with one degree of freedom (DOF), which we denote by $\phi(x)$.[2] They correspond to spin-0 particles and are invariant under Lorentz transformations. The respective creation and annihilation operators satisfy commutation relations as well. As a consequence, scalar and vector particles obey Bose-Einstein statistics. The Lagrange density of the free theory is given by

$$\mathcal{L}_{\text{Klein-Gordon}} = \partial_\mu\phi^*(x)\partial^\mu\phi(x) - m^2|\phi(x)|^2\,. \tag{1.5}$$

Here, m is interpreted as the mass of the particle. The classical EOM is again obtained by applying the variational principle. One finds the Klein-Gordon equation $(\Box + m^2)\phi(x) = 0$, where $\Box \equiv \partial_\mu\partial^\mu$. If we insert the plane-wave solution of $\phi(x)$, we find $p^2 = m^2$, were p is the four momentum of the moving spin-0 particle, which is confined to its mass shell. Indeed, this was the original motivation for writing down a Lorentz invariant generalization

[1] Ghost fields are Grassman variables, that is scalar fields that obey anti-commutation relations. As a consequence, they only show up as intermediate states which can only be produced/annihilated in pairs.

[2] $\phi(x)$ could be any scalar field, do not confuse with the electric potential.

of Schroedinger's equation. Within an interacting theory, particles do not necessarily have to be on-shell. We will come back to this point below.

For the moment, we will instead continue dealing with free theories and study the two-component spinor representation of the Lorentz group. The related quantum fields describe spin-1/2 particles. Let us define a Lorentz vector via $\sigma_\mu = \hat{\sigma}^\mu \equiv (\sigma_0, \boldsymbol{\sigma}) = (\sigma_0, \sigma_1, \sigma_2, \sigma_3)$, where $\sigma_0 = \mathbf{1}_{2\times 2}$, and σ_i are the Pauli matrices

$$\sigma_1 = \begin{pmatrix} 0 & 1 \\ 1 & 0 \end{pmatrix}, \qquad \sigma_2 = \begin{pmatrix} 0 & -i \\ i & 0 \end{pmatrix}, \qquad \sigma_3 = \begin{pmatrix} 1 & 0 \\ 0 & -1 \end{pmatrix}. \tag{1.6}$$

The position vector x, which transforms as $x' = \boldsymbol{\Lambda} x$ under Lorentz transformations $\boldsymbol{\Lambda}$, is mapped on a two-dimensional hermitian matrix $\boldsymbol{X}$ via

$$x^\mu \to \boldsymbol{X} = \sigma_\mu x^\mu . \tag{1.7}$$

Next we have to find a representation for Lorentz transformations, such that

$$\boldsymbol{X} = \boldsymbol{X}' = \boldsymbol{A}(\boldsymbol{\Lambda})\boldsymbol{X}\boldsymbol{A}^\dagger(\boldsymbol{\Lambda}) . \tag{1.8}$$

As $\det\boldsymbol{X} = x^2$ and $x^2 = x'^2$ is an invariant, we have to require $\det \boldsymbol{A} = 1$. The complex 2×2 matrices with determinant equal one form a group, the so-called special linear group $SL(2, \mathbb{C})$. Its elements can be represented by

$$\boldsymbol{A} = e^{\frac{1}{2}\boldsymbol{\sigma}\boldsymbol{\lambda}} e^{\frac{i}{2}\boldsymbol{\sigma}\boldsymbol{\theta}} , \tag{1.9}$$

where $\boldsymbol{\lambda}$, $\boldsymbol{\theta}$ correspond to six real parameters, and the exponential functions are defined via power expansion. The first factor corresponds to special Lorentz transformations (boosts), and $\boldsymbol{\lambda} = \lambda\hat{\boldsymbol{v}}$ is the rapidity parameter into the direction of the velocity $\boldsymbol{v} = \hat{\boldsymbol{v}}\,\mathrm{tanh}\lambda$. The second factor corresponds to rotations. If we define

$$\epsilon = i\sigma_2 = \begin{pmatrix} 0 & 1 \\ -1 & 0 \end{pmatrix} = \epsilon^{-1} = \epsilon^T = -\epsilon \in SL(2, \mathbb{C}) , \tag{1.10}$$

we find that $\epsilon\, \sigma_\mu^* \epsilon^{-1} = (\sigma_0, -\boldsymbol{\sigma}) \equiv \hat{\sigma}_\mu = \sigma^\mu$, and, as a consequence,

$$\epsilon \boldsymbol{A}^* \epsilon^{-1} = e^{-\frac{1}{2}\boldsymbol{\sigma}\boldsymbol{\lambda}} e^{\frac{i}{2}\boldsymbol{\sigma}\boldsymbol{\theta}} \equiv \hat{\boldsymbol{A}} . \tag{1.11}$$

Thus, we have constructed a second representation, where the boost has a relative sign. Next, one defines two-component complex-valued Weyl spinors ϕ and χ, that transform under $\boldsymbol{A}$ and $\hat{\boldsymbol{A}}$ respectively. Due to (1.11), the spinors are related by a parity transformation. They can also be transformed to each other via

$$\chi(p) = \hat{\boldsymbol{A}}(\boldsymbol{L}_{\boldsymbol{p}})\boldsymbol{A}^{-1}(\boldsymbol{L}_{\boldsymbol{p}})\phi(p) , \tag{1.12}$$

where we switched to momentum space, and $\boldsymbol{L}_{\boldsymbol{p}}$ is a Lorentz boost with momentum $\boldsymbol{p}$. It is interesting to note that $\chi^\dagger\phi$ and $\phi^\dagger\chi$ form Lorentz invariants. This can be seen from (1.11) and the relation $\epsilon\boldsymbol{A}^T\epsilon^{-1} = \boldsymbol{A}^{-1}$, which implies

$$\chi'^\dagger\phi' = \chi^\dagger\hat{\boldsymbol{A}}^\dagger\boldsymbol{A}\phi = \chi^\dagger(\epsilon\boldsymbol{A}^T\epsilon^{-1})\boldsymbol{A}\phi = \chi^\dagger\phi , \tag{1.13}$$

and vice versa for $\phi^\dagger\chi$. Making use of the relations $\cosh\lambda = p^0/m$ and $\sinh\lambda = |\boldsymbol{p}|/m$, it can be shown that equation (1.12) is equivalent to

$$m\,\chi(p) = p^\mu\hat{\sigma}_\mu\phi(p) = p_\mu\hat{\sigma}^\mu\phi(p)\,, \tag{1.14}$$

or

$$m\,\phi(p) = p^\mu\sigma_\mu\chi(p) = p_\mu\sigma^\mu\chi(p)\,. \tag{1.15}$$

It is thus convenient to define a four-component Dirac spinor $u(p) = (\phi(p), \chi(p))^T$, and to introduce the Dirac matrices

$$\gamma^\mu = \begin{pmatrix} \mathbf{0} & \sigma^\mu \\ \hat{\sigma}^\mu & \mathbf{0} \end{pmatrix}\,. \tag{1.16}$$

The equations (1.14) and (1.15) can now be combined into

$$(\gamma^\mu p_\mu - m\,\mathbf{1}_{4\times4})u(p) = 0\,. \tag{1.17}$$

In the limit $m = 0$, the spinors $\phi(p)$ and $\chi(p)$ are eigenstates of the helicity operator $h = \boldsymbol{\sigma}\cdot\boldsymbol{p}/(2p^0)$, with eigenvalues $\mp1/2$. The EOMs (1.14) and (1.15) are known as Weyl equations for that case. Defining $\gamma^5 = i\gamma^0\gamma^1\gamma^2\gamma^3 = \mathrm{diag}(-\mathbf{1}, \mathbf{1})$, which satisfies $\gamma^5\gamma^\mu + \gamma^\mu\gamma^5 = 0$, we can build projection operators

$$P_L = \frac{1}{2}\,(1-\gamma^5)\,, \qquad P_R = \frac{1}{2}\,(1+\gamma^5)\,, \tag{1.18}$$

and define the chiral spinors

$$u_L(p) = P_L\,u(p) = \begin{pmatrix} \phi(p) \\ 0 \end{pmatrix}\,, \qquad u_R(p) = P_R\,u(p) = \begin{pmatrix} 0 \\ \chi(p) \end{pmatrix}\,. \tag{1.19}$$

The distinction between left-handed ($u_L(p)$) and right-handed spinors ($u_R(p)$) becomes necessary, if different interactions for the more fundamental Weyl spinors are introduced. For massive fermions, the chiral components are superpositions of states where the spin points into the moving direction in the one case, and into the opposite direction in the other. For a left-handed fermion at high energy $E \gg m$ for instance, the fraction of the former state is suppressed compared to the fraction of the latter by the ratio m/E.

As the spinor product

$$u^\dagger(p)\gamma^0 u(p) = \chi^\dagger\phi + \phi^\dagger\chi \tag{1.20}$$

is a Lorentz invariant, it is convenient to define the Dirac conjugate $\overline{u}(p) \equiv u(p)^\dagger\gamma^0$. The Dirac matrices satisfy the Clifford algebra

$$\gamma^\mu\gamma^\nu + \gamma^\nu\gamma^\mu \equiv \{\gamma^\mu, \gamma^\nu\} = 2\eta^{\mu\nu}\mathbf{1}_{4\times4}\,, \tag{1.21}$$

where we use the convention $\eta^{\mu\nu} = \mathrm{diag}(1, -1, -1, -1)$ for the Minkowski metric. Useful identities which directly follow from the algebra are

$$\gamma^0(\gamma^\mu)^\dagger\gamma^0 = \gamma^\mu\,, \qquad (\gamma^0)^2 = \mathbf{1}_{4\times4}\,, \qquad \text{and} \qquad (\gamma^i)^2 = -\mathbf{1}_{4\times4}\,. \tag{1.22}$$

Here, $i = 1, 2, 3$ label the space coordinates. Contracting (1.21) with $p_\mu p_\nu$ and using (1.17), one finds $p^2 \mathbf{1}_{4\times 4} = m^2 \mathbf{1}_{4\times 4}$. The operator $\gamma^\mu p_\mu$ has the eigenvalues $\pm m$. Indeed, there exists a second spinor $v(p) = (\epsilon\chi^*(p), -\epsilon\phi^*(p))^T$, which satisfies

$$(\gamma^\mu p_\mu + m\,\mathbf{1}_{4\times 4})v(p) = 0\,. \tag{1.23}$$

The two EOMs (1.17) and (1.23) are known as the Dirac equations in momentum space.

Due to Pauli's spin-statistic theorem, spin-1/2 particles should behave like fermions. Therefore, the creation and annihilation operators have to satisfy anti-commutation relations. Switching back to position space and introducing creation (annihilation) operators $a_{\boldsymbol{p}}^{(s)\dagger}$ ($a_{\boldsymbol{p}}^{(s)}$) for fermions with momentum $\boldsymbol{p}$ and spin s, and $b_{\boldsymbol{p}}^{(s)\dagger}$ ($b_{\boldsymbol{p}}^{(s)}$) for anti-fermions, the field operators are given by

$$\begin{aligned} \psi(x) &= \frac{1}{(2\pi)^{3/2}} \sum_s \int \frac{d^3p}{2E_p} \Big(a_{\boldsymbol{p}}^{(s)}\, e^{-ipx}\, u^{(s)}(p) + b_{\boldsymbol{p}}^{(s)\dagger}\, e^{ipx}\, v^{(s)}(p) \Big)\,, \\ \overline{\psi}(x) &= \frac{1}{(2\pi)^{3/2}} \sum_s \int \frac{d^3p}{2E_p} \Big(a_{\boldsymbol{p}}^{(s)\dagger}\, e^{ipx}\, \overline{u}^{(s)}(p) + b_{\boldsymbol{p}}^{(s)}\, e^{-ipx}\, \overline{v}^{(s)}(p) \Big)\,. \end{aligned} \tag{1.24}$$

It satisfies the Dirac equation in position space

$$(i\gamma^\mu \partial_\mu - m\,\mathbf{1}_{4\times 4})\psi(x) = 0\,. \tag{1.25}$$

The conjugate equation can be derived with the help of the relations (1.22) and reads

$$\overline{\psi}(x)(i\gamma^\mu \overleftarrow{\partial_\mu} + m\,\mathbf{1}_{4\times 4}) = 0\,, \tag{1.26}$$

where the arrow indicates that the derivative is acting to the left.

In a general d-dimensional space-time, the Clifford algebra (1.21) forms a 2^d dimensional vector space. In four dimensions, we can choose

$$\Gamma = \{\Gamma_S = \mathbf{1}_{4\times 4}, \Gamma_P = \gamma^5, \Gamma_V = \gamma^\mu, \Gamma_A = \gamma^\mu\gamma^5, \Gamma_T = \sigma^{\mu\nu}\} \tag{1.27}$$

with $\mu < \nu$ as its 16 basis elements. Here, we introduced the definition $\sigma^{\mu\nu} \equiv i/2\,[\gamma^\mu, \gamma^\nu]$ and the superscripts S, P, V, A, T stand for scalar, pseudo scalar, vector, axial vector, and tensor, respectively. The names refer to the transition behavior of the current $\overline{\psi}(x)\,\Gamma\,\psi(x)$ under general Lorentz transformations. Indeed, in QFT the usual vector current j^μ known from electrodynamics is replaced by the (normal ordered) product of field operators $j^\mu = \overline{\psi}(x)\gamma^\mu\psi(x)$, and one proves $\partial_\mu j^\mu = 0$ with the help of (1.25) and (1.26). If the theory distinguishes between the chiralities, it is often more convenient to work with the chiral basis [5]

$$\begin{aligned} \Gamma^M &= \{P_R, P_L, P_R\gamma^\mu, P_L\gamma^\mu, \sigma^{\mu\nu}\}\,, \\ \Gamma_M &= \{P_R, P_L, P_L\gamma_\mu, P_R\gamma_\mu, \frac{1}{2}\,\sigma_{\mu\nu}\}\,, \end{aligned} \tag{1.28}$$

instead of (1.27). Here, the second line is the dual basis to the first line and we again take $\mu < \nu$. Finally, we want to quote the Lagrange density of the free Dirac theory

$$\mathcal{L}_{\mathrm{Dirac}} = \overline{\psi}(x) \left(\frac{i}{2} \gamma^\mu \overleftrightarrow{\partial_\mu} - m\, \mathbf{1}_{4\times 4} \right) \psi(x)\,, \tag{1.29}$$

where $\overleftrightarrow{\partial_\mu} \equiv \partial_\mu - \overleftarrow{\partial_\mu}$. It is sometimes convenient to use integration by parts within the action (or making use of the relations between ϕ and χ) in order to replace the Dirac operator in (1.29) by $(i\gamma^\mu \partial_\mu - m\,\mathbf{1})$. Another common abbreviation is provided by the slash notation $\not\partial \equiv \gamma^\mu \partial_\mu$ or $\not A = \gamma^\mu A_\mu$.

1.2 The gauge principle

As we discussed above, there is a gauge freedom in defining the classical vector potential $A_\mu(x)$ at any point x, which is not affected by field quantization. Now, the question arises if there is something similar for fermions. Obviously, the Dirac Lagrange density (1.29) is invariant under global phase rotations $\psi(x) \to \exp(i\alpha)\,\psi(x)$, where α is a real parameter. On the other hand, a local phase rotation

$$\psi(x) \to e^{i\alpha(x)} \psi(x) \tag{1.30}$$

will change $\mathcal{L}_D$ due to the derivative in the kinetic term. In order to obtain local gauge invariance, the partial derivative (which connects the point x with its vicinity) has to be replaced by a covariant derivative. The latter takes care of the fact that fields at different positions have different transformations (1.30). In general, we write

$$D_\mu = \partial_\mu - igA_\mu(x)\,, \tag{1.31}$$

where we pulled a constant g out of the vector field $A_\mu(x)$, which serves as a connection. In order to obtain a gauge-invariant Lagrangian, the latter has to transform as

$$A_\mu(x) \to A_\mu(x) + \frac{1}{g}\, \partial_\mu \alpha(x)\,. \tag{1.32}$$

One now identifies $A_\mu(x)$ with the photon field of the Maxwell theory. For interaction terms of fermions with photons, it is common to replace the general coupling constant g by the elementary charge e times the quantum number q, which denotes the fermion charge in units of e.

We now see how electromagnetic interactions can be motivated from the theory side: As the theory is described in terms of local field operators $\psi(x)$, $A_\mu(x)$, *etc.*, which are themselves non-observable quantities (in analogy to classical potentials), we assume local gauge freedom of the quantum fields for any point x of the space-time. However, this assumption requires a so-called minimal substitution of the partial derivative in the fermion action, which adds an interaction term to the Lagrange density. This is what we call the gauge principle. If we now include a kinetic term for the gauge fields $A_\mu(x)$, we have constructed the Lagrange density of quantum electro-dynamics (QED)

$$\mathcal{L}_{\rm QED} = -\frac{1}{4}\, F_{\mu\nu}(x)F^{\mu\nu}(x) + i\,\overline{\psi}(x)\gamma^\mu D_\mu\psi(x) - m\,\overline{\psi}(x)\psi(x)\,. \tag{1.33}$$

Some remarks are in order. The field-strength tensor $F_{\mu\nu}(x)$ itself is a gauge-invariant object. This is however not true for a mass term $\propto A_\mu(x)A^\mu(x)$. Thus, the photon has to be massless in QED. We do not include a Lorentz- and gauge invariant term $\propto F_{\mu\nu}\tilde{F}^{\mu\nu}$, as it violates parity.

The symmetry group of the above phase rotations (1.30) is the Lie group $U(1)$. It is now straight-forward to extend to more general cases. In general, fermions are assumed to live in the fundamental (vector) representation of the chosen Lie group. For the special unitary group $SU(N)$ for instance, there have to be N copies of any field, which we label by Latin indices from the middle of the alphabet. Gauge fields live in the adjoint representation, labeled by indices from the beginning of the alphabet. Their number is equal to the dimension of the group, which is N^2-1 for $SU(N)$. The covariant derivative generalizes to

$$D_\mu = \partial_\mu - ig\,T^a G^a_\mu(x)\,, \tag{1.34}$$

where T^a are the generators of the Lie group. For $SU(N)$, they satisfy the identities

$$\mathrm{Tr}[T^aT^b] = \frac{1}{2}\,\delta^{ab}\,, \quad T^aT^a = C_F\mathbf{1}\,, \tag{1.35}$$

with $C_F = (N^2-1)/(2N)$, as well as

$$(T^a)_{ij}(T^a)_{kl} = \frac{1}{2}\left(\delta_{il}\delta_{jk} - \frac{1}{N}\delta_{ij}\delta_{kl}\right)\,. \tag{1.36}$$

The quantum theory of strong interactions for instance is based on $SU(3)$ transformations. Thus, there are three copies of any fermion which transforms as a vector, and it has become common to talk about the color of a given field. The theory is therefore known as quantum chromo-dynamics (QCD). Its gauge fields $G^a_\mu(x)$ with $a=1,..,8$ are known as gluons. The generalization of the field-strength tensor $G^a_{\mu\nu}$, given by $[D_\mu, D_\nu] \equiv -igG^a_{\mu\nu}T^a$, is however not a gauge invariant object. Furthermore, it involves an additional term, as the generators of $SU(3)$ do not commute with each other[3]. Explicitly, one finds

$$G^a_{\mu\nu} = \partial_\mu G^a_\nu - \partial_\nu G^a_\mu + g_s f^{abc} G^b_\mu G^c_\nu\,, \tag{1.37}$$

where f^{abc} denotes the structure constant of $SU(3)$. In order to obtain a gauge invariant kinetic term, we have to take the trace $\mathrm{Tr}[T^aG^a_{\mu\nu}T^bG^{b\,\mu\nu}]$ with respect to the adjoint index a. Thus, we find the QCD Lagrangian as a generalization of (1.33)

$$\mathcal{L}_{\rm QCD} = -\frac{1}{4}\,G^a_{\mu\nu}(x)G^{a\,\mu\nu}(x) + i\,\overline{\psi}_i(x)\gamma^\mu D_\mu\psi_i(x) - m\,\overline{\psi}_i(x)\psi_i(x)\,, \tag{1.38}$$

[3]It is said that QCD is a non-abelian gauge theory opposed to QED, which is abelian.

where a summation over $a = 1, .., 8$ and $i = 1, 2, 3$ is understood. An important difference to QED is that due to (1.37), the kinetic term induces interaction terms which are cubic or quartic in the gluon fields. The $U(1)$ group is thus exceptional as its gauge fields do not directly interact with each other. Nevertheless, QED provides the possibility of photon-photon scattering via intermediate exchange of charged fermions.

At this stage, one needs to distinguish between classical- and quantum field theories. Within a quantum theory, there is the possibility of creating off-shell particle/anti-particle pairs, with subsequent annihilation of the latter. In a free theory, these so-called vacuum fluctuations would be non-observable. Within an interacting theory however, one can have fluctuations within the propagation of a photon for instance. On the other hand, a propagating fermion can emit an off-shell photon, and absorb it again. Within a classical theory of course, there is no possibility of creating off-shell particles, as energy-momentum conservation holds exactly. Thus, there is only the possibility of emitting an on-shell photon, which of course also works within the quantized theory. In order to take care of several quantum effects within the calculation of a scattering process, the mathematical framework of QFT is needed.

1.3 Spontaneous symmetry breaking

Our goal is to write down a Lagrange density, which describes all physics that have directly been discovered at collider experiments. Thus, it should contain the phenomena of electromagnetism, as well as strong and weak interactions. The latter is needed to describe the decay of heavy fermions and is mediated by the exchange of heavy gauge bosons. Before we are going to introduce the required gauge fields, we have to face another problem first: As mentioned above, there is no way of writing down a (fundamental) mass term for gauge fields without violating the local gauge symmetry of the theory. As we want to keep the gauge principle as a basic concept, we have to find a way of creating some kind of effective mass term, which stems from a gauge invariant interaction. This can be achieved with the help of a so-called hidden or spontaneously broken symmetry. The idea goes as follows: Let us assume that there exists a self-interacting (complex) scalar field $\phi(x)$. Its Lagrange density is given by

$$\mathcal{L}^{\phi^4} = \frac{1}{2}\,\partial_\mu \phi^*(x) \partial^\mu \phi(x) + \mu^2 |\phi(x)|^2 - \lambda |\phi(x)|^4 \,. \tag{1.39}$$

For $\mu^2 > 0$ and $\lambda > 0$ the potential $V(\phi) = -\mu^2|\phi(x)|^2 + \lambda|\phi(x)|^4$ develops a minimum at

$$\phi_0 = \left(\frac{\mu^2}{2\lambda}\right)^{1/2} . \tag{1.40}$$

Within the quantized theory, this minimum is associated with the vacuum expectation value (VEV) $v = \langle \phi(x) \rangle$ of the scalar field. It is convenient to write

$$\phi(x) = \sigma(x) + i\varphi(x) \equiv \phi_0 + h(x) + i\varphi(x) \,. \tag{1.41}$$

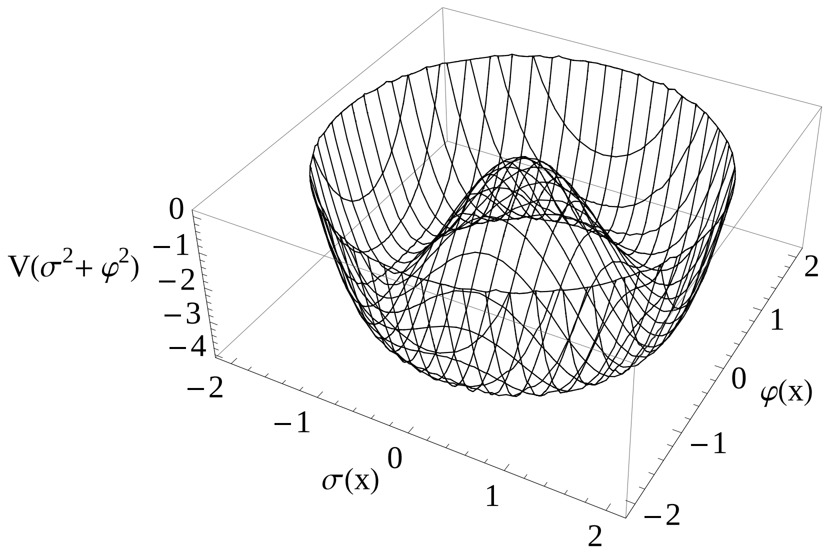

Figure 1.1: Potential $V(\phi)$ of the ϕ^4 theory for $-\mu^2 < 0$. See text for details.

The massless field $\varphi(x)$ is a left-over DOF within in the minimum of the potential $V(\phi)$ (see Figure 2.1), which is known as Goldstone boson (GB). The field $h(x)$, on the other hand, will receive a mass term. Note that the scalar field $\phi(x)$ could either be an elementary or a bound state, as long as it appears as a single particle at the scale v. Let us further assume, that $\phi(x)$ is charged under a given gauge symmetry. In this case, we have to replace the partial derivatives in (1.39) by covariant derivatives $D_\mu = \partial_\mu - igV_\mu(x)$, where we consider a $U(1)$ vector field for simplicity. We now find that an interaction term $\propto \phi^*(x)\phi(x)V_\mu(x)V^\mu(x)$, as well as further tri-linear terms are induced. If we take the VEV, we will generate a quadratic term $v^2\, V_\mu(x)V^\mu(x)/2$ among others. This is the desired mass term of the vector field $V_\mu(x)$, which on its own is not invariant under a local gauge transformation. Nevertheless, the combination of interaction and mass terms preserves local gauge freedom. This is all we require and the reason why we talk about hidden symmetry here: The theory as a whole is covariant, where the ground state is not.

There is a formal relation to statistical mechanics. If one tries to find a continuum description of a ferromagnet for instance, the theory should be invariant with respect to rotations in space. Nevertheless, the ground state picks out on arbitrary direction, when the elementary magnets are aligned. That is where the name spontaneous symmetry breaking comes from. The procedure of creating gauge-boson masses from spontaneous symmetry breaking is nowadays known as Higgs mechanism.

It should be noted that the insertion of the covariant derivative into (1.39) also induces terms of the form $g\, V_\mu(x)\partial^\mu\varphi(x)$, which have no sensible physical interpretation. Here we can make use of the gauge freedom and apply the method of gauge fixing, which allows us to get rid of those by adding the Lagrangian

$$\mathcal{L}_{\text{GF}} = -\frac{1}{2\xi}\left(\partial^\mu V_\mu(x) - \xi\,\frac{gv}{2}\,\varphi(x)\right)^2 \tag{1.42}$$

to the theory. Here, ξ is the gauge-fixing parameter, which can take any value from zero to infinity. As it can be worked out, the undesired terms cancel, and we obtain an additional (gauge dependent) contribution to the kinetic term of the vector field, as well as a mass term $m_\varphi = \xi v^2 g^2 |\varphi(x)|^2/2$ for the Goldstone boson. It is therefore called pseudo- or would-be Goldstone boson.

One might be worried that the gauge dependent terms spoil the predictivity of the theory. However, one will always find that the related contributions cancel within the calculation of a scattering or decay amplitude. An interesting remark is that in Feynman gauge ($\xi = 1$), the propagator of a massive vector field equals that one of the photon (apart from the mass in the denominator), while the propagator of the would-be GB is that of an ordinary scalar particle. It is said that the latter carries the longitudinal DOF of the heavy vector field, which is absent for a photon. The would-be GB is therefore not a particle on its own, but rather part of the quantum field theoretical description of a heavy gauge boson. Note that the quantization of the photon also goes along with a gauge-fixing Lagrangian, which however does not contain a scalar DOF. If we extend the discussion to a non-abelian gauge group, we need to add a further ingredient, the so-called ghost Lagrangian. It is a byproduct of the gauge-fixing procedure and guarantees the overall gauge invariance of the theory. As it is only important for calculations involving loops of gauge bosons (which is not a topic of this thesis), we will not go into detail here.

1.4 The Standard model of elementary particle physics

The Standard model of elementary particle physics (SM) is the basic playground for theoretical computations. It consists of QCD and a unified theory of electromagnetic and weak interactions. The theory of electroweak (EW) interactions, invented by *Sheldon Glashow, Abdus Salam* and *Steven Weinberg*, is based on the direct product $SU(2) \times U(1)$. The associated gauge fields are denoted as W^a_μ ($a = 1, 2, 3$), and B_μ. It further includes the Higgs mechanism in order to generate masses, where the Higgs is charged under both symmetry groups. As it turns out, the mass matrix has off-diagonal entries in the above basis of gauge fields. Moreover, one of the $SU(2)$ generators is imaginary. Therefore, one applies a basis transformation to a set of fields for which the generators are real, and the mass matrix is diagonal. These quantum fields are understood to describe the physical (that is propagating) particles, which are given by the heavy charged $W^\pm_\mu$ bosons, the heavy neutral Z^0, and the massless photon. Indeed, the existence of the heavy gauge bosons has been postulated by the above authors before the direct observation at the LEP experiment. The covariant derivative of the (non-abelian) theory of weak interactions is given by

$$D_\mu = \partial_\mu - igT^a W^a_\mu - ig'YB_\mu\,. \tag{1.43}$$

The generators of $SU(2)$ are given by (half of) the Pauli matrices $T^a = \sigma^a/2$, and we assign the so-called hyper-charge Y to $U(1)$. Furthermore, we need kinetic terms for the gauge fields consisting of the square of the field strength tensors

$$W^a_{\mu\nu} = \partial_\mu W^a_\nu - \partial_\nu W^a_\mu + g\,\epsilon^{abc}\,W^b_\mu W^c_\nu\,, \qquad \text{and} \qquad B_{\mu\nu} = \partial_\mu B_\nu - \partial_\nu B_\mu\,. \tag{1.44}$$

Here, the antisymmetric Levi-Cevita symbol ϵ^{abc} is the structure constant of $SU(2)$. In analogy to QCD, there will be interactions among the fields W^a_μ. As a next step, we take the covariant derivative (1.43) of the Higgs field, which is assumed to be a fundamental complex scalar field, which transforms as a doublet under $SU(2)$. As discussed in the previous section, it can obtain a vacuum-expectation value different from zero by the introduction of a self interaction. Explicitely, we write the Higgs-doublet as

$$\Phi(x) = \frac{1}{\sqrt{2}}\begin{pmatrix} -i(\varphi_1(x) - i\varphi_2(x)) \\ v + (h(x) + i\varphi_3(x)) \end{pmatrix}_{\frac{1}{2}}\,, \qquad \langle\Phi(x)\rangle = \frac{1}{\sqrt{2}}\begin{pmatrix} 0 \\ v \end{pmatrix}_{\frac{1}{2}}\,, \tag{1.45}$$

where the subscript denotes its hyper-charge. The Higgs-Lagrangian has the form

$$\mathcal{L}_{\text{Higgs}} = (D_\mu\Phi)^\dagger\,(D^\mu\Phi) - V(\Phi)\,, \qquad V(\Phi) = -\mu^2\Phi^\dagger\Phi + \lambda\left(\Phi^\dagger\Phi\right)^2\,. \tag{1.46}$$

Due to the non-vanishing VEV, the kinetic term in (1.46) gives rise to mass terms for the gauge bosons. As mentioned above, these are not diagonal in the basis (W^a_μ, B_μ). There is a mixture between W^3_μ and B_μ. The change to the mass eigenbasis, where each field has individual mass and kinetic terms, is achieved by the field rotation

$$\begin{pmatrix} Z_\mu \\ A_\mu \end{pmatrix} = \frac{1}{\sqrt{g^2 + g'^2}}\begin{pmatrix} g & -g' \\ g' & g \end{pmatrix}\begin{pmatrix} W^3_\mu \\ B_\mu \end{pmatrix}\,. \tag{1.47}$$

The fields Z_μ and A_μ are identified with the massive Z^0 and the massless photon respectively. It is common to introduce the weak-mixing angle θ_w

$$\sin\theta_w = \frac{g'}{\sqrt{g^2 + g'^2}}\,, \qquad \cos\theta_w = \frac{g}{\sqrt{g^2 + g'^2}} \tag{1.48}$$

in the above expression. One further defines

$$W^\pm_\mu = \frac{1}{\sqrt{2}}\left(W^1_\mu \mp iW^2_\mu\right)\,, \qquad T^\pm = (T^1 \pm iT^2)\,, \tag{1.49}$$

where the generators

$$T^+ = \begin{pmatrix} 0 & 1 \\ 0 & 0 \end{pmatrix} \qquad \text{and} \qquad T^- = \begin{pmatrix} 0 & 0 \\ 1 & 0 \end{pmatrix} \tag{1.50}$$

mediate between particles, which are identified as upper and lower components of $SU(2)$ doublets. We will come back to this point below. The masses of the gauge fields are found to be

$$m_W = \frac{g\,v}{2}\,, \qquad m_Z = \frac{\sqrt{g^2 + g'^2}\,v}{2}\,, \qquad \text{and} \qquad m_A = 0\,. \tag{1.51}$$

The would-be GBs are rewritten in analogy to (1.49) such that $\varphi^{\pm} = (\varphi_1 \mp i\varphi_2)/\sqrt{2}$. We remember that the latter serve as longitudinal DOFs of $W_\mu^{\pm}$. The GB ϕ_3 is absorbed by the Z^0 boson. The field $h(x)$ however stays within the theory as an additional DOF. It is known as Higgs field and is the only particle of the theory, which has not been observed so far. Its mass is given by $m_h = \sqrt{2\lambda}v$, where λ is the self-coupling as introduced in (1.39). It should be stressed that the above expressions for the masses m_Z, m_W and m_h are LO relations. There will be modifications from quantum corrections to the respective propagators, given by vacuum-polarization diagrams. Here, one talks of oblique corrections [6, 7]. The weak mixing angle is determined from measurements of various EW decay processes. The Higgs VEV v can be extracted from the observed gauge boson masses and is found to be $v \approx 246\,\text{GeV}$ within the SM. Considering the Higgs mass, there is a theoretical upper bound

$$m_h < \left(\frac{8\pi\sqrt{2}}{3G_F}\right)^{1/2} \approx 1\,\text{TeV}\,, \tag{1.52}$$

if one wants to preserve unitarity in the longitudinal component of heavy gauge boson scattering amplitudes at high energies [8]. Here, we have introduced Fermi's constant

$$\frac{G_F}{\sqrt{2}} = \frac{g^2}{8m_W^2}\,. \tag{1.53}$$

It is useful to write (1.43) in the mass eigenbasis. If we define the charges

$$e = \frac{gg'}{\sqrt{g^2+g'^2}} = g\sin\theta_w\,, \qquad \text{and} \qquad g_Z = \sqrt{g^2+g'^2} = \frac{g}{\cos\theta_w} \tag{1.54}$$

as well as the charge quantum numbers

$$Q = T^3 + Y, \qquad \text{and} \qquad Q_Z = T^3 - \frac{g'^2}{\sqrt{g^2+g'^2}}\,Q = T^3 - \sin^2\theta_w\,Q\,, \tag{1.55}$$

we can write ($s_w \equiv \sin\theta_w,\ c_w \equiv \cos\theta_w$)

$$D_\mu = \partial_\mu - i\,\frac{g}{\sqrt{2}}\left(W_\mu^+T^+ + W_\mu^-T^-\right) - ig_z\,Z_\mu\left(T^3 - s_w^2 Q\right) - ieA_\mu Q\,. \tag{1.56}$$

The first connection term induces charged-current interactions. This can be understood from the explicit form of the generators (1.50) and the definition of the quantum number Q in (1.55). For a given hyper-charge, the value of Q differs by 1 for components of an $SU(2)$ doublet for which $T^3 = \pm 1/2$. As mentioned above, the generators $T^{\pm}$ link the different components. On the other hand, Q is identified as the quantum number related to the electric charge, as evident from the third term in the covariant derivative. The latter gives rise to photon exchange, where e is the elementary electron charge. Finally, the second term induces the exchange of neutral-current interactions mediated by a heavy Z^0 boson.

Before we are able to write down the full Lagrange density of the SM, we need to specify the particles of the theory, and list there quantum numbers under the SM gauge group

$$SU(3)_c \times SU(2)_L \times U(1)_Y\,. \tag{1.57}$$

The subscripts c and Y indicate color and hyper-charge respectively. The subscript L however refers to chirality. From angular distributions in scattering experiments it is known that charged current interactions only occur for left-handed fermions. Therefore, we have to choose the latter to be doublets under $SU(2)_L$, where right-handed fermions are taken to be singlets. This assignment is however problematic if we want to insist on local gauge invariance and describe massive fermions at the same time. From (1.19) and (1.20) it is evident that the Dirac mass term in (1.29) couples left to right-handed spinors and vice versa. If the corresponding quantum fields are assigned with different quantum numbers, the mass term does not form an invariant under the respective gauge group. Fortunately, we have the solution to face the problem already at hand. If the Higgs doublet is part of the theory, we are allowed to write down further coupling terms. For instance, if we define the doublet $L_L^e = (\nu_e, e_L)^T$, which consists of the electron neutrino and the left-handed electron, we can write the gauge-invariant term

$$\mathcal{L}^e_{\text{Yukawa}} = -y_e \overline{L}^e_L(x)\Phi(x)e_R(x) + \text{h.c.}\,, \tag{1.58}$$

where y_e is a complex-valued coupling constant. After spontaneous symmetry breaking, a mass term $m_e = \lambda_e v/\sqrt{2}$ is generated. One now introduces Yukawa interactions for all fermions, where the Yukawa couplings are further input variables of the theory. If there is more than one generation of particles, we have again to distinguish between weak eigenstates and mass eigenstates. Before we go into detail here, we first specify the particle content of the SM.

Within the SM, fermions are classified by their color, their electric charge (quantum number Q), their weak isospin T_L^3, and their mass. Fermions which are charged under $SU(3)_c$ are known as quarks. Considering electric charge, there are two types of them: up-type quarks with charge $2/3\,e$ and down-type quarks with charge $-1/3\,e$. Left-handed up- and down-type quarks are combined into doublets Q_L of $SU(2)_L$. Right-handed quarks transform as singlets. Today, we know about three generations of up and down-type quarks, which differ by their masses. In the up-sector we have $u_i = (u, c, t)$, where i is the generation index.[4] They are referred to as up quark, charm quark, and top quark respectively. In the down sector we have $d_i = (d, s, b)$, which are known as down quark, strange quark, and bottom (or beauty) quark. A similar picture arises for leptons, which are singlets under $SU(3)_c$. We have $e_i = (e, \mu, \tau)$ with charge $-e$, known as electron, muon and τ-lepton. The neutrinos with electric charge zero are labeled by $\nu_i = (\nu_e, \nu_\mu, \nu_\tau)$ and carry the name of the corresponding charged lepton. Note that there are no right-handed so-called sterile neutrinos in the SM, as they would be singlets under the complete group (1.57). As a consequence, there is no Dirac mass term for the neutrino. In summary, the

[4]Do not confuse with the color index which we will suppress for the rest of the discussion.

	Q	Y	T_L^3
u_{i_L}	$2/3$	$1/6$	$1/2$
d_{i_L}	$-1/3$	$1/6$	$-1/2$
u_{i_R}	$2/3$	$2/3$	0
d_{i_R}	$-1/3$	$-1/3$	0
ν_{i_L}	0	$-1/2$	$1/2$
e_{i_L}	-1	$-1/2$	$-1/2$
e_{i_R}	-1	-1	0

Table 1.1: Quantum numbers of the SM quarks and leptons. See text for details.

fermion content of the SM is given by

$$\begin{aligned} Q_L &= \left(\begin{pmatrix} u_L \\ d_L \end{pmatrix}, \begin{pmatrix} c_L \\ s_L \end{pmatrix}, \begin{pmatrix} b_L \\ t_L \end{pmatrix} \right) , \quad u_R = (u_R, c_R, t_R) \ , \quad d_R = (d_R, s_R, b_R) \\ L_L &= \left(\begin{pmatrix} \nu_e \\ e_L \end{pmatrix}, \begin{pmatrix} \nu_\mu \\ \mu_L \end{pmatrix}, \begin{pmatrix} \nu_\tau \\ \tau_L \end{pmatrix} \right) , \quad e_R = (e_R, \mu_R, \tau_R) \ . \end{aligned} \tag{1.59}$$

The respective quantum numbers are collected in Table 1.1. Ignoring chirality, it is said that there are six different flavors u, d, s, c, b, t. Only the lightest up and the down quarks are stable. The additional quarks decay either hadronically into lighter quarks (finally into u or d), or semileptonically into leptons via charged current interactions. Concerning the latter, only the electron is a stable particle.

At this point, we need to discuss the phenomenon of quark (lepton) mixing. The Yukawa Lagrangian of the quark sector in the three generation case is given by

$$\mathcal{L}^q_{\text{Yukawa}} = -(\boldsymbol{Y}_d)_{ij} \overline{Q}_{i_L}(x)\, \Phi(x)\, d_{j_R}(x) - (\boldsymbol{Y}_u)_{ij} \overline{Q}_{i_L}(x)\, \epsilon \Phi^*(x)\, u_{j_R}(x) + \text{h.c.} \,, \tag{1.60}$$

where $\boldsymbol{Y}_{d,u}$ are complex-valued 3×3 matrices and ϵ is defined in (1.10). The hermitian products $\boldsymbol{Y}_q \boldsymbol{Y}_q^\dagger$ and $\boldsymbol{Y}_q^\dagger \boldsymbol{Y}_q$ with $q = u, d$ can be diagonalized via the unitary transformations

$$\boldsymbol{Y}_q \boldsymbol{Y}_q^\dagger = \boldsymbol{U}_q \tilde{\boldsymbol{Y}}_q^2 \boldsymbol{U}_q^\dagger \,, \qquad \boldsymbol{Y}_q^\dagger \boldsymbol{Y}_q = \boldsymbol{W}_q \tilde{\boldsymbol{Y}}_q^2 \boldsymbol{W}_q^\dagger \,. \tag{1.61}$$

It follows that the Yukawa matrices $\boldsymbol{Y}_q$ are diagonalized by a bi-unitary transformation

$$\boldsymbol{Y}_q = \boldsymbol{U}_q \tilde{\boldsymbol{Y}}_q \boldsymbol{W}_q^\dagger \,. \tag{1.62}$$

If we now transform the quark fields according to

$$q_{i_L} \to q'_{i_L} = (\boldsymbol{U}_q)_{ij} q_{j_L} \,, \qquad q_{i_R} \to q'_{i_R} = (\boldsymbol{W}_q)_{ij} q_{j_R} \,, \tag{1.63}$$

we can identify the quark masses $m_{q_i} = v\, (\tilde{\boldsymbol{Y}}_q)_{ii}/\sqrt{2}$. The fields q form the flavor or weak interaction basis, where the fields q' are denoted as mass eigenstates. Due to the unitarity of

$\boldsymbol{U}_q$ and $\boldsymbol{W}_q$, the field redefinition (1.63) drops out if one studies neutral-current interactions. For the same reason, there is no flavor-changing neutral current (FCNC) interaction in the SM. This is not the case for charged currents. If we rotate to the mass basis, the current will transform as

$$J_\mu^+ = \frac{1}{\sqrt{2}}\,\bar{u}_{i_L}(x)\gamma_\mu d_{i_L} \rightarrow \frac{1}{\sqrt{2}}\,\bar{u}'_{i_L}(x)\gamma_\mu(\boldsymbol{V}_{\text{CKM}})_{ij}d'_{i_L}\,, \tag{1.64}$$

where we introduced the *Cabibbo-Kobayashi-Maskawa* (CKM) quark-mixing matrix.

$$\boldsymbol{V}_{\text{CKM}} = \boldsymbol{U}_u^\dagger \boldsymbol{U}_d\,. \tag{1.65}$$

It is the only source of flavor violation in the SM, and can be parametrized by three mixing angles and one complex phase. The latter gives rise to CP violating interactions [9] and does not appear in a reduced scenario which features only two generations. Indeed, the existence of a third generation has been postulated by Kobayashi and Maskawa in order to obtain a CP violing phase, before there was a direct experimental evidence for the bottom and the top-quark.

The Yukawa Lagrangian of the lepton sector is given by

$$\mathcal{L}^l_{\text{Yukawa}} = -(\boldsymbol{Y}_l)_{ij}\overline{L}_{i_L}(x)\Phi(x)e_{j_R}(x) + \text{h.c.}\,, \tag{1.66}$$

with a complex-valued 3×3 coupling matrix $\boldsymbol{Y}_l$. In analogy to (1.62), it can be diagonalized, by introducing unitary matrices $\boldsymbol{U}_l$ and $\boldsymbol{W}_l$. If the neutrinos are massless, these matrices can however always be eliminated from the theory by imposing the field redefinitions

$$e_{i_L} \rightarrow e'_{i_L} = (\boldsymbol{U}_l)_{ij}e_{j_L}\,, \qquad \nu_{i_L} \rightarrow \nu'_{i_L} = (\boldsymbol{U}_l)_{ij}\nu_{j_L}\,, \qquad e_{i_R} \rightarrow e'_{i_R} = (\boldsymbol{W}_l)_{ij}e_{j_R}\,. \tag{1.67}$$

As a consequence, there will be no mixing among different generations in the lepton sector. If the neutrinos carry mass on the other hand, we need a second set of transformation matrices and the situation is analog to quark mixing.

We have finally collected all ingredients to write down the full SM Lagrangian. Within the weak interaction basis, it reads

$$\mathcal{L}_{\text{SM}} = \mathcal{L}_{\text{Gauge}} + \mathcal{L}_{\text{Higgs}} + \mathcal{L}_{\text{GF}} + \mathcal{L}_{\text{FP}} + \mathcal{L}_{\text{Fermion}} + \mathcal{L}_{\text{Yukawa}}\,, \tag{1.68}$$

where

$$\begin{aligned}\mathcal{L}_{\text{Gauge}} &= -\frac{1}{4}\,G^a_{\mu\nu}G^{a\mu\nu} - \frac{1}{4}\,W^a_{\mu\nu}W^{a\mu\nu} - \frac{1}{4}\,B_{\mu\nu}B^{\mu\nu}\,,\\ \mathcal{L}_{\text{GF}} &= -\frac{1}{2\xi_a}\left(\partial^\mu W^a_\mu - \xi_a\,\frac{gv}{2}\,\varphi_a\right)^2 - \frac{1}{2\xi}\left(\partial^\mu B_\mu + \xi\,\frac{g'v}{2}\,\varphi_3\right)^2\,,\end{aligned} \tag{1.69}$$

and

$$\mathcal{L}_{\text{Fermion}} = \bar{Q}_L\,i\not{D}\,Q_L + \bar{u}_R\,i\not{D}\,u_R + \bar{d}_R\,i\not{D}\,d_R + \bar{L}_L\,i\not{D}\,L_L + \bar{e}_R\,i\not{D}\,e_R\,. \tag{1.70}$$

For the case of quarks, the covariant derivative D_μ combines the connection terms of (1.34) and (1.56). For leptons it is given by the latter formula only. The required quantum numbers are listed in in Table 1.1. The Higgs Lagrangian $\mathcal{L}_{\text{Higgs}}$ is given in (1.46), and $\mathcal{L}_{\text{Yukawa}}$ is the sum of (1.60) and (1.66). As it is not needed in this thesis, we will not specify the Faddeev-Popov ghost Lagrangian $\mathcal{L}_{\text{FP}}$. However, it will turn out to be useful to translate (1.69) into the mass eigenbasis. Therefore, we define $W^\pm_{\mu\nu} = \partial_\mu W^\pm_\nu - \partial_\nu W^\pm_\mu$ and $Z_{\mu\nu} = \partial_\mu Z_\nu - \partial_\nu Z_\mu$, and obtain

$$\mathcal{L}_{\text{Gauge}} = -\frac{1}{4}\, G^a_{\mu\nu} G^{a\mu\nu} - \frac{1}{2}\, W^+_{\mu\nu} W^{-\mu\nu} - \frac{1}{4}\, Z_{\mu\nu} Z^{\mu\nu} - \frac{1}{4}\, F_{\mu\nu} F^{\mu\nu} + \text{weak interaction terms}\,, \tag{1.71}$$

$$\mathcal{L}_{\text{GF}} = -\frac{1}{2\xi}\big(\partial^\mu A_\mu\big)^2 - \frac{1}{2\xi}\big(\partial^\mu Z_\mu - \xi\, m_Z \varphi_3\big)^2 - \frac{1}{\xi}\big(\partial^\mu W^+_\mu - \xi\, m_W \varphi^+\big)\big(\partial^\nu W^-_\nu - \xi\, m_W \varphi^-\big).$$

Here, we have chosen a common gauge parameter ξ for simplicity. A complete list of Feynman rules deduced from (1.68) can be found in [3]. If one takes into account all symmetry restrictions, the SM has 18 independent free parameters, which have to be fixed by experiment. These consist of six quark masses, three lepton masses, three CKM mixing angles, one CP-violating CKM phase, three gauge couplings (g_c, g, g'), as well as the parameters μ and λ of the Higgs potential.

Before we are going to discuss the prosperities and short-comings of the SM, we first want to give some short remarks about renormalization and effective theories. As it is given above, the SM is a renormalizable theory. On the other hand, there are obvious reasons, why it should be regarded as an effective theory only. Therefore, we want to repeat the main facts about that topic. Let us close this section by noting that the SM of elementary particle physics is a relativistic quantum field theory based on the concept of local gauge freedom. It is widely believed that any extension should fall into the same category of theories.

1.5 Effective theories and higher dimensional operators

In the early days it was widely believed that only renormalizable quantum field theories make sense as a theory of nature, as only for those there is a finite number of counter terms needed in the process of renormalization. Here, ultra-violet (UV) divergences due to loop integrations are absorbed into singular (non-observable) relations between bare input parameters and measurable quantities. The related renormalization constants have to be fixed by measurement. Infra-red (IR) divergences cancel out when real state emission is taken into account. Therefore, they do not have to be removed by a renormalization procedure. Non-renormalizable theories involve so-called higher dimensional operators, for which additional counter terms are induced at any order of the perturbative expansion of the scattering matrix. Thus, predictivity is lost. On the other hand, if one cuts the loop integration at some finite momentum (or energy) scale, there are no UV divergences at all. The question now is, do we really expect our theory to hold to all energies? Indeed, this assumption seems to be very venturous. In the history of physics, it turned out again and again that the validity of a well understood and experimentally verified theory can break down, when one tries to test the theory on smaller length scales or higher energies. Another important observation is that physics at different scales turn out to be disentangled from each other. Back in the seventies, the physical meaning of renormalization has been reinterpreted by *Kenneth Wilson*. Nowadays, it is accepted that renormalizability in the original sense is no requirement in order to have a sensible theory of nature. Instead, nature may be described in terms of so-called effective theories (EFTs). The price one has to pay is that an EFT goes along with a hard energy/momentum cut-off M, to which it is valid.

In the discussion of the previous sections we emphasized, that the Lagrange density of an interacting theory has to satisfy Poincaré- and gauge invariance. In other words, the action should transform as a scalar under the related symmetry transformations. By inspection of (1.33) and (1.38) or (1.68) on the other hand, one observes that we have not written down all possible terms. Indeed, there is an infinite amount of combinations of spinors, vector and scalar fields, as well as derivatives, that are both gauge- and Lorentz invariant. In order to be able to make a prediction from the theory, these extra terms should either vanish, or be suppressed in a certain sense we have to specify.

In natural units ($\hbar = c = 1$), energy, mass, and momentum, as well as inverse time and length scales have the same (mass) dimension: $[E] = [p] = [m] = [1/x] = [1/t] = 1$. The action S has no physical dimension (otherwise it could not show up in the exponential of a generating functional). Due to (1.2), the Lagrange density then has to have a mass dimension of four. As derivatives scale like $1/x$, we conclude by "naive dimensional analysis", that the fields have the dimensions $[\psi] = 3/2$, and $[\phi] = [A_\mu] = 1$. If we want to construct operators with a higher mass dimension (or simply higher dimensional operators), we have to include an additional energy scale. For instance, the four fermion operator $\overline{\Psi}_1(x)\Psi_2(x)\,\overline{\Psi}_3(x)\Psi_4(x)$ has dimension six. Thus, it should be accompanied by an inverse energy scale squared. Let us assume that this scale is identified with the cut-off M of the theory. In the limit $M \to \infty$, all higher dimensional operators vanish. This is exactly what happens for renormalizable theories, such as QED (1.33), QCD (1.38), and the theory of EW interactions.

As it turns out, EFTs do not only offer the possibility of having a scale of ignorance, beyond which the appropriate theory is not known, but also provide useful tools for the analysis of multi-scale problems.[5] In practice, the hard cut-off is identified with some physical mass scale. Let us take the Fermi theory of EW interactions as an example. Before the theory of weak interactions has been invented it was assumed, that β-decay is a local four-fermion process. The respective coupling constant G_F has to be proportional to some inverse scale $1/m_W^2$. With the increase of available energies at collider experiments it turned out that β-decay is instead mediated by a local charged-current interaction, featuring an intermediate heavy gauge boson $W_\mu^\pm$ of mass m_W. To LO in perturbation

[5]A thorough discussion of the most important aspects is given in [10] or [11] for instance.

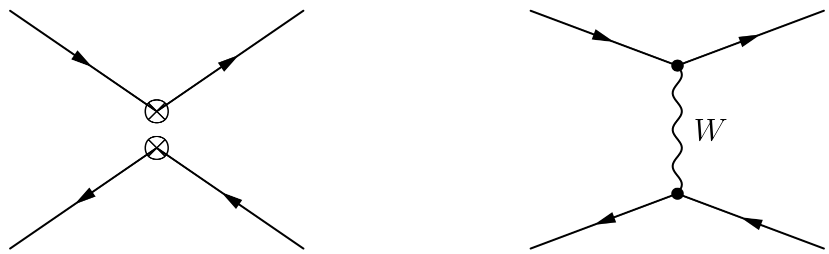

Figure 1.2: Effective four-fermion interaction versus exchange of a W-boson in the full theory.

theory, its two-point correlation function (in Feynman gauge) reads

$$\int d^4x\, e^{ipx}\, \langle 0|\, T\, W_\mu^+(x) W_\nu^-(x)\, |0\rangle = \frac{-i\eta_{\mu\nu}}{p^2 - m_W^2 + i\epsilon}\,. \tag{1.72}$$

At low energies $p^2 \ll m_W^2$, the $W_\mu^\pm$ boson is far from its mass shell and the right-hand side of (1.72) is proportional to $1/m_W^2$. Thus, the four-fermion interaction indeed seems to be point-like. Going up to higher energies, the non-renormalizable four-fermion operator is replaced by two renormalizable charged-current operators, which are connected by the propagator of the $W_\mu^\pm$ (see Figure 1.5). In this sense, the theory of weak interactions is the UV completion of Fermi's theory.

Next, we want to understand how we can separate short distance from long distance physics by the use of the EFT language. Therefore, one has to split the quantum fields of the theory into low-frequency and high-frequency modes, separated by a scale μ

$$\omega_L < \mu < \omega_H\,. \tag{1.73}$$

Here, $\omega_{L,H}$ denote the energies of the fields under consideration. Next, one wants to remove the high-frequency modes as propagating particles and write down a low-energy theory, where the quantum effects of the latter are absorbed into effective coupling constants. Formally this corresponds to the situation where the path integral of those modes is explicitly performed. It is said that the heavy modes have been integrated out. They do no longer show up as individual DOFs. For instance, if $\mu < m_W$, the W boson is no longer part of the effective theory. The effective Lagrangian is defined as the sum off all operators Q_i allowed by the symmetries of the theory, multiplied by some coupling coefficients C_i. These have to be determined by computing appropriate scattering amplitudes[6] in the full theory (including $W^\pm$ etc.) to a given order in perturbation theory, and comparing the result to the matrix elements of the effective theory

$$\mathcal{A} = \sum_i C_i(\mu)\, \langle Q_i(\mu)\rangle \Big|_{\mu=\Lambda}\,. \tag{1.74}$$

[6]The term "amplitude" is used for "amputated Greens function" here.

This procedure is known as matching. The scale $\Lambda < M$ is denoted as the matching scale and serves as an intermediate cut-off, where the field that sets the scale is removed from the theory. At LO matching, the so-called Wilson-coefficients C_i are either zero (if the respective vertices do not exist), or given by the coupling constant times a numerical factor with negative mass dimension. In the theory of weak decays, we would obtain Fermi's constant. If we now go to higher order in perturbation theory in QCD for instance, the matrix elements involve terms $\propto \alpha_s(\mu)\ln(\mu^2/(-p^2))$, where the full theory gives rise to $\alpha_s(\mu)\ln(m_W^2/(-p^2))$. The idea is now to apply the following matching scheme [11]

$$\underbrace{1+\frac{\alpha_s(\mu)}{4\pi}\ln\left(\frac{m_W^2}{-p^2}\right)}_{\text{full theory}} = \underbrace{\left(1+\frac{\alpha_s(\mu)}{4\pi}\ln\left(\frac{m_W^2}{\mu^2}\right)\right)}_{C(\mu)}\underbrace{\left(1+\frac{\alpha_s(\mu)}{4\pi}\ln\left(\frac{\mu^2}{-p^2}\right)\right)}_{\langle Q(\mu)\rangle} + \mathcal{O}\left(\alpha_s^2\right) , \tag{1.75}$$

where the separation into long distance (matrix elements) and short distance effects (Wilson coefficients) becomes apparent. The choice of matrix elements from which the coefficients are extracted is arbitrary, as long as the respective operators show up in the result of the full theory calculation. The Wilson coefficients are therefore process independent. Once they are calculated, they can be used for any operator insertion within an EFT calculation.

1.6 Renormalization group running for Wilson coefficients

The separation of scales as given in (1.75) only makes sense, if there is a reasonable convergence of the power series in α_s. Let us assume, we want to calculate the matrix element of four-fermion operators at the scale $\mu \approx 1\,\text{GeV}$, where $\Lambda = m_W$. Then we have $\ln(m_W^2/\mu^2) \approx \ln(80^2) \approx 6$, which has to be multiplied by $\alpha_s(1\text{GeV})/4\pi \approx 0.03$. Thus we find $\alpha_s/4\pi\ \ln(m_W^2/\mu^2) \approx 0.25$. If the cut-off of the theory is about $1\,\text{TeV}$, the latter expression evaluates to ≈ 0.4. As we see, there is the danger of large logarithms spoiling the perturbativity of the expansion, if we consider a large separation of scales. For that reason, we require a resummation of the power expansion in such a way that $\alpha_s\ln(\Lambda/\mu)$ counts as an $\mathcal{O}(1)$ parameter. Therefore, all terms of the form $(\alpha_s\ln(\Lambda/\mu))^n$ with $n \in \mathbb{N}_0$ need to be summed, where terms of the form $\alpha_s(\alpha_s\ln(\Lambda/\mu))^n$ count as $\mathcal{O}(\alpha_s)$ and so on. At this point, the concept of renormalization group (RG)-improved perturbation theory enters the game. Let us assume, the operators given in (1.74) form a complete set (basis) for a given scattering process. It is clear that the amplitude should depend on the input momentum p and the cut-off scale, but not on the choice of the separation scale Λ. Therefore, we require

$$\frac{d}{d\ln\mu}\sum_i C_i(\mu)\langle Q_i(\mu)\rangle = 0\,. \tag{1.76}$$

As the Q_i form a basis, we can expand

$$\frac{d}{d\ln\mu}\langle Q_i(\mu)\rangle = -\sum_j \hat{\gamma}_{ij}(\mu)\,\langle Q_j(\mu)\rangle\,, \tag{1.77}$$

where the expansion coefficients $\hat{\gamma}_{ij}$ form the entries of the so-called anomalous dimension matrix $\hat{\gamma}$. They can be understood as the answer of the matrix element $\langle Q_j(\mu)\rangle$ to a scale variation of $\langle Q_i(\mu)\rangle$. Inserting the definition (1.77) into (1.76), and using the fact that the basis operators Q_i are linearly independent, we conclude that

$$\frac{d}{d\ln\mu}\,C_j(\mu) - \sum_i C_i(\mu)\,\hat{\gamma}_{ij}(\mu) = 0 \qquad \Leftrightarrow \qquad \frac{d}{d\ln\mu}\,\vec{C}(\mu) - \hat{\gamma}^T(\mu)\,\vec{C}(\mu) = 0\,. \tag{1.78}$$

This is known as RG equation for Wilson coefficient functions, which we expressed in matrix notation on the right-hand side for convenience. Let us now remember the definition of the QCD β-function $\beta \equiv d\alpha_s(\mu)/d\ln(\mu)$, which describes the running of α_s due to quantum corrections in a given process. The scale dependence of the matrix element $\langle Q_i(\mu)\rangle$ can be traced back to the scale dependence of the couplings and the separation of scales according to (1.75). The anomalous dimension matrix depends on μ only through the running of $\alpha_s(\mu)$. Thus, we can recast the RG equation (1.78) into the form

$$\frac{d}{d\alpha_s(\mu)}\,\vec{C}(\mu) - \frac{\hat{\gamma}^T(\alpha_s(\mu))}{\beta(\alpha_s(\mu))}\,\vec{C}(\mu) = 0\,. \tag{1.79}$$

This equation is now solved by integration. If we define the quantities $\hat{\gamma}_0$ and β_0 via the expansion

$$\hat{\gamma}(\alpha_s) = \hat{\gamma}_0\,\frac{\alpha_s}{4\pi} + \mathcal{O}(\alpha_s^2)\,, \quad \beta(\alpha_s) = -2\alpha_s\left(\beta_0\,\frac{\alpha_s}{4\pi} + \mathcal{O}(\alpha_s^2)\right)\,, \quad C_i(\Lambda) = 1 + \mathcal{O}(\alpha_s)\,, \tag{1.80}$$

and insert the latter expressions into the equation (1.79), we find to LO in α_s (see [10, 11] for more details)

$$\vec{C}(\mu) = \hat{V}\left(\frac{\alpha_s(\Lambda)}{\alpha_s(\mu)}\right)_D^{\frac{\vec{\gamma}_0}{2\beta_0}}\hat{V}^{-1}\,\vec{C}(\Lambda) \equiv \hat{U}(\mu,\Lambda)\,\vec{C}(\Lambda)\,. \tag{1.81}$$

Here, $\hat{V}$ diagonalizes $\hat{\gamma}_0^T$ via $\hat{\gamma}_{0D} = \hat{V}^{-1}\hat{\gamma}_0^T\,\hat{V}$, and $\vec{\gamma}_0$ contains the entries of $\hat{\gamma}_{0D}$. If there is only one operator under consideration, $\hat{\gamma}_0$ is just a number γ_0, and there is no diagonalization required. In order to see that we have indeed achieved a summation of large logarithms by solving the RG equation (1.78), we insert the LO expression

$$\alpha_s(\mu) = \frac{\alpha_s(\Lambda)}{1 - \beta_0\,\frac{\alpha_s(\Lambda)}{2\pi}\,\ln\left(\frac{\Lambda}{\mu}\right)} \tag{1.82}$$

into (1.81). Another expansion is α_s then gives

$$\left(\frac{\alpha_s(\Lambda)}{\alpha_s(\mu)}\right)^{\frac{\gamma_0}{2\beta_0}} = \left(1 - \beta_0\,\frac{\alpha_s(\Lambda)}{4\pi}\,\ln\frac{\Lambda^2}{\mu^2}\right)^{\frac{\gamma_0}{2\beta_0}} = 1 - \frac{\gamma_0}{2}\,\frac{\alpha_s}{4\pi}\,\ln\frac{\Lambda^2}{\mu^2} + \mathcal{O}\left(\alpha_s^2\ln^2\frac{\Lambda^2}{\mu^2}\right)\,. \tag{1.83}$$

Finally, we want to mention that

$$\beta_0(n_f) = \frac{1}{3}\,(11N_c - 2n_f) \tag{1.84}$$

is a function of the number of active flavors n_f contributing to the running of α_s, which have not been integrated out at a given energy. This number might be different at the matching scale and the scale we want to evolve to. The number of QCD colors $N_c = 3$ is fixed. The anomalous dimension matrices might also depend on n_f. In general, the running is performed in several steps according to

$$\vec{C}(\mu_1) = \hat{U}^{(n_{f1})}(\mu_1, \mu_2)\, \hat{U}^{(n_{f2})}(\mu_2, \mu_3) \ldots \hat{U}^{(n_{fn})}(\mu_n, \Lambda)\, \vec{C}(\Lambda)\,, \tag{1.85}$$

where the matrices $\hat{U}$ are defined as in (1.81). The latter formula is extremely useful. If the anomalous dimension matrices for a given operator basis have been calculated once at a given order in α_s, they can be used for any process which shares the same operators. Of course, a similar treatment holds for corrections in powers of the fine-structure constant α. For the purpose of this thesis, all we have to do is to perform the matching of the required operators at the cut-off scale. If the matrix element is needed at a lower energy, we can use the general formula (1.85) together with anomalous dimension matrices listed in the literature.

1.7 The need for new physics

As we have now collected the main facts about renormalizability and the meaning of an EFT description, we want to come back to the statement at the end of Section 1.4, where we claimed that the SM should be regarded as an EFT only. First of all, although the theory is renormalizable in the sense that only a finite number of renormalization constants need to be fixed, there is no meaning in studying the SM at arbitrarily high energies by using perturbation theory. This is simply due to the behavior of $\alpha(\mu)$, which runs into a pole at $\mu \approx 10^{277}$ GeV. However, if this was the only short-coming, we probably would not worry.

The SM does not describe effects of gravity. Of course, those can be safely neglected within a high energy collision of elementary particles. Nevertheless, we expect modifications due to a yet unknown quantum gravity at energies of the order of the reduced Planck mass $M_{\mathrm{Pl}} \approx 10^{18}$GeV. The latter may therefore serve as a natural cut-off scale. However, there are many ideas and reasons, why we expect new physics (NP) at lower scales.

From the theoretical side, there are non-understood hierarchies in the particle spectrum and the quark-mixing matrix. The input parameters are just matched to the empirical observation, but there is no "theory of flavor".

Inspired by the unification of electromagnetic and weak interactions, one might appreciate the idea of Grand Unified Theories (GUTs) [12], where all elementary forces are combined into a single force at the scale $M_{GUT} \approx 10^{16}$GeV. The latter number is motivated by the running of the coupling constants g_s, g, and g', which cross at the so-called GUT scale. However, this crossing does not take place simultaneously for all couplings at the same energy. Therefore, new particles are needed at a lower scale in order to modify the RG running. Typical candidates are the superpartners of the SM fields in supersymmetric theories.

While grand unification is a rather aesthetic motivation to believe in new physics, there are empirical facts, which seem to make an extension of the SM unavoidable. For instance, the SM model has no candidate for dark matter. Furthermore, its CP-violating phase fails to reproduce the observed matter-antimatter asymmetry of the universe. Due to observed neutrino-oscillations, the neutrinos need to have a mass. The latter requirement can be fulfilled, by adding sterile neutrinos to the SM as a trivial extension. These may also play a role in the explanation of dark matter [13, 14]. However, if one expects the SM to be an effective theory, there is a further possibility by writing down the dimension-five operator $\bar{\nu}_L H H^\dagger \nu_L$. The latter will give rise to a Majorana mass term, that violates any additive quantum number, which is assigned to the neutrino (for instance lepton number). Therefore, there is an ongoing search for neutrino less double β-decays, which would be a direct evidence for lepton-number violation. If we have a high cut-off scale, the $1/M$ suppression of the latter operator will naturally predict light neutrino masses.

As we see, there are good reasons why the SM should be provided with a cut-off. Therefore, one should write down all higher dimensional operators which are invariant under the gauge group (1.57). However, doing so, one immediately runs into various problems. Today, the SM has been tested to high accuracy. Up to some deviations (up to 3σ), the theoretical predictions are in astonishing good agreement with the experimental estimates. As a consequence we have tough bounds for the impact of many higher dimensional operators (especially from flavor physics). This requires either a cancellation of various NP corrections (typically due to a symmetry, which has been imposed), or a large value of the cut-off scale.

Let us now assume, we have chosen such a large cut-off, for example $M = M_{\rm Pl}$. Nevertheless, we are not confident. If we calculate quantum corrections to the Higgs mass due to a particle of mass m, we will find

$$\delta m_h^2 = -A\, M^2 + B\, m^2 \ln\left(\frac{M}{m}\right) + \dots . \tag{1.86}$$

If we now want to have $v^2 \approx m_h^2 = m_{h_0}^2 + \delta m_h^2$, where m_h is the renormalized Higgs mass, we require a huge fine-tuning of the bare mass m_{h_0}. The amount of tuning is given by the ratio $m_h/M_{\rm Pl} \approx 1/10^{16}$. In other words, compared to the cut-off scale, we have to adjust the value of the bare Higgs mass in the first 16 significant numbers. This seems to be very unnatural. The problem of an unstable Higgs mass against quantum corrections goes under the name gauge-hierarchy problem, or simply hierarchy problem (HP) of the SM. It arises, as there are two widely separated scales of physical importance, the electroweak scale M_W, and the Planck scale $M_{\rm Pl}$. A possible solution is to add NP not too far away from M_W, which cancels the quadratic dependence on the cut-off scale within the Higgs boson self energy. This is exactly what happens in super-symmetric models. On the other hand, one might wonder why there is such a large discrepancy between M_W and $M_{\rm Pl}$. In other words, one might ask why gravity is so weak compared to EW gauge interactions.

In 1998, a new proposal has been made by *Nima Arkani-Hamed, Savas Dimopoulos*, and *Gia Dvali*. They claimed that the weakness of gravity may be related to the existence of additional spacial dimensions, in which only gravity is allowed to propagate [15]. These extra dimensions (EDs) have to be smaller than the distance, to which the $1/r$ potential of the gravitational force is tested. Going to smaller distances, the potential is proportional to $1/r^{n+1}$, where n is the number of EDs. Thus, the gravitational force gets diluted. At larger distances, we observe

$$V(r) \sim \frac{m_1 m_2}{{M_{\mathrm{Pl}}}_{(4+n)}^{n+2} R^n} \frac{1}{r}\,, \tag{1.87}$$

where R is the size of the EDs, and $M_{\mathrm{Pl}(4+n)}$ is the fundamental Planck scale, which is taken to be roughly of the order of the weak scale. The "observed" effective Planck mass is then of the order

$$M_{\mathrm{Pl}}^2 \sim {M_{\mathrm{Pl}}}_{(4+n)}^{n+2} R^n\,. \tag{1.88}$$

For $n = 2$, one requires $R > 100\,\mu m$. However, the current experimental bound is given by $R \leq 44\,\mu\mathrm{m}$ [16]. For $n = 3$, R has to be about a nanometer. On the other hand, for a low number n, the fundamental Planck scale must not be too small. The reason is, that compactified EDs give rise to an infinite sum of so-called Kaluza-Klein excitations of the graviton with masses $\propto k/R$ ($k \in \mathbb{N}_0$). These would give rise to missing energy at collider experiments [17]. Furthermore, there are astrophysical constraints which require $M_{\mathrm{Pl}(7)} > 4\,\mathrm{TeV}$ for instance [18].

It should be stated that the ADD model of large extra dimensions [15] is not really satisfactory as a solution to the HP, unless the number n of EDs is huge. For low n, the hierarchy between M_{Pl} and M_W has been reduced to a somewhat milder but still strong hierarchy between R and the Planck length, which scales as $1/M_{\mathrm{Pl}}$. Nevertheless, the proposal of using additional spatial dimensions in order to explain the weakness of gravity, opened a new way of thinking. In 1999, *Lisa Randall* and *Raman Sundrum* came up with the idea of warped extra dimensions [19]. Here, all fundamental energy and inverse length scales can be chosen to have the same order of magnitude, while the hierarchy problem is solved by gravitational red-shifting. Opposed to ADD, the Randall-Sundrum model features one ED in between two boundaries. This is the model we are going to study in detail.

1.8 Outline

This thesis is organized as follows. In the next section, we introduce the Randall-Sundrum (RS) model of warped extra dimensions (WEDs) and explain how it solves the HP, when the Higgs sector is localized on (or near) the IR brane. We motivate that SM gauge and matter fields should live in the whole higher dimensional space-time, which we call the bulk. As the terminology of parametrizing the ED differs in the literature, we explain how the different notations can be transformed to each other. In Section 3, we discuss the gauge sector of the minimal RS model, which consists of the SM gauge and matter fields living in the bulk, and the Higgs located on the IR boundary. The concept of Kaluza-Klein (KK) decomposition is introduced and performed in the presence of electroweak symmetry breaking (EWSB). The solution of the bulk EOMs gives us the profile functions of the

KK modes, which describe their localization within the bulk. A summation over the KK tower, needed for tree level gauge interactions, is performed. Corrections to the Fermi constant, the gauge boson masses, and the related electroweak precision observables are computed and compared to experimental bounds. In Section 4, we repeat the analysis of Section 3 for the custodial model [20], which features an extended gauge group $SU(3)_c \times SU(2)_L \times SU(2)_R \times U(1)_X$. The latter is broken down to the gauge group of the SM by an appropriate choice of boundary conditions. We show in detail, how this extension leads to a protection of the Peskin-Takeuchi T-parameter, up to small effects due to symmetry breaking on the UV boundary. In Section 5, we discuss an alternative ansatz to KK decomposition, the holographic approach [21, 22, 23]. Up to small boundary breaking effects, the holographic approach is equivalent to the KK decomposition. The leading expressions for the electroweak precision observables are verified. In Section 6, we discuss the 5D action of fermions for the case of the minimal model. The KK-decomposition is performed in the presence of EWSB and the flavor mixing among the different KK modes is discussed. Hierarchies in the fermion masses and the CKM-mixing pattern appear as a natural prediction and can be generated from anarchic $\mathcal{O}(1)$ 4D Yukawa couplings. The observed spectrum and mixing angles, as well as the CKM phase, can be obtained by an appropriate choice of bulk mass parameters, which however does not involve any fine-tuning. In Section 7, we derive expressions for neutral and charged currents. It is briefly explained how a protection for the $Z^0 b_L \bar{b}_L$ vertex can be achieved from a specific embedding of the fermion fields into the enlarged gauge group [24]. Furthermore, we study four-fermion charged current interactions and derive generalized expressions for the CKM matrix and Wilson coefficients for the effective low-energy theory. In Section 8 we derive expressions for the Higgs couplings, which require a proper regularization of the brane-localized Higgs. As an application, we study the modification of the Higgs-production cross section at the LHC.

The last part of this thesis is devoted to the phenomenology of selected four-fermion interactions, which have been (and still are) of great interest from the theoretical and experimental side. In Section 9, we study RS corrections to the forward-backward asymmetry in $t\bar{t}$-production, going beyond the LO in QCD. The calculatations are performed within a general EFT approach and can be applied to other NP models by replacing the Wilson coefficients. For the RS model we find that, because of the normalization with respect to the production cross-section, the corrections to the assymetry turn out to be marginal. The situation is different for flavor-tagged B_s^0 decays, studied in Section 10. Here, the RS model can induce sizeable modifications to the relative phase ϕ_s between the $\bar{B}_s^0$-B_s^0 mixing amplitude M_{12}^s and the related decay amplitude Γ_{12}^s. The prediction for the semileptonic CP asymmetry $A_{\rm SL}^s$ can come close to the experimental favored value. We calculate general NP corrections to the magnitude of Γ_{12}^s, where we include effects of right-handed charged current interactions for the first time. In the model at hand these turn out to give the dominant contribution. Again, a description in terms of local four-fermion operators is used. The required running of the coefficients is performed as explained above. Formulas for the various RS Wilson coefficients are collected in the appendices. Finally, we summarize our findings in Section 11.

Note that in the current version, some typos have been corrected compared to the original printout.

2 Warped extra dimensions

The RS model [19] of WEDs is formulated on a five-dimensional space-time. The ED is compactified to a circle, labeled by a dimensionless coordinate $\phi \in [-\pi, \pi]$ for instance. In addition, the authors impose a Z_2-parity, which identifies points (x, ϕ) with $(x, -\phi)$. Therefore, the set-up effectively corresponds to an interval and goes under the name S_1/Z_2-orbifold. There are two fixed points at $\phi = 0$ and $\phi = \pi$, which act as boundaries of the ED. The idea is now that the usual 4D space-time is rescaled by a so-called warp factor, such that length scales in the 4D subspace depend on the position in the ED. This is achieved by the metric

$$ds^2 = e^{-2\sigma(\phi)}\eta_{\mu\nu}\, dx^\mu dx^\nu - r^2 d\phi^2\,, \qquad \sigma(\phi) = kr|\phi|\,, \tag{2.1}$$

where we have chosen the convention $\eta_{\mu\nu} = \mathrm{diag}(1, -1, -1, -1)$. Here, k and r denote the curvature and the radius of the fifth dimension, which are of the order of the (inverse) Planck scale. The first task is to prove that the ansatz (2.1) is a solution to Einstein's equations in five dimensions. In [19] it has been shown that the solution asks for a negative (5D) cosmological constant. The 5D bulk is therefore a slice of five-dimensional Anti-de Sitter space AdS_5. Another crucial point is that the ansatz (2.1) guarantees four-dimensional Poincaré invariance.

2.1 Features of the Randall-Sundrum model

Let us now understand, how the RS model solves the HP. If $\phi = 0$, the warp factor vanishes, and the Planck mass is taken to be the fundamental scale of the theory. For $\phi = \pi$, each coordinate x is multiplied by a factor $\epsilon \equiv e^{-kr\pi}$ with $\epsilon \ll 1$. If we rescale the coordinates according to $x \to e^{\sigma(\phi)}x$, length scales are blown up when going from 0 to π. As a consequence, energy scales are warped down $\propto e^{-kr\phi}$. Thus, they are suppressed by a factor ϵ at the IR or TeV brane ($\phi = \pi$), while they keep their fundamental size at the UV or Planck brane ($\phi = 0$). The set-up is depicted in Figure 2.1.

If the Higgs is localized on the IR brane, we have $v = \epsilon\, v_0$, where v_0 is to be taken of the order of the Planck scale. In this thesis, we denote the scale of EW interactions by $M_W \approx 100\,\mathrm{GeV}$. Explicitly, one has to choose

$$L \equiv kr\pi \,\approx\, \ln\left(\frac{M_{\mathrm{Pl}}}{M_W}\right) \approx \ln\left(10^{16}\right) \approx 37\,, \tag{2.2}$$

in order to reproduce the observed hierarchy, which is thus understood by gravitational red-shifting. The original hierarchy of 10^{16} between the fundamental scales M_W and M_{Pl}

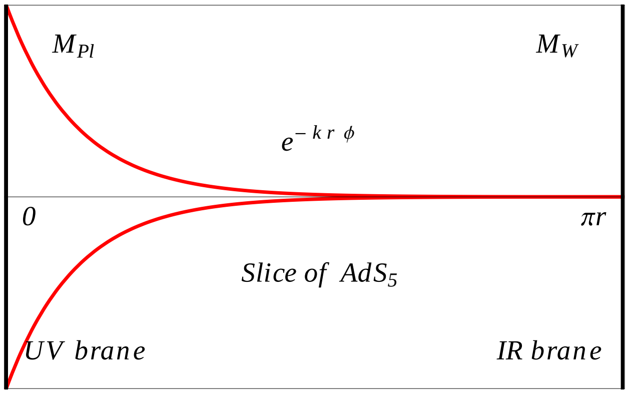

Figure 2.1: 5D bulk of the RS model. See text for details.

has been replaced by the small hierarchy $kr \approx 12$ compared to the natural value of about one. Thus we require some mechanism to stabilize the size of the ED. A solution has been proposed in [25], where a bulk scalar field with quartic interactions on the boundaries creates a potential, which is minimized by an appropriate choice of kr. One adjusts the coupling constants to obtain the desired value. The factor L will sometimes be denoted as the "volume" of the ED below.

Besides M_W and $M_{\rm Pl}$, there is a third scale of (phenomenological) importance, the so-called KK-scale

$$M_{\rm KK} = k\epsilon = \mathcal{O}(\text{few TeV})\,. \tag{2.3}$$

It is the mass scale of the low-lying KK excitations and thus sets the size of possible RS corrections to higher dimensional operators. In the original formulation, the SM particle content is confined on the IR brane. Thus, there is only new physics in the gravity sector due to the presence of KK excitations of the graviton. The KK decomposition has been worked out on [26]. It has been found that the zeroth excitation, which is identified with the ordinary graviton, couples with the usual $1/M_{\rm Pl}$ suppression to the stress-energy tensor. The KK-gravitons however couple with the reduced $1/(\epsilon M_{\rm Pl})$ suppression. Therefore, the effects of gravity can not be treated perturbatively at energies of several TeV. A UV completion would be required instead. For instance, one could ask if it is possible to realize the RS scenario as a low-energy limit of a String theory. Up to now, no UV completion for the RS model is known. That is why it should only be regarded as an EFT with the hard cut-off $\Lambda_{\rm IR} \approx M_{\rm KK}$ on the IR brane, and $\Lambda_{\rm UV} = M_{\rm Pl}$ on the IR brane. For our calculations of low-energy observables, we will use $\Lambda = M_{\rm KK}$ as matching scale.

After the proposal of WEDs, it was soon realized that the warping gives rise to dangerous four-fermion interactions [27]. For instance, if we want to study Grand unification in the context of RS models, the GUT scale will also be warped down if all particles are confined to the IR brane. As a consequence, we are immediately in conflict with the tough bounds from the yet unobserved proton-decay. If we decide to localize light fermions close to the UV brane, these dangerous couplings can be suppressed sufficiently. Fortunately, a bulk fermion scenario allows for a localization of the latter due to the free choice of their so-called bulk mass. The localization of fermions at different positions of the WED moreover gives a solution to the flavor problem. We will briefly discuss all this issues in Section 6. The main focus of this thesis is the gauge sector, which is released into the bulk in analogy to the fermions. In principle, the Higgs field can be released into the bulk too, as long as it is kept close to the IR-brane. However, the brane-Higgs scenario can be solved exactly. That is what we will discuss in the next sections.

2.2 Conventions and notations

One has to take care about the fact, that different signatures for the Minkowski metric are used in the literature. For instance, *Randall* and *Sundrum* use $\eta_{\mu\nu} = (-1, 1, 1, 1)$, which is the common choice in String theory. Therefore, the sign in front of the fifth coordinate is switched in [19] compared to (2.1).

It is often convenient to introduce a dimensionless coordinate $t = \epsilon\, e^{\sigma(\phi)}$ [28], in favor of ϕ. The former equals ϵ on the UV brane and 1 on the IR brane. When we integrate over the ED, we make use of the orbifold-symmetry and replace

$$\int_{-\pi}^{\pi} d\phi \;\to\; \frac{2\pi}{L}\int_{\epsilon}^{1}\frac{dt}{t}\,, \qquad \int_{-\pi}^{\pi} d\phi\, e^{\sigma(\phi)} \;\to\; \frac{2\pi}{L\epsilon}\int_{\epsilon}^{1} dt\,, \qquad \partial_\phi = krt\partial_t = \frac{L}{\pi}\,\partial_t\,, \qquad etc.. \tag{2.4}$$

Despite the fact that we perform our integrations over the half of the orbifold only, we will always normalize our fields to the whole circle $\phi \in [-\pi, \pi]$. The coordinate t is related to the widely used (dimensionful) coordinate z, which shows up in the conformally flat RS metric [29]

$$ds^2 = \left(\frac{R}{z}\right)^2 \left(\eta_{\mu\nu}\, dx^\mu dx^\nu - dz^2\right). \tag{2.5}$$

The relations needed for comparison are given by

$$z = \frac{t}{M_{\rm KK}}\,, \qquad R = \frac{1}{k}\,, \qquad R' = \frac{1}{M_{\rm KK}}\,, \qquad \ln\frac{R'}{R} = L\,, \tag{2.6}$$

where R and R' denote the positions of the UV and IR branes respectively. A dimensionless coordinate however is more comfortable for numerical calculations. That is why we decide to use t in favor of z.

3 Gauge fields in the minimal RS model

The KK decomposition of bulk gauge fields has been performed in [30, 31] first. Here, the authors studied the decomposition of a 5D photon. Obviously, the treatment of the gluon is identical. If the gauge fields are coupled to the Higgs however, the IR boundary conditions (BCs) are modified. There are two possible ways of performing the KK decomposition in the presence of EWSB, namely the perturbative and the exact treatment.

The first approach is mostly used in the literature. Here, the couplings of bulk fields to the Higgs sector are neglected within the KK decomposition, but introduced afterwards as a perturbation. This requires a diagonalization of an infinite-dimensional mass matrix consisting of bare KK masses and Higgs couplings between various KK modes. We have shown that an exact equation for the physical masses can be derived [32]. However, its solution requires a truncation of the KK tower. The theory is then expanded in powers of v^2/M_{KK}^2.

In this thesis, we choose the method of [33, 34], where exact solutions to the bulk EOMs are constructed, which take into account the boundary terms imposed by the couplings to the Higgs sector. We obtain exact results for the masses and profiles of the various SM particles and their KK excitations, as a diagonalization of an infinite-dimensional mass matrix is avoided. If we study the corrections to the light boson masses and couplings, it is nevertheless convenient to expand the exact results in powers of v^2/M_{KK}^2.

3.1 Action of the 5D theory

We want to find a 5D generalization for the EW gauge sector in the presence of a brane-localized Higgs. Therefore we need to decide, whether the components of the bulk gauge fields W_M^a ($a = 1,2,3$) and B_M with $M = 0,1,2,3,5$ are even or odd under the Z_2-orbifold symmetry. The latter choice determines the BCs of the bulk profiles and fixes the spectrum for given scales v, M_{KK}, and volume L. After KK decomposition, we should obtain light SM-like fields accompanied by heavy KK excitations. It turns out that only fields with even Z_2-parity possess a zero mode. As a consequence, we choose the vector components W_μ^a and B_μ to be even, and the scalar components W_5^a and B_5 to be odd. Thus, we obtain light mass eigenstates, which we denote as zero modes. The action can be split up as

$$S_{\mathrm{Gauge}} = \int d^4x\, r \int_{-\pi}^{\pi} d\phi \left(\mathcal{L}_{\mathrm{W,B}} + \mathcal{L}_{\mathrm{Higgs}} + \mathcal{L}_{\mathrm{GF}} + \mathcal{L}_{\mathrm{FP}} \right), \tag{3.1}$$

with the Lagrangian of the 5D gauge theory

$$\mathcal{L}_{\mathrm{W,B}} = \frac{\sqrt{G}}{r}\, G^{KM} G^{LN} \left(-\frac{1}{4}\, W^a_{KL} W^a_{MN} - \frac{1}{4}\, B_{KL} B_{MN} \right), \tag{3.2}$$

which satisfies 5D gauge invariance. Within the integration over the warped space-time, we have to take into account the volume element $\sqrt{G}$, where $G = r^2 e^{-8\sigma(\phi)}$ is the determinant of the warped 5D metric G_{MN}. Furthermore, the inverse metric is given by $G^{MN} = \mathrm{diag}(e^{2\sigma}, -e^{2\sigma}, -e^{2\sigma}, -e^{2\sigma}, -1/r^2)$. Note that the bulk-gauge fields of the 5D theory have mass dimension 3/2, as the Lagrangian has mass dimension five. The Higgs-sector Lagrangian

$$\mathcal{L}_{\mathrm{Higgs}} = \frac{\delta(|\phi| - \pi)}{r} \left[(D_\mu \Phi)^\dagger \, (D^\mu \Phi) - V(\Phi) \right], \qquad V(\Phi) = -\mu^2 \Phi^\dagger \Phi + \lambda \left(\Phi^\dagger \Phi \right)^2 \tag{3.3}$$

equals that one of the SM with the Higgs-doublet given in (1.45). We also perform the usual field redefinitions of the gauge fields

$$\begin{aligned} W^\pm_M &= \frac{1}{\sqrt{2}} \left(W^1_M \mp i W^2_M \right), \\ Z_M &= \frac{1}{\sqrt{g_5^2 + g_5'^2}} \left(g_5 W^3_M - g_5' B_M \right), \\ A_M &= \frac{1}{\sqrt{g_5^2 + g_5'^2}} \left(g_5' W^3_M + g_5 B_M \right), \end{aligned} \tag{3.4}$$

where g_5 and g_5' are the 5D gauge couplings of $SU(2)_L$ and $U(1)_Y$, respectively. They are related to 4D couplings via $g_5 = g\,\sqrt{2\pi r}$ (same for g') [30]. In analogy to (1.51), we define

$$M_W = \frac{v g_5}{2}, \qquad M_Z = \frac{v \sqrt{g_5^2 + g_5'^2}}{2}, \tag{3.5}$$

with mass dimension 1/2. For the photon we have $M_A = 0$.

At this stage, we want to comment on the precise meaning of the expression $\delta(|\phi| - \pi)$. In order to ensure that the Lagrangian is hermitian, we need to be able to apply integration by parts without encountering boundary terms. On the other hand, the presence of δ-functions on the IR brane gives rise to discontinuities of the fields at $|\phi| = \pi$, which ask for a proper regularization. Thus, we will always understand the brane-localized δ-functions via the limiting procedure

$$\delta(|\phi| - \pi) \equiv \lim_{\theta \to 0^+} \frac{1}{2} \Big[\delta(\phi - \pi + \theta) + \delta(\phi + \pi - \theta) \Big]. \tag{3.6}$$

In this way the discontinuities are moved into the bulk, and we can assign proper BCs to the fields, which are consistent with the hermiticity of the theory. Alternatively, one could perform all calculations with a regularized δ-function, where a finite regulator η is sent to zero at the end. Indeed, as we will see below, such a treatment becomes necessary in order to derive the BCs of the fermion fields. When we switch to t-notation, we have to replace

$$\delta(|\phi| - \pi) \to \frac{1}{2}\, kr\, \delta(t-1) \tag{3.7}$$

In the following, we use the notation $f(1^-) \equiv \lim_{\theta\to 0^+} f(1-\theta)$, whenever a function f is discontinuous at $t=1$.

As in the SM, the kinetic terms of the Higgs field give rise to mixed terms involving the gauge bosons and the would-be GBs $\varphi^\pm$ and φ_3 (with ordinary mass dimension one), which can be read off from

$$D_\mu \Phi = \frac{1}{\sqrt{2}} \begin{pmatrix} -i\sqrt{2}\left(\partial_\mu \varphi^+ + M_W\, W_\mu^+\right) \\ \partial_\mu h + i\left(\partial_\mu \varphi_3 + M_Z\, Z_\mu\right) \end{pmatrix} + \text{terms bi-linear in fields} \ . \tag{3.8}$$

In addition, the kinetic terms of the gauge fields in (3.2) contain mixed terms consisting of the gauge bosons and the scalar components $W_5^\pm$, Z_5, and A_5. All of these mixed terms can be removed with a suitable choice of the gauge-fixing Lagrangian. We find

$$\begin{aligned} \mathcal{L}_{\rm GF} = &-\frac{1}{2\xi}\left(\partial^\mu A_\mu - \frac{\xi}{2}\left[M_{\rm KK}^2\,\frac{2\pi}{L}\,t\partial_t\,t^{-2}A_5\right]\right)^2 \\ &- \frac{1}{2\xi}\left(\partial^\mu Z_\mu - \frac{\xi}{2}\left[\delta(t-1)\,kM_Z\,\varphi_3 + M_{\rm KK}^2\,\frac{2\pi}{L}\,t\partial_t\,t^{-2}Z_5\right]\right)^2 \\ &- \frac{1}{\xi}\left(\partial^\mu W_\mu^+ - \frac{\xi}{2}\left[\delta(t-1)\,kM_W\,\varphi^+ + M_{\rm KK}^2\,\frac{2\pi}{L}\,t\partial_t\,t^{-2}W_5^+\right]\right) \\ &\times\left(\partial^\mu W_\mu^- - \frac{\xi}{2}\left[\delta(t-1)\,kM_W\,\varphi^- + M_{\rm KK}^2\,\frac{2\pi}{L}\,t\partial_t\,t^{-2}W_5^-\right]\right) \end{aligned} \tag{3.9}$$

as a straightforward generalization of (1.71), where we choose one common gauge-fixing parameter ξ for simplicity. The reader might worry about squaring the δ-functions in the above expression. We will see below that the contributions of the latter are canceled by the derivatives of the scalar components of the gauge fields $W_5^\pm$ and Z_5, when we apply the bulk EOMs. Therefore, we do not need to introduce a separate gauge-fixing Lagrangian on the IR boundary, contrary to the treatment in [35].

In order to derive the spectrum of the effective four-dimensional theory, we write down all quadratic terms of the action (3.1), omitting the Faddeev-Popov Lagrangian,

$$
\begin{aligned}
S_{\text{Gauge},2} = & \int d^4x\, r\, \frac{2\pi}{L} \int_\epsilon^1 \frac{dt}{t} \qquad (3.10)\\
& \Bigg\{ -\frac{1}{4} F_{\mu\nu}F^{\mu\nu} - \frac{1}{2\xi}\left(\partial^\mu A_\mu\right)^2 + \frac{1}{2} M_{\text{KK}}^2\, t^{-2} \left(\frac{\pi^2}{L^2}\, \partial_\mu A_5 \partial^\mu A_5 + (t\partial_t A_\mu)(t\partial_t A^\mu) \right) \\
& - \frac{1}{4} Z_{\mu\nu}Z^{\mu\nu} - \frac{1}{2\xi}\left(\partial^\mu Z_\mu\right)^2 + \frac{1}{2} M_{\text{KK}}^2\, t^{-2} \left(\frac{\pi^2}{L^2}\, \partial_\mu Z_5 \partial^\mu Z_5 + (t\partial_t Z_\mu)(t\partial_t Z^\mu) \right) \\
& - \frac{1}{2} W^+_{\mu\nu}W^{-\mu\nu} - \frac{1}{\xi}\, \partial^\mu W^+_\mu\, \partial^\nu W^-_\nu + M_{\text{KK}}^2\, t^{-2} \left(\frac{\pi^2}{L^2}\, \partial_\mu W^+_5 \partial^\mu W^-_5 + (t\partial_t W^+_\mu)(t\partial_t W^{-\mu}) \right) \\
& + \frac{k\,\delta(t-1)}{2} \left(\frac{1}{2}\partial_\mu h \partial^\mu h - \lambda v^2 h^2 + \partial_\mu \varphi^+ \partial^\mu \varphi^- + \frac{1}{2}\partial_\mu \varphi_3 \partial^\mu \varphi_3 + \frac{M_Z^2}{2}\, Z_\mu Z^\mu + M_W^2\, W^+_\mu W^{-\mu} \right) \\
& - \frac{\xi}{8} \left(M_{\text{KK}}^2\, \frac{2\pi}{L}\, t\partial_t\, t^{-2} A_5 \right)^2 - \frac{\xi}{8} \left(\delta(t-1)\, k M_Z\, \varphi_3 + M_{\text{KK}}^2\, \frac{2\pi}{L}\, t\partial_t\, t^{-2} Z_5 \right)^2 \\
& - \frac{\xi}{4} \left(\delta(t-1)\, k M_W\, \varphi^+ + M_{\text{KK}}^2\, \frac{2\pi}{L}\, t\partial_t\, t^{-2} W^+_5 \right) \left(\delta(t-1)\, k M_W\, \varphi^- + M_{\text{KK}}^2\, \frac{2\pi}{L}\, t\partial_t\, t^{-2} W^-_5 \right) \Bigg\} .
\end{aligned}
$$

The next step consists of decomposing the vector and scalar components of the gauge fields, what we will do now.

3.2 Kaluza-Klein decomposition

The KK decompositions of the various 5D fields can be written in the form [34, 36]

$$
\begin{aligned}
A_\mu(x,t) &= \frac{1}{\sqrt{r}} \sum_n A_\mu^{(n)}(x)\, \chi_n^A(t)\,, & A_5(x,t) &= \frac{1}{\sqrt{r}} \sum_n a_n^A\, \varphi_A^{(n)}(x)\, \frac{L}{\pi}\, t\partial_t\, \chi_n^A(t)\,, \\
Z_\mu(x,t) &= \frac{1}{\sqrt{r}} \sum_n Z_\mu^{(n)}(x)\, \chi_n^Z(t)\,, & Z_5(x,t) &= \frac{1}{\sqrt{r}} \sum_n a_n^Z\, \varphi_Z^{(n)}(x)\, \frac{L}{\pi}\, t\partial_t\, \chi_n^Z(t)\,, \\
W_\mu^\pm(x,t) &= \frac{1}{\sqrt{r}} \sum_n W_\mu^{\pm(n)}(x)\, \chi_n^W(t)\,, & W_5^\pm(x,t) &= \frac{1}{\sqrt{r}} \sum_n a_n^W\, \varphi_W^{\pm(n)}(x)\, \frac{L}{\pi}\, t\partial_t\, \chi_n^W(t)\,,
\end{aligned}
\tag{3.11}
$$

where $A_\mu^{(n)}$ *etc.* are the 4D mass eigenstates. The related profiles χ_n^a with $a = A, Z, W$[1], form complete sets of even functions on the orbifold and obey the orthonormality condition

$$
\frac{2\pi}{L} \int_\epsilon^1 \frac{dt}{t}\, \chi_m^a(t)\, \chi_n^a(t) = \delta_{mn}\,. \tag{3.12}
$$

As the scalar components of the gauge fields go along with a derivative of even profiles, they are odd under Z_2-parity. The longitudinal DOFs are given by the corresponding 4D

[1] Do not confuse with the superscript $a = 1, 2, 3$ for weak interaction eigenstates.

scalar fields $\varphi_a^{(n)}$. The would-be GBs of the Higgs sector can be expanded in the same basis of mass eigenstates

$$\varphi^{\pm}(x) = \sum_n b_n^W \, \varphi_W^{\pm(n)}(x) \, , \qquad \varphi_3(x) = \sum_n b_n^Z \, \varphi_Z^{(n)}(x) \, . \tag{3.13}$$

Inserting these decompositions into the action, and matching the result on the canonical form of a 4D Lagrangian, one finds that the profiles χ_n^a have to satisfy the EOMs [30, 31]

$$-M_{\rm KK}^2 \, t\partial_t \, t^{-1}\partial_t \, \chi_n^a(t) = (m_n^a)^2 \, \chi_n^a(t) - \frac{1}{2} \, \delta(t-1) \, kM_a^2 \, \chi_n^a(t) \, , \tag{3.14}$$

where we have introduced the masses m_n^a of the 4D vector fields. The masses of the scalar fields $\varphi_a^{(n)}$ are related to those by gauge invariance. In order to derive the explicit form of the profiles and eigenvalues m_n^a from the second order EOM, we need to fix the boundary conditions. The UV BCs immediately follow from the Z_2-parity assignment, which states that derivative of even fields should vanish at the orbifold-fix points. If there is no EWSB as in the case of the photon, the same statement applies to the IR boundary. If we want to include EW symmetry-breaking effects into the derivation of the profiles, we have to integrate the EOMs over an infinitesimal interval around the IR boundary [33, 34]. Thus, we obtain

$$\begin{aligned} \partial_t \, \chi_n^a(t)\Big|_{t=\epsilon} &\equiv \partial_t \, \chi_n^a(\epsilon) = 0 \, , && \text{(UV brane)} \\ \partial_t \, \chi_n^a(t)\Big|_{t=1^-} &\equiv \partial_t \, \chi_n^a(1^-) = -\frac{kM_a^2}{2M_{\rm KK}^2} \, \chi_n^a(t) \, . && \text{(IR brane)} \end{aligned} \tag{3.15}$$

Having all this at hand, one finds that the action takes the desired form

$$\begin{aligned} S_{\rm Gauge,2} = \sum_n \int d^4x \bigg\{ & -\frac{1}{4} \, F_{\mu\nu}^{(n)} F^{\mu\nu(n)} - \frac{1}{2\xi} \left(\partial^\mu A_\mu^{(n)}\right)^2 + \frac{(m_n^A)^2}{2} \, A_\mu^{(n)} A^{\mu(n)} \\ & - \frac{1}{4} \, Z_{\mu\nu}^{(n)} Z^{\mu\nu(n)} - \frac{1}{2\xi} \left(\partial^\mu Z_\mu^{(n)}\right)^2 + \frac{(m_n^Z)^2}{2} \, Z_\mu^{(n)} Z^{\mu(n)} \\ & - \frac{1}{2} \, W_{\mu\nu}^{+(n)} W^{-\mu\nu(n)} - \frac{1}{\xi} \, \partial^\mu W_\mu^{+(n)} \, \partial^\nu W_\nu^{-(n)} + (m_n^W)^2 \, W_\mu^{+(n)} W^{-\mu(n)} \\ & + \frac{1}{2} \partial_\mu \varphi_A^{(n)} \partial^\mu \varphi_A^{(n)} - \frac{\xi (m_n^A)^2}{2} \, \varphi_A^{(n)} \varphi_A^{(n)} + \frac{1}{2} \partial_\mu \varphi_Z^{(n)} \partial^\mu \varphi_Z^{(n)} - \frac{\xi (m_n^Z)^2}{2} \, \varphi_Z^{(n)} \varphi_Z^{(n)} \\ & + \partial_\mu \varphi_W^{+(n)} \partial^\mu \varphi_W^{-(n)} - \xi (m_n^W)^2 \, \varphi_W^{+(n)} \varphi_W^{-(n)} \bigg\} + \int d^4x \left(\frac{1}{2} \partial_\mu h \partial^\mu h - \lambda v^2 h^2 \right) , \end{aligned} \tag{3.16}$$

if and only if

$$a_n^a = -\frac{1}{m_n^a} \, , \qquad b_n^a = \frac{M_a}{\sqrt{r}} \, \frac{\chi_n^a(\pi^-)}{m_n^a} \, . \tag{3.17}$$

Thus, we have constructed an effective 4D Lagrangian, where all SM gauge fields are accompanied by a tower of massive KK gauge bosons. The 4D gauge-fixing Lagrangian derived from (3.9) takes the simple form

$$r \int_{-\pi}^{\pi} d\phi \, \mathcal{L}_{\mathrm{GF}} = \sum_n \mathcal{L}_{\mathrm{GF}}^{(n)} , \tag{3.18}$$

with

$$\begin{aligned} \mathcal{L}_{\mathrm{GF}}^{(n)} = & -\frac{1}{2\xi} \left(\partial^\mu A_\mu^{(n)} - \xi m_n^A \varphi_A^{(n)} \right)^2 - \frac{1}{2\xi} \left(\partial^\mu Z_\mu^{(n)} - \xi m_n^Z \varphi_Z^{(n)} \right)^2 \\ & - \frac{1}{\xi} \left(\partial^\mu W_\mu^{+(n)} - \xi m_n^W \varphi_W^{+(n)} \right) \left(\partial^\nu W_\nu^{-(n)} - \xi m_n^W \varphi_W^{-(n)} \right) . \end{aligned} \tag{3.19}$$

For each KK mode these expressions are identical to those of the SM. We see that the δ-terms have been canceled by the use of (3.11) and (3.14). It is interesting to realize that the KK excitations of the scalar components of the 5D gauge fields act as would-be GBs for the related vector excitations. Therefore, the related profiles have to be odd under Z_2-parity, such that the zero modes of the vector fields do not obtain a longitudinal DOF in the absence of EWSB.

3.3 Bulk profiles

It is now straightforward to derive the explicit form of the profiles χ_n^a from the bulk EOMs (3.14). Replacing the 5D mass parameters M_a by the 4D counter parts m_a (1.51), and defining the dimensionless parameters

$$x_n^a = \frac{m_n^a}{M_{\mathrm{KK}}} , \qquad x_a = \frac{m_a}{M_{\mathrm{KK}}} , \tag{3.20}$$

the EOMs are given by

$$\left(t\partial_t \, t^{-1} \partial_t \;\; + (x_n^a)^2 \right) \chi_n^a(t) = \delta(t-1) \, L \, x_a^2 \, \chi_n^a(t) . \tag{3.21}$$

The solution is formally the same for all gauge fields, as the boundary terms only enter the BCs. If we choose the ansatz

$$\chi_n^a(t) \propto t \, c_n^+(t) , \tag{3.22}$$

we can recast (3.21) into a first order Bessel equation [30, 31] with the general solution

$$c_n^+(t) = A \, J_1(x_n^a t) + B \, Y_1(x_n^a t) . \tag{3.23}$$

We see that the nature "a" of the gauge boson only affects the eigenvalues x_n^a within the argument of the Bessel functions. The coefficients A and B are determined from the UV BC given in (3.15) and the orthonormality relation (3.12). We find

$$\chi_n^a(t) = N_n \sqrt{\frac{L}{\pi}} \, t \, c_n^+(t) , \tag{3.24}$$

with the normalization factor

$$N_n^{-2} = \left[c_n^+(1)\right]^2 + \left[c_n^-(1)\right]^2 - \frac{2}{x_n}\, c_n^+(1)\, c_n^-(1) - \epsilon^2 \left[c_n^+(\epsilon)\right]^2 , \tag{3.25}$$

and the explicit form of the profiles and their derivatives

$$\begin{aligned} c_n^+(t) &= Y_0(x_n^a\epsilon)\, J_1(x_n^a t) - J_0(x_n^a\epsilon)\, Y_1(x_n^a t)\,, \\ c_n^-(t) &= \frac{1}{x_n^a t}\,\frac{d}{dt}\left[t\, c_n^+(t)\right] = Y_0(x_n^a\epsilon)\, J_0(x_n^a t) - J_0(x_n^a\epsilon)\, Y_0(x_n^a t)\,. \end{aligned} \tag{3.26}$$

As $c_n^-(\epsilon) = 0$, the solution (3.24) satisfies the UV BC $\partial_t \chi_n(\epsilon) = 0$. The eigenvalues x_n^a are determined from the IR BC (3.15), which requires

$$x_n^a\, c_n^-(1) = -x_a^2\, L\, c_n^+(1)\,. \tag{3.27}$$

For the case of the photon (or gluon), the right-hand side is zero and there is a massless zero-mode solution with a flat profile $\chi_{\gamma(g)}(t) = 1/\sqrt{2\pi}$.

In the presence of EWSB, we find $m_0 \neq 0$. The results for the SM-like gauge bosons can be simplified by expanding (3.27) in powers of $x_0^{W,Z} \ll 1$. Doing so, we recover the tree-level SM relations (1.51), augmented by corrections of the order v^2/M_{KK}^2. Therefore, we re-define the explicit expressions (1.51) for m_W and m_Z according to

$$\begin{aligned} m_W^2 &\equiv \frac{g^2 v^2}{4}\left[1 - \frac{g^2 v^2}{8M_{\text{KK}}^2}\left(L - 1 + \frac{1-\epsilon^2}{2L}\right) + \mathcal{O}\left(\frac{v^4}{M_{\text{KK}}^4}\right)\right], \\ m_Z^2 &\equiv \frac{(g^2+g'^2)\, v^2}{4}\left[1 - \frac{(g^2+g'^2)\, v^2}{8M_{\text{KK}}^2}\left(L - 1 + \frac{1-\epsilon^2}{2L}\right) + \mathcal{O}\left(\frac{v^4}{M_{\text{KK}}^4}\right)\right]. \end{aligned} \tag{3.28}$$

It will further be useful to have an approximate expression for the ground-state profiles

$$\chi_{W,Z}(t) = \frac{1}{\sqrt{2\pi}}\left[1 + \frac{m_{W,Z}^2}{4M_{\text{KK}}^2}\left(1 - \frac{1-\epsilon^2}{L} + t^2\,(1 - 2L - 2\ln t)\right) + \mathcal{O}\left(\frac{m_{W,Z}^4}{M_{\text{KK}}^4}\right)\right], \tag{3.29}$$

which are obtained from expansion of the exact solution (3.24) in $x_n^a \ll 1$ and the use of (3.28). Contrary to the zero-mode profile of the photon (and the gluon), the latter profiles depend on the coordinate t of the ED. As $L \approx 37$, we can approximate the above result by $\chi_{W,Z}(t) \approx \chi_\gamma[1 + x_{W,Z}^2(1 - 2L\,t^2)/4]$. We see that the profiles $\chi_{W,Z}(t)$ are more or less flat in the UV regime, but receive a dip near the IR brane [33]. From the perturbative point of view, this behavior can be understood from an admixture of the KK profiles, when the diagonalization of the mass matrix is performed. As we will see later, the dependence on t will give rise to non-universal gauge couplings with respect to different flavors. As a consequence, the Z^0 induces FCNC interactions at tree-level.

For the KK gauge bosons, we are not able to perform an expansion of the Bessel functions. The shape of their profiles is controlled by the prefactor $\sqrt{L}\, t$ in (3.24), which gives rise to an IR localization of the KK modes.

3.4 Summing over Kaluza-Klein modes

If we compute the tree-level exchange of a SM gauge boson accompanied by its KK tower in a generic Feynman diagram, we have to sum over the corresponding propagators in combination with the boson profiles, which show up in the vertex functions. In the low-energy limit, *i.e.*, for small momentum transfer q^2, we can expand

$$\sum_n \frac{\chi_n(t)\,\chi_n(t')}{m_n^2 - q^2} = \sum_{N=1}^{\infty} \left(q^2\right)^{N-1} \sum_n \frac{\chi_n(t)\,\chi_n(t')}{\left(m_n^2\right)^N} . \tag{3.30}$$

For simplicity, we have dropped the superscript a, which labels the type of the gauge field. The KK index n runs from 0 to ∞ in general. If the zero mode is massless, it has to be treated separately. For most applications, it is sufficient to consider just the first term ($N = 1$) in the above expansion. It can be evaluated in closed form by generalizing a method developed in [37]. Here, one makes use of the fact that the profiles $\chi_n(t)$ form a complete set of even functions on the orbifold. The required completeness relation can be deduced from (3.12), and is given by

$$\frac{2\pi}{L} \sum_n \frac{1}{t}\,\chi_n(t)\,\chi_n(t') = \delta(t - t'). \tag{3.31}$$

We first integrate the EOM (3.14) twice, accounting for the UV BC. This yields

$$\chi_n(t) - \chi_n(\epsilon) = -x_n^2 \int_\epsilon^t dt'\,t' \int_\epsilon^{t'} dt''\,\frac{1}{t''}\,\chi_n(t'') . \tag{3.32}$$

Using the latter result along with the completeness relation (3.31), the sums over profiles in (3.30) can be evaluated iteratively [34]. We will restrict ourselves to the first approximation with $N = 1$, and normalize the sum with respect to M_{KK}^{-2}. For the case of massive gauge bosons with $m_0 > 0$, we obtain

$$\sum_n \frac{\chi_n(t)\,\chi_n(t')}{x_n^2} = \sum_n \frac{\chi_n^2(\epsilon)}{x_n^2} - \frac{L}{4\pi}\left(t_>^2 - \epsilon^2\right) , \tag{3.33}$$

where we have introduced $t_> \equiv \max(t, t')$. The remaining sum over profiles $\chi_n^2(\epsilon)$ on the UV brane can be performed by multiplicating (3.33) with $\chi_0(t)$, and performing an integration over the entire orbifold. If we now use the orthonormality condition (3.12) on the one hand, and the explicit form of the zero-mode profiles (3.29) on the other hand, we find

$$\sum_n \frac{\chi_n^2(\epsilon)}{x_n^2} = \frac{1}{2\pi x_0^2} + \frac{1}{4\pi}\left[1 - \frac{1}{2L} - \epsilon^2\left(L - \frac{1}{2L}\right)\right] + \mathcal{O}\left(x_0^2\right) . \tag{3.34}$$

The terms $\propto \epsilon^2$ can be ignored for all practical purposes. Inserting the latter expression into (3.33), and substituting $t_>^2 = t^2 + t'^2 - t_<^2$ with $t_< \equiv \min(t, t')$, we obtain the final result

$$\sum_n \frac{\chi_n(t)\,\chi_n(t')}{x_n^2} = \frac{1}{2\pi x_0^2} + \frac{1}{4\pi}\left[L\,t_<^2 - L\left(t^2 + t'^2\right) + 1 - \frac{1}{2L} + \mathcal{O}\left(x_0^2\right)\right] . \tag{3.35}$$

If there exists a massless zero mode, one has to remove its contribution from the sum over states. This can be done by subtracting the square of the zero-mode profiles from both sides of the completeness relation (3.31), where the explicit expression for the flat zero-mode profile is used on the right-hand side. In this way we find

$$\sum_n{}' \frac{\chi_n(t)\,\chi_n(t')}{x_n^2} = \frac{1}{4\pi}\left[L\,t_<^2 - t^2\left(\frac{1}{2}-\ln t\right) - t'^2\left(\frac{1}{2}-\ln t'\right) + \frac{1}{2L}\right], \tag{3.36}$$

where the prime on the sum indicates that n runs from 1 to ∞.

In order to understand the origin of the corrections in the above relations, we explicitly evaluate the zero-mode contribution in (3.35) with the help of (3.28) and (3.29). We find

$$\frac{\chi_0(t)\,\chi_0(t')}{x_0^2} = \frac{1}{2\pi x_0^2} - \frac{L}{4\pi}\left[t^2+t'^2\right] + \frac{1}{4\pi}\left[1-\frac{1}{L}+t^2\left(\frac{1}{2}-\ln t\right)+t'^2\left(\frac{1}{2}-\ln t'\right)\right]. \tag{3.37}$$

By comparison of (3.37) and (3.35), we see that beside the non-factorizable contribution proportional to $t_<^2$, the L-enhanced terms in the latter formula arise from zero-mode exchange. The terms proportional to t^2 and t'^2 in (3.36) on the other hand do not receive an enhancement. This has important consequences for the phenomenology of flavor-violating processes [38]. It implies that the RS corrections to $\Delta F = 2$ processes are dominated by tree-level KK gluon exchange. Concerning $\Delta F = 1$ processes, the main modifications compared to the SM are given by FCNC couplings of the Z^0 boson to fermions. An extended analysis of the summation over the KK towers is provided in [34] for $N = 2$.

Another important consequence is a modification of the theoretical expression for the Fermi constant G_F. The latter is determined from muon decay $\mu \to \bar{\nu}_e \nu_\mu e$, which is mediated by a charged-current interaction. Staying at tree level, the W^- exchange of the SM has to be replaced by the exchange of the whole K tower in the RS model. The relevant sum over these intermediate states is given in (3.35). The terms proportional to t^2 or t'^2 in this relation give rise to non-universal corrections, if the fermions live in the bulk. Therefore, we have to perform the KK decomposition of the fermion sector and determine the relevant profiles. It will turn out that fermions with light zero modes should be localized near the UV brane. As a consequence, the upper terms are exponential suppressed for the light leptons involved in muon decay and can be neglected to excellent approximation. The correction to G_F is thus given by the constant terms in (3.35), for which the fermion profiles are combined to a factor one due their orthonormalitiy condition. We obtain

$$\frac{G_F}{\sqrt{2}} = \frac{g^2}{8m_W^2}\left[1+\frac{m_W^2}{2M_{\mathrm{KK}}^2}\left(1-\frac{1}{2L}\right)+\mathcal{O}\left(\frac{m_W^4}{M_{\mathrm{KK}}^4}\right)\right]. \tag{3.38}$$

The correction term receives a contribution $(1-1/L)$ from the zero mode of the W^- boson (3.37), and a contribution $1/(2L)$ from the KK tower (3.36). If the RS model is realized in nature, the measurement of the Fermi constant always involves the exchange of the KK tower. Therefore, we have to account for this universal correction factor, when we pull out a factor G_F of the effective Hamiltonian for charged currents.

Before we proceed, we want to mention that there is another possibility for the calculation of two-point functions within a five-dimensional theory. For internal states, there is no need to perform a KK decomposition. Instead, one could solve the generalized Greens functions in five dimensions in the presence of the brane-localized Higgs sector. This gives rise to 5D propagators [36], which are equivalent to the infinite sum over KK modes. We will however not entertain this possibility here.

3.5 Electroweak precision observables

A first phenomenological test of the RS model can be obtained from the gauge sector only, if we study the impact on electroweak precision observables. In the SM, these are defined as universal corrections stemming from vacuum polarization diagrams, known as oblique corrections. They are collected in correlator functions, which can be expanded for small momenta (squared) according to $\Pi(p^2) \approx \Pi(0) + p^2\Pi'(0)$. Within the study of NP, one defines the parameters S, T, and U as shifts to the corresponding SM values, which are therefore set to zero. The definition of the so-called Peskin-Takeuchi parameters is given in [6, 7]

$$\begin{aligned} S &= \frac{16\pi s_w^2 c_w^2}{e^2}\left[\Pi'_{ZZ}(0) + \frac{s_w^2 - c_w^2}{s_w c_w}\,\Pi'_{ZA}(0) - \Pi'_{AA}(0)\right], \\ T &= \frac{4\pi}{e^2 c_w^2 m_Z^2}\Big[\Pi_{WW}(0) - c_w^2\,\Pi_{ZZ}(0) - 2\,s_w c_w\,\Pi_{ZA}(0) - s_w^2\,\Pi_{AA}(0)\Big], \\ U &= \frac{16\pi s_w^2}{e^2}\Big[\Pi'_{WW}(0) - c_w^2\,\Pi'_{ZZ}(0) - 2\,s_w c_w\,\Pi'_{ZA}(0) - s_w^2\,\Pi'_{AA}(0)\Big]. \end{aligned} \tag{3.39}$$

Here, s_w (c_w) denotes the sine (cosine) of the weak-mixing angle. Of particular interest is the T-parameter, which is sensitive to the difference between the corrections to the W and Z^0 boson vacuum-polarization functions, and thus measures isospin violation. For the RS scenario (and any other NP model which involves heavy gauge bosons that mix with those of the SM), the oblique parameters can be computed in an effective Lagrangian approach [29]. The quantities $\Pi'_{aa}(0)$ collect modifications due to universal vertex corrections, which for the case of the $W^\pm$ and the Z^0 bosons are given by $1 + m_{W,Z}^2/(4M_{\mathrm{KK}}^2)(1 - 1/L)$. The idea is to rescale the fields with the inverse factor, such that the interaction vertices take their canocical form. Thereafter, one has to match the resulting expression to the effective Lagrangian

$$\begin{aligned} \mathcal{L}_{\text{eff}} = &-\frac{1}{2}\big(1 - \Pi'_{WW}(0)\big)W^+_{\mu\nu}W^{-\mu\nu} - \frac{1}{4}\big(1 - \Pi'_{ZZ}(0)\big)Z_{\mu\nu}Z^{\mu\nu} - \frac{1}{4}\big(1 - \Pi'_{AA}(0)\big)F_{\mu\nu}F^{\mu\nu} \\ &+ \left(\frac{g^2 v^2}{4} + \Pi_{WW}(0)\right) W^+_{\mu\nu}W^{-\mu\nu} + \left(\frac{(g^2 + g'^2)v^2}{4} + \Pi_{ZZ}(0)\right) Z_{\mu\nu}Z^{\mu\nu}. \end{aligned} \tag{3.40}$$

Note that the photon (and the gluon) do not receive a vertex correction. Therefore the correlator $\Pi'_{AA}(0)$ vanishes. The quantities $\Pi_{aa}(0)$ additionally pick up corrections of the

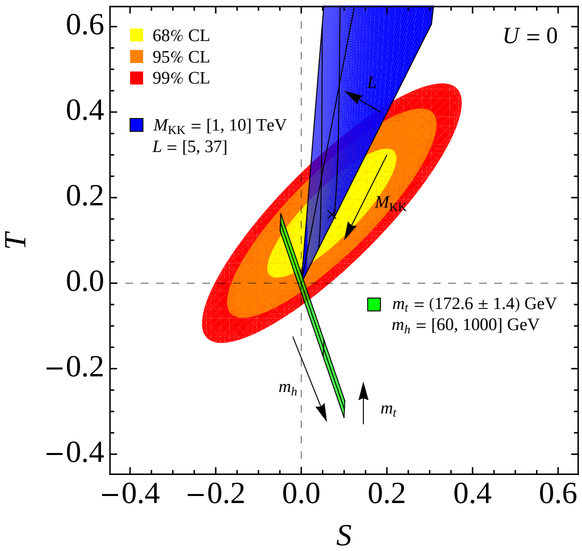

Figure 3.1: Regions of 68%, 95%, and 99% probability in the S-T plane for the minimal RS model. The green (medium gray) shaded stripes in both panels indicate the SM predictions for $m_t = (172.6 \pm 1.4)\,\text{GeV}$ and $m_h \in [60, 1000]\,\text{GeV}$. The blue (dark gray) shaded area represents the RS corrections for $M_{\rm KK} \in [1, 10]\,\text{TeV}$ and $L \in [5, 37]$. Figure taken from [34]. See text for details.

zero-mode masses. Gauge invariance guarantees that $\Pi_{AA}(0) = 0$ holds to all orders in perturbation theory, and one further has $\Pi_{ZA}(0) = \Pi'_{ZA}(0) = 0$ as long as one works at tree-level. For the minimal RS model we find

$$\begin{aligned}
\Pi_{WW}(0) &= -\frac{g^4 v^4}{32 M_{\rm KK}^2}\left(L - \frac{1}{2L}\right), \\
\Pi'_{WW}(0) &= \frac{g^2 v^2}{8 M_{\rm KK}^2}\left(1 - \frac{1}{L}\right), \\
\Pi_{ZZ}(0) &= -\frac{\left(g^2 + g'^2\right)^2 v^4}{32 M_{\rm KK}^2}\left(L - \frac{1}{2L}\right), \\
\Pi'_{ZZ}(0) &= \frac{\left(g^2 + g'^2\right) v^2}{8 M_{\rm KK}^2}\left(1 - \frac{1}{L}\right).
\end{aligned} \tag{3.41}$$

Inserting these expressions into (3.39) yields [34, 39, 40]

$$S = \frac{2\pi v^2}{M_{\rm KK}^2}\left(1 - \frac{1}{L}\right), \qquad T = \frac{\pi v^2}{2\, c_w^2 M_{\rm KK}^2}\left(L - \frac{1}{2L}\right), \qquad U = 0\,. \tag{3.42}$$

As we see, a potential problem arises from the T-parameter, which goes along with a factor L. In Figure 3.1, we show the experimental 68% , 95%, and 99% confidence levels (CLs) in the S-T plane, corrected to the present world average of the top-quark mass [41].

Details about the generation of the confidence ellipses are given in [34], from where the plots are taken from. The light-shaded stripe indicates the SM predictions for different values of m_h and m_t, where $m_h = 150\,\text{GeV}$ corresponds to $S = T = 0$. The dark-shaded area represents the RS corrections for different values of M_{KK} and L. For a SM-like Higgs mass $m_h < 150\,\text{GeV}$, we find that

$$M_{\text{KK}} > 4.0\,\text{TeV} \quad (99\%\ \text{CL})\,. \tag{3.43}$$

As the first eigenvalue of the bulk EOM (3.14) is about $x_1 = 2.45$ in warped extra dimensions, the bounds from the T-parameter will force the first gauge-boson KK excitation to have a mass of at least 10 TeV. The energy cut-off on the IR brane is about the same size. This will re-introduce a little HP due to (1.86), as we have to tune 150 GeV against the latter number. If, on the other hand, the Higgs mass is raised compared to the SM, the problem is cured by two different effects. First, a larger Higgs mass requires less tuning against the cut-off. Secondly, the SM reference values for S and T will be corrected at the loop level [42, 43, 44, 45, 46]. In particular the T-parameter receives a negative correction, which partially cancels the positive RS correction. Keeping only the leading logarithmic loop effects in the SM, the shifts in S and T due to a Higgs-boson mass different from the reference value $m_h^{\text{ref}} = 150\,\text{GeV}$ read [7]

$$\Delta S = \frac{1}{6\pi}\,\ln\frac{m_h}{m_h^{\text{ref}}}\,, \qquad \Delta T = -\frac{3}{8\pi c_w^2}\,\ln\frac{m_h}{m_h^{\text{ref}}}\,, \tag{3.44}$$

while U remains unchanged. For example, taking $m_h = 1\,\text{TeV}$,[2] the lower bound (3.43) is relaxed to

$$M_{\text{KK}} > 2.6\,\text{TeV} \quad (99\%\ \text{CL})\,. \tag{3.45}$$

This feature is illustrated by the upper sets of bands in the panels of Figure 3.2, which show the regions of 68%, 95%, and 99% probability in the m_h-M_{KK} and m_h-L planes for $L = \ln(10^{16})$ (left plot) and $M_{\text{KK}} = 3\,\text{TeV}$ (right plot).

An additional possibility is to give up the solution to the full HP by working in a volume-truncated RS background [48]. The so-called little RS model with $L = \ln(10^3)$ has a lower bound of

$$M_{\text{KK}} > 1.5\,\text{TeV} \quad (99\%\ \text{CL})\,. \tag{3.46}$$

Since the lightest mass eigenvalue is about $x_1 = 2.65$, resulting in KK mass of around 4 TeV. As in the case of the original RS scenario, the bound (3.46) relaxes further for a larger Higgs-boson mass. This feature is illustrated by the lower sets of bands in the panels of Figure 3.2, where we take $L = \ln(10^3)$ (left plot) and $M_{\text{KK}} = 1.5\,\text{TeV}$ (right plot). For example, using $m_h = 500\,\text{GeV}$ relaxes the limit (3.46) to 1.1 TeV. In this thesis however, we are not going to consider the little RS scenario.

Another way to satisfy the bounds from EW precision data, keeping the masses of the first KK gauge-bosons of the order of 5 TeV, is to introduce large brane-localized kinetic

[2] Note that the unitarity bound for W-boson scattering can be satisfied for values of $m_h > 1\,\text{TeV}$ in the RS model [47].

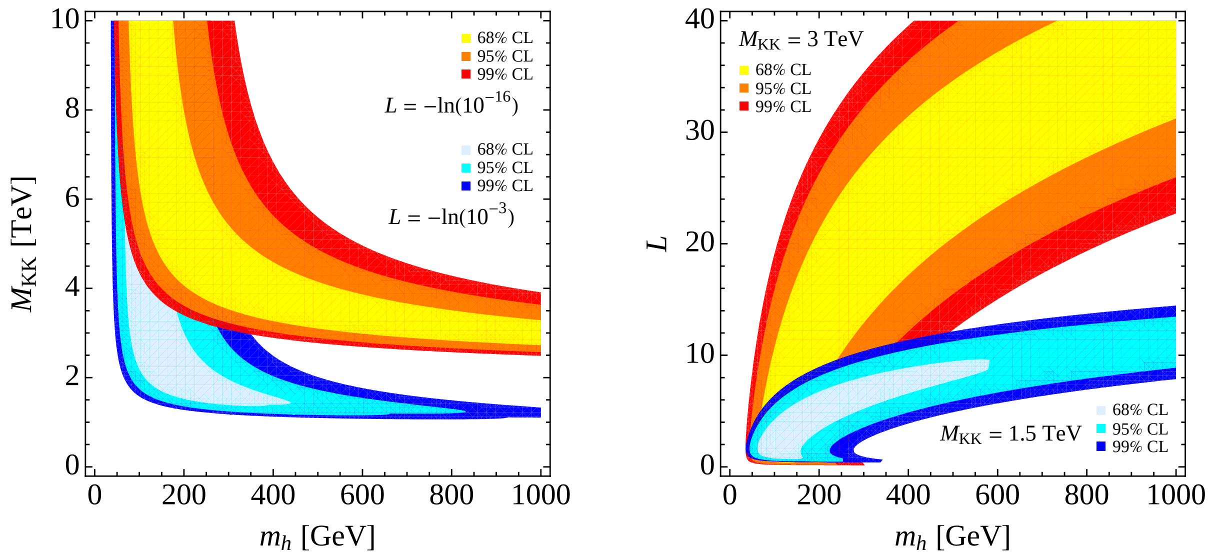

Figure 3.2: Regions of 68%, 95%, and 99% probability in the m_h–$M_{\rm KK}$ (left panel) and m_h–L (right panel) plane in the RS scenario without custodial protection. The upper (lower) area in the left and right panel corresponds to $L = \ln(10^{16})$ ($L = \ln(10^3)$) and $M_{\rm KK} = 3\,\text{TeV}$ ($M_{\rm KK} = 1.5\,\text{TeV}$), respectively. Figure taken from [34]. See text for details.

terms for the gauge fields [40, 49, 50]. Since such terms are generated at the loop level [51, 52] and turn out to be UV divergent, bare contributions to the brane-kinetic terms encode unknown UV physics at or above the cut-off scale. In order to retain the predictivity of the model, we simply assume that these bare contributions are small.

The perhaps most elegant method to protect the T-parameter from vast corrections is the implementation of a gauged custodial symmetry [20]. Within the SM, the ratio $m_W/m_Z = \cos\theta_w$ is a consequence of the symmetry-breaking mechanism. Within the weak interaction basis, the mass matrix for the vector $(W_\mu^1, W_\mu^2, W_\mu^3, B_\mu)^T$ has the form

$$\mathcal{M}_{\text{mass}}^{\text{weak}} = \begin{pmatrix} M_W^2 & 0 & 0 & 0 \\ 0 & M_W^2 & 0 & 0 \\ 0 & 0 & M_W^2 & M^2 \\ 0 & 0 & M^2 & M_0^2 \end{pmatrix} . \tag{3.47}$$

Here, the masses in the upper-left 3×3 block have to be identical due to a global $O(3)$ rotation symmetry of (1.46), which exchanges the would-be GBs with each other. As the orthogonal group $O(3)$ is locally isomorph to the unitary group $SU(2)$, it is said that the EW sector is invariant under a custodial $SU(2)$ symmetry. The idea of [20] is to promote the global custodial symmetry of the SM to be a local one. This is achieved by replacing the hyper-charge group $U(1)_Y$ by the direct product $SU(2)_R \times U(1)_X$, which is broken down to the former by an appropriate choice of UV BCs of the respective gauge fields. As we will see in the next section, this will remove the leading L-enhanced contribution to the T-parameter.

4 Gauge fields in the custodial RS model

In this section we repeat the analysis of the minimal model for the extended gauge group

$$SU(3)_c \times SU(2)_L \times SU(2)_R \times U(1)_X \,, \tag{4.1}$$

as suggested in [20]. Again, we keep the Higgs sector on the IR brane and decompose the 5D theory into a tower of mass eigenstates. This allows for a compact notation [53], which makes the generalization of the minimal gauge sector straightforward. Furthermore, the exact treatment allows for a clear understanding of the custodial protection mechanism, which arises from the interplay of UV and IR boundary conditions. An exhaustive treatment within perturbative approach, featuring a truncation of the KK tower after the first mode, can be found in [54].

4.1 Action of the 5D theory

According to (4.1), we have to introduce a second set of $SU(2)$ gauge fields. Omitting the Faddeev-Popov Lagrangian, the 5D action of the gauge sector takes the form

$$S_{\text{Gauge}} = \int d^4x\, r \int_{-\pi}^{\pi} d\phi \left(\mathcal{L}_{\text{L,R,X}} + \mathcal{L}_{\text{Higgs}} + \mathcal{L}_{\text{GF}} \right), \tag{4.2}$$

with the kinetic terms ($a = 1, 2, 3$)

$$\mathcal{L}_{\text{L,R,X}} = \frac{\sqrt{G}}{r}\, G^{KM} G^{LN} \left(-\frac{1}{4}\, L^a_{KL} L^a_{MN} - \frac{1}{4}\, R^a_{KL} R^a_{MN} - \frac{1}{4}\, X_{KL} X_{MN} \right). \tag{4.3}$$

The Higgs Lagrangian is generalized to

$$\mathcal{L}_{\text{Higgs}} = \frac{\delta(|\phi| - \pi)}{r} \left(\frac{1}{2}\, \text{Tr}\, |(D_\mu \Phi)|^2 - V(\Phi) \right), \tag{4.4}$$

where the Higgs is assumed to transform as a bi-doublet $(\mathbf{2}, \mathbf{2})_0$. It explicitly reads

$$\Phi(x) = \frac{1}{\sqrt{2}} \begin{pmatrix} v + h(x) - i\varphi_3(x) & -i\sqrt{2}\, \varphi^+(x) \\ -i\sqrt{2}\, \varphi^-(x) & v + h(x) + i\varphi_3(x) \end{pmatrix}, \tag{4.5}$$

where again $\varphi^\pm = (\varphi_1 \mp i\varphi_2)/\sqrt{2}$. $SU(2)_L$ transformations act from the left on the bi-doublet, while the $SU(2)_R$ transformations act from the right. The covariant derivative[1]

$$D_\mu \Phi = \partial_\mu \Phi - i g_{L5}\, L_\mu^a T_L^a\, \Phi + i g_{R5}\, \Phi\, R_\mu^a T_R^a\,, \tag{4.6}$$

with $T^a_{L,R} = \sigma^a/2$, can be worked out in analogy to (3.8),

$$\begin{aligned} D_\mu \Phi = \frac{1}{\sqrt{2}} &\begin{pmatrix} \partial_\mu (h - i\varphi_3) - i\frac{v}{2}\left(g_{L5} L_\mu^3 - g_{R5} R_\mu^3\right) & -\partial_\mu i\sqrt{2}\varphi^+ - i\frac{v}{2}\left(g_{L5} L_\mu^+ - g_{R5} R_\mu^+\right) \\ -\partial_\mu i\sqrt{2}\varphi^- - i\frac{v}{2}\left(g_{L5} L_\mu^- - g_{R5} R_\mu^-\right) & \partial_\mu (h + i\varphi_3) + i\frac{v}{2}\left(g_{L5} L_\mu^3 - g_{R5} R_\mu^3\right) \end{pmatrix} \\ &+ \text{terms bi-linear in fields}\,. \end{aligned} \tag{4.7}$$

Here, we have introduced the linear combinations

$$L_\mu^\pm = \frac{1}{\sqrt{2}}\left(L_\mu^1 \mp i L_\mu^2\right), \qquad R_\mu^\pm = \frac{1}{\sqrt{2}}\left(R_\mu^1 \mp i R_\mu^2\right). \tag{4.8}$$

The structure of (4.7) motivates for a further field rotation [55]

$$\begin{pmatrix} \tilde{A}_M^a \\ V_M^a \end{pmatrix} = \frac{1}{\sqrt{g_L^2 + g_R^2}} \begin{pmatrix} g_L & -g_R \\ g_R & g_L \end{pmatrix} \begin{pmatrix} L_M^a \\ R_M^a \end{pmatrix}, \tag{4.9}$$

which gives rise to a diagonal mass matrix, and we have replaced the 5D gauge couplings by 4D ones. The rotations are analogous to the usual definitions of the Z^0 boson and photon fields in the SM (4.16). The 5D mass term related to EWSB adopts the form

$$\mathcal{L}_{\text{mass}} = \frac{\delta(|\phi| - \pi)}{r}\, \frac{(g_{L5}^2 + g_{R5}^2)\, v^2}{8}\, \tilde{A}_\mu^a \tilde{A}^{\mu\, a} \tag{4.10}$$

$$\to \delta(t-1)\, \frac{k}{4}\, \frac{(g_{L5}^2 + g_{R5}^2)\, v^2}{4}\, \tilde{A}_\mu^a \tilde{A}^{\mu\, a} \equiv \delta(t-1)\, \frac{k}{4}\, M_{\tilde{A}}^2\, \tilde{A}_\mu^a \tilde{A}^{\mu\, a}\,, \tag{4.11}$$

where we changed to t-notation again. There is no mass term for the fields V_μ^a. Thus, the Higgs VEV $\langle \Phi \rangle = v/\sqrt{2}\, \mathbf{1}$ breaks the bulk gauge symmetry down to a diagonal subgroup $SU(2)_V$ on the IR brane

$$SU(2)_L \times SU(2)_R \xrightarrow{\text{IR}} SU(2)_V\,. \tag{4.12}$$

The SM gauge group is obtained by an additional symmetry breaking on the UV boundary

$$SU(2)_R \times U(1)_X \xrightarrow{\text{UV}} U(1)_Y\,, \tag{4.13}$$

which is achieved by an appropriate choice of the UV BCs. Therefore, we define the linear combinations

$$\begin{pmatrix} Z_M' \\ B_M^Y \end{pmatrix} = \frac{1}{\sqrt{g_R^2 + g_X^2}} \begin{pmatrix} g_R & -g_X \\ g_X & g_R \end{pmatrix} \begin{pmatrix} R_M^3 \\ X_M \end{pmatrix}, \tag{4.14}$$

[1]The plus sign in front of g_{R_5} is chosen for convenience.

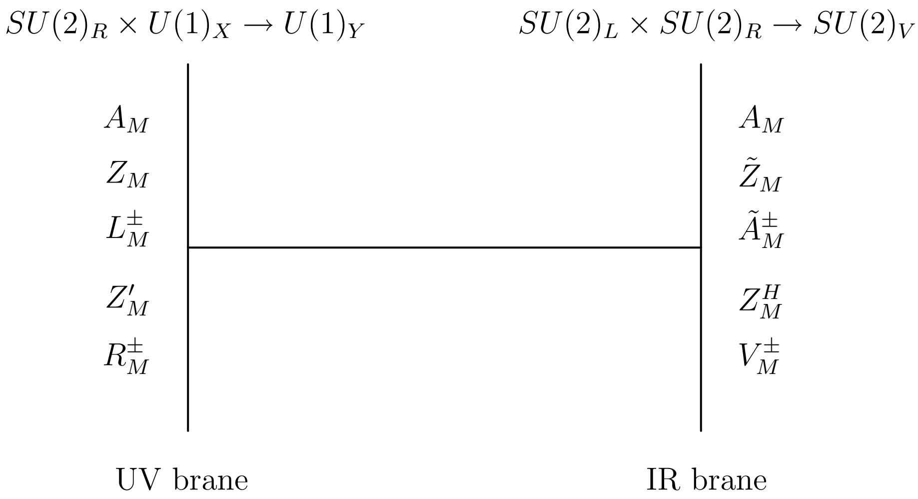

Figure 4.1: UV and IR basis ⇔ gauge fields with individual BCs at the corresponding branes. If EWSB is neglected, the fields which are related to the UV basis and depicted in the upper half, possess a zero mode, while the fields in the lower half do not.

and assign Dirichlet BCs to Z'_μ and $R_\mu^{1,2}$ on the UV brane. The $U(1)_Y$ hyper-charge coupling is related to the $SU(2)_R \times U(1)_X$ couplings by

$$g_Y = \frac{g_R\, g_X}{\sqrt{g_R^2 + g_X^2}} \,. \tag{4.15}$$

The SM-like neutral electroweak gauge bosons are defined in the standard way through

$$\begin{pmatrix} Z_M \\ A_M \end{pmatrix} = \frac{1}{\sqrt{g_L^2 + g_Y^2}} \begin{pmatrix} g_L & -g_Y \\ g_Y & g_L \end{pmatrix} \begin{pmatrix} L_M^3 \\ B_M^Y \end{pmatrix}, \tag{4.16}$$

where the SM coupling constants g and g' are now denoted as g_L and g_Y, respectively. The SM definition of the weak-mixing angle (1.48) is kept. The fields A_M, Z_M, $L_M^\pm$, Z'_M, and $R_M^\pm$ form a basis. As we are going to assign individual UV BCs for each of those, we will refer to them as the UV or weak basis.

Starting from (4.9), we will construct a second basis for which we will assign individual IR BCs. As EWSB takes place at the IR boundary, we will therefore speak of the IR or mass basis. The fields V_M^3 and X_M for instance can be rotated to the photon field A_M and a state Z_M^H via

$$\begin{pmatrix} Z_M^H \\ A_M \end{pmatrix} = \frac{1}{g_{LRX}^2} \begin{pmatrix} g_L\, g_R & -g_X \sqrt{g_L^2 + g_R^2} \\ g_X \sqrt{g_L^2 + g_R^2} & g_L\, g_R \end{pmatrix} \begin{pmatrix} V_M^3 \\ X_M \end{pmatrix}, \tag{4.17}$$

$\partial_t A_\mu(x,\epsilon)=0$	$A_5(x,\epsilon)=0$	$\partial_t A_\mu(x,1)=0$	$A_5(x,1)=0$
$\partial_t Z_\mu(x,\epsilon)=0$	$Z_5(x,\epsilon)=0$	$\partial_t \tilde{Z}_\mu(x,1^-)=-kM_{\tilde{A}}^2/(2M_{\rm KK}^2)\tilde{Z}_\mu(x,1)$	$\tilde{Z}_5(x,1)=0$
$\partial_t L^\pm_\mu(x,\epsilon)=0$	$L^\pm_5(x,\epsilon)=0$	$\partial_t \tilde{A}^\pm_\mu(x,1^-)=-kM_{\tilde{A}}^2/(2M_{\rm KK}^2)\tilde{A}^\pm_\mu(x,1)$	$\tilde{A}^\pm_5(x,1)=0$
$Z'_\mu(x,\epsilon)=0$	$Z'_5(x,\epsilon)=0$	$\partial_t Z^H_\mu(x,1)=0$	$Z^H_5(x,1)=0$
$R^\pm_\mu(x,\epsilon)=0$	$R^\pm_5(x,\epsilon)=0$	$\partial_t V^\pm_\mu(x,1)=0$	$V^\pm_5(x,1)=0$

Table 4.1: BCs for UV basis (left) and IR basis (right).

where

$$g_{LRX}^2=\sqrt{g_L^2\,g_R^2+g_R^2\,g_X^2+g_X^2\,g_L^2}\,. \tag{4.18}$$

We further write $\tilde{Z}_M\equiv\tilde{A}^3_M$, as it is a linear combination of Z_M and Z'_M, which is orthogonal to Z^H_M. The two bases can be transformed to each other with the help of the relations

$$\begin{aligned}
\begin{pmatrix}\tilde{Z}_M\\ Z^H_M\end{pmatrix}&=\begin{pmatrix}\cos\theta_Z & -\sin\theta_Z\\ \sin\theta_Z & \cos\theta_Z\end{pmatrix}\begin{pmatrix}Z_M\\ Z'_M\end{pmatrix}\equiv\boldsymbol{R}_Z\begin{pmatrix}Z_M\\ Z'_M\end{pmatrix},\\
\begin{pmatrix}\tilde{A}^\pm_M\\ V^\pm_M\end{pmatrix}&=\begin{pmatrix}\cos\theta_W & -\sin\theta_W\\ \sin\theta_W & \cos\theta_W\end{pmatrix}\begin{pmatrix}L^\pm_M\\ R^\pm_M\end{pmatrix}\equiv\boldsymbol{R}_W\begin{pmatrix}L^\pm_M\\ R^\pm_M\end{pmatrix},
\end{aligned} \tag{4.19}$$

where

$$\begin{aligned}
\sin\theta_Z&=\frac{g_R^2}{\sqrt{(g_L^2+g_R^2)(g_R^2+g_X^2)}}\,, & \cos\theta_Z&=\frac{g_{LRX}^2}{\sqrt{(g_L^2+g_R^2)(g_R^2+g_X^2)}}\,,\\
\sin\theta_W&=\frac{g_R}{\sqrt{g_L^2+g_R^2}}\,, & \cos\theta_W&=\frac{g_L}{\sqrt{g_L^2+g_R^2}}\,.
\end{aligned} \tag{4.20}$$

The latter quantities will be abbreviated by s_Z, c_Z, s_W, and c_W from now on.

In Table 4.1 we give the various BCs needed to obtain the correct mass spectrum for the SM gauge bosons. The 5D photon field A_μ has individual and source-free Neumann BCs at both branes. Therefore its zero mode remains massless, and there is no need to distinguish between the two bases. In contrast to the the minimal model, which features the two parameters M_Z and M_W (3.5), there is just one parameter $M_{\tilde{A}}$ entering the IR BCs. The different masses for the lightest electroweak $W^\pm$ and Z^0 bosons are generated through the mixed UV BCs of the gauge fields in the IR basis. The fact that there is just one fundamental mass parameter is crucial for the custodial protection of the T-parameter. We will elaborate on this in Section 4.6.

As it is the case in the minimal model, the action of the theory contains mixing terms between the vector components of the gauge fields and the various scalars, which can be removed by an appropriate gauge-fixing. As the Higgs sector is localized on the IR brane, it is natural to work in the IR basis for that purpose. For this reason, we define the 5D theory in the IR basis. For the KK decomposition however, it is convenient to rotate to the weak basis. The expression for the extended gauge-fixing Lagrangian will be given below, after the introduction of some useful notation.

4.2 Kaluza-Klein decomposition

For the KK decomposition of the 5D fields it is convenient to work with profiles that obey definite Neumann (+) or Dirichlet (−) BCs at the UV brane. Therefore we include a rotation to the weak basis, for which the UV BCs are decoupled. As different UV fields get mixed by the IR BCs, these fields should be expressed through the same 4D basis. Thus, we introduce the vectors

$$\vec{Z}_M = (\tilde{Z}_M, Z_M^H)^T\,, \qquad \text{and} \qquad \vec{W}_M^{\pm} = (\tilde{A}_M^{\pm}, V_M^{\pm})^T\,, \tag{4.21}$$

and define the diagonal matrix consisting of profiles in the UV basis,

$$\boldsymbol{\chi}_n^a(t) = \begin{pmatrix} \chi_n^{a(+)}(t) & 0 \\ 0 & \chi_n^{a(-)}(t) \end{pmatrix} \tag{4.22}$$

for $a = W, Z$. The superscripts (+) and (−) label the type of BC we impose at the UV brane, *i.e.*, they indicate untwisted and twisted even functions on the orbifold. We use the term twisted even functions for profiles with even Z_2-parity, which obey Dirichlet BC on the UV brane and are thus not smooth at this orbifold fix point. These fields are sometimes called odd, as they look like an odd function if one just considers half of the orbifold. Untwisted even functions correspond to ordinary profiles with Neumann UV BCs. Remember from Table 4.1 that both profiles satisfy a Neumann BC at the IR boundary, which we do not indicate explicitly by a superscript (+) to avoid unnecessary clutter of notation.

We further define two-component vectors $\vec{A}_n^a$, which are supposed to parametrize the mixings between the different UV gauge fields and their KK excitations due to the EWSB on the IR brane. As a straightforward generalization of (3.11) we are now able to write

$$\begin{aligned}
A_\mu(x,t) &= \frac{1}{\sqrt{r}} \sum_n \chi_n^{A(+)}(t)\, A_\mu^{(n)}(x)\,, & A_5(x,t) &= \frac{1}{\sqrt{r}} \sum_n \frac{L}{\pi}\, t\partial_t\, \chi_n^{A(+)}(t)\, a_n^A\, \varphi_A^{(n)}(x)\,, \\
\vec{Z}_\mu(x,t) &= \frac{\boldsymbol{R}_Z}{\sqrt{r}} \sum_n \boldsymbol{\chi}_n^Z(t)\, \vec{A}_n^Z\, Z_\mu^{(n)}(x)\,, & \vec{Z}_5(x,t) &= \frac{\boldsymbol{R}_Z}{\sqrt{r}} \sum_n \frac{L}{\pi}\, t\partial_t\, \boldsymbol{\chi}_n^W(t)\, \vec{A}_n^Z a_n^Z\, \varphi_Z^{(n)}(x)\,, \\
\vec{W}_\mu^{\pm}(x,t) &= \frac{\boldsymbol{R}_W}{\sqrt{r}} \sum_n \boldsymbol{\chi}_n^W(t) \vec{A}_n^W W_\mu^{\pm(n)}(x), & \vec{W}_5^{\pm}(x,t) &= \frac{\boldsymbol{R}_W}{\sqrt{r}} \sum_n \frac{L}{\pi}\, t\partial_t \boldsymbol{\chi}_n^W(t) \vec{A}_n^W a_n^W\, \varphi_W^{\pm(n)}(x).
\end{aligned} \tag{4.23}$$

Again, the fields $A_\mu^{(n)}(x)$ *etc.* are the 4D mass eigenstates and the lightest modes are identified with the SM gauge bosons. The matrices $\boldsymbol{R}_{Z,W}$ are defined in (4.19). The mixing vectors are normalized according to

$$(\vec{A}_n^a)^T \vec{A}_n^a = 1\,. \tag{4.24}$$

As the profile matrices (4.22) are always combined with the mixing vector $\vec{A}_n^a$, it is natural to define the vectors

$$\vec{\chi}_n^Z(t) = \begin{pmatrix} \chi_n^{Z(+)}(t) \\ \chi_n^{Z'(-)}(t) \end{pmatrix} = \boldsymbol{\chi}_n^Z(t)\,\vec{A}_n^Z\,, \qquad \vec{\chi}_n^W(t) = \begin{pmatrix} \chi_n^{L(+)}(t) \\ \chi_n^{R(-)}(t) \end{pmatrix} = \boldsymbol{\chi}_n^W(t)\,\vec{A}_n^W\,, \tag{4.25}$$

for the profiles of the UV fields. A crucial point is that the profiles $\chi_n^{a(+)}(t)$ and $\chi_n^{a(-)}(t)$ do not obey exact orthonormality conditions separately, as the related fields are mixed by the IR BCs, and decomposed into the same 4D gauge-boson basis. The complete vectors $\vec{\chi}_n^a(t)$ on the other hand are orthonormal on each other,

$$\frac{2\pi}{L}\int_\epsilon^1 \frac{dt}{t}\,\vec{\chi}_m^{a\,T}(t)\,\vec{\chi}_n^a(t) = \delta_{mn}\,. \tag{4.26}$$

Indeed, within our exact treatment, one should never consider the components of the gauge-field vectors (4.21) separately. Instead, one should always take the expressions (4.25) as a starting point [53]. Within the perturbative approach, the situation is different. Here, the gauge fields are decoupled within the KK decomposition such that one obtains individual orthonormality relations for all of them. The mixing is induced after truncation via diagonalization of the mass matrix. The photon and gluon are exceptional as they obey the standard orthonormality condition (3.12) in both approaches. In analogy to (3.13), we also expand the 4D Goldstone bosons in the basis of mass eigenstates $\varphi_Z^{(n)}(x)$ and $\varphi_W^{\pm(n)}(x)$ by writing

$$\vec{\varphi}^3(x) = \sum_n \vec{b}_n^Z\,\varphi_Z^{(n)}(x)\,, \qquad \vec{\varphi}^\pm(x) = \sum_n \vec{b}_n^W\,\varphi_W^{\pm(n)}(x)\,. \tag{4.27}$$

Employing the notation introduced in this section, it is now straightforward to write down the generalized gauge-fixing Lagrangian

$$\begin{aligned}
\mathcal{L}_{\rm GF} = &-\frac{1}{2\xi}\left(\partial^\mu A_\mu - \frac{\xi}{2}\left[M_{\rm KK}^2\,\frac{2\pi}{L}\,t\partial_t\,t^{-2}A_5\right]\right)^2 \\
&-\frac{1}{2\xi}\left(\partial^\mu \vec{Z}_\mu - \frac{\xi}{2}\left[\delta(t-1)\,kM_Z\,\vec{\varphi}_3 + M_{\rm KK}^2\,\frac{2\pi}{L}\,t\partial_t\,t^{-2}\vec{Z}_5\right]\right)^2 \\
&-\frac{1}{\xi}\left(\partial^\mu \vec{W}_\mu^+ - \frac{\xi}{2}\left[\delta(t-1)\,kM_W\,\vec{\varphi}^+ + M_{\rm KK}^2\,\frac{2\pi}{L}\,t\partial_t\,t^{-2}\vec{W}_5^+\right]\right)^T \\
&\times\left(\partial^\mu \vec{W}_\mu^- - \frac{\xi}{2}\left[\delta(t-1)\,kM_W\,\vec{\varphi}^- + M_{\rm KK}^2\,\frac{2\pi}{L}\,t\partial_t\,t^{-2}\vec{W}_5^-\right]\right)\,.
\end{aligned} \tag{4.28}$$

The same philosophy applies to the generalization of the expression (3.10). If we insert the decomposition (4.23) into the action and define the projectors $\boldsymbol{P}_{(+)} = \mathrm{diag}(1,0)$ and $\boldsymbol{P}_{(-)} = \mathrm{diag}(0,1)$, we find the generalized EOMs [53]

$$\Big(t\partial_t\, t^{-1}\partial_t\, + (x_n^a)^2\Big)\boldsymbol{R}_a\, \boldsymbol{\chi}_n^a(t)\vec{A}_n^a = \delta(t-1)L\,\frac{(g_L^2+g_R^2)v^2}{4M_{\mathrm{KK}}^2}\,\boldsymbol{P}_{(+)}\boldsymbol{R}_a\,\boldsymbol{\chi}_n^a(t)\vec{A}_n^a\,. \tag{4.29}$$

for $a = W, Z$. The EOM for the photon can be written in the same form by defining $\boldsymbol{R}_A = \mathbf{1}$ and $\vec{A}_n^A = (1,0)^T$, and setting the brane-localized mass term to zero. The appropriate IR BCs are derived as above. They read

$$\boldsymbol{R}_a\,\partial_t\,\boldsymbol{\chi}_n^a(1^-)\vec{A}_n^a = -X^2\,L\,\boldsymbol{P}_{(+)}\boldsymbol{R}_a\,\boldsymbol{\chi}_n^a(1)\vec{A}_n^a\,, \tag{4.30}$$

where $X^2 \equiv (g_L^2+g_R^2)\,v^2/(4M_{\mathrm{KK}}^2)$, and, for the photon, the right-hand side is equal to zero. The UV BCs are given by

$$\partial_t\,\chi_n^{(+)}(\epsilon) = \chi_n^{(-)}(\epsilon) = 0\,. \tag{4.31}$$

After applying the EOMs and the orthonormality condition (4.26), we observe that the 4D action takes the desired canonical form (3.16), if

$$a_n^a = -\frac{1}{m_n^a}\,, \qquad \vec{b}_n^a = \sqrt{2\pi}\,\frac{\sqrt{g_L^2+g_R^2}\,v}{2m_n^a}\,\boldsymbol{P}_{(+)}\boldsymbol{R}_a\,\boldsymbol{\chi}_n^a(1^-)\vec{A}_n^a\,. \tag{4.32}$$

With these definitions, the desired 4D form of the gauge-fixing Lagrangian (3.19) is recovered.

4.3 Bulk profiles

We now derive expressions for the profiles $\chi_n^{a(\pm)}(t)$. In order to get the EOMs for the UV basis, we multiply (4.29) with $\boldsymbol{R}_a^T$ from the left. The solutions of $\chi_n^{a(+)}(t)$ are identical to those derived in Section 3.3. The profiles $\chi_n^{a(-)}(t)$ have to vanish on the UV boundary. As a consequence, there is no zero-mode solution for the latter fields. We find

$$\chi_n^{(+)}(t) = N_n^{(+)}\sqrt{\frac{L}{\pi}}\,t\,c_n^{(+)+}(t)\,, \qquad \chi_n^{(-)}(t) = N_n^{(-)}\sqrt{\frac{L}{\pi}}\,t\,c_n^{(-)+}(t)\,, \tag{4.33}$$

with

$$\begin{aligned}
c_n^{(+)+}(t) &= Y_0(x_n^a\epsilon)J_1(x_n^a t) - J_0(x_n^a\epsilon)\,Y_1(x_n^a t)\,,\\
c_n^{(-)+}(t) &= Y_1(x_n^a\epsilon)J_1(x_n^a t) - J_1(x_n^a\epsilon)\,Y_1(x_n^a t)\,,\\
c_n^{(+)-}(t) &= \frac{1}{x_n^a t}\,\frac{d}{dt}\Big(t\,c_n^{(+)+}(t)\Big) = Y_0(x_n^a\epsilon)\,J_0(x_n^a t) - J_0(x_n^a\epsilon)\,Y_0(x_n^a t)\,,\\
c_n^{(-)-}(t) &= \frac{1}{x_n^a t}\,\frac{d}{dt}\Big(t\,c_n^{(-)+}(t)\Big) = Y_1(x_n^a\epsilon)\,J_0(x_n^a t) - J_1(x_n^a\epsilon)\,Y_0(x_n^a t)\,.
\end{aligned} \tag{4.34}$$

As $c_n^{(+)-}(\epsilon) = c_n^{(-)+}(\epsilon) = 0$, it is apparent that the UV BCs are satisfied. The normalization factor is given by

$$\begin{aligned}\left(N_n^{(\pm)}\right)^{-2} &= \left[c_n^{(\pm)+}(1)\right]^2 + \left[c_n^{(\pm)-}(1^-)\right]^2 - \frac{2}{x_n}\Big(c_n^{(\pm)+}(1)\,c_n^{(\pm)-}(1^-) - \epsilon\, c_n^{(\pm)+}(\epsilon)\, c_n^{(\pm)-}(\epsilon^+)\Big) \\ &\quad - \epsilon^2\left(\left[c_n^{(\pm)+}(\epsilon)\right]^2 + \left[c_n^{(\pm)-}(\epsilon^+)\right]^2\right), \end{aligned} \tag{4.35}$$

where $\epsilon^+ \equiv \lim_{\theta\to 0^+}(\epsilon+\theta)$. Note that, depending on the type of the UV BCs, some of the terms in (4.35) vanish identically.

The spectrum of the theory is determined by the IR BCs (4.30). The eigenvalues x_n^a are solutions of

$$\det\left[\,\partial_t\,\boldsymbol{\chi}_n^a(1^-) + LX^2\boldsymbol{D}_a\boldsymbol{\chi}_n^a(1)\,\right] = 0\,, \tag{4.36}$$

with

$$\boldsymbol{D}_a = \boldsymbol{R}_a^{-1}\boldsymbol{P}_{(+)}\boldsymbol{R}_a = \begin{pmatrix} c_a^2 & -s_a c_a \\ -s_a c_a & s_a^2 \end{pmatrix}, \tag{4.37}$$

and the mixing angles s_a and c_a are defined in (4.20). The presence of the new gauge fields doubles the number of KK excitations in such a way that there are always two KK modes with similar masses. This already suggests, that there may be cancellations within the calculation of weak-interaction amplitudes. To see that this can indeed happen, one needs to determine the eigenvectors $\vec{A}_n^a$ from (4.30), once the eigenvalues are known.

If we expand (4.33) in powers of $v^2/M_{\rm KK}^2$ and ignore tiny terms $\propto \epsilon^2$, we find the simple analytic expressions

$$\begin{aligned} m_W^2 &= \frac{g_L^2 v^2}{4}\left[1 - \frac{g_L^2 v^2}{8M_{\rm KK}^2}\left(L - 1 + \frac{1}{2L}\right) - \frac{g_R^2 v^2}{8M_{\rm KK}^2}\,L + \mathcal{O}\left(\frac{v^4}{M_{\rm KK}^4}\right)\right], \\ m_Z^2 &= \frac{(g_L^2+g_Y^2)\,v^2}{4}\left[1 - \frac{(g_L^2+g_Y^2)\,v^2}{8M_{\rm KK}^2}\left(L - 1 + \frac{1}{2L}\right) - \frac{(g_R^2-g_Y^2)\,v^2}{8M_{\rm KK}^2}\,L + \mathcal{O}\left(\frac{v^4}{M_{\rm KK}^4}\right)\right], \end{aligned} \tag{4.38}$$

for the masses of the $W^\pm$ and Z^0 bosons. The last terms inside the square brackets are new compared to the minimal model. Interestingly, these are responsible for the custodial protection of the T-parameter. Expanding (4.30) in $v^2/M_{\rm KK}^2$, the zero-mode profiles are found to be

$$\begin{aligned} \chi_0^{(+)}(t) &= \frac{1}{\sqrt{2\pi}}\left[1 + \frac{x_a^2}{4}\left(1 - \frac{1}{L} + t^2\left(1 - 2L - 2\ln t\right)\right) + \mathcal{O}\left(x_a^4\right)\right], \\ \chi_0^{(-)}(t) &= \sqrt{\frac{L}{2\pi}}\,t^2\left[-2 + \frac{x_a^2}{4}\left(t^2 - \frac{2}{3}\right) + \mathcal{O}\left(x_a^4\right)\right], \end{aligned} \tag{4.39}$$

for $a = W, Z$ and $x_a = m_a/M_{\rm KK}$. The profiles $\chi_0^{(+)}(t)$ with Neumann IR BC are identical to those of the minimal model (3.29). The profiles $\chi_0^{(-)}(t)$ satisfying Dirichlet IR BC scale like $\sqrt{L}$, reflecting the admixture of KK modes close to the IR boundary. Indeed, the contribution of profile the $\chi_0^{(-)}(t)$ is a higher order effect in $v^2/M_{\rm KK}^2$ due to the respective entry of the mixing vector

$$\vec{A}_0^a = \begin{pmatrix} 1 \\ -s_a c_a \, \dfrac{X^2}{4} \sqrt{L} \end{pmatrix} + \mathcal{O}\left(X^4\right). \tag{4.40}$$

As we will see below, the results (4.39) and the minus sign in (4.40) play a crucial role in the custodial protection mechanism of the $Z^0 b_L \bar{b}_L$ vertex.

4.4 Interactions among gauge bosons

For some applications, one requires the RS corrections of cubic and quartic gauge couplings. For instance, one may think of a Higgs decaying into a photon and a Z^0 boson via a triangle W-boson loop. We will show that the RS corrections to cubic and quartic couplings of zero modes are of higher order.

Due to the unbroken $U(1)_{\rm e.m.}$ gauge group, the $WW\gamma$ coupling is unchanged with respect to the SM to all orders in $v^2/M_{\rm KK}^2$. The WWZ^0 coupling will receive a correction, but not at the order $v^2/M_{\rm KK}^2$. This can be understood by the following observations: First, the bulk integral over a single zero-mode profile of a heavy gauge field is given by

$$\frac{2\pi}{L} \int_\epsilon^1 \frac{dt}{t} \, \chi_0^{(+)}(t) \; = \sqrt{2\pi} + \mathcal{O}\left(\frac{v^4}{M_{\rm KK}^4}\right). \tag{4.41}$$

Second, within the custodial model, the contributions from the additional gauge bosons are of higher order as $\left[(\vec{A}_0^a)_2 \, \chi_0^{(-)}(t)\right]^2 = \mathcal{O}(v^4/M_{\rm KK}^4)$. Collecting all factors appearing in the decomposed action apart from the 4D gauge fields, the result (4.41) immediately implies that the RS coupling of the triple-gauge boson vertex WWZ^0 is given by

$$r g_{L_5} c_w \, \frac{2\pi}{L} \int_\epsilon^1 \frac{dt}{t} \, \frac{1}{r^{3/2}} \left(\chi_0^{W(+)}(t)\right)^2 \chi_0^{Z(+)}(t) \; = g_L c_w \left[1 + \mathcal{O}\left(\frac{v^4}{M_{\rm KK}^4}\right)\right]. \tag{4.42}$$

Thus, corrections compared to the SM appear at the order $v^4/M_{\rm KK}^4$ [54], which are therefore irrelevant for all practical purposes. The same line of reasoning applies to the quartic vertex WWZ^0Z^0.

In the example of the Higgs decay, one further involves overlaps of KK $W^\pm$ bosons and the zero mode Z^0, which in the custodial model with $g_L = g_R$ are given by [53]

$$\begin{aligned} \mathcal{I}_{nn0}^{WWZ} = \frac{(2\pi)^{3/2}}{L} \int_\epsilon^1 \frac{dt}{t} \Big[& \chi_0^{(+)Z} \left(\chi_n^{(+)W^2} (\vec{A}_n^W)_1^2 + \frac{g_Y^2}{g_L^2} \, \chi_n^{(-)W^2} (\vec{A}_n^W)_2^2 \right) \\ & - \sqrt{1 - g_Y^4/g_L^4} \; \chi_0^{(-)Z} (\vec{A}_0^Z)_2 \, \chi_n^{(-)W^2} (\vec{A}_n^W)_2^2 \Big]. \end{aligned} \tag{4.43}$$

Here, $\big(A_n^W(t)\big)_i$ denotes the i^{th} component of the corresponding mixing vector. Within the minimal model, one just keeps the first term on the right-hand side. Note that we have to choose the same KK index n for both W bosons, whenever the triangle loop is coupled to photon. The generalization to the more general case is obvious. The overlap integral (4.43) has to be performed numerically, as we do not have simple expressions for the profiles of the KK modes in simple powers or logarithms of t. However, as the sum over KK propagators of $W^{(n)\pm}$ bosons is already suppressed with v^2/M_{KK}^2 compared to the zero-mode exchange, one only requires (4.43) to 0^{th} order in the latter ratio. This gives rise to the more simple expression

$$\mathcal{I}_{nn0}^{WWZ} = \frac{2\pi}{L} \int_\epsilon^1 \frac{dt}{t} \left(\chi_n^{(+)W\,2} \big(\vec{A}_n^W\big)_1^2 + \frac{g_Y^2}{g_L^2}\, \chi_n^{(-)W\,2} \big(\vec{A}_n^W\big)_2^2 \right) + \mathcal{O}\left(\frac{v^2}{M_{\text{KK}}^2}\right) . \qquad (4.44)$$

An analogous result is obtained for the interaction $W^{(m)}W^{(n)}Z^0Z^0$. The extension to the most general vertex $W^{(m)}W^{(n)}Z^{(k)}Z^{(l)}$ is also straightforward.

4.5 Summing over Kaluza-Klein modes

In this section we are going generalize the computations of KK sums of the heavy $W^\pm$ and Z^0 bosons. We define the expression

$$\boldsymbol{\Sigma}_a(t,t') \equiv \sum_n \frac{\vec{\chi}_n^a(t)\, \vec{\chi}_n^{a\,T}(t')}{\big(x_n^a\big)^2} , \qquad (4.45)$$

which arises within the calculation of the tree-level exchange of a SM electroweak gauge boson accompanied by its KK excitations in the limit of zero (or negligibly small) momentum transfer. In analogy to the minimal model, we integrate the EOM (4.29) twice, but accounting for the BCs on both branes [53]. We observe

$$\vec{\chi}_n^a(t) \;=\; (x_n^a)^2\, \vec{\mathcal{I}}_n^a(t) - (x_n^a)^2 \left(t^2-\epsilon^2\right) \boldsymbol{X}_a\, \vec{\mathcal{I}}_n^a(1) + \left[\,\boldsymbol{1} - \left(t^2-\epsilon^2\right) \boldsymbol{X}_a\,\right] \boldsymbol{P}_{(+)}\, \vec{\chi}_n^a(\epsilon) , \qquad (4.46)$$

where we have defined

$$\vec{\mathcal{I}}_n^a(t) \equiv \int_\epsilon^t dt'\, t' \int_{t'}^{1^-} \frac{dt''}{t''}\, \vec{\chi}_n^a(t'') , \qquad \boldsymbol{X}_a \equiv \tilde{X}^2\, \boldsymbol{D}_a \equiv \frac{LX^2}{2+LX^2\,(1-\epsilon^2)}\, \boldsymbol{D}_a . \qquad (4.47)$$

Using the generalized completeness relation

$$\frac{2\pi}{L} \sum_n \frac{1}{t}\, \vec{\chi}_n^a(t)\, \vec{\chi}_n^{a\,T}(t') = \delta(t-t')\, \boldsymbol{1} , \qquad (4.48)$$

one derives

$$\begin{aligned} \boldsymbol{\Sigma}_a(t,t') = \frac{L}{4\pi} &\Big[\left(t_<^2-\epsilon^2\right) \boldsymbol{1} + \left(t^2-\epsilon^2\right) \left(t'^2-\epsilon^2\right) \boldsymbol{X}_a \Big] \\ &+ \left[\,\boldsymbol{1} - \left(t^2-\epsilon^2\right) \boldsymbol{X}_a\,\right] \boldsymbol{P}_{(+)}\, \boldsymbol{\Sigma}_a(\epsilon,\epsilon)\, \boldsymbol{P}_{(+)} \left[\,\boldsymbol{1} - \left(t'^2-\epsilon^2\right) \boldsymbol{X}_a\,\right]^T . \end{aligned} \qquad (4.49)$$

The latter result is exact to all orders in $v^2/M_{\rm KK}^2$ and the straight-forward generalization of (3.33). Again, the orthonormality relation (4.26) is used to perform the remaining sum over gauge profiles evaluated at the UV brane, which yields

$$\begin{aligned}\boldsymbol{P}_{(+)}\,\boldsymbol{\Sigma}_a(\epsilon,\epsilon)\,\boldsymbol{P}_{(+)} = \frac{L}{2\pi x_a^2}\left(\vec{\chi}_0^{\,a}(\epsilon)\right)_1\Bigg[\int_\epsilon^1\frac{dt}{t}\Big[&\left(1-c_a^2\tilde{X}^2\left(t^2-\epsilon^2\right)\right)\left(\vec{\chi}_0^{\,a}(t)\right)_1\\ &+s_ac_a\tilde{X}^2\left(t^2-\epsilon^2\right)\left(\vec{\chi}_0^{\,a}(t)\right)_2\Big]\Bigg]^{-1}\boldsymbol{P}_{(+)}\,.\end{aligned}\tag{4.50}$$

This formula can be easily expanded in powers of $v^2/M_{\rm KK}^2$, after inserting the explicit expression for the profiles (4.39) and the mixing vectors (4.40). Thus, we obtain

$$\boldsymbol{P}_{(+)}\,\boldsymbol{\Sigma}_a(\epsilon,\epsilon)\,\boldsymbol{P}_{(+)} = \left(\frac{1}{2\pi x_a^2}+\frac{1}{4\pi}\left[1-\frac{1}{2L}-\epsilon^2\left(L-\frac{1}{2L}\right)\right]+\mathcal{O}(x_a^2)\right)\boldsymbol{P}_{(+)}\,. \tag{4.51}$$

Keeping in mind that $X^2 = x_a^2/c_a^2 + O(x_a^4)$ and dropping phenomenologically irrelevant terms $\propto \epsilon^2$, we finally arrive at

$$\boldsymbol{\Sigma}_a(t,t') = \frac{L}{4\pi}\left[t_<^2\,\boldsymbol{1}-\boldsymbol{P}_a\,t^2-\boldsymbol{P}_a^T\,t'^2\right]+\left[\frac{1}{2\pi x_a^2}+\frac{1}{4\pi}\left(1-\frac{1}{2L}\right)\right]\boldsymbol{P}_{(+)}+\mathcal{O}(x_a^2)\,, \tag{4.52}$$

where

$$\boldsymbol{P}_a = \begin{pmatrix} 1 & 0\\ -\frac{s_a}{c_a} & 0\end{pmatrix}. \tag{4.53}$$

The zero-mode contribution to the KK sum(4.45) can be obtained from (4.39) and (4.40), and is explicitly given by

$$\begin{aligned}\frac{\vec{\chi}_0^{\,a}(t)\,\vec{\chi}_0^{\,a\,T}(t')}{x_a^2} &= \frac{1}{2\pi x_a^2}\,\boldsymbol{P}_{(+)}-\frac{L}{4\pi}\left[\boldsymbol{P}_a\,t^2+\boldsymbol{P}_a^T\,t'^2\right]\\ &+\left[\frac{1}{4\pi}\left(1-\frac{1}{L}+t^2\left(\frac{1}{2}-\ln t\right)+t'^2\left(\frac{1}{2}-\ln t'\right)\right)\right]\boldsymbol{P}_{(+)}+\mathcal{O}(x_a^2)\,.\end{aligned}\tag{4.54}$$

We see that the results for the minimal model (3.35) and (3.37) are contained in the extended results (4.52) and (4.54). The additional terms due to the custodial extension go along with a factor s_a/c_a and, under certain circumstances, play a crucial role in the custodial protection of the $Z^0 b_L\bar{b}_L$ coupling. We will postpone the necessary discussion to Section 7. Of course, the KK sums involving photon and gluon excitations do not depend on whether the electroweak gauge group is minimal or extended. Thus, the result (3.36) derived in the previous section stays valid.

4.6 Electroweak precision observables

Finally, we want to repeat the analysis of Section 3.5. The non-zero tree-level correlators $\Pi_{aa}(0)$ with $a = W, Z$ are calculated from the corrections to the zero-mode masses (4.38)

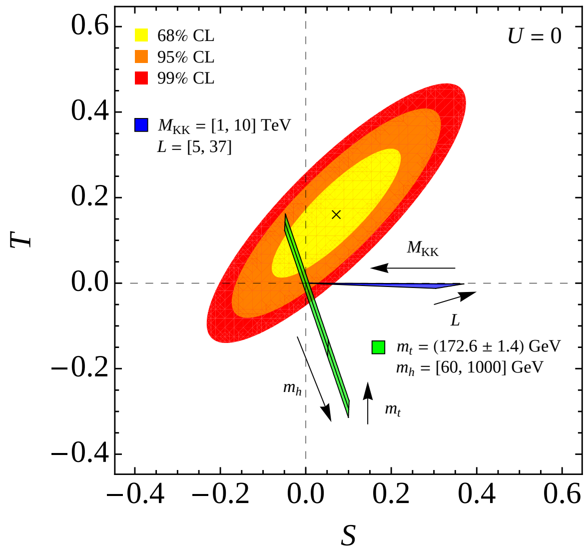

Figure 4.2: Regions of 68%, 95%, and 99% probability in the S-T plane for the custodial RS model. Figure taken from [34].

and profiles (4.39), where the latter also give rise to non-zero derivatives $\Pi'_{aa}(0)$ of the correlators at zero momentum. The expressions (3.41) generalize to

$$\begin{aligned}
\Pi_{WW}(0) &= -\frac{g_L^2 v^4}{32 M_{\rm KK}^2} \left[g_L^2 \left(L - \frac{1}{2L} \right) + g_R^2 L \right] , \\
\Pi'_{WW}(0) &= \frac{g_L^2 v^2}{8 M_{\rm KK}^2} \left(1 - \frac{1}{L} \right) , \\
\Pi_{ZZ}(0) &= -\frac{(g_L^2 + g_Y^2)\, v^4}{32 M_{\rm KK}^2} \left[(g_L^2 + g_Y^2) \left(L - \frac{1}{2L} \right) + (g_R^2 - g_Y^2)\, L \right] , \\
\Pi'_{ZZ}(0) &= \frac{(g_L^2 + g_Y^2)\, v^2}{8 M_{\rm KK}^2} \left(1 - \frac{1}{L} \right) .
\end{aligned} \tag{4.55}$$

Compared to the expressions of the minimal model (3.41), the correlators $\Pi_{WW}(0)$ and $\Pi_{ZZ}(0)$ receive additional L-enhanced contributions from the extended mass formula (4.38), that cancel the leading contribution to the T-parameter. This can also be understood as follows: The contributions of the the fields $L_\mu^\pm$ and Z_μ to the mass eigenstates $\tilde{A}_\mu^\pm$ and $\tilde{Z}_\mu$ are multiplied by c_W and c_Z, respectively. On the other hand, if one combines the definitions (1.48), (4.15), and (4.20), one can show that $c_W^2 = c_w^2 c_Z^2$. As a consequence, there is a cancellation of the volume enhanced terms in the expression $\Pi_{WW}(0) - c_w^2\, \Pi_{ZZ}(0)$, which enters the definition of the T-parameter. Indeed, if we insert the expressions (4.55) into (3.39), we obtain

$$S = \frac{2\pi v^2}{M_{\rm KK}^2} \left(1 - \frac{1}{L} \right) , \qquad T = -\frac{\pi v^2}{4\, c_w^2 M_{\rm KK}^2} \frac{1}{L} , \qquad U = 0 , \tag{4.56}$$

in agreement with [39, 20]. The tree-level results for S and U are unchanged with respect to the minimal model. A related discussion including estimates of loop effects on the T-parameter has been given in [56, 57].

In Figure 4.2, we depict the corrections (4.56) to S and T compared to the SM reference value. Opposed to the minimal model, tree-level RS corrections to the T-parameter are essentially zero. On the other hand, shifts due to a heavy Higgs boson can not be compensated anymore. Thus, the custodial RS model prefers a light, SM-like Higgs with $m_h < 150\,\text{GeV}$.

One-loop corrections to the S-parameter, arising from Higgs loops in the KK-gauge boson tower, have been calculated in [55]. They are found to be logarithmically UV divergent and scale like $m_W^2/M_{\text{KK}}^2 \ln(\Lambda_{IR}^2/m_h^2)$. For $\Lambda_{IR} \approx$ few TeV, this correction is of the order of the tree-level result. Therefore, low-lying KK scales of $M_{\text{KK}} \approx 1\,\text{TeV}$ seem to be excluded also for the custodial RS model.

5 The holographic approach

In this section, we want to discuss an alternative to KK decomposition, invented in [23]. It is known as holographic approach and features the idea of separating the 5D gauge field from its boundary value, which is kept fixed during the variation of the 5D action. When one inserts the solutions to the (classical) bulk EOM into the 5D action, the latter reduces to a 4D action on the UV boundary. It is said that the bulk has been integrated out. The idea of holography goes back to the conjectured duality between a $3+1$-dimensional $\mathcal{N}=4$ conformal Yang-Mills theory and a supergravity formulated on $AdS_5 \times S^5$ [58]. Taking only a slice of AdS_5, Green's functions of the former in the large N limit can be calculated by mapping the conformal theory on the boundaries of the supergravity [21, 22]. The authors of [59] therefore refer to the method as the boundary-effective action approach. We will give a more detailed discussion at the end of this section.

At this point, we want to state that the holographic approach is not completely equivalent to KK decomposition. This is evident from the solutions $\chi_n^{(\pm)}(t)$ (4.33), which have different (but rather similar) values on the UV brane for different KK numbers n. Therefore, the ansatz of pulling out a common UV boundary value can not lead to exactly the same low-energy theory, that we have discussed above. Naively speaking, it rejects the possibility of having a quantized momentum within the fifth dimension, and therefore corresponds to a classical solution. On the other hand we will learn that the boundary breaking effects due to the presence of the UV brane are small, as they scale like $1/L$.

The holographic approximation nevertheless is a practical tool, which allows for an easy derivation of effective 4D correlator functions. We will demonstrate this for the custodial model.

5.1 Integrating out the bulk

We follow the calculation of [55] and work with the fields $\tilde{A}_M$, V_M defined in (4.9), and X_M. Besides kinetic terms, the action contains the mass term (4.10), as well as mixing terms of the vector components with the respective fifth component of the gauge fields. In addition, there is an IR-brane localized mixing term between the would-be GBs ϕ_a and the fields $\tilde{A}^a_\mu$. Thus, we impose the gauge-fixing Lagrangian

$$\begin{aligned}\mathcal{L}_{\mathrm{GF}} = &-\frac{1}{2\xi}\left(\partial^\mu \tilde{A}^a_\mu - \xi\, M_{\mathrm{KK}}^2\,\frac{\pi}{L}\, t\partial_t\, t^{-2}\tilde{A}^a_5\right)^2 - \delta(t-1)\,\frac{1}{2\xi}\left(\partial^\mu \tilde{A}^a_\mu - \frac{\xi}{2}\, kM_{\tilde{A}}\phi_a\right)^2 \\ &-\frac{1}{2\xi}\left(\partial^\mu V^a_\mu - \xi\, M_{\mathrm{KK}}^2\,\frac{\pi}{L}\, t\partial_t\, t^{-2}V^a_5\right)^2 - \frac{1}{2\xi}\left(\partial^\mu X_\mu - \xi\, M_{\mathrm{KK}}^2\,\frac{\pi}{L}\, t\partial_t\, t^{-2}X_5\right)^2 .\end{aligned} \tag{5.1}$$

Compared to the previous section, we have chosen a separate gauge-fixing for the would-be GBs, as we are not going to expand the latter in a set of orthonormalized KK-profile functions. As a consequence, we can not use the EOMs to cancel δ^2-terms, as we did in (4.28).

In order to solve the classical bulk EOM, it is convenient to change to momentum space for the 4D coordinates[1]. As mentioned above, we will separate the UV boundary value from the gauge fields by writing

$$\tilde{A}^a_\mu = \sqrt{k}\,\tilde{A}^{a\epsilon}_\mu(p)\,f_{\tilde{A}}(p,t)\,,\qquad V^a_\mu = \sqrt{k}\,V^{a\epsilon}_\mu(p)\,f_V(p,t)\,,\qquad X_\mu = \sqrt{k}\,V^\epsilon_\mu(p)\,f_V(p,t)\,. \tag{5.2}$$

Note that we have chosen the same bulk function $f_V(p,t)$ for the fields V_μ and X_μ, as the respective IR BCs are the same,

$$\partial_t V^a_\mu(1) = V^a_5(1) = \partial_t X_\mu(1) = X_5(1) = 0\,. \tag{5.3}$$

The components of the massive 5D vector field $\tilde{A}_M$ satisfy the IR BCs

$$\left(\partial_t + \frac{kM^2_{\tilde{A}}}{2M^2_{\mathrm{KK}}}\right)\tilde{A}^a_\mu(1^-) = \left(\partial_t + L\,\frac{(g_L^2+g_R^2)v^2}{4M^2_{\mathrm{KK}}}\right)\tilde{A}^a_\mu(1^-) = \tilde{A}^a_5(1) = 0\,. \tag{5.4}$$

Inserting the gauge-fixing Lagrangian (5.1) into the action (4.2), and using integration by parts, we obtain

$$\begin{aligned}S = &-\frac{1}{2}\int\frac{d^4p}{(2\pi)^4}\,2\int_\epsilon^1\frac{dt}{k\,t}\left\{\tilde{A}^a_\mu\left(p^2\eta^{\mu\nu} - p^\mu p^\nu\Big(1-\frac{1}{\xi}\Big)\right)\tilde{A}^a_\nu\right.\\ &\left.\qquad + M^2_{\mathrm{KK}}\,\tilde{A}^a_\mu\,t\partial_t\,t^{-1}\,\partial_t\tilde{A}^{a\mu} - \delta(t-1)\,L\,\frac{(g_L^2+g_R^2)v^2}{4}\,\tilde{A}^a_\mu\tilde{A}^{a\mu} + \,\ldots\right\}\\ &+\frac{1}{2}\int\frac{d^4p}{(2\pi)^4}\,\frac{2}{k\,t}\,M^2_{\mathrm{KK}}\left[\tilde{A}^a_\mu\partial_t\tilde{A}^{a\mu} + V^a_\mu\partial_t V^{a\mu} + X_\mu\partial_t X^\mu\right]\Bigg|^1_{t=\epsilon}\end{aligned} \tag{5.5}$$

Due to the BCs (5.3) and (5.4), all IR boundary terms vanish identically or cancel each other. The bulk is integrated out by demanding the fields to fulfill the classical bulk EOM

$$\left(M^2_{\mathrm{KK}}\,t\partial_t\,t^{-1}\partial_t + p^2\right)\tilde{A}^a_\mu(p,t) = 0\quad etc.\,, \tag{5.6}$$

Choosing Feynman gauge ($\xi = 1$), we are left with the effective-boundary action

$$S = -\int\frac{d^4p}{(2\pi)^4}\,M_{\mathrm{KK}}\left(\tilde{A}^a_\mu\partial_t\tilde{A}^{a\mu} + V^a_\mu\partial_t V^{a\mu} + X_\mu\partial_t X^\mu\right)\Bigg|_{t=\epsilon} \tag{5.7}$$

of the gauge fields. The solution to (5.6) is derived in analogy to the bulk profiles. If one normalizes the fields according to $f_{\tilde{A}}(p,\epsilon) = f_V(p,\epsilon) = 1$, and implements the above IR

[1] As a consequence, the mass dimensions of the fields are reduced by four, $[\tilde{A}_\mu(p,t)] = -5/2$, *etc.*.

BCs, one finds [55]

$$
\begin{aligned}
f_V(p,t) &= \frac{t\big[Y_0(x_p)J_1(x_pt) - J_0(x_p)Y_1(x_pt)\big]}{\epsilon\big[Y_0(x_p)J_1(x_p\epsilon) - J_0(x_p)Y_1(x_p\epsilon)\big]}\,, \\
f_{\tilde{A}}(p,t) &= \frac{t\big[\big(pY_0(x_p)+MY_1(x_p)\big)J_1(x_pt) - \big(pJ_0(x_p)+MJ_1(x_p)\big)Y_1(x_pt)\big]}{\epsilon\big[\big(pY_0(x_p)+MY_1(x_p)\big)J_1(x_p\epsilon) - \big(pJ_0(x_p)+MJ_1(x_p)\big)Y_1(x_p\epsilon)\big]}\,,
\end{aligned}
\tag{5.8}
$$

where $p = \sqrt{p^2}$, $x_p = p/M_{\mathrm{KK}}$, and $M = kM_{\tilde{A}}^2/(2M_{\mathrm{KK}})$.

5.2 Low-energy theory

The effective low-energy Lagrangian for the gauge fields is now written in the form

$$
\mathcal{L}_{\mathrm{eff}}^{\mathrm{Gauge}} = \frac{\eta^{\mu\nu}}{2}\Big(\tilde{A}_\mu^{a\epsilon}\Pi_{\tilde{A}\tilde{A}}(p^2)\tilde{A}_\nu^{a\epsilon} + V_\mu^{a\epsilon}\Pi_{VV}(p^2)V_\nu^{a\epsilon} + X_\mu^{\epsilon}\Pi_{VV}(p^2)X_\nu^{\epsilon}\Big)\,, \tag{5.9}
$$

where the correlators are obtained by inserting the solutions (5.8) into the boundary action (5.7). If one uses the identity[2]

$$
\frac{d}{dz}\big[z^nJ_n(z)\big] = z^nJ_{n-1}(z) \tag{5.10}
$$

with $n=1$ and $z = x_pt$, one finds

$$
\begin{aligned}
\Pi_{VV}(p^2) &= -\,kp\,\frac{\big[Y_0(x_p)J_0(x_p\epsilon) - J_0(x_p)Y_0(x_p\epsilon)\big]}{\big[Y_0(x_p)J_1(x_p\epsilon) - J_0(x_p)Y_1(x_p\epsilon)\big]}\,, \\
\Pi_{\tilde{A}\tilde{A}}(p^2) &= -\,kp\,\frac{\big[\big(pY_0(x_p)+MY_1(x_p)\big)J_0(x_p\epsilon) - \big(pJ_0(x_p)+MJ_1(x_p)\big)Y_0(x_p\epsilon)\big]}{\big[\big(pY_0(x_p)+MY_1(x_p)\big)J_1(x_p\epsilon) - \big(pJ_0(x_p)+MJ_1(x_p)\big)Y_1(x_p\epsilon)\big]}\,,
\end{aligned}
\tag{5.11}
$$

For the following discussion, we will drop the superscript ϵ in (5.9) and always assume the fields to be four-dimensional ones. The next step consists of using the field rotations (4.9), (4.14), and (4.16) to write the effective Lagrangian in the form

$$
\mathcal{L}_{\mathrm{eff}}^{\mathrm{Gauge}} = \frac{\eta^{\mu\nu}}{2}\Big(L_\mu^{a=1,2}\Pi_{LL}(p^2)L_\nu^{a=1,2} + Z_\mu\Pi_{ZZ}(p^2)Z_\nu + A_\mu\Pi_{AA}(p^2)A_\nu\Big)\,. \tag{5.12}
$$

One derives

$$
\Pi_{LL} \equiv \Pi_{WW} = s_W^2\Pi_{VV} + c_W^2\Pi_{\tilde{A}\tilde{A}} \quad \Pi_{ZZ} = s_Z^2\Pi_{VV} + c_Z^2\Pi_{\tilde{A}\tilde{A}} \quad \Pi_{AA} = \Pi_{VV}\,, \tag{5.13}
$$

[2] An analogous relation holds for the Bessel functions of second kind.

where the mixing angles are defined in (4.20). If we expand the correlators (5.11) in x_p and, for the case of $\Pi_{\tilde{A}\tilde{A}}$ in v/M_{KK} afterwards, we find to LO (neglecting terms $\propto \epsilon^2$)

$$\begin{aligned} &\Pi_{VV}(p^2) \approx p^2 \Pi'_{VV}(0) = -p^2 L\,, \\ &\Pi_{\tilde{A}\tilde{A}}(p^2) \approx \Pi_{\tilde{A}\tilde{A}}(0) + p^2 \Pi'_{\tilde{A}\tilde{A}}(0) = L\,\frac{(g_L^2+g_R^2)v^2}{4} - p^2 L\left[1 - L\,\frac{(g_L^2+g_R^2)v^2}{8M_{\text{KK}}^2}\right]. \end{aligned} \tag{5.14}$$

Thus, we can easily identify the correlators at zero momentum and their derivatives. Inserting this result into the definitions of the Peskin-Takeuchi parameters (3.39), and using the relations $c_W^2 = c_w^2 c_Z^2$, as well as $s_w^2 c_w^2 c_Z^2/e^2 = c_W^2/g_L^2 = 1/(g_L^2+g_R^2)$, one finally obtains

$$S = \frac{2\pi v^2}{M_{\text{KK}}^2}\,, \qquad T = 0\,, \qquad U = 0\,. \tag{5.15}$$

Up to the tiny $1/L$ corrections, we have re-derived the result (4.56) of the previous section.

The holographic approximation can also be applied to the fermion sector [60]. It has been used for the construction of composite Higgs models [61, 62], where the Higgs is realized as a would-be GB of a strongly coupled four-dimensional conformal field theory (CFT). The latter can be described by means of an effective boundary action of a weakly coupled gravity theory in a slice of AdS_5. Here, the warped ED is introduced as a computing aid to make perturbative calculations within a strongly coupled theory feasible.

Indeed, the concept of holography opened a new branch in theoretical physics. For instance, there are attempts to perform (perturbative) QCD calculations in the region of confinement, where the running of α_s can be neglected. Therefore, it is worth to say a few words about this remarkable correspondence between 4D CFTs and 5D warped models. A very nice and more thorough introduction can be found in [63] for instance.

The original conjecture states that a type IIB string theory on $AdS_5 \times S^5$ is dual to a $\mathcal{N} = 4$ $SU(N)$ 4D Super Yang-Mills theory. The latter has to be a conformal field theory, as the isometry group of AdS_5 is equivalent to the conformal group in four dimensions. If we want to neglect string corrections and rather study a classical gravity theory on AdS_5, the duality relations require that the CFT has to be strongly coupled, and that one assumes a large number of colors.

A purely CFT is invariant under conformal transformations and therefore does not involve a mass scale. As a consequence, its gauge couplings do not run with energy. The invariance of conformal transformations corresponds of having the whole AdS_5 space on the gravity side with $-\infty < \phi < \infty$. If we now locate a UV brane at $\phi = 0$, this introduces a UV cutoff Λ_{UV} on the CFT side, which explicitly breaks conformal invariance. If one runs down to lower energies, the conformal behavior is restored again. Therefore, only higher dimensional operators come in question as symmetry breaking terms [64, 65, 66]. Fields which are located on the UV brane are elementary, and act as source fields when coupled to CFT operators. The introduction of an IR brane on the other hand corresponds to a spontaneous breaking of the conformal symmetry [64, 65], and goes along with an IR cut-off Λ_{IR}. Physical states of the strongly coupled conformal sector in the region of the IR cut-off correspond to composite particles.

At this point, we want to stress again that in AdS/CFT, the dual description of strongly coupled 4D conformal Yang-Mills theories in the large N limit relies on a classical gravity theory. In some sense, the invention of the fifth dimension can be understood as a mathematical trick. In this thesis however, we will assume the fifth dimension to be physical. Therefore, we have to account for all the quantum effects of the bulk, if the fields are assumed to propagate in the whole space-time. Therefore, the method of KK-decomposition is mandatory to obtain the correct low-energy description.

6 Fermions in the bulk

In this section, we want to study fermions in the 5D bulk. The appropriate 5D action has been given in [28] first. Due to the curvature of the fifth dimension, one needs to introduce the inverse vielbein $E_m^M(x)$, defined via the inverse RS metric G^{MN}

$$E_m^M \eta^{mn} E_n^M = G^{MN} = \mathrm{diag}(e^{2\sigma}, -e^{2\sigma}, -e^{2\sigma}, -e^{2\sigma}, -1/r^2)\,. \tag{6.1}$$

As before, capital Latin indices refer to the coordinates of the warped space-time, where $m, n = 0, 1, 2, 3, 5$ refer to the five-dimensional flat space. Within the fermion action, we have to replace $\gamma^\mu \to \gamma^M = E_m^M \gamma^m$. Therefore, the Clifford algebra (1.21) has to be extended according to

$$\{\Gamma_m, \Gamma_n\} = 2\,\eta_{mn} \mathbf{1}_{4\times 4}\,, \tag{6.2}$$

As a consequence, the 5D QFT for fermions is no longer a chiral theory, as the fields can no longer be separated into independent left- and right-handed representations of the Lorentz group[1]. It should be stressed that due the chosen signature $\eta_{mn} = \eta^{mn} = \mathrm{diag}(1, -1, -1, -1, -1)$, one has to distinguish $\gamma^5 = \eta^{55}\gamma_5 = -\gamma_5 = \mathrm{diag}(-\mathbf{1}, \mathbf{1})$. We define $\Gamma^m = (\gamma^\mu, i\gamma^5)$ and $\Gamma_m = (\gamma_\mu, -i\gamma^5) = (\gamma_\mu, i\gamma_5)$. In general, a curved background asks for a spin connection, which has to be added to the partial derivative within the kinetic term $\partial_M \to \partial_M + \omega_M$. For the RS model we find [27]

$$\omega_\mu = -i\,\frac{k}{2}\,\mathrm{sgn}(\phi) e^{\sigma(\phi)} \gamma^5 \gamma_\mu\,, \qquad \omega_5 = 0\,. \tag{6.3}$$

The 4D space-time components of the spin connection are odd under Z_2 orbifold symmetry, and therefore vanish within the integration over the bulk from $-\pi$ to π. The fifth component on the other hand is identical to zero.

Before we are able to proceed, we first have to answer the following question: How can we get a chiral low-energy 4D theory out of a non-chiral 5D one? At this point, the Z_2-parity enters the stage. As already mentioned, it is still possible to define projection operators. Therefore, we may assign different parities to the Dirac spinors Ψ_L and Ψ_R. A crucial point is that only even fields possess a zero mode. Thus, we are able to construct a theory which involves a massless ground state with one specific chirality, and a tower of massive non-chiral Dirac spinors. As we need a massless ground state for both the left-handed and the right-handed fields, we need to introduce a second set of fermions with opposite Z_2-parity assignments [27]. As a consequence, the number of KK modes gets doubled.

[1] Of course, one is still allowed to define projectors $P_{L,R}$ (1.18) in order to write $\Psi = \Psi_L + \Psi_R$, where $\Psi_{L,R}$ are four-component Dirac spinors with the last (first) two elements are equal to zero.

In this thesis, we consider three generations of 5D fermions in the bulk. They are grouped into $SU(2)_L$ doublets Q and singlets u^c and d^c, where each of them is a three-component vector in flavor space. It follows that the KK tower is made up of bunches, each with six KK excitations of similar masses. We will denote these bunches as KK levels in the following.

6.1 Action of the 5D theory

For the purpose of this thesis, we will only study the decomposition of quark fields. The extension to leptons is obvious. After switching to t-notation, and taking into account the IR boundary terms from EWSB[2], the quadratic terms in the 5D action of the minimal RS model can be written in the form[3] [34, 67]

$$\begin{aligned} S_{\text{ferm},2} = & \int d^4x\, r\, \frac{2\pi}{L} \int_\epsilon^1 \frac{dt}{t} \\ & \Bigg\{ \frac{\epsilon^3}{t^3} \Big(\bar{Q}\, i\partial\!\!\!/\, Q + \sum_{q=u,d} \bar{q}^c\, i\partial\!\!\!/\, q^c \Big) - \frac{\epsilon^4}{t^4} \Big(\bar{Q}\, \boldsymbol{M}_Q\, Q + \sum_{q=u,d} \bar{q}^c\, \boldsymbol{M}_q\, q^c \Big) \\ & - k\epsilon^4 t^{-1} \Big[\bar{Q}_L\, \partial_t t^{-2}\, Q_R - \bar{Q}_R\, \partial_t t^{-2}\, Q_L + \sum_{q=u,d} \Big(\bar{q}_L^c\, \partial_t t^{-2}\, q_R^c - \bar{q}_R^c\, \partial_t t^{-2}\, q_L^c \Big) \Big] \\ & - \delta(t-1)\, \frac{\epsilon^3 v}{2\sqrt{2} r} \Big[\bar{u}_L\, \boldsymbol{Y}_u^{(5\text{D})}\, u_R^c + \bar{d}_L\, \boldsymbol{Y}_d^{(5\text{D})}\, d_R^c + \bar{u}_R\, \boldsymbol{Y}_u^{(5\text{D})}\, u_L^c + \bar{d}_R\, \boldsymbol{Y}_d^{(5\text{D})}\, d_L^c + \text{h.c.} \Big] \Bigg\}. \end{aligned} \tag{6.4}$$

Here, $\boldsymbol{M}_{Q,q}$ are diagonal matrices containing the (real) bulk masses, which can be positive or negative. In fact, phenomenology requires that the bulk masses are clustered around the values $M_{Q_i} \approx -k/2$ and $M_{q_i} \approx +k/2$. Note that the choice of diagonal bulk masses is convenient, but not necessary in general. However, as the diagonal structure can always be achieved by appropriate field redefinitions [34], there is no need to study the more complicated case of off-diagonal entries. We will refer to our choice as the bulk-mass basis. The 5D Yukawa matrices $\boldsymbol{Y}_q^{(5\text{D})}$ correspond to the latter basis. Up to them, all other terms in (6.4) are invariant under a basis rotation. In the following, we define the dimensionless 4D Yukawa matrices via

$$\boldsymbol{Y}_q^{(5\text{D})} \equiv \frac{2\boldsymbol{Y}_q}{k}, \qquad q = u, d\,. \tag{6.5}$$

Of course, the latter definition is not unique. For instance, one could define $\boldsymbol{Y}_q' \equiv \boldsymbol{Y}_q^{(5\text{D})}/(2\pi r) = \boldsymbol{Y}_q/L$ [34] in analogy to the relation between the 5D and 4D gauge couplings, which seems to be a more natural choice. The definition (6.5) therefore absorbs a factor L, which appears in the square of the fermion profiles evaluated at the IR brane, as

[2]Here, we have already implemented a rescaling of the Higgs field in order to obtain canonical normalized kinetic terms [19].

[3]We use a superscript c to label $SU(2)_L$ singlets.

we will see in a moment. Nevertheless, we choose the defintion (6.5), as it is common in the literature.

The left-handed (right-handed) components of the $SU(2)_L$ doublet Q are chosen to have even (odd) Z_2-parity. Likewise, the right-handed (left-handed) components of the singlets u^c and d^c are even (odd). As mentioned above, without the Yukawa interactions, each 5D fermion would decompose into a massless Weyl fermion and a tower of massive KK excitations. After EWSB, the Yukawa couplings replace the massless modes by light SM-like fermions.

One may wonder, why we have written down terms of the form $\bar{q}_R \boldsymbol{Y}_u^{(5\mathrm{D})} q_L^c$, which would not be there in the SM. From the 5D point of view, this is just explained by the vector-like nature of 5D quarks. Within the KK decomposition in the presence of EWSB, KK fermions of left-handed $SU(2)_L$ doublets will be mixed with left-handed $SU(2)_L$ singlets. On the other hand, the right-handed singlets will be mixed with right-handed doublets. Moreover, the presence of the Higgs sector will change the bare profiles of the unbroken scenario. The profiles of quark fields become discontinuous at the IR brane [68]. The Z_2-odd profiles of q_R and q_L^c gain a non-vanishing value at $t = 1^-$, while they have to be zero at $t = 1$. Indeed, the treatment of the Higgs couplings to fermions and the derivation of the BCs for the fermionic bulk EOMs, requires a proper regularization of the δ-function [67].

6.2 Kaluza-Klein decomposition

For the following discussion, Dirac spinors in the effective 4D theory are separated according to $q^{(n)} = q_L^{(n)} + q_R^{(n)}$. In formal analogy to the extended gauge boson sector, we introduce three-vectors in flavor space $Q_{L,R}(x,t)$ and $q_{L,R}^c(x,t)$, which are supposed to be decomposed into the same 4D basis of quark fields. We have to discriminate between the left- and right-handed components, as we want them to have different Z_2-parity assignments. At this point one can make use of the fact that the fields $Q_{L,R}(x,t)$ and $q_{L,R}^c(x,t)$ can be expanded in terms of the same three-component mixing vectors $\vec{a}_n^Q$ and $\vec{a}_n^q$, respectively. As a consequence, the Z_2-even and odd profiles are normalized in the same way. Having all this in mind, we write the KK decomposition of the 5D fields in the form [34, 53]

$$\begin{aligned} Q_L(x,t) &= \frac{1}{\sqrt{r}}\,\frac{t^2}{\epsilon^2}\sum_n \boldsymbol{C}_n^Q(t)\,\vec{a}_n^Q\,q_L^{(n)}(x)\,, \quad & Q_R(x,t) &= \frac{1}{\sqrt{r}}\,\frac{t^2}{\epsilon^2}\sum_n \boldsymbol{S}_n^Q(t)\,\vec{a}_n^Q\,q_R^{(n)}(x)\,, \\ q_L^c(x,t) &= \frac{1}{\sqrt{r}}\,\frac{t^2}{\epsilon^2}\sum_n \boldsymbol{S}_n^q(t)\,\vec{a}_n^q\,q_L^{(n)}(x)\,, \quad & q_R^c(x,t) &= \frac{1}{\sqrt{r}}\,\frac{t^2}{\epsilon^2}\sum_n \boldsymbol{C}_n^q(t)\,\vec{a}_n^q\,q_R^{(n)}(x)\,, \end{aligned} \tag{6.6}$$

where $Q = U, D$, $q = u, d$ and we pulled out a factor $e^\sigma = t^2/\epsilon^2$ for convenience. The index n labels the mass eigenstates with fermion masses m_n. The vectors $\vec{a}_n^{Q,q}$ parametrize the flavor mixing of the “bare” fermion profiles, which are collected into the diagonal 3×3 matrices of $\boldsymbol{C}_n^{Q,q}$ and $\boldsymbol{S}_n^{Q,q}$, where each entry refers to a different bulk mass parameter (in the bulk mass basis). Here, the matrices $\boldsymbol{C}_n^{Q,q}$ contain profiles with even Z_2-parity, while

$\boldsymbol{S}_n^{Q,q}$ collect the odd ones. Note that we have to distinguish the associated vectors $\vec{a}_n^U$ and $\vec{a}_n^D$.

Inserting these relations into the action (6.4), and applying the 5D variational principle, one derives the equations of motion [34, 53]

$$\begin{aligned}
\Big(-t\partial_t - c_Q\Big)\,\boldsymbol{S}_n^Q(t)\,\vec{a}_n^Q &= -x_n\,t\,\boldsymbol{C}_n^Q(t)\,\vec{a}_n^Q + \delta(t-1)\,\frac{v}{\sqrt{2}M_{\text{KK}}}\,\boldsymbol{Y}_q\,\boldsymbol{C}_n^q(t)\,\vec{a}_n^q\,,\\
\Big(t\partial_t + c_q\Big)\,\boldsymbol{S}_n^q(t)\,\vec{a}_n^q &= -x_n\,t\,\boldsymbol{C}_n^q(t)\,\vec{a}_n^q + \delta(t-1)\,\frac{v}{\sqrt{2}M_{\text{KK}}}\,\boldsymbol{Y}_q^\dagger\,\boldsymbol{C}_n^Q(t)\,\vec{a}_n^Q\,,\\
\Big(t\partial_t - c_Q\Big)\,\boldsymbol{C}_n^Q(t)\,\vec{a}_n^Q &= -x_n\,t\,\boldsymbol{S}_n^Q(t)\,\vec{a}_n^Q + \delta(t-1)\,\frac{v}{\sqrt{2}M_{\text{KK}}}\,\boldsymbol{Y}_q\,\boldsymbol{S}_n^q(t)\,\vec{a}_n^q\,,\\
\Big(-t\partial_t + c_q\Big)\,\boldsymbol{C}_n^q(t)\,\vec{a}_n^q &= -x_n\,t\,\boldsymbol{S}_n^q(t)\,\vec{a}_n^q + \delta(t-1)\,\frac{v}{\sqrt{2}M_{\text{KK}}}\,\boldsymbol{Y}_q^\dagger\,\boldsymbol{S}_n^Q(t)\,\vec{a}_n^Q\,,
\end{aligned} \tag{6.7}$$

where again $x_n = m_n/M_{\text{KK}}$, and we have defined the dimensionless bulk mass parameters $c_{Q,q} = \pm M_{Q,q}/k$.

For $t \neq 1$, the general solutions [28, 27] to the above equations can be written as linear combinations of Bessel functions. The presence of the source terms on the IR brane dictates the boundary behavior of the fields. Finding the correct IR BCs requires a proper regularization [67]. The most simple possibility consists of replacing the δ-functions appearing in (6.7) by a rectangular function

$$\delta^\eta(t-1) = \begin{cases} \dfrac{1}{\eta}\,, & t \in [1-\eta, 1]\,,\\[2mm] 0\,, & \text{otherwise}\,, \end{cases} \tag{6.8}$$

where the limit $\eta \to 0$ is to be taken at the end. Keeping only terms which may become singular in the infinitesimal range $t \in [1-\eta, 1]$, the EOMs (6.7) close to the IR brane take the simpler form

$$\begin{aligned}
-\partial_t\,\boldsymbol{S}_n^Q(t)\,\vec{a}_n^Q &= \delta^\eta(t-1)\,\frac{v}{\sqrt{2}M_{\text{KK}}}\,\boldsymbol{Y}_q\,\boldsymbol{C}_n^q(t)\,\vec{a}_n^q\,,\\
\partial_t\,\boldsymbol{S}_n^q(t)\,\vec{a}_n^q &= \delta^\eta(t-1)\,\frac{v}{\sqrt{2}M_{\text{KK}}}\,\boldsymbol{Y}_q^\dagger\,\boldsymbol{C}_n^Q(t)\,\vec{a}_n^Q\,,\\
\partial_t\,\boldsymbol{C}_n^Q(t)\,\vec{a}_n^Q &= \delta^\eta(t-1)\,\frac{v}{\sqrt{2}M_{\text{KK}}}\,\boldsymbol{Y}_q\,\boldsymbol{S}_n^q(t)\,\vec{a}_n^q\,,\\
-\partial_t\,\boldsymbol{C}_n^q(t)\,\vec{a}_n^q &= \delta^\eta(t-1)\,\frac{v}{\sqrt{2}M_{\text{KK}}}\,\boldsymbol{Y}_q^\dagger\,\boldsymbol{S}_n^Q(t)\,\vec{a}_n^Q\,.
\end{aligned} \tag{6.9}$$

Combining the first (second) with the fourth (third) relation and using (6.8), we obtain

$$\left[\partial_t^2 - \left(\frac{\boldsymbol{X}_q}{\eta}\right)^2\right]\boldsymbol{S}_n^Q(t) = 0\,, \qquad \left[\partial_t^2 - \left(\frac{\bar{\boldsymbol{X}}_q}{\eta}\right)^2\right]\boldsymbol{S}_n^q(t) = 0\,, \tag{6.10}$$

where

$$\boldsymbol{X}_q \equiv \frac{v}{\sqrt{2}M_{\rm KK}}\sqrt{\boldsymbol{Y}_q\,\boldsymbol{Y}_q^\dagger}\,, \qquad \bar{\boldsymbol{X}}_q \equiv \frac{v}{\sqrt{2}M_{\rm KK}}\sqrt{\boldsymbol{Y}_q^\dagger\,\boldsymbol{Y}_q}\,. \tag{6.11}$$

Imposing the BCs $\boldsymbol{S}_n^{Q,q}(1) = 0$ and matching $\boldsymbol{S}_n^{Q,q}(1-\eta)$ onto the bulk solutions of (6.7), evaluated in the limit $t \to 1^-$, we find that the differential equations (6.10) are solved by

$$\boldsymbol{S}_n^Q(t) = \frac{\sinh\left(\frac{\boldsymbol{X}_q}{\eta}\,(1-t)\right)}{\sinh\left(\boldsymbol{X}_q\right)}\,\boldsymbol{S}_n^Q(1^-)\,, \qquad \boldsymbol{S}_n^q(t) = \frac{\sinh\left(\frac{\bar{\boldsymbol{X}}_q}{\eta}\,(1-t)\right)}{\sinh\left(\bar{\boldsymbol{X}}_q\right)}\,\boldsymbol{S}_n^q(1^-)\,. \tag{6.12}$$

This implies that in the interval $t \in [1-\eta, 1]$ the Z_2-even fermion profiles take the form

$$\boldsymbol{C}_n^Q(t) = \frac{\cosh\left(\frac{\boldsymbol{X}_q}{\eta}\,(1-t)\right)}{\cosh\left(\boldsymbol{X}_q\right)}\,\boldsymbol{C}_n^Q(1^-)\,, \qquad \boldsymbol{C}_n^q(t) = \frac{\cosh\left(\frac{\bar{\boldsymbol{X}}_q}{\eta}\,(1-t)\right)}{\cosh\left(\bar{\boldsymbol{X}}_q\right)}\,\boldsymbol{C}_n^q(1^-)\,. \tag{6.13}$$

Reinserting the solutions (6.12) and (6.13) into (6.9), allows us to determine the IR BCs, which relate the Z_2-even profiles with the odd ones at $t = 1^-$. The resulting expressions read

$$\begin{aligned} \boldsymbol{S}_n^Q(1^-)\,\vec{a}_n^Q &= \frac{v}{\sqrt{2}M_{\rm KK}}\,\boldsymbol{Y}_q\left(\bar{\boldsymbol{X}}_q\right)^{-1}\tanh\left(\bar{\boldsymbol{X}}_q\right)\boldsymbol{C}_n^q(1^-)\,\vec{a}_n^q\,,\\ -\boldsymbol{S}_n^q(1^-)\,\vec{a}_n^q &= \frac{v}{\sqrt{2}M_{\rm KK}}\,\boldsymbol{Y}_q^\dagger\left(\boldsymbol{X}_q\right)^{-1}\tanh\left(\boldsymbol{X}_q\right)\boldsymbol{C}_n^Q(1^-)\,\vec{a}_n^Q\,. \end{aligned} \tag{6.14}$$

Next, we introduce the rescaled Yukawa matrices [53]

$$\tilde{\boldsymbol{Y}}_q \equiv \boldsymbol{f}\left(\frac{v}{\sqrt{2}M_{\rm KK}}\sqrt{\boldsymbol{Y}_{\vec{q}}\boldsymbol{Y}_{\vec{q}}^\dagger}\right)\boldsymbol{Y}_q\,, \qquad \boldsymbol{f}(\boldsymbol{A}) = \boldsymbol{A}^{-1}\tanh\left(\boldsymbol{A}\right)\,, \tag{6.15}$$

which are given by the original ones plus some higher order correction, *i.e.*$\tilde{\boldsymbol{Y}}_q = \boldsymbol{Y}_q + \mathcal{O}(v^2/M_{\rm KK}^2)$. Thus, the IR BCs at $t = 1^-$ are given by

$$\begin{aligned} \boldsymbol{S}_n^Q(1-)\,\vec{a}_n^Q &= \frac{v}{\sqrt{2}M_{\rm KK}}\,\tilde{\boldsymbol{Y}}_q\,\boldsymbol{C}_n^q(1-)\,\vec{a}_n^q\,,\\ -\boldsymbol{S}_n^q(1-)\,\vec{a}_n^q &= \frac{v}{\sqrt{2}M_{\rm KK}}\,\tilde{\boldsymbol{Y}}_q^\dagger\,\boldsymbol{C}_n^Q(1-)\,\vec{a}_n^Q\,. \end{aligned} \tag{6.16}$$

In [53], the same result has been derived in a complete general manner, which does not rely on the concrete choice of the regularization function.

Without the brane-localized Yukawa terms, the profiles $\boldsymbol{C}_n^{(Q,u)}$ and $\boldsymbol{S}_n^{(Q,u)}$ form complete sets of even and odd functions on the orbifold, which can be chosen to obey orthonormality conditions independent from each other [28] . As it turns out, the δ-function terms in the above EOMs (6.7) are inconsistent with these. We thus impose the generalized orthonormality conditions

$$
\begin{aligned}
\frac{2\pi}{L\epsilon}\int_\epsilon^1 dt\, \boldsymbol{C}_m^{(Q,u)}(t)\, \boldsymbol{C}_n^{Q,u}(t) &= \delta_{mn}\,\mathbf{1} + \boldsymbol{\Delta C}_{mn}^{Q,u}\,, \\
\frac{2\pi}{L\epsilon}\int_\epsilon^1 dt\, \boldsymbol{S}_m^{(Q,u)}(t)\, \boldsymbol{S}_n^{Q,u}(t) &= \delta_{mn}\,\mathbf{1} + \boldsymbol{\Delta S}_{mn}^{Q,u}\,,
\end{aligned}
\tag{6.17}
$$

and find that the 4D action reduces to the desired canonical form

$$
S_{\text{ferm},2} = \sum_n \int d^4x \left[\bar{u}^{(n)}(x)\, i\not{\partial}\, u^{(n)}(x) - m_n\, \bar{u}^{(n)}(x)\, u^{(n)}(x)\right], \tag{6.18}
$$

if and only if, in addition to the BCs, the relation

$$
\vec{a}_m^{Q,q\,\dagger}\left(\delta_{mn}\mathbf{1} + \boldsymbol{\Delta C}_{mn}^{Q,q}\right)\vec{a}_n^{Q,q} + \vec{a}_m^{q,Q\,\dagger}\left(\delta_{mn}\mathbf{1} + \boldsymbol{\Delta S}_{mn}^{q,Q}\right)\vec{a}_n^{q,Q} = \delta_{mn} \tag{6.19}
$$

is fulfilled. Without loss of generality, we can choose

$$
\vec{a}_n^{Q\,\dagger}\,\vec{a}_n^{Q} + \vec{a}_n^{q\,\dagger}\,\vec{a}_n^{q} = 1\,, \qquad \vec{a}_m^{Q,q\,\dagger}\,\boldsymbol{\Delta C}_{mn}^{Q,q}\,\vec{a}_n^{Q,q} + \vec{a}_m^{q,Q\,\dagger}\,\boldsymbol{\Delta S}_{mn}^{q,Q}\,\vec{a}_n^{q,Q} = 0\,. \tag{6.20}
$$

This is possible due to the freedom of exchanging normalization factors between the flavor vectors $\vec{a}_n^{Q,q}$ and the corresponding profiles.

The fact that the profiles do not fulfill separate orthonormality conditions is in complete analogy to the situation within the extended gauge sector. Indeed, from (6.19) it is apparent that the vectors

$$
\vec{\psi}_{L_n}(t) = \sqrt{\frac{2\pi}{L\epsilon}}\begin{pmatrix} \boldsymbol{C}_n^{Q}(t)\,\vec{a}_n^{Q} \\ \boldsymbol{S}_n^{q}(t)\,\vec{a}_n^{q}\end{pmatrix} \qquad \text{and} \qquad \vec{\psi}_{R_n}(t) = \sqrt{\frac{2\pi}{L\epsilon}}\begin{pmatrix} \boldsymbol{C}_n^{q}(t)\,\vec{a}_n^{q} \\ \boldsymbol{S}_n^{Q}(t)\,\vec{a}_n^{Q}\end{pmatrix} \tag{6.21}
$$

fulfill the canonical orthonormality relations

$$
\int_\epsilon^1 dt\, \vec{\psi}_{L_m}^{\,\dagger}(t)\,\vec{\psi}_{L_n}(t) = \int_\epsilon^1 dt\, \vec{\psi}_{R_m}^{\,\dagger}(t)\,\vec{\psi}_{R_n}(t) = \delta_{mn}\,. \tag{6.22}
$$

This has to be the case as the corresponding 5D fields are decomposed into the same set of 4D fields (6.6). Opposed to the gauge sector, it is however not sensible to express the theory in terms of the latter objects. The reason is that the components of (6.21) have different gauge quantum numbers with respect to $SU(2)_L$. Therefore, weak interactions will distinct the entries. As a consequence, the corrections to the separate orthonormality relations (6.17) will give rise to observable effects. Therefore, we have to derive explicit expressions for the corretion terms $\boldsymbol{\Delta C}_{mn}^{q,Q}$ and $\boldsymbol{\Delta S}_{mn}^{q,Q}$. With the help of the EOMs, one can show that

$$
m_m\,\boldsymbol{\Delta C}_{mn}^{Q,q} - m_n\,\boldsymbol{\Delta S}_{mn}^{Q,q} = \pm\frac{2}{r}\,\boldsymbol{C}_n^{Q,q}(1^-)\,\boldsymbol{S}_m^{Q,q}(1^-)\,. \tag{6.23}
$$

Using the symmetry of the relations (6.17) in m and n, we obtain for $m \neq n$

$$\begin{aligned}
\boldsymbol{\Delta C}_{mn}^{Q,q} &= \pm\frac{2}{r}\,\frac{m_m\,\boldsymbol{C}_n^{Q,q}(1^-)\,\boldsymbol{S}_m^{Q,q}(1^-) - m_n\,\boldsymbol{C}_m^{Q,q}(1^-)\,\boldsymbol{S}_n^{Q,q}(1^-)}{m_m^2 - m_n^2}\,, \\
\boldsymbol{\Delta S}_{mn}^{Q,q} &= \mp\frac{2}{r}\,\frac{m_m\,\boldsymbol{C}_m^{Q,q}(1^-)\,\boldsymbol{S}_n^{Q,q}(1^-) - m_n\,\boldsymbol{C}_n^{Q,q}(1^-)\,\boldsymbol{S}_m^{Q,q}(1^-)}{m_m^2 - m_n^2}\,.
\end{aligned} \tag{6.24}$$

Finally, using the explicit results for the bulk profiles which are derived in Section 6.3, one finds that

$$\boldsymbol{\Delta C}_{nn}^{Q,q} = -\boldsymbol{\Delta S}_{nn}^{Q,q} = \pm\frac{1}{r m_n}\,\boldsymbol{C}_n^{Q,q}(1^-)\,\boldsymbol{S}_n^{Q,q}(1^-)\,. \tag{6.25}$$

One would naively expect that the extra terms in the generalized orthonormality conditions (6.17) are small corrections of the order v/M_{KK}. However, as we will see below, these terms are of $\mathcal{O}(1)$ for the profiles of the light SM-like fields.

Finally, we want to derive the spectrum from the regularized BCs (6.16). These relations can be written as a system of linear equations for the components of the vectors $\vec{a}_n^{Q,q}$

$$\begin{aligned}
\boldsymbol{S}_n^Q(1^-)\,\vec{a}_n^Q &= -\frac{v^2}{2M_{\text{KK}}^2}\,\tilde{\boldsymbol{Y}}_u\,\boldsymbol{C}_n^q(1^-)\left[\boldsymbol{S}_n^q(1^-)\right]^{-1}\tilde{\boldsymbol{Y}}_u^\dagger\,\boldsymbol{C}_n^Q(1^-)\,\vec{a}_n^Q\,, \\
\boldsymbol{S}_n^q(1^-)\,\vec{a}_n^q &= -\frac{v^2}{2M_{\text{KK}}^2}\,\tilde{\boldsymbol{Y}}_u^\dagger\,\boldsymbol{C}_n^Q(1^-)\left[\boldsymbol{S}_n^Q(1^-)\right]^{-1}\tilde{\boldsymbol{Y}}_u\,\boldsymbol{C}_n^q(1^-)\,\vec{a}_n^q\,,
\end{aligned} \tag{6.26}$$

where we have used that the matrices $\boldsymbol{S}_n^{Q,q}$ are non-singular, such that the inverse matrices exist. The mass eigenvalues x_n are solutions to the equation

$$\det\left(\boldsymbol{1} - \frac{v^2}{2M_{\text{KK}}^2}\left[\boldsymbol{S}_n^Q(1^-)\right]^{-1}\tilde{\boldsymbol{Y}}_q\,\boldsymbol{C}_n^q(1^-)\left[-\boldsymbol{S}_n^q(1^-)\right]^{-1}\tilde{\boldsymbol{Y}}_q^\dagger\,\boldsymbol{C}_n^Q(1^-)\right) = 0\,. \tag{6.27}$$

Once they are known, the eigenvectors $\vec{a}_n^{Q,q}$ follow from (6.26). Note that the latter are complex-valued objects in general.

6.3 Bulk profiles

The explicit form of the profiles $(C_n^{Q,q})_i$ and $(S_n^{Q,q})_i$ associated with bulk mass parameters c_{Q_i,q_i} (with $q = u, d$) has been obtained in [27, 28]. For the following discussion, we will drop the flavor index i. In analogy to the gauge sector, one can derive a Bessel equation, which is solved by

$$\begin{aligned}
C_n^{Q,q}(t) &= \mathcal{N}_n(c_{Q,q})\,\sqrt{\frac{L\epsilon t}{\pi}}\,f_n^+(t, c_{Q,q})\,, \\
S_n^{Q,q}(t) &= \pm\mathcal{N}_n(c_{Q,q})\,\sqrt{\frac{L\epsilon t}{\pi}}\,f_n^-(t, c_{Q,q})\,,
\end{aligned} \tag{6.28}$$

where

$$f_n^{\pm}(t,c) = J_{-\frac{1}{2}-c}(x_n\epsilon)\, J_{\mp\frac{1}{2}+c}(x_n t) \pm J_{\frac{1}{2}+c}(x_n\epsilon)\, J_{\pm\frac{1}{2}-c}(x_n t)\,. \tag{6.29}$$

If we would perform our calculations using the coordinate $\phi \in [-\pi,\pi]$, we would have to include a factor $\mathrm{sgn}(\phi)$ to the odd profiles. In t-notation, integrants with overall odd Z_2-parity like $C_m^{Q,q}(t)\, S_n^{Q,q}(t)$ have to be set to zero, as long as those expressions are not evaluated by means of a δ-function. From the orthonormality relations (6.17) it follows that

$$2\int_\epsilon^1 dt\, t\, \big[f_n^{\pm}(t,c)\big]^2 = \frac{1}{\mathcal{N}_n^2(c)} \pm \frac{f_n^+(1^-,c)\, f_n^-(1^-,c)}{x_n}\,, \tag{6.30}$$

and the normalization factor in (6.28) is given by

$$\begin{aligned}\mathcal{N}_n^{-2}(c) = {}& \big[f_n^+(1^-,c)\big]^2 + \big[f_n^-(1^-,c)\big]^2 - \frac{2c}{x_n}\, f_n^+(1^-,c)\, f_n^-(1^-,c) \\ & - \epsilon^2\Big(\big[f_n^+(\epsilon,c)\big]^2 + \big[f_n^-(\epsilon^+,c)\big]^2 \Big)\,.\end{aligned} \tag{6.31}$$

For the odd fermion profiles of the minimal model, the last term in the latter expression vanishes due to the UV BC. The custodial RS model however may contain odd fermion profiles with a non-vanishing UV boundary value at the point $\epsilon^+ \equiv \lim_{\theta\to 0^+}(\epsilon+\theta)$. For the special cases where $c+1/2$ is an integer, the profiles must be obtained by a limiting procedure.

As even the top-quark is much lighter than the KK scale, it is a very good approximation to expand the above results in $x_n \ll 1$ for all the zero modes. We find

$$\begin{aligned} C_n^{Q,q}(t) &\approx \sqrt{\frac{L\epsilon}{\pi}}\, F(c_{Q,q})\, t^{c_{Q,q}}\,, \\ S_n^{Q,q}(t) &\approx \pm\sqrt{\frac{L\epsilon}{\pi}}\, x_n F(c_{Q,q})\, \frac{t^{1+c_{Q,q}} - \epsilon^{1+2c_{Q,q}}\, t^{-c_{Q,q}}}{1+2c_{Q,q}}\,, \end{aligned} \tag{6.32}$$

where we have introduced the "zero-mode profile" [27, 28] on the IR brane

$$F(c) \equiv \mathrm{sgn}[\cos(\pi c)]\sqrt{\frac{1+2c}{1-\epsilon^{1+2c}}}\,. \tag{6.33}$$

The sign factor in (6.33) is chosen such that the signs in (6.32) agree with those derived from the exact profiles (6.28). The bulk-mass parameter c controls the localization of the fermions within the bulk. For $c < -1/2$, the profiles are UV-localized, while they grow towards the IR brane for $c > -1/2$. The quantity $F(c)$ decreases exponentially with increasing UV-localization of the fermions, where it is $\mathcal{O}(1)$ for IR-localized ones. Explicitly we find the behavior

$$F(c) \approx \begin{cases} -\sqrt{-1-2c}\; \epsilon^{-c-\frac{1}{2}}\,, & -3/2 < c < -1/2\,, \\ \sqrt{1+2c}\,, & -1/2 < c < 1/2\,. \end{cases} \tag{6.34}$$

The latter observation is crucial for the suppression of dangerous four-fermion operators. As it turns out, all KK-modes (fermions and gauge bosons) are localized towards the IR brane. As a consequence, KK-gauge boson couplings to light quarks ($c < -1/2$) will always receive an exponential suppression, and therefore minimize NP corrections within light-quark interactions. This is known as RS-GIM mechanism [69, 70]. From now on, we will refer to the first order in the expansion of the exact profiles in terms of $x_n \ll 1$ as the zero-mode approximation (ZMA). The so-obtained expressions agree with those of the perturbative approach, where one first solves the bulk EOMs (6.7) without the Yukawa couplings and then treats the latter as a perturbation [28, 27, 71].

6.4 Hierarchies of fermion masses and mixings

In order to study the mixing among different fermion generations, we need the profiles evaluated at the IR brane. We start our analysis with the zero modes and show how the hierarchical quark-mass pattern of the SM can be obtained from $\mathcal{O}(1)$ input parameters. Therefore, we apply the ZMA and insert the IR boundary values

$$C_n^{(Q,q)}(1^-) = \sqrt{\frac{L\epsilon}{\pi}}\, F(c_{Q,q})\,, \qquad S_n^{(Q,q)}(1^-) = \pm\sqrt{\frac{L\epsilon}{\pi}}\, \frac{x_n}{F(c_{Q,q})}\,. \tag{6.35}$$

into the BCs (6.16). These can now be written as

$$\frac{\sqrt{2}\, m_n}{v}\, \hat{a}_n^Q = \boldsymbol{Y}_u^{\text{eff}}\, \hat{a}_n^q\,, \qquad \frac{\sqrt{2}\, m_n}{v}\, \hat{a}_n^q = (\boldsymbol{Y}_q^{\text{eff}})^\dagger\, \hat{a}_n^Q\,, \tag{6.36}$$

with $n = 1, 2, 3$, where the effective Yukawa matrices

$$\boldsymbol{Y}_q^{\text{eff}} \equiv \text{diag}\left[F(c_{Q_i})\right] \tilde{\boldsymbol{Y}}_q\, \text{diag}\left[F(c_{q_j})\right] = \frac{\sqrt{2}}{v}\, \boldsymbol{U}_q\, \text{diag}\left[m_{q1}, m_{q2}, m_{q3}\right] \boldsymbol{W}_q^\dagger \tag{6.37}$$

factorize into a product of zero-mode profiles and rescaled Yukawa couplings $(\tilde{\boldsymbol{Y}}_q)_{ij}$. As we will explain below, the latter can taken to be anarchic $\mathcal{O}(1)$ complex numbers within the RS model. The rescaled vectors $\hat{a}_n^A \equiv \sqrt{2}\, \vec{a}_n^A$ obey the normalization conditions

$$\hat{a}_n^{Q\dagger}\, \hat{a}_n^Q = \hat{a}_n^{q\dagger}\, \hat{a}_n^q = 1\,. \tag{6.38}$$

From (6.36), we thus obtain the simple equations

$$\left(m_n^2\, \mathbf{1} - \frac{v^2}{2}\, \boldsymbol{Y}_q^{\text{eff}}\, (\boldsymbol{Y}_q^{\text{eff}})^\dagger\right) \hat{a}_n^Q = 0\,, \qquad \left(m_n^2\, \mathbf{1} - \frac{v^2}{2}\, (\boldsymbol{Y}_q^{\text{eff}})^\dagger\, \boldsymbol{Y}_q^{\text{eff}}\right) \hat{a}_n^q = 0\,. \tag{6.39}$$

The mass eigenvalues are the solutions to

$$\det\left(m_n^2\, \mathbf{1} - \frac{v^2}{2}\, \boldsymbol{Y}_q^{\text{eff}}\, (\boldsymbol{Y}_q^{\text{eff}})^\dagger\right) = 0\,. \tag{6.40}$$

Notice that in the ZMA, but not in general, the vectors a_m^A and $\hat{a}_n^A$ with $m \neq n$ are orthogonal on each other.

The eigenvectors $\hat{a}_n^Q$ and $\hat{a}_n^q$ of the matrices $\boldsymbol{Y}_q^{\rm eff} \left(\boldsymbol{Y}_q^{\rm eff}\right)^\dagger$ and $\left(\boldsymbol{Y}_q^{\rm eff}\right)^\dagger \boldsymbol{Y}_q^{\rm eff}$ form the columns of the unitary matrices $\boldsymbol{U}_q$ and $\boldsymbol{W}_q$ appearing in the singular-value decomposition introduced in (6.37). It follows that in the ZMA, the transformation between the SM-like weak interaction eigenstates and mass eigenstates is provided by the matrices $\boldsymbol{U}_q$ and $\boldsymbol{W}_q$. The former apply to the $SU(2)_L$ doublets with bulk mass parameters c_{Q_i}, the latter to singlets with masses c_{q_i}. Thus, to the zeroth order in $v/M_{\rm KK}$, the CKM mixing matrix is given by

$$\boldsymbol{V}_{\rm CKM} = \boldsymbol{U}_u^\dagger \, \boldsymbol{U}_d \,. \tag{6.41}$$

Due to the expression (6.37), the RS model has a build-in Froggatt-Nielsen mechanism [72]. The latter relates hierarchies in the quark-mass pattern to those appearing in the CKM matrix, provided there is a theory of flavor, which gives rise to a factorizing Yukawa structure. In our case, the hierarchies of the quark masses can be adsorbed into the zero-mode profiles by an appropriate choice of the bulk mass parameters. Due to the exponential behavior for $c < -1/2$ (6.34), we can generate light quark masses with $\mathcal{O}(1)$ Yukawa couplings for bulk mass parameters slightly below $-1/2$. The mass of the top quark is of the order of the EW scale[4], and therefore should not receive a suppression due to its profile. As a consequence, the latter should be IR localized.

Let us now understand, how the warped-space Froggatt-Nielsen mechanism [70, 34] works: The products of up- and down-type quark masses is obtained from the determinant of the equation (6.37),

$$\begin{aligned} m_u \, m_c \, m_t &= \frac{v^3}{2\sqrt{2}} \left|\det\left(\boldsymbol{Y}_u\right)\right| \prod_{i=1,2,3} \left|F(c_{Q_i}) \, F(c_{u_i})\right| , \\ m_d \, m_s \, m_b &= \frac{v^3}{2\sqrt{2}} \left|\det\left(\boldsymbol{Y}_d\right)\right| \prod_{i=1,2,3} \left|F(c_{Q_i}) \, F(c_{d_i})\right| , \end{aligned} \tag{6.42}$$

where one uses $\det(\boldsymbol{U}_q) = \det(\boldsymbol{W}_q) = 1$. If we assume a little hierarchy in the bulk mass parameters, giving rise to a sizable hierarchy in

$$|F(c_{A_1})| < |F(c_{A_2})| < |F(c_{A_3})| \,, \tag{6.43}$$

we can consistently evaluate all the eigenvalues to leading order in hierarchies. Thus, we obtain

$$\begin{aligned} m_u &= \frac{v}{\sqrt{2}} \frac{|\det(\boldsymbol{Y}_u)|}{|(M_u)_{11}|} \left|F(c_{Q_1})F(c_{u_1})\right| , & m_d &= \frac{v}{\sqrt{2}} \frac{|\det(\boldsymbol{Y}_d)|}{|(M_d)_{11}|} \left|F(c_{Q_1})F(c_{d_1})\right| , \\ m_c &= \frac{v}{\sqrt{2}} \frac{|(M_u)_{11}|}{|(Y_u)_{33}|} \left|F(c_{Q_2})F(c_{u_2})\right| , & m_s &= \frac{v}{\sqrt{2}} \frac{|(M_d)_{11}|}{|(Y_d)_{33}|} \left|F(c_{Q_2})F(c_{d_2})\right| , \\ m_t &= \frac{v}{\sqrt{2}} \left|(Y_u)_{33}\right| \left|F(c_{Q_3})F(c_{u_3})\right| , & m_b &= \frac{v}{\sqrt{2}} \left|(Y_d)_{33}\right| \left|F(c_{Q_3})F(c_{d_3})\right| , \end{aligned} \tag{6.44}$$

[4]Indeed, within the SM the top-quark mass is the only one which seems to be natural, as the required Yukawa coupling is $\mathcal{O}(1)$. The existence of light quark masses is part of what is called the “flavor puzzle” today.

where $(M_q)_{ij}$ denotes the minor of $\boldsymbol{Y}_q$, *i.e.*, the determinant of the square matrix formed by removing the i^{th} row and the j^{th} column from $\boldsymbol{Y}_q$.

To leading order in hierarchies, the elements of the matrices $\boldsymbol{U}_q$ and $\boldsymbol{W}_q$ are given by

$$(U_q)_{ij} = (u_q)_{ij} \begin{cases} \dfrac{F(c_{Q_i})}{F(c_{Q_j})}, & i \le j\,, \\[2ex] \dfrac{F(c_{Q_j})}{F(c_{Q_i})}, & i > j\,, \end{cases} \qquad (W_q)_{ij} = (w_q)_{ij}\, e^{i\phi_j} \begin{cases} \dfrac{F(c_{q_i})}{F(c_{q_j})}, & i \le j\,, \\[2ex] \dfrac{F(c_{q_j})}{F(c_{q_i})}, & i > j\,. \end{cases} \tag{6.45}$$

The non-hierarchical entries of the matrices $\boldsymbol{u}_q$ and $\boldsymbol{w}_q$, as well as the phase factor $e^{i\phi_j}$, are given in [34]. There, we also collect approximate expressions for the Wolfenstein parameters

$$\lambda = \frac{|V_{us}|}{\sqrt{|V_{ud}|^2 + |V_{us}|^2}}, \qquad A = \frac{1}{\lambda}\left|\frac{V_{cb}}{V_{us}}\right|, \qquad \bar{\rho} - i\bar{\eta} = -\frac{V_{ud}^* V_{ub}}{V_{cd}^* V_{cb}}\,, \tag{6.46}$$

in terms of zero-mode profiles and entries of the up- and down-type Yukawa matrices $\tilde{\boldsymbol{Y}}_u$ and $\tilde{\boldsymbol{Y}}_d$. These, in combination with (6.44), can be used for the generation of RS parameter sets consisting of bulk masses and the Yukawa matrices, which reproduce the observed masses and CKM structure. As an example, we quote the scaling behavior of the $SU(2)_L$ doublet profiles in terms of the parameter $\lambda \approx 0.225$,

$$\frac{|F(c_{Q_1})|}{|F(c_{Q_2})|} \sim \lambda\,, \quad \frac{|F(c_{Q_2})|}{|F(c_{Q_3})|} \sim \lambda^2\,, \quad |F(c_{Q_3})| \sim \mathcal{O}(1)\,. \tag{6.47}$$

The related ratios of the singlet profiles can be obtained from (6.47) with the help of (6.44). The ZMA formulas (6.44) and the expressions for the CKM parameters given in [34] are used for the random generation of RS parameter sets. It is interesting to note that to LO order, the size of the chosen KK scale has no impact on the spectrum and the quark mixing. It is solely controlled by the localization pattern and the choice of Yukawa couplings.

Finally, we want to discuss the mass spectrum and flavor mixing of KK modes. Therefore, we make use of the exact relations derived in the previous subsections. As an example, we study the first level of KK quarks numerically, using default parameters given in Appendix A.1 and assuming $M_{\text{KK}} = 2\,\text{TeV}$. Due to the existence of two fermion sets with opposite Z_2-parity assignments, we obtain six mass states for each KK-level in each sector. In Figure 6.1 we compare the exact mass spectrum of these states with the spectrum obtained without Yukawa couplings. The "undisturbed states" correspond to pure $SU(2)_L$ doublets and singlets, labeled by Q_1, Q_2, Q_3 and u, c, t or d, s, b, respectively. The Yukawa couplings induce mixings between fields with different flavor and $SU(2)_L$ quantum numbers, which are visualized by the bar charts at the bottom of each panel. The area of each colored region is proportional to the square of the absolute value of the corresponding entry in the mixing vectors $\vec{a}_{4-9}^{(U,D)}$ and $\vec{a}_{4-9}^{(u,d)}$, which appear in the KK decomposition (6.6) of the fermion fields.

Naively, one might expect the flavor mixings between KK fermions to be small, as the KK scale is much larger than the Higgs vacuum expectation value. However, as it is evident

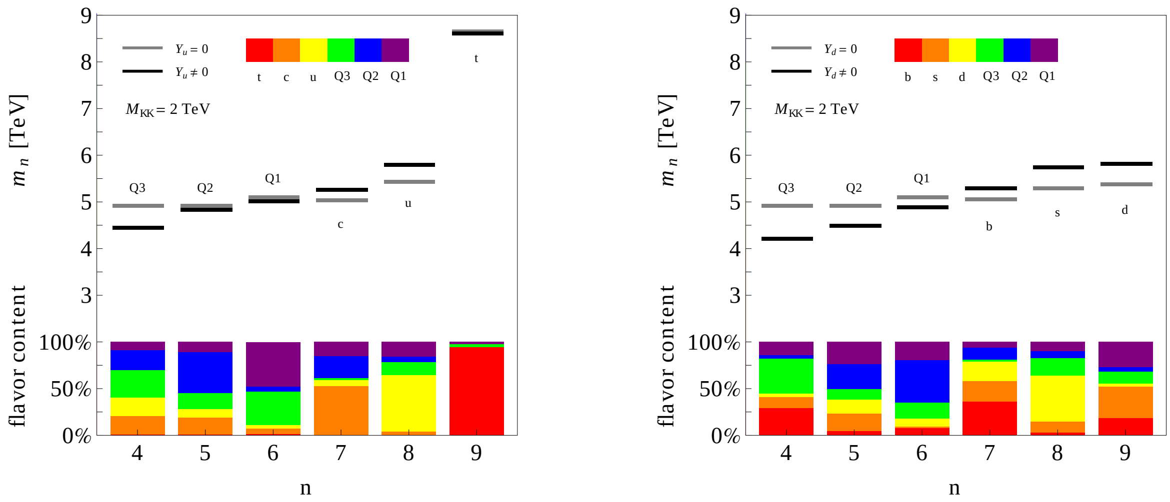

Figure 6.1: Mass spectrum of the first KK excitations of the up- (left) and down-type (right) quarks. Black lines show the exact masses, while gray lines show the masses obtained by switching off the Yukawa couplings. The mixings of the mass eigenstates are visualized by the bar charts at the bottom of each panel. See text for details.

from Figure 6.1, we find $\mathcal{O}(1)$ mixing effects. This is explained by the near degeneracy of the 5D bulk masses of the corresponding fermion fields. The mass splittings of the undisturbed KK states turn out to be of order of the Higgs VEV v. Therefore, the latter induces $\mathcal{O}(1)$ mixings among the KK excitations of the same KK level. The top singlet is an exception due to its strong IR localization. As a consequence, its bare KK mass differs from the others about some TeV, and is close to the masses of the next KK level. The related flavor mixing is therefore at the percent level of the order v^2/M_{KK}^2. Note that in our reference point, we have chosen a rather large bulk mass $c_{t_R} = 0.874$. One could also choose a negative value, as long as it is larger than $-1/2$. The fact that the zero-mode profiles behave like $\sqrt{1+c}$ in the infra-red region (opposed to the exponential scaling behavior in the ultra-violet) allows for a big scattering range.

The generation mixing of KK modes is an important example where the approach of treating the Yukawa couplings as a small perturbation is inadequate in general. On the other hand, we have shown explicitly that the spectrum can be reproduced perturbatively to good approximation [32]. This is achieved by solving the bulk EOM (6.7) without Yukawa couplings, which are then introduced as interactions afterwards. The resulting mass matrix is then diagonalized for a truncated basis of KK-states [73].

	Q	Q_X	Y	T_L^3	T_R^3
$u_L^{(+,+)}$	2/3	1/6	1/6	1/2	0
$d_L^{(+,+)}$	−1/3	1/6	1/6	−1/2	0
$u_R^{c\,(+,+)}$	2/3	1/6	1/6	0	−1/2

	Q	Q_X	Y	T_L^3	T_R^3
$d_R^{\prime\,(-,+)}$	−1/3	1/6	1/6	0	1/2
$u_R^{\prime\,(-,+)}$	2/3	1/6	1/6	0	−1/2
$d_R^{c\,(+,+)}$	−1/3	1/6	1/6	0	1/2

Table 6.1: Charge assignments of the different quark fields in the left-right symmetric custodial RS model. Of course, the same values hold for the Z_2-odd counterparts.

6.5 Embeddings into the custodial gauge group

We will now give a short discussion of possible fermion embeddings into the extended gauge group (4.1) of the custodial RS model. Here, one has to carefuly distinguish between the chiralities L, R of the quark fields, and the gauge-group charge assignments. These are labeled by the same capital letters, but have a different theoretical meaning. Of course, within the SM the left-handed quark is taken to be charged under $SU(2)_L$, while the right-handed is not. As the RS model deals with heavy vector-like particles, one has, already in the minimal model, both chiralities coupled to one specific gauge group. The presence of a gauged $SU(2)_R$ may therefore lead to additional confusion.

Coming back to the possibilities of embeddings, one may choose all left-handed quark fields, which have zero mode in the weak-interaction basis, to be doublets (singlets) under $SU(2)_L$ ($SU(2)_R$). Fields with a right-handed zero-mode are taken to be doublets under $SU(2)_R$ and singlets under $SU(2)_L$. This left-right symmetric assignment has been used in [88] recently, for instance. The covariant derivative (4.6) implies the relation

$$Q = T_L^3 - T_R^3 + Q_X = T_L^3 + Y\,, \tag{6.48}$$

and fixes the quantum numbers of the other fields uniquely. The following multiplet structure for the quark fields of even (first line) and odd (second line) Z_2-parity is observed:

$$\begin{gathered}
\mathcal{Q}_L \equiv \begin{pmatrix} u_L^{(+,+)} \\ d_L^{(+,+)} \end{pmatrix}_{\frac{1}{6}}\,, \qquad U_R \equiv \Big(d_R^{\prime\,(-,+)}, u_R^{c\,(+,+)}\Big)_{\frac{1}{6}}\,, \qquad D_R \equiv \Big(d_R^{c\,(+,+)}, u_R^{\prime\,(-,+)}\Big)_{\frac{1}{6}}\,, \\
\mathcal{Q}_R \equiv \Big(d_L^{(-,-)}, u_R^{(-,-)} \Big)_{\frac{1}{6}}\,, \qquad U_L \equiv \begin{pmatrix} u_L^{c\,(-,-)} \\ d_L^{\prime\,(+,-)} \end{pmatrix}_{\frac{1}{6}}\,, \qquad D_L \equiv \begin{pmatrix} u_L^{\prime\,(+,-)} \\ d_L^{c\,(-,-)} \end{pmatrix}_{\frac{1}{6}}\,.
\end{gathered} \tag{6.49}$$

The $SU(2)_L$ transformations act vertically, while the $SU(2)_R$ transformations act horizontally on the multiplets. All quark fields are understood to be three-vectors in flavor space. The superscripts specify the type of BCs on the UV/IR boundary for the respective chirality, which have been chosen such to obtain the desired low-energy spectrum. As in the gauge sector, we denote Neumann BCs by (+) and Dirichlet BCs by (−). The subscripts

	Q	Q_X	Y	T_L^3	T_R^3
$u_L^{(+)}$	$2/3$	$2/3$	$1/6$	$1/2$	$1/2$
$d_L^{(+)}$	$-1/3$	$2/3$	$1/6$	$-1/2$	$1/2$
$\lambda_L^{(-)}$	$5/3$	$2/3$	$7/6$	$1/2$	$-1/2$
$u_L^{\prime(-)}$	$2/3$	$2/3$	$7/6$	$-1/2$	$-1/2$

	Q	Q_X	Y	T_L^3	T_R^3
$u_R^{c\,(+)}$	$2/3$	$2/3$	$2/3$	0	0
$\Lambda_R^{\prime(-)}$	$5/3$	$2/3$	$2/3$	1	0
$U_R^{\prime(-)}$	$2/3$	$2/3$	$2/3$	0	0
$D_R^{\prime(-)}$	$-1/3$	$2/3$	$2/3$	-1	0

	Q	Q_X	Y	T_L^3	T_R^3
$D_R^{(+)}$	$-1/3$	$2/3$	$-1/3$	0	1
$U_R^{(-)}$	$2/3$	$2/3$	$2/3$	0	0
$\Lambda_R^{(-)}$	$5/3$	$2/3$	$5/3$	0	-1

Table 6.2: Charge assignments of the different quark fields in the extended custodial model.

correspond to the $U(1)_X$ charges, where the charge under $U(1)_{\text{e.m.}}$ is evident from the naming of the quark fields. The quantum numbers are summarized in Table 6.1. Altogether there are nine different quark fields in the up and down sector, respectively. Due to the BCs, there will be six light modes in each sector, three left-handed $SU(2)_L$ doublets and three right-handed $SU(2)_L$ singlets. These are to be identified with the SM quarks. The three zero modes of a given chirality are accompanied by KK towers, which contain nine modes of similar masses at each KK level.

A much more popular though more complicated embedding has been proposed in [24], where the authors achieved a protection of the $Z^0 b_L \bar{b}_L$ vertex from vast corrections by an appropriate choice of the gauge quantum numbers of the third generation. The left-handed $SU(2)_L$ doublet of the SM is extended to a bi-doublet under $SU(2)_L \times SU(2)_R$. The left-handed bottom quark has isospin quantum numbers $T_L^3 = -T_R^3 = -1/2$. This fixes the quantum numbers of the other fields uniquely and implies the following multiplet structure for the quark fields with even Z_2 parity:

$$\begin{aligned} Q_L &\equiv \begin{pmatrix} u_L^{(+,+)}{}_{\frac{2}{3}} & \lambda_L^{(-,+)}{}_{\frac{5}{3}} \\ d_L^{(+,+)}{}_{-\frac{1}{3}} & u_L^{\prime(-,+)}{}_{\frac{2}{3}} \end{pmatrix}_{\frac{2}{3}} , \qquad u_R^c \equiv \left(u_R^{c\,(+,+)}{}_{\frac{2}{3}} \right)_{\frac{2}{3}} , \\ \mathcal{T}_R \equiv \mathcal{T}_{1R} \oplus \mathcal{T}_{2R} &\equiv \begin{pmatrix} \Lambda_R^{\prime(-,+)}{}_{\frac{5}{3}} \\ U_R^{\prime(-,+)}{}_{\frac{2}{3}} \\ D_R^{\prime(-,+)}{}_{-\frac{1}{3}} \end{pmatrix}_{\frac{2}{3}} \oplus \left(D_R^{(+,+)}{}_{-\frac{1}{3}} \; U_R^{(-,+)}{}_{\frac{2}{3}} \; \Lambda_R^{(-,+)}{}_{\frac{5}{3}} \right)_{\frac{2}{3}} . \end{aligned} \tag{6.50}$$

Here, we have chosen the same $SU(2)_L \times SU(2)_R$ representations for all three generations, in order to consistently incorporate quark mixing in the fully anarchic approach to flavor in WEDs. The choice of the parities is again motivated by the low-energy spectrum of the theory. The quantum numbers of the quark fields are summarized in Table 6.2. The right-handed down-type quarks have to be embedded in a $SU(2)_R$ triplet in order to arrive at an $U(1)_X$-invariant Yukawa coupling [54]. Altogether, the embedding (6.50) features 15 different quark fields in the up-type and nine in the down-type sector. Moreover one also has a KK tower of exotic fermion fields of electric charge 5/3, which has nine excitations in each level. In addition to (6.50) we have a second set of multiplets, belonging to the components of opposite chirality. The corresponding states have opposite BCs and Z_2-parity assignments. In particular, they all obey Dirichlet BCs at the IR brane and do not posses a zero mode in the weak-interaction basis. The mechanism of the custodial protection of the $Z^0 b_L \bar{b}_L$ vertex is discussed in the next section, where we study gauge couplings to fermions.

At this point, we want to shortly explain, how the analysis of the decomposition within the minimal model is extended to fermions in the custodial one. By virtue of our exact treatment, the generalization is straightforward. To get started, one collects all fields which should be decomposed into the same basis of 4D fields (that is states with equal chirality and electric charge) into a common 5D vector. Within the left-right symmetric model for instance, we define

$$\vec{U} \equiv u \,, \quad \vec{u} \equiv \begin{pmatrix} u^c \\ u' \end{pmatrix} , \quad \vec{D} \equiv d \,, \quad \vec{d} \equiv \begin{pmatrix} d' \\ d^c \end{pmatrix} . \tag{6.51}$$

In the extended custodial model, we obtain

$$\vec{U} \equiv \begin{pmatrix} u \\ u' \end{pmatrix} , \quad \vec{u} \equiv \begin{pmatrix} u^c \\ U' \\ U \end{pmatrix} , \quad \vec{D} \equiv d \,, \quad \vec{d} \equiv \begin{pmatrix} D \\ D' \end{pmatrix} , \quad \vec{\Lambda} \equiv \lambda \,, \quad \vec{\lambda} \equiv \begin{pmatrix} \Lambda' \\ \Lambda \end{pmatrix} . \tag{6.52}$$

The KK decomposition is now performed into analogy to (6.6), where the diagonal profile matrices and the flavor mixing vectors have to be replaced by larger objects, if required. For the latter representation, this has been explicitly done in [53]. We are therefore not going to repeat the whole analysis again, but rather close this section with some useful remarks.

The profiles of the $(+,+)$ fields in (6.51) and (6.52) are given by the Z_2-even solution in (6.28). We rename the solution $f_n^{(+)+}(t,c) \equiv f_n^{+}(t,c)$, where the plus sign in brackets denotes the type of the UV BC. Though they are even, the profiles of the $(-,+)$ fields satisfy the UV BC of "ordinary" Z_2-odd fields. The solution of the former is denoted by $f_n^{(-)+}(t,c)$, where the solution of the latter is $f_n^{(+)-}(t,c) \equiv f_n^{-}(t,c)$. Here, the plus sign in brackets refers to the UV BC of the related even profile. In other words, all fields that are present in the minimal model carry a superscript $(+)$. Furthermore, we have odd solutions with Neumann UV BC $f_n^{(-)-}(t,c)$, where $(-)$ refers to the Dirichlet BC of the related even profile. Although this notation may seem to be confusing at first sight, it turns out to be very convenient, as it allows for a compact notation for many calculations. If we define the bulk mass parameters in analogy to the minimal model as $c_Q = M_Q/k$, and $c_A = -M_A/k$ for $A = u^c, \mathcal{T}_1, \mathcal{T}_1$, we find that the $(-)$ fields have to be related to the known $(+)$ fields by the equalities

$$f_n^{(+)+}(t,c) = f_n^{(-)-}(t,-c) \,, \qquad \text{and} \qquad f_n^{(+)-}(t,c) = -f_n^{(-)+}(t,-c) \,. \tag{6.53}$$

By inspection of the zero-mode solutions (6.32) we conclude that within the mass eigenbasis, the profiles of the additional even fermions are suppressed by x_n. The profiles of the additional odd solutions on the other hand do not receive such a suppression. However, as it turns out, there is a factor x_n in the ZMA expression of the respective entries of the generalized flavor mixing matrices. Thus, any corrections to light-fermion interactions caused by the additional heavy states receives a chiral suppression $m_n m_{n'}/v^2$ times the usual $v^2/M_{\rm KK}^2$ RS factor. The interested reader is referred to our paper [53], where all analytic results have been given. If we however study processes with KK fermions in the loop, such as Higgs production via gluon fusion, the high multiplicity of states will give rise to sizable effects.

7 Gauge interactions with fermions

In this section we work out the various gauge couplings to quarks. The results can applied to leptons by obvious replacements of the gauge quantum numbers. Considering the Z^0 coupling, we reexamine how a custodial protection for left-handed down type quarks (and right-handed up-type quarks [74]) can be achieved for equal gauge couplings $g_L = g_R$ and the embedding (6.50). The phenomenological impact of neutral currents within the minimal RS model has been studied in great detail in [38]. For the custodial model, $\Delta F = 2$ processes have been examined in [74]. Recently, we have studied the effective Hamiltonian of the charged-current sector for both models, where the possibility of right-handed charged currents is taken into account [53, 75]. We will present the latter analysis here and derive the generalized quark mixing matrices.

7.1 Fermion couplings to gluons, photons, and KK excitations

As a start, we will examine the gauge couplings for the cases without symmetry breaking, that is the photon and the gluon couplings. The 4D QCD Lagrangian contains the terms

$$\begin{aligned}\mathcal{L}_{4\text{D}} \ni \sum_{k,m,n} \Big\{ &\left[\vec{a}_m^{Q\dagger}\, \boldsymbol{I}_{kmn}^{C(Q)}\, \vec{a}_n^{Q} + \vec{a}_m^{q\dagger}\, \boldsymbol{I}_{kmn}^{S(q)}\, \vec{a}_n^{q}\right] \bar{q}_L^{(m)} g_s \slashed{A}^{(k)a}\, t^a\, q_L^{(n)} \\ &+ \left[\vec{a}_m^{q\dagger}\, \boldsymbol{I}_{kmn}^{C(q)}\, \vec{a}_n^{q} + \vec{a}_m^{Q\dagger}\, \boldsymbol{I}_{kmn}^{S(Q)}\, \vec{a}_n^{Q}\right] \bar{q}_R^{(m)} g_s \slashed{A}^{(k)a}\, t^a\, q_R^{(n)} \Big\}\,,\end{aligned} \tag{7.1}$$

where we have defined the overlap integrals

$$\boldsymbol{I}_{kmn}^{C(A)} = \frac{2\pi}{L\epsilon} \int_\epsilon^1 dt\, \sqrt{2\pi}\, \chi_k(\phi)\, \boldsymbol{C}_m^A(t)\, \boldsymbol{C}_n^A(t)\,, \qquad A = Q, u, d\,, \tag{7.2}$$

and similarly $\boldsymbol{I}_{kmn}^{S(A)}$ in terms of integrals over odd profiles $\boldsymbol{S}_n^{(A)}$. Obviously, analogous relations hold for the (KK) photon couplings, where we have to replace $g_s t^a \to e Q_q$. For the gluon (photon) zero mode, the factor $\sqrt{2\pi}$ cancels with the result for the zero-mode profile, and we can use the orthonormality relations (6.17). The condition (6.19) then implies that

$$\vec{a}_m^{Q\dagger}\, \boldsymbol{I}_{0mn}^{C(Q)}\, \vec{a}_n^{Q} + \vec{a}_m^{q\dagger}\, \boldsymbol{I}_{0mn}^{S(q)}\, \vec{a}_n^{q} = \vec{a}_m^{q\dagger}\, \boldsymbol{I}_{0mn}^{C(q)}\, \vec{a}_n^{q} + \vec{a}_m^{Q\dagger}\, \boldsymbol{I}_{0mn}^{S(Q)}\, \vec{a}_n^{Q} = \delta_{mn}\,. \tag{7.3}$$

Thus, the gluon and the photon couple flavor diagonal with couplings g_s and e, as they do not mix with their KK excitations. This is a direct consequence of the unbroken $SU(3)_c \times U(1)_{\rm e.m.}$ symmetry, which assures that there are no NP corrections to the interactions of massless gauge bosons. Note that the couplings of KK gluons (photons) are not flavor diagonal and have to be computed from the general expression (7.1). It is interesting to note that the couplings of KK gauge bosons to heavy fermions, which live close to the IR brane, are enhanced by a factor $\sqrt{L}$ [30, 31] compared to the zero-mode coupling. This follows from the explicit shape of the KK profiles, as discussed in Section 3.3.

7.2 Fermion couplings to heavy gauge bosons

As we have learned above, the heavy Z^0 and $W^\pm$ bosons develop a non-trivial profile within the ED, which gives rise to a non-universal gauge coupling. Furthermore, the heavy gauge bosons couple differently to the $SU(2)_L$ doublet and singlet fermions. Thus, the condition (6.19) can not be used, even if we just consider the constant part of the ground state profiles (3.29), which gives the dominant contribution. As a consequence we have FCNC couplings of the Z^0 boson for two reasons: first, due to the non-constant terms in (3.29); secondly, due to the correction terms $\Delta C_{mn}^{Q,q}$ and $\Delta S_{mn}^{Q,q}$ in the orthonormality relation (6.17). In the perturbative approach, the latter effect would be interpreted as an $SU(2)_L$ singlet admixture in the wave functions of the $SU(2)_L$ doublet SM fermions (and vice versa) due to mixing with their KK excitations [73, 76, 77].

In order to derive the gauge couplings of Z^0 and $W^\pm$, we give the covariant derivative in the mass eigenbasis

$$\begin{aligned} D_\mu = \partial_\mu - i\,\frac{g_{L5}}{\sqrt{2}}\left(L_\mu^+ T_L^+ + L_\mu^- T_L^-\right) + i\,\frac{g_{R5}}{\sqrt{2}}\left(R_\mu^+ T_R^+ + R_\mu^- T_R^-\right) \\ - i\,g_{Z5}\,Q_Z Z_\mu - i\,g_{Z'5}\,Q_{Z'} Z'_\mu - i\,e_5 Q A_\mu\,. \end{aligned} \tag{7.4}$$

In analogy to the SM model we define

$$g_Z = \sqrt{g_L^2 + g_Y^2}\,,\quad g_{Z'} = \sqrt{g_R^2 + g_X^2}\,,\quad Q_Z = T_L^3 - \frac{g_Y^2}{g_Z^2}Q\,,\quad Q_{Z'} = -T_R^3 - \frac{g_X^2}{g_{Z'}^2}Y\,, \tag{7.5}$$

and it will be useful to introduce $\vec{g}_Z = (g_Z Q_Z, g_{Z'} Q_{Z'})^T$.

The explicit form of the $SU(2)_{L,R}$ generators depends on the multiplets they are acting on. For the case of doublets or bi-doublets, the generators $T_{L,R}^i$ with $i = 1,2,3$ are given by the Pauli matrices (1.6) times a factor of 1/2. As usual we define $T_{L,R}^\pm = T_{L,R}^1 \pm i\,T_{L,R}^2$. The generators T_L^i act on the multiplets from the left, where the T_R^i act from the right. If, on the other hand, the generators act on $SU(2)_{L,R}$ triplets, one has to choose the representation

$$T_{L,R}^+ = \begin{pmatrix} 0 & \sqrt{2} & 0 \\ 0 & 0 & \sqrt{2} \\ 0 & 0 & 0 \end{pmatrix},\qquad T_{L,R}^- = \begin{pmatrix} 0 & 0 & 0 \\ \sqrt{2} & 0 & 0 \\ 0 & \sqrt{2} & 0 \end{pmatrix},\qquad T_{L,R}^3 = \begin{pmatrix} 1 & 0 & 0 \\ 0 & 0 & 0 \\ 0 & 0 & -1 \end{pmatrix}. \tag{7.6}$$

The charged-current operators involve a trace with respect to the fundamental gauge indices. Therefore, we define the generalized charged-current vectors of the custodial model as

$$\begin{aligned} \vec{J}^{\mu\pm}_{W_Q} &= \frac{1}{\sqrt{2}} \left(g_L \,\mathrm{Tr}\left[\bar{Q}\,\gamma^\mu\, T^\pm\, Q\right], g_R \,\mathrm{Tr}\left[\bar{Q}\,\gamma^\mu\, Q\, T^\pm\right] \right), \\ \vec{J}^{\mu\pm}_{W_\mathcal{T}} &= \frac{1}{\sqrt{2}} \left(g_L \bar{\mathcal{T}}_1\,\gamma^\mu\, T^\pm\, \mathcal{T}_1\,,\; g_R \,\mathrm{Tr}\left[\bar{\mathcal{T}}_2\,\gamma^\mu\, \mathcal{T}_2\, T^\pm\right] \right). \end{aligned} \tag{7.7}$$

These act on $\left(L^\pm_\mu\,, R^\pm_\mu\right)^T$ from the left and are the starting point for the calculation of the generalized quark-mixing matrices.

7.3 Custodial protection of the $Z^0 b_L \bar{b}_L$ vertex

Using (4.39) and (4.40), we find that the neutral current is proportional to

$$\begin{aligned} \left(\vec{g}^{\,q}_Z\right)^T \vec{\chi}^{\,Z}_0(\phi) = \frac{g_Z Q^q_Z}{\sqrt{2\pi}} &\left\{ 1 + \frac{m_Z^2}{4M^2_{\mathrm{KK}}} \left[1 - \frac{1}{L} - 2L\, t^2 \omega^q_Z + 2\, t^2 \left(\frac{1}{2} - \ln t \right) \right] \right\} \\ &+ \mathcal{O}\left(\frac{m_Z^4}{M^4_{\mathrm{KK}}} \right), \end{aligned} \tag{7.8}$$

with $\omega^q_Z = 1$ in the minimal RS model, where it is given by

$$\omega^q_Z = 1 - \frac{s_Z}{c_Z}\, \frac{g_{Z'} Q^q_{Z'}}{g_Z Q^q_Z} \tag{7.9}$$

in the custodial one. This formula allows us to understand (part of) the custodial protection mechanism of the $Z^0 b_L \bar{b}_L$ vertex. If the gauge couplings and quantum numbers of the fermions are chosen such that

$$\omega^{b_L}_Z = 0 \quad \Longleftrightarrow \quad g_Z Q^{b_L}_Z = \frac{s_Z}{c_Z}\, g_{Z'} Q^{b_L}_{Z'}\,, \tag{7.10}$$

the dominant correction to the Z^0 coupling vanishes. Numerically, the corrections arising from the gauge sector are thus suppressed by a factor of $L \approx 37$ in the custodial model relative to the minimal RS model.

In order to see which quantum number assignments are necessary to achieve a custodial protection, we recast (7.9) into the form

$$\omega^q_Z = \frac{c_w^2}{2g_L^2}\, \frac{(g_L^2 + g_R^2)\,(T^{3\,q}_L + T^{3\,q}_R) + (g_L^2 - g_R^2)\,(T^{3\,q}_L - T^{3\,q}_R)}{T^{3\,q}_L - s_w^2 Q_q}\,. \tag{7.11}$$

This allows one to read off the possible choices

$$T^{3\,q}_L = T^{3\,q}_R = 0\,, \qquad (P_C \text{ symmetry}) \tag{7.12}$$

and

$$g_L = g_R\,, \qquad T_L^{3\,q} = -T_R^{3\,q}\,, \qquad (P_{LR} \text{ symmetry}). \tag{7.13}$$

Since the representation (6.50) features $T_L^{3\,d_L} = -T_R^{3\,d_L} = -1/2$ and $T_L^{3\,u_R} = T_R^{3\,u_R} = 0$, the $Zd_L^i\bar{d}_L^j$ and $Zu_R^i\bar{u}_R^j$ vertices are protected by the P_{LR} and P_C symmetries, respectively. It is interesting to observe that only the leading term in L can be protected, while no such mechanism is available for the sub-leading terms, since they arise from the fact that the fields $\chi_0^{(\pm)}(t)$ obey different UV BCs. The latter effects hence represent an irreducible source of the P_{LR}-symmetry breaking.

We will see below that the terms arising from the non-orthonormality of the fermion profiles also give rise to sizable corrections. The leading contribution of these can be eliminated by setting the bulk masses of the triplets equal $c_{\mathcal{T}_1} = c_{\mathcal{T}_2}$ [78]. Formally, this corresponds to an exchange symmetry of the fields D and D' [53], which is broken by the distinct UV BCs. As a consequence, we obtain parametrically suppressed correction terms, which can not be eliminated, but turn out to be insignificant. From now on we will always choose the fermion representation (6.50) for the custodial model and assume that extended P_{LR} symmetry ($g_L = g_R,\ T_L^{3\,d_{iL}} = -T_R^{3\,d_{iL}},\ c_{\mathcal{T}_1} = c_{\mathcal{T}_2}$) is at work.

Let us now explicitly work out the Z^0-boson couplings to left- and right-handed quarks. The 4D Lagrangian can be written in the form

$$\mathcal{L}_{4\mathrm{D}} \ni \frac{g_L}{c_w}\left[1 + \frac{m_Z^2}{4M_{\mathrm{KK}}^2}\left(1 - \frac{1}{L}\right)\right] \sum_{q,m,n} \left[\left(\boldsymbol{g}_L^q\right)_{mn}\left(\bar{q}_L^{(m)}\gamma_\mu q_L^{(n)}\right) + \left(\boldsymbol{g}_R^q\right)_{mn}\left(\bar{q}_R^{(m)}\gamma_\mu q_R^{(n)}\right)\right] Z^\mu\,, \tag{7.14}$$

where we pulled out the universal correction factor due to the t-independent terms in (3.29). The left- and right-handed couplings $\boldsymbol{g}_{L,R}^q$ are infinite-dimensional matrices in the space of quark modes, and can be parametrized as

$$\begin{aligned}
\boldsymbol{g}_L^q &= \left(T_L^{3\,q_L} - s_w^2 Q_q\right)\left[\mathbf{1} - \frac{m_Z^2}{2M_{\mathrm{KK}}^2}\left(\omega_Z^{q_L} L\,\boldsymbol{\Delta}_Q - \boldsymbol{\Delta}_Q'\right)\right] - T_L^{3\,q_L}\left[\boldsymbol{\delta}_Q - \frac{m_Z^2}{2M_{\mathrm{KK}}^2}\left(\frac{c_w^2}{g_L^2}\,L\,\boldsymbol{\varepsilon}_Q - \boldsymbol{\varepsilon}_Q'\right)\right],\\
\boldsymbol{g}_R^q &= -s_w^2 Q_q\left[\mathbf{1} - \frac{m_Z^2}{2M_{\mathrm{KK}}^2}\left(\omega_Z^{q_R} L\,\boldsymbol{\Delta}_q - \boldsymbol{\Delta}_q'\right)\right] + T_L^{3\,q_L}\left[\boldsymbol{\delta}_q - \frac{m_Z^2}{2M_{\mathrm{KK}}^2}\left(\frac{c_w^2}{g_L^2}\,L\,\boldsymbol{\varepsilon}_q - \boldsymbol{\varepsilon}_q'\right)\right].
\end{aligned} \tag{7.15}$$

The isospin quantum-numbers are always those of the SM-like fermions, also in the case of the custodial model, where new fermion species contribute[1]. These will modify the expressions for the matrices $\boldsymbol{\Delta}_A^{(\prime)}$, $\boldsymbol{\epsilon}_A^{(\prime)}$, and $\boldsymbol{\delta}_A$, which contain certain overlap integrals. The matrices $\boldsymbol{\Delta}_A^{(\prime)}$ and $\boldsymbol{\epsilon}_A^{(\prime)}$ arise from the t dependent terms of the Z^0-boson profile. The former

[1] We do not consider exotic λ and $\Lambda^{(\prime)}$ quarks at this point, as these fields do not possess zero modes.

are formally equal for the minimal and the custodial model and read

$$
\begin{aligned}
(\Delta_Q)_{mn} &= \frac{2\pi}{L\epsilon}\int_\epsilon^1 dt\, t^2 \left[\vec{a}_m^{Q\dagger}\,\boldsymbol{C}_m^Q(t)\,\boldsymbol{C}_n^Q(t)\,\vec{a}_n^Q + \vec{a}_m^{q\dagger}\,\boldsymbol{S}_m^q(t)\,\boldsymbol{S}_n^q(t)\,\vec{a}_n^q\right],\\
(\Delta_q)_{mn} &= \frac{2\pi}{L\epsilon}\int_\epsilon^1 dt\, t^2 \left[\vec{a}_m^{q\dagger}\,\boldsymbol{C}_m^q(t)\,\boldsymbol{C}_n^q(t)\,\vec{a}_n^q + \vec{a}_m^{Q\dagger}\,\boldsymbol{S}_m^Q(t)\,\boldsymbol{S}_n^Q(t)\,\vec{a}_n^Q\right],\\
\left(\Delta'_Q\right)_{mn} &= \frac{2\pi}{L\epsilon}\int_\epsilon^1 dt\, t^2 \left(\frac{1}{2}-\ln t\right) \left[\vec{a}_m^{Q\dagger}\,\boldsymbol{C}_m^Q(t)\,\boldsymbol{C}_n^Q(t)\,\vec{a}_n^Q + \vec{a}_m^{q\dagger}\,\boldsymbol{S}_m^q(t)\,\boldsymbol{S}_n^q(t)\,\vec{a}_n^q\right],\\
\left(\Delta'_q\right)_{mn} &= \frac{2\pi}{L\epsilon}\int_\epsilon^1 dt\, t^2 \left(\frac{1}{2}-\ln t\right) \left[\vec{a}_m^{q\dagger}\,\boldsymbol{C}_m^q(t)\,\boldsymbol{C}_n^q(t)\,\vec{a}_n^q + \vec{a}_m^{Q\dagger}\,\boldsymbol{S}_m^Q(t)\,\boldsymbol{S}_n^Q(t)\,\vec{a}_n^Q\right].
\end{aligned}
\tag{7.16}
$$

The latter differ for the various RS models. In the minimal model, the matrices $\boldsymbol{\epsilon}_A^{(\prime)}$ are equal to the expressions (7.16), where the even profiles have been removed. If one considers the coupling to light SM-like fermions, these terms are highly suppressed. The same is true for the custodial model, where the expressions are slightly more complicated due to the different isospin quantum numbers.

The matrices $\boldsymbol{\delta}_A$ arise due to the non-orthonormality of the fermion profiles. For zero modes, they are of the order v^2/M_{KK}^2. In the minimal model, they are given by

$$
(\delta_Q)_{mn} = \vec{a}_m^{q\,\dagger}\left(\delta_{mn} + \Delta\boldsymbol{S}_{mn}^q\right)\vec{a}_n^q\,, \qquad (\delta_q)_{mn} = \vec{a}_m^{Q\,\dagger}\left(\delta_{mn} + \Delta\boldsymbol{S}_{mn}^Q\right)\vec{a}_n^Q\,, \tag{7.17}
$$

while in the custodial model, they read

$$
\begin{aligned}
(\delta_Q)_{mn} &= \frac{2\pi}{L\epsilon}\int_\epsilon^1 dt \left[\vec{a}_m^{Q\,\dagger}\,\boldsymbol{C}_m^Q(t)\left(\mathbf{1} - \boldsymbol{T}_L^{3\,Q}/T_L^{3\,q_L}\right)\boldsymbol{C}_n^Q(t)\,\vec{a}_n^Q\right.\\
&\qquad\qquad\left. + \,\vec{a}_m^{q\dagger}\,\boldsymbol{S}_m^q(t)\,\left(\mathbf{1} - \boldsymbol{T}_L^{3\,q}/T_L^{3\,q_L}\right)\boldsymbol{S}_n^q(t)\,\vec{a}_n^q\right],\\
(\delta_q)_{mn} &= \frac{2\pi}{L\epsilon}\int_\epsilon^1 dt \left[\vec{a}_m^{q\,\dagger}\,\boldsymbol{C}_m^q(t)\,\boldsymbol{T}_L^{3\,q}/T_L^{3\,q_L}\,\boldsymbol{C}_n^q(t)\,\vec{a}_n^q + \vec{a}_m^{Q\dagger}\,\boldsymbol{S}_m^Q(t)\,\boldsymbol{T}_L^{3\,Q}/T_L^{3\,q_L}\,\boldsymbol{S}_n^Q(t)\,\vec{a}_n^Q\right].
\end{aligned}
\tag{7.18}
$$

In the expressions above we have used the charge matrices $\boldsymbol{T}_{L,R}^{3\,Q,q}$, defined as $\boldsymbol{T}_{L,R}^{3\,u} = \mathbf{0}$,

$$
\boldsymbol{T}_{L,R}^{3\,U} = \begin{pmatrix} T_{L,R}^{3\,u} & 0 \\ 0 & T_{L,R}^{3\,u'} \end{pmatrix}, \qquad \boldsymbol{T}_{L,R}^{3\,D} = T_{L,R}^{3\,d}\,, \qquad \boldsymbol{T}_{L,R}^{3\,d} = \begin{pmatrix} T_{L,R}^{3\,D} & 0 \\ 0 & T_{L,R}^{3\,D'} \end{pmatrix}. \tag{7.19}
$$

Note that up to the expansion of the Z^0-boson profile, the expression (7.15) is exact to all orders in v/M_{KK}. Nevertheless, of particular interest are the ZMA results of the overlap matrices. In the minimal model we find for $m, n = 1, 2, 3$ (see also [20, 79])

$$
\begin{aligned}
\boldsymbol{\Delta}_Q &\to \boldsymbol{U}_q^\dagger \ \mathrm{diag}\left[\frac{F^2(c_{Q_i})}{3+2c_{Q_i}}\right] \boldsymbol{U}_q \,, \\
\boldsymbol{\Delta}_f &\to \boldsymbol{W}_q^\dagger \ \mathrm{diag}\left[\frac{F^2(c_{q_i})}{3+2c_{q_i}}\right] \boldsymbol{W}_q \,, \\
\boldsymbol{\Delta}'_F &\to \boldsymbol{U}_q^\dagger \ \mathrm{diag}\left[\frac{5+2c_{Q_i}}{2(3+2c_{Q_i})^2}\, F^2(c_{Q_i})\right] \boldsymbol{U}_q \,, \\
\boldsymbol{\Delta}'_q &\to \boldsymbol{W}_q^\dagger \ \mathrm{diag}\left[\frac{5+2c_{q_i}}{2(3+2c_{q_i})^2}\, F^2(c_{q_i})\right] \boldsymbol{W}_q \,,
\end{aligned}
\tag{7.20}
$$

and

$$
\begin{aligned}
\boldsymbol{\delta}_Q &\to \boldsymbol{x}_q\, \boldsymbol{W}_q^\dagger \ \mathrm{diag}\left[\frac{1}{1-2c_{q_i}}\left(\frac{1}{F^2(c_{q_i})} - 1 + \frac{F^2(c_{q_i})}{3+2c_{q_i}}\right)\right] \boldsymbol{W}_q\, \boldsymbol{x}_q \,, \\
\boldsymbol{\delta}_q &\to \boldsymbol{x}_q\, \boldsymbol{U}_q^\dagger \ \mathrm{diag}\left[\frac{1}{1-2c_{Q_i}}\left(\frac{1}{F^2(c_{Q_i})} - 1 + \frac{F^2(c_{Q_i})}{3+2c_{Q_i}}\right)\right] \boldsymbol{U}_q\, \boldsymbol{x}_q \,,
\end{aligned}
\tag{7.21}
$$

where $\boldsymbol{x}_u = \mathrm{diag}(m_u, m_c, m_t)/M_{\mathrm{KK}}$, $\boldsymbol{x}_d = \mathrm{diag}(m_d, m_s, m_b)/M_{\mathrm{KK}}$ [34]. The leading terms in the latter expressions are those proportional to $1/F^2(c_i)$, which will be exponentially enhanced for $c_i < -1/2$. However, exactly these terms will be canceled, if we have a custodial protection. From (7.18) we obtain

$$
\begin{aligned}
\boldsymbol{\delta}_D &\to \boldsymbol{x}_d\, \boldsymbol{W}_d^\dagger \ \mathrm{diag}\left[\frac{1}{1-2c_{\mathcal{T}_{2i}}}\left(\frac{1}{F^2(c_{\mathcal{T}_{2i}})}\left[1 - \frac{1-2c_{\mathcal{T}_{2i}}}{F^2(-c_{\mathcal{T}_{1i}})}\right] - 1 + \frac{F^2(c_{\mathcal{T}_{2i}})}{3+2c_{\mathcal{T}_{2i}}}\right)\right] \boldsymbol{W}_d\, \boldsymbol{x}_d \,, \\
\boldsymbol{\delta}_u &\to \boldsymbol{x}_u\, \boldsymbol{U}_u^\dagger \ \mathrm{diag}\left[\frac{1}{1-2c_{Q_i}}\left(\frac{1}{F^2(c_{Q_i})}\left[1 - \frac{1-2c_{Q_i}}{F^2(-c_{Q_i})}\right] - 1 + \frac{F^2(c_{Q_i})}{3+2c_{Q_i}}\right)\right] \boldsymbol{U}_u\, \boldsymbol{x}_u \,.
\end{aligned}
\tag{7.22}
$$

Assuming extended P_{LR} symmetry ($c_{\mathcal{T}_1} = c_{\mathcal{T}_2}$), and observing that all bulk mass parameters (besides c_{Q_3} and c_{u_3}) typically satisfy $c < -1/2$, we can apply (6.34) and therefore obtain $1 - (1-2c)/F^2(-c) = 0$ to excellent approximation.

Now, as we have discussed how to protect the $Z^0 b_L \bar{b}_L$ vertex, we want to understand why this is desired, and to what extent such a protection is necessary. Therefore, we have to discuss the $Z^0 \to b\bar{b}$ "pseudo observables". These are given by the ratio of the width of the Z^0-boson decay into bottom quarks and the total hadronic width, R_b^0, the bottom quark left-right asymmetry parameter A_b, and the forward-backward asymmetry for bottom quarks $A_{\mathrm{FB}}^{0,b}$. They can be expressed as functions of the left- and right-handed bottom quark couplings [80]

$$\begin{aligned} R_b^0 &= \left[1 + \frac{4\sum_{q=u,d}[(g_L^q)^2 + (g_R^q)^2]}{\eta_{\rm QCD}\,\eta_{\rm QED}\left[(1-6z_b)(g_L^b - g_R^b)^2 + (g_L^b + g_R^b)^2\right]}\right]^{-1}, \\ A_b &= \frac{2\sqrt{1-4z_b}\,\dfrac{g_L^b + g_R^b}{g_L^b - g_R^b}}{1 - 4z_b + (1+2z_b)\left(\dfrac{g_L^b + g_R^b}{g_L^b - g_R^b}\right)^2}\,, \qquad A_{\rm FB}^{0,b} = \frac{3}{4}\,A_e\,A_b\,, \end{aligned} \tag{7.23}$$

where $\eta_{\rm QCD} = 0.9954$ and $\eta_{\rm QED} = 0.9997$ are QCD and QED radiative correction factors. The parameter $z_b \equiv m_b^2(m_Z)/m_Z^2 = 0.997 \cdot 10^{-3}$ describes corrections from a non-zero bottom quark mass. Due to the RS-GIM suppression, we can neglect the RS contributions to the left- and right-handed couplings of the light quarks and the asymmetry parameter of the electron, A_e. We will therefore fix these quantities to their SM values $g_L^u = 0.34674$, $g_R^u = -0.15470$, $g_L^d = -0.42434$, $g_R^d = 0.077345$ [81], $A_e = 0.1462$ [82, 83].

Inserting the SM expectations $g_L^b = -0.42114$ and $g_R^b = 0.077420$ [81] into the relations (7.23), we obtain the central values

$$R_b^0 = 0.21579\,, \qquad A_b = 0.935\,, \qquad A_{\rm FB}^{0,b} = 0.1025\,. \tag{7.24}$$

These should be compared to the experimentally extracted values for the three "pseudo observables" [81]

$$\begin{aligned} R_b^0 &= 0.21629 \pm 0.00066\,, \\ A_b &= 0.923 \pm 0.020\,, \\ A_{\rm FB}^{0,b} &= 0.0992 \pm 0.0016\,, \end{aligned} \qquad \rho = \begin{pmatrix} 1.00 & -0.08 & -0.10 \\ -0.08 & 1.00 & 0.06 \\ -0.10 & 0.06 & 1.00 \end{pmatrix}. \tag{7.25}$$

Here, ρ is the correlation matrix. We see that while the R_b^0 and A_b measurements agree within $+0.8\sigma$ and -0.6σ with their SM predictions, the $A_{\rm FB}^{0,b}$ measurement is almost -2.1σ away from its SM value.

In Figure 7.1 we plot the predictions of the minimal (blue/dark gray) and the custodial (orange/light gray) RS model in the g_L^b-g_R^b plane for 10000 random parameter sets, which produce the correct zero-mode masses and CKM parameters. The KK scale is set to $M_{\rm KK} = 2\,$TeV. The ellipses mark the 68% , 95% , and 99% confidence regions with respect to the experimental favored values. While the corrections relative to the SM value of g_L are strictly positive and potentially large in the minimal model, they turn out to be negative and tiny in the custodial model with extended P_{LR} symmetry. Note that the latter also allows for moderate positive and negative corrections to g_L, if we allow for different bulk masses $c_{\mathcal{T}_1} \neq c_{\mathcal{T}_2}$ [53]. In either case, the corrections to g_R turn out to be small and negative. However, we can reach a sizable shift of the latter by varying the Higgs mass against the SM reference value $m_h = 150\,$GeV. The individual leading logarithmic Higgs-mass corrections are well approximated by [34]

$$\Delta R_b^0 = 3.3\cdot 10^{-5} \ln\frac{m_h}{m_h^{\rm ref}}\,, \quad \Delta A_b = -2.7\cdot 10^{-4} \ln\frac{m_h}{m_h^{\rm ref}}\,, \quad \Delta A_{\rm FB}^{0,b} = -2.7\cdot 10^{-3} \ln\frac{m_h}{m_h^{\rm ref}}\,. \tag{7.26}$$

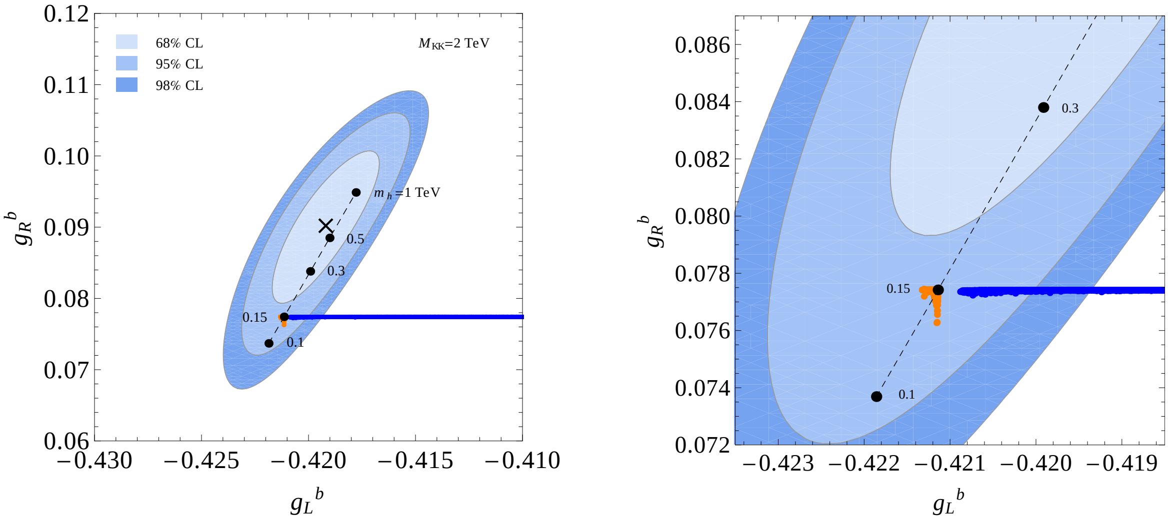

Figure 7.1: Predictions of the minimal (blue/dark gray) and the custodial (orange/light gray) RS model in the g_L^b-g_R^b plane for 10000 parameter sets. See text for details.

Within the plots in Figure 7.1, we have sketched the shifts of the SM prediction for $m_h = (100, 300, 500, 1000)\text{GeV}$. We conclude that for a Higgs mass of around 500 GeV, one can come close to the central value. As the minimal RS model favors a large Higgs mass in order to compensate corrections to the T-parameter, the overall fit can be significantly improved. Note especially that, despite appearance, the chance of obtaining a moderate correction to g_L in the minimal RS model is not so bad at all. Indeed, using the above ZMA expressions for the $Z^0 b_L \bar{b}_L$ coupling, we find that nearly 20% of the respective scatter points lie within the 2σ confidence region. Here, the combined fit sets an upper limit on the value of $c_{b_L} \equiv c_{Q_3}$, depending on the value of the KK scale. For $M_{\text{KK}} = 2\,\text{TeV}$ we find $c_{b_L} \lesssim -0.43$ for our set of scatter points. For $M_{\text{KK}} = 3\,\text{TeV}$, the limit is extended to $c_{b_L} \lesssim -0.35$. A lower limit comes from the top mass, which requires $c_{b_L} = c_{t_L} \gtrsim -0.5$ for $|(\boldsymbol{Y}_u)_{ij}| \leq 3$. For the custodial model on the other hand, a large Higgs mass seems to be excluded from the T-parameter. Therefore, the choice of the embedding (6.50) is well motivated as one safely stays within the 2σ confidence region.

7.4 Charged-current interactions

In this section, we want to elaborate an effective theory of charged four-quark interactions in the framework of the RS scenario, which we can apply for $\Lambda < m_W$. The effective Hamiltonian can be written as

$$\begin{aligned}\mathcal{H}_{\text{eff}}^{(W)} = 2\sqrt{2}\,G_F \Big\{ & [\,\bar{d}_{m_L}\gamma_\mu(\mathbf{V}_L^\dagger)_{mn}u_{n_L} + \bar{d}_{m_R}\gamma_\mu(\mathbf{V}_R^\dagger)_{mn}u_{n_R}] \\ & \otimes [\,\bar{u}_{m'_L}\gamma^\mu(\mathbf{V}_L)_{m'n'}d_{n'_L} + \bar{u}_{m'_R}\gamma^\mu(\mathbf{V}_R)_{m'n'}d_{n'_R}] + \text{h.c.}\Big\}\,,\end{aligned} \tag{7.27}$$

where $m, n, m', n' \in \{1,2,3\}$ and we assume $m+n > m'+n'$. Furthermore, a summation over repeated indices is understood. The tensor symbol merely indicates that the full analytic result contains terms that can not be separated into independent matrix products. This is because of the sums over W-gauge boson profiles (3.35) and (4.52) which contain a term $\propto t_<^2$, that prevents a factorization into separate vertex factors.

Before we are going to derive the Wilson coefficients of four-quark interactions, we first want to study the case of a semileptonic decay, for which we replace (7.27) by

$$\mathcal{H}_{\text{eff}}^{(W)} = 2\sqrt{2}\,G_F \sum_l \Big\{ \big[\, \bar{u}_L \gamma^\mu \boldsymbol{V}_L\, d_L + \bar{u}_R \gamma^\mu \boldsymbol{V}_R\, d_R \big] \, (\bar{l}_L \gamma_\mu \nu_{l\,L}) + \text{h.c.} \Big\} \,. \tag{7.28}$$

If the leptons are light, their profiles have to be localized close to the UV brane. Therefore, we can drop the $t_<^2$ term to excellent approximation. We can further assume that the lepton current is SM-like, if we are just interested to determine the elements of the quark-mixing matrices $\boldsymbol{V}_{L,R}$. The latter have to be computed from the product $\vec{J}^{\mu\pm}_{W_{\text{quarks}}}(t) \cdot \boldsymbol{\Sigma}_a(t,t') \cdot \vec{J}^{W_{\text{leptons}}}_{\mu\pm}(t')$. The current vectors and the sum over the KK-tower are given in (7.7) and (4.52), where the simplification to the minimal model is straightforward. We find the general result

$$\begin{aligned} \boldsymbol{V}_L &= \boldsymbol{\Delta}^{+\,Q} + \sqrt{2}\,\boldsymbol{\varepsilon}^{+\,q} - \frac{m_W^2}{2M_{\text{KK}}^2}\, L \left(\bar{\boldsymbol{\Delta}}^{+\,Q} + \sqrt{2}\,\bar{\boldsymbol{\varepsilon}}^{+\,q} \right), \\ \boldsymbol{V}_R &= \sqrt{2}\,\boldsymbol{\Delta}^{+\,q} + \boldsymbol{\varepsilon}^{+\,Q} - \frac{m_W^2}{2M_{\text{KK}}^2}\, L \left(\sqrt{2}\,\bar{\boldsymbol{\Delta}}^{+\,q} + \bar{\boldsymbol{\varepsilon}}^{+\,Q} \right), \end{aligned} \tag{7.29}$$

with

$$\begin{aligned} \Delta_{mn}^{+\,Q,q} &= \frac{2\pi}{L\epsilon} \int_\epsilon^1 dt\; \vec{a}_m^{\,U,u\dagger}\, \boldsymbol{C}_m^{U,u}(t)\, \boldsymbol{\Omega}^{Q,q}\, \boldsymbol{C}_n^{D,d}(t)\, \vec{a}_n^{\,D,d}\,, \\ \epsilon_{mn}^{+\,Q,q} &= \frac{2\pi}{L\epsilon} \int_\epsilon^1 dt\; \vec{a}_m^{\,U,u\dagger}\, \boldsymbol{S}_m^{U,u}(t)\, \boldsymbol{\Omega}^{Q,q}\, \boldsymbol{S}_n^{D,d}(t)\, \vec{a}_n^{\,D,d}\,, \\ \bar{\Delta}_{mn}^{+\,Q,q} &= \frac{2\pi}{L\epsilon} \int_\epsilon^1 dt\; t^2\, \vec{a}_m^{\,U,u\dagger}\, \boldsymbol{C}_m^{U,u}(t)\, \bar{\boldsymbol{\Omega}}^{Q,q}\, \boldsymbol{C}_n^{D,d}(t)\, \vec{a}_n^{\,D,d}\,, \\ \bar{\epsilon}_{mn}^{+\,Q,q} &= \frac{2\pi}{L\epsilon} \int_\epsilon^1 dt\; t^2\, \vec{a}_m^{\,U,u\dagger}\, \boldsymbol{S}_m^{U,u}(t)\, \bar{\boldsymbol{\Omega}}^{Q,q}\, \boldsymbol{S}_n^{D,d}(t)\, \vec{a}_n^{\,D,d}\,. \end{aligned} \tag{7.30}$$

The matrices $\boldsymbol{\Omega}^{Q,q}$ and $\bar{\boldsymbol{\Omega}}^{Q,q}$ contain the information, which fields in the generalized flavor vectors (6.52) are linked through the respective overlap integrals. In the custodial model, we observe

$$\boldsymbol{\Omega}^Q = \begin{pmatrix} \mathbf{1} \\ \mathbf{0} \end{pmatrix}, \quad \boldsymbol{\Omega}^q = \begin{pmatrix} \mathbf{0} & \mathbf{0} \\ \mathbf{0} & \mathbf{1} \\ \mathbf{0} & \mathbf{0} \end{pmatrix}, \quad \bar{\boldsymbol{\Omega}}^Q = \begin{pmatrix} \mathbf{1} \\ -\frac{g_R^2}{g_L^2}\,\mathbf{1} \end{pmatrix}, \quad \bar{\boldsymbol{\Omega}}^q = \begin{pmatrix} \mathbf{0} & \mathbf{0} \\ \mathbf{0} & \mathbf{1} \\ -\frac{g_R^2}{g_L^2}\,\mathbf{1} & \mathbf{0} \end{pmatrix}, \tag{7.31}$$

where the entries are 3×3 matrices. In the minimal model we have $\boldsymbol{\Omega}^Q = \bar{\boldsymbol{\Omega}}^Q = \mathbf{1}$, and $\boldsymbol{\Omega}^q = \bar{\boldsymbol{\Omega}}^q = \mathbf{0}$. Note that our definitions of $\boldsymbol{V}_{L,R}$ include the exchange of the entire W-boson tower. Here, we have already absorbed the universal correction factor $\big(1+m_W^2/(2M_{\rm KK}^2)[1-1/(2\,L)]\big)$ (3.38) into the definition of the Fermi constant. As any measurement of a charged-current interaction involves the exchange of the whole KK-tower, this universal factor is non-observable in the measurement of the combination $G_F \boldsymbol{V}_{L,R}$ [38].

Opposed to the neutral-current sector, no custodial protection mechanism is at work for charged currents [24]. The leading contribution to $(\boldsymbol{V}_L)_{mn}$ stems from Δ_{mn}^{+Q}. Corrections of the order $v^2/M_{\rm KK}^2$ arise from the non-universality of KK gauge bosons encoded in $\bar{\Delta}_{mn}^{+Q}$ and, in the custodial model, from the admixture of U' and D' quarks described by ϵ_{mn}^{+q}. Contributions arising from the admixture of U, D, u', U', and D' quarks, which are collected $\bar{\epsilon}_{mn}^{+Q,q}$, do not contribute at the order $\mathcal{O}(v^2/M_{\rm KK}^2)$. The full ZMA expression for $\boldsymbol{V}_L$ reads

$$
\begin{aligned}
\boldsymbol{V}_L = \boldsymbol{U}_u^\dagger \Bigg(\mathbf{1} - \frac{m_W^2}{2M_{\rm KK}^2}\, L \,\text{diag}\left[\frac{F^2(c_{Q_i})}{3+2c_{Q_i}}\right] \\
+ \frac{v^2}{2M_{\rm KK}^2}\,\text{diag}\left[F(c_{Q_i})\right] \boldsymbol{Y}_d \,\text{diag}\left(F^{-2}(-c_{\mathcal{T}_{1i}})\right) \boldsymbol{Y}_d^\dagger \,\text{diag}\left[F(c_{Q_i})\right] \Bigg) \boldsymbol{U}_d \,,
\end{aligned} \tag{7.32}
$$

where the first line holds for both scenarios, while the second arises from the admixture of U' and D' in the custodial model. Obviously, the result (7.32) is not unitary. The amount of unitarity violation has been estimated in [53] and has been found to be below the current experimental uncertainty, at least within the minimal RS model. A detailed discussion of the breakdown of the unitarity of the quark-mixing matrix in the framework of the RS model with custodial protection has been presented in [78]. Unfortunately, the authors defined the CKM matrix via the $W u_L^i d_L^j$ vertex only, and did not take into account the non-universal corrections stemming from the exchange of the KK excitations.

For the mixing matrix of right-handed quarks $(\boldsymbol{V}_R)_{mn}$, the dominant contribution is given by ϵ_{mn}^{+Q}, which is equal for both scenarios. All other contributions are of the order $v^4/M_{\rm KK}^4$, which we will neglect. Explicitly, we find the ZMA expression [75]

$$
\boldsymbol{V}_R = \boldsymbol{x}_u \boldsymbol{U}_u^\dagger \,\text{diag}\big[f(c_{Q_i})\big]\, \boldsymbol{U}_d\, \boldsymbol{x}_d \,, \tag{7.33}
$$

where

$$
f(c) = \frac{1}{F^2(c)(1-2c)} - \frac{1}{1-2c} + \frac{F^2(c)}{(1+2c)^2}\left(\frac{1}{1-2c} - 1 + \frac{1}{3+2c}\right) . \tag{7.34}
$$

The factors $\boldsymbol{x}_{u,d}$ reflect the fact that to LO the right-handed charged-current interactions of zero modes originate from quark mixing, and not, as one might naively expect, from the presence of a gauged $SU(2)_R$ group. The product $x_{u_i} x_{d_i}$ can be split up into the usual $v^2/M_{\rm KK}^2$ suppression and a chiral factor $m_{u_i} m_{d_i}/v^2$. As the latter is tiny for all quarks besides the top, one might think that the contributions of right-handed charged currents are completely negligible against the RS corrections to the left-handed ones. However, the ZMA expressions (7.33) also involve exponentially enhanced terms proportional to $1/F(c_i)^2$, in analogy to the quantities $\boldsymbol{\delta}_{Q,q}$ (7.21), (7.22). In fact, the resulting NP corrections dominate those of the left-handed sector, as to LO the latter solely arise from parametrically suppressed non-factorizable RS corrections, which can not be absorbed into the definition of the Fermi constant and CKM matrix elements.

Coming back to four-quark interactions, we perform the necessary overlap integrals and find $(m,n,m',n'=1,2,3)$

$$\begin{aligned}(\mathbf{V}_L^\dagger)_{mn}\otimes(\mathbf{V}_L)_{m'n'} &= \left(\boldsymbol{U}_d^\dagger\left[1+\mathcal{O}\left(\frac{v^2}{M_{\mathrm{KK}}^2}\right)\right]\boldsymbol{U}_n\right)_{mn}\left(\boldsymbol{U}_u^\dagger\left[1+\mathcal{O}\left(\frac{v^2}{M_{\mathrm{KK}}^2}\right)\right]\boldsymbol{U}_d\right)_{m'n'}\\ &\quad+\frac{m_W^2}{2M_{\mathrm{KK}}^2}\,L\,(\boldsymbol{U}_d^\dagger)_{mi}(\boldsymbol{U}_u)_{in}(\widetilde{\boldsymbol{\Delta}}_{QQ})_{ij}(\boldsymbol{U}_u^\dagger)_{m'j}(\boldsymbol{U}_d)_{jn'}\end{aligned}\tag{7.35}$$

with the non-factorizable correction [84]

$$(\widetilde{\boldsymbol{\Delta}}_{QQ})_{ij}=\frac{F^2(c_{Q_i})}{3+2c_{Q_i}}\,\frac{3+c_{Q_i}+c_{Q_j}}{2+c_{Q_i}+c_{Q_j}}\,\frac{F^2(c_{Q_j})}{3+2c_{Q_{ij}}}\,.\tag{7.36}$$

A summation over repeated indices is understood. The $\mathcal{O}(v^2/M_{\mathrm{KK}}^2)$ terms in the brackets are simply given by the RS corrections in (7.32). The factorizable terms in the first line are universal for all interactions involving the given vertices, and therefore should be identified with the measured values of the respective CKM-matrix elements. Thus, they are only observable through unitarity violations. For a given four-fermion interaction, the RS correction to the amplitude is given by the non-factorizable terms (7.36), and the Wilson coefficients have to be deduced from the latter.

For the interference of left- and right-handed currents, we find at LO in v^2/M_{KK}^2

$$\begin{aligned}(\mathbf{V}_L^\dagger)_{mn}\otimes(\mathbf{V}_R)_{m'n'} &= \frac{1}{M_{\mathrm{KK}}^2}\,(\boldsymbol{U}_d^\dagger\boldsymbol{U}_u)_{mn}(\boldsymbol{m}_u\boldsymbol{U}_u^\dagger)_{m'j}\,f(c_{Q_j})\,(\boldsymbol{U}_d\,\boldsymbol{m}_d)_{jn'}\,,\\ (\mathbf{V}_R^\dagger)_{mn}\otimes(\mathbf{V}_L)_{m'n'} &= \frac{1}{M_{\mathrm{KK}}^2}\,(\boldsymbol{m}_d\boldsymbol{U}_d^\dagger)_{mi}\,f(c_{Q_i})\,(\boldsymbol{U}_u\,\boldsymbol{m}_u)_{in}(\boldsymbol{U}_u^\dagger\boldsymbol{U}_d)_{m'n'}\,.\end{aligned}\tag{7.37}$$

The double insertion of right-handed currents contributes at the order v^4/M_{KK}^2, and therefore can safely be neglected in the models at hand.

8 Higgs-boson couplings

In this section we present analytic results for the vertices of Higgs couplings to fermions. The latter are not flavor diagonal in the mass basis due the mixing of zero-modes with their KK excitations. Thus, WED scenarios give rise to flavor-changing Higgs couplings [85]. These require a proper localization of the δ-function, as couplings to Z_2-odd fermions are involved [67]. Naively, one would set these terms to zero as the odd profiles vanish on the boundaries. In fact, we will use the latter property below. However, as we have learned above, the fermion profiles develop a discontinuity in the limit $\eta \to 0$, where η is the regulator. For the odd profiles, this means that within the interval $t \in [1-\eta, 1]$, they are rising to a finite value according to the solution (6.12) of EOMs in the vicinity of the IR brane (6.9). At this point we should stress that the latter have a restricted region of validity. Within their derivation, we have dropped the term that multiplies the bulk mass, and the one proportional to the eigenvalue x_n. As the first term never becomes singular, its omission is well justified for the brane-Higgs scenario. The second one, however, becomes singular in the limit $n \to \infty$. Going back to a regularized scenario with η finite, its omission is only justified for $x_n \ll 1/\eta$. On the other hand, we have learned that the IR cut-off has to be in the vicinity of the KK scale. For (IR) brane-localized interactions, one should not sum up modes with masses $m_n > \Lambda_{\rm IR}$. As we safely fulfill $\Lambda_{\rm IR}/M_{\rm KK} \ll 1/\eta$, our solution is trustworthy in the low-energy effective theory.

We further give results for Higgs couplings to gauge bosons. These are required along with the results from the fermion sector to make estimations of Higgs production amplitudes normalized to the known SM results.

8.1 Higgs couplings to fermions

In [67] it has been pointed out that the contributions of the Z_2-odd fermions provide the dominant corrections to tree-level Higgs FCNCs in the case of light quark flavors. The authors performed their calculations within the perturbative approach and obtained results valid to $\mathcal{O}(v^2/M_{\rm KK}^2)$. In [53], we re-derived these results within our exact treatment and thus to all orders in $v/M_{\rm KK}$, both for the minimal as well as the custodial RS model. Working in unitary gauge, the relevant terms in the 4D Lagrangian describing the couplings of the Higgs boson to quarks are given by

$$\mathcal{L}_{\rm 4D} \ni -\sum_{q,m,n} (g_h^q)_{mn}\, h\, \bar{q}_L^m\, q_R^n + \text{h.c.}\,, \tag{8.1}$$

and the coefficients $(g_h^q)_{mn}$ are given by

$$(g_h^q)_{mn} = \sqrt{2}\,\frac{\pi}{L\epsilon}\int_\epsilon^1 dt\,\delta(t-1)\,\left[\vec{a}_m^{Q\,\dagger}\,\boldsymbol{C}_m^Q(t)\boldsymbol{Y}_q\,\boldsymbol{C}_n^q(t)\,\vec{a}_n^q + \vec{a}_m^{q\,\dagger}\,\boldsymbol{S}_m^q(t)\boldsymbol{Y}_q^\dagger\,\boldsymbol{S}_n^Q(t)\,\vec{a}_n^Q\right]. \tag{8.2}$$

To simplify this expression, we follow [67] and observe that the EOMs (6.7) imply

$$\begin{aligned}&\vec{a}_m^{Q\,\dagger}\,\left(x_n t\,\boldsymbol{C}_m^Q(t)\boldsymbol{C}_n^Q(t) - \boldsymbol{S}_m^Q(t)\boldsymbol{S}_n^Q(t)\,t\,x_m - t\partial_t\,\boldsymbol{C}_m^Q(t)\boldsymbol{S}_n^Q(t)\right)\,\vec{a}_n^Q \\ &- \frac{v}{\sqrt{2}M_{\mathrm{KK}}}\,\delta(t-1)\,\left[\vec{a}_m^{Q\,\dagger}\,\boldsymbol{C}_m^Q(t)\,\boldsymbol{Y}_q\,\boldsymbol{C}_n^q(t)\,\vec{a}_n^q - \vec{a}_m^{q\,\dagger}\,\boldsymbol{S}_m^q(t)\,\boldsymbol{Y}_q^\dagger\,\boldsymbol{S}_n^Q(t)\,\vec{a}_n^Q\right] = 0\,.\end{aligned} \tag{8.3}$$

After integrating this relation over the orbifold $t\in[\epsilon,1]$, the derivative in (8.3) does not contribute since the Z_2-odd profiles obey $\boldsymbol{S}_n^{Q,q}(\epsilon) = \boldsymbol{S}_n^{Q,q}(1) = 0$. Using the orthonormality (6.17) and the normalization condition (6.19), we find the expression

$$\begin{aligned}x_m\,\delta_{mn} = \frac{2\pi}{L}\int_\epsilon^1 dt\,\Bigg\{&x_n t\,\vec{a}_m^{q\,\dagger}\,\boldsymbol{S}_m^q(t)\,\boldsymbol{S}_n^q(t)\,\vec{a}_n^q + \vec{a}_m^{Q\,\dagger}\,\boldsymbol{S}_m^Q(t)\,\boldsymbol{S}_n^Q(t)\,\vec{a}_n^Q\,t\,x_m \\ &+ \frac{v}{\sqrt{2}M_{\mathrm{KK}}}\,\delta(t-1)\left[\vec{a}_m^{Q\,\dagger}\,\boldsymbol{C}_m^Q(t)\,\boldsymbol{Y}_q\,\boldsymbol{C}_n^q(t)\,\vec{a}_n^q - \vec{a}_m^{q\,\dagger}\,\boldsymbol{S}_m^q(t)\,\boldsymbol{Y}_q^\dagger\,\boldsymbol{S}_n^Q(t)\,\vec{a}_n^Q\right]\Bigg\}\,.\end{aligned} \tag{8.4}$$

This result allows to eliminate the term bi-linear in the Z_2-even profiles from (8.2), and to express the tree-level Higgs FCNCs solely in terms of overlap integrals involving Z_2-odd fields. Doing so, we find that the Higgs couplings to fermions can be written as

$$(g_h^q)_{mn} \equiv \delta_{mn}\,\frac{m_m^q}{v} - (\Delta g_h^q)_{mn}\,, \tag{8.5}$$

where the misalignment $(\Delta g_h^q)_{mn}$ between the SM masses and the Yukawa couplings is given by

$$(\Delta g_h^q)_{mn} = \frac{m_m^q}{v}\,(\Phi_q)_{mn} + (\Phi_Q)_{mn}\,\frac{m_n^q}{v} + (\Delta\tilde{g}_h^q)_{mn}\,, \tag{8.6}$$

with

$$(\Phi_q)_{mn} = \frac{2\pi}{L\epsilon}\int_\epsilon^1 dt\,\vec{a}_m^{Q\dagger}\,\boldsymbol{S}_m^Q(t)\,\boldsymbol{S}_n^Q(t)\,\vec{a}_n^Q\,, \qquad (\Phi_Q)_{mn} = \frac{2\pi}{L\epsilon}\int_\epsilon^1 dt\,\vec{a}_m^{q\dagger}\,\boldsymbol{S}_m^q(t)\,\boldsymbol{S}_n^q(t)\,\vec{a}_n^q\,, \tag{8.7}$$

and

$$(\Delta\tilde{g}_h^q)_{mn} = -\sqrt{2}\,\frac{2\pi}{L\epsilon}\int_\epsilon^1 dt\,\delta(t-1)\,\vec{a}_m^{q\,\dagger}\,\boldsymbol{S}_m^q(t)\,\boldsymbol{Y}_{\vec{q}}^\dagger\,\boldsymbol{S}_n^Q(t)\,\vec{a}_n^Q\,. \tag{8.8}$$

For Higgs couplings to fermion zero-modes, the corrections (8.7) receive a chiral suppression. For light quarks, these terms are negligible to first approximation. In the minimal model, the definitions of (8.7) are identical to the quark-mixing corrections $(\delta_{q,Q})_{mn}$ in the Z^0 couplings (7.17). The ZMA expressions are given in (7.21). In the custodial model, the corrections to the Higgs couplings differ in general from those of the Z^0. The respective ZMA results can be found in [53].

Our last task is to regularize the integrand of (8.8). Employing the regularization (6.8) for the δ-function, we get

$$(\Delta\tilde{g}_h^q)_{mn} = -\sqrt{2}\,\frac{2\pi}{L\epsilon}\int_{1-\eta}^{1} dt\,\frac{1}{\eta}\,\vec{a}_m^{q\,\dagger}\,\boldsymbol{S}_m^q(t)\,\boldsymbol{Y}_{\vec{q}}^\dagger\,\boldsymbol{S}_n^Q(t)\,\vec{a}_n^Q\,. \tag{8.9}$$

Now we combine the solutions (6.12) and (6.13) with the expressions for the boundary values at $t = 1^-$ (6.14) and apply the relation

$$\int_{1-\eta}^{1} dt\,\frac{1}{\eta}\,\sinh^2\left(\frac{\boldsymbol{A}}{\eta}(1-t)\right) = \frac{1}{2}\left(\sinh\left(2\boldsymbol{A}\right)\left(2\boldsymbol{A}\right)^{-1} - \boldsymbol{1}\right) \tag{8.10}$$

(valid for any invertible matrix $\boldsymbol{A}$) to the integral (8.9). Thus, we obtain

$$(\Delta\tilde{g}_h^q)_{mn} = \frac{1}{\sqrt{2}}\,\frac{2\pi}{L\epsilon}\,\frac{v^2}{3M_{\rm KK}^2}\,\vec{a}_m^{Q\,\dagger}\,\boldsymbol{C}_m^Q(1^-)\,\boldsymbol{Y}_{\vec{q}}\boldsymbol{Y}_{\vec{q}}^\dagger\,\boldsymbol{g}\left(\frac{v}{\sqrt{2}M_{\rm KK}}\sqrt{\boldsymbol{Y}_{\vec{q}}\boldsymbol{Y}_{\vec{q}}^\dagger}\right)\boldsymbol{Y}_{\vec{q}}\,\boldsymbol{C}_n^q(1^-)\,\vec{a}_n^q\,, \tag{8.11}$$

with

$$\boldsymbol{g}(\boldsymbol{A}) = \frac{3}{2}\left[\sinh\left(2\boldsymbol{A}\right)\left(2\boldsymbol{A}\right)^{-1} - \boldsymbol{1}\right]\left(\cosh\left(\boldsymbol{A}\right)\boldsymbol{A}\right)^{-2}\,. \tag{8.12}$$

This expression has to be rewritten in terms of rescaled Yukawa matrices (6.15), which we use as numerical input. Using

$$\frac{v}{\sqrt{2}M_{\rm KK}}\sqrt{\boldsymbol{Y}_{\vec{q}}\boldsymbol{Y}_{\vec{q}}^\dagger} = \tanh^{-1}\left(\frac{v}{\sqrt{2}M_{\rm KK}}\sqrt{\tilde{\boldsymbol{Y}}_{\vec{q}}\tilde{\boldsymbol{Y}}_{\vec{q}}^\dagger}\right)\,, \tag{8.13}$$

we obtain

$$(\Delta\tilde{g}_h^q)_{mn} = \frac{1}{\sqrt{2}}\,\frac{2\pi}{L\epsilon}\,\frac{v^2}{3M_{\rm KK}^2}\,\vec{a}_m^{Q\,\dagger}\,\boldsymbol{C}_m^Q(1^-)\,\tilde{\boldsymbol{Y}}_q\,\bar{\boldsymbol{Y}}_q^\dagger\,\tilde{\boldsymbol{Y}}_q\,\boldsymbol{C}_n^q(1^-)\,\vec{a}_n^q\,, \tag{8.14}$$

where

$$\bar{\boldsymbol{Y}}_q^\dagger \equiv \tilde{\boldsymbol{Y}}_q^\dagger\,\boldsymbol{h}\left(\frac{v}{\sqrt{2}M_{\rm KK}}\sqrt{\tilde{\boldsymbol{Y}}_q\tilde{\boldsymbol{Y}}_q^\dagger}\right)\,,\qquad \boldsymbol{h}(\boldsymbol{A}) = \frac{3}{2}\left[\boldsymbol{A}^{-2} + \tanh^{-1}\left(\boldsymbol{A}\right)\boldsymbol{A}^{-1}\left(\boldsymbol{1} - \boldsymbol{A}^{-2}\right)\right]. \tag{8.15}$$

In analogy to the rescaled Yukawa matrices $\tilde{\boldsymbol{Y}}_q$, the definition (8.15) satisfies $\bar{\boldsymbol{Y}}_q^\dagger = \boldsymbol{Y}_q^\dagger + \mathcal{O}(v^2/M_{\rm KK}^2)$. This implies that, as long as one is interested in the ZMA results for $(\Delta\tilde{g}_h^q)_{mn}$ only, one can simply replace $\tilde{\boldsymbol{Y}}_q\,\bar{\boldsymbol{Y}}_q^\dagger\,\tilde{\boldsymbol{Y}}_q$ by the product $\boldsymbol{Y}_q\,\boldsymbol{Y}_q^\dagger\,\boldsymbol{Y}_q$ of original Yukawa matrices. Applying the ZMA to the exact expression in (8.14), we find

$$\boldsymbol{\Delta\tilde{g}}_h^q = \frac{\sqrt{2}\,v^2}{3M_{\rm KK}^2}\,\boldsymbol{U}_q^\dagger\,\mathrm{diag}\left[F(c_{Q_i})\right]\boldsymbol{Y}_q\boldsymbol{Y}_q^\dagger\boldsymbol{Y}_q\,\mathrm{diag}\left[F(c_{q_i})\right]\boldsymbol{W}_q\,. \tag{8.16}$$

An analysis of the flavor misalignment of the SM fermion masses and the Yukawa couplings has also been presented in [86] for composite Higgs models. There it has been shown that chirally unsuppressed contributions to flavor-changing Higgs-fermion vertices arise from dimension-six operators of the form $\bar{q}_L^i\,H q_R^j\,(H^\dagger H)$. They generically dominate over the chiral suppressed contributions from $\bar{q}_L^i \not{D}\, q_L^j\, (H^\dagger H)$, because the couplings y_{q*} of the composite Higgs to the other strongly interacting states can be large, resulting in $y_{q*}^2/(16\pi^2) \gg m_q/v$. Within our model, one could also perform an analysis within the mass insertion approximation, keeping all relevant dimension-six operators in lowest order [67]. Doing so, one obtains the above ZMA expressions. We emphasize that in our exact solutions (8.5), (8.6), (8.7), and (8.14), all NP effects induced by the mass insertions are resummed to all orders in $v^2/M_{\rm KK}^2$ at tree level.

8.2 Higgs couplings to gauge bosons

In order to be able to calculate the production rates of the Higgs boson via vector-boson fusion, we still need to evaluate the RS corrections to the WWh and ZZh tree-level vertices. The weak couplings involving the Higgs boson are derived from the cubic and quartic interactions due to (4.6). In unitary gauge, the 4D Lagrangian involves

$$\mathcal{L}_{\rm 4D} \ni \left(h^2 + 2\,v\,h\right) \left[\frac{g_L^2}{4} \left(1 - \Delta g_h^W\right) W_\mu^+ W^{-\mu} + \frac{g_L^2 + g_Y^2}{8} \left(1 - \Delta g_h^Z\right) Z_\mu Z^\mu \right], \tag{8.17}$$

where

$$\Delta g_h^V = x_V^2 \left[L \left(1 + \frac{s_V^2}{c_V^2}\right) - 1 + \frac{1}{2L} \right] + \mathcal{O}\left(x_V^4\right), \tag{8.18}$$

and $x_V \equiv m_V/M_{\rm KK}$ for $V = W, Z$. For the case of P_{LR} symmetry (7.13), we have $s_W^2/c_W^2 = 1$ and $s_Z^2/c_Z^2 = 1 - 2s_w^2$. This implies that the leading correction due to $\Delta g_h^{W,Z}$ simplifies to $-2\,m_W^2/M_{\rm KK}^2\,L$. For $M_{\rm KK} = 2\,\text{TeV}$ ($3\,\text{TeV}$) these terms lead to a suppression of the WWh and ZZh couplings by about -10% (-5%) compared to the SM. In the minimal RS model the expressions (8.18) hold in the limit $s_{W,Z} \to 0$, and consequently the corrections to the couplings of the Higgs to massive gauge bosons are smaller by a factor of about 2.

In principle, one has to include another effect. As the Higgs VEV is extracted from the masses of the heavy gauge bosons, one would assume a correction of $\mathcal{O}(v^2/M_{\rm KK}^2)$ to the SM estimation $v = 246\,\text{GeV}$. In order to get a precise prediction here, one needs to calculate vacuum polarization diagrams that involve KK particles in the loop. In this thesis however, we fix the VEV to its SM value. The inclusion of a VEV shift [87] would partially cancel the correction terms (8.18) [88]. Our finding that the couplings WWh and ZZh experience a reduction from their SM expectations confirms the model-independent statements made in [89].

8.3 RS effects in Higgs production at the LHC

In this section, we estimate the impact of the RS scenario on Higgs production cross sections. At hadron colliders such as the Tevatron or the LHC, the leading production mechanism of the Higgs boson is gluon fusion. This process is mediated by a triangle

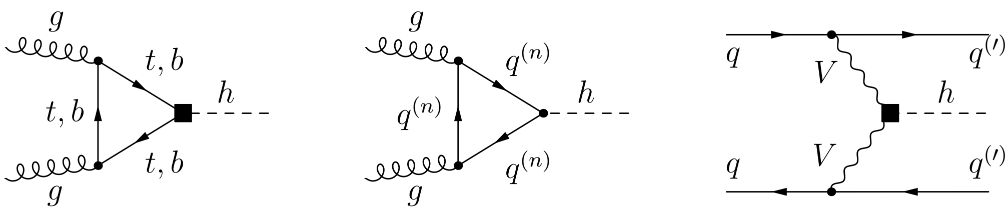

Figure 8.1: Feynman diagrams contributing to Higgs production via gluon and vector-boson fusion ($V = W, Z$). For the exchange of zero modes, the vertex indicated by a black square can receive a sizable shift in the RS model relative to the SM coupling. See text for details.

quark loop, where the dominant SM contribution stems from the top-quark. Within the RS framework, we further have to take into account KK modes of all quark flavors. The corresponding Feynman diagrams are depicted in Figure 8.1. It is evident that the treatment of the various KK-quark loops is analogous to the SM calculation. Due to the flatness of the zero-mode gluons in the initial state, there is no possibility of a flavor change inside the loop. Therefore, we can rescale the SM prediction of the production cross section, employing

$$\sigma(gg \to h)_{\rm RS} = |\kappa_g|^2 \; \sigma(gg \to h)_{\rm SM}\,, \tag{8.19}$$

where

$$\kappa_g = \frac{\sum_{i=t,b} \kappa_i A_q^h(\tau_i) + \sum_n \kappa_n^{\rm KK} A_q^h(\tau_n)}{\sum_{i=t,b} A_q^h(\tau_n)}\,, \tag{8.20}$$

with $\tau_i \equiv 4m_i^2/m_h^2$ and $\tau_n \equiv 4(m_n^q)^2/m_h^2$. The first term in the numerator encodes the effects due to zero modes running in the loop and the corresponding sum includes both the virtual top- and bottom-quark contributions. The form factor $A_q^h(\tau_i)$ arises from the calculation of the loop and approaches 1 for $\tau_i \to \infty$, whereas it vanishes proportional to τ_i for $\tau_i \to 0$. Its analytic form is given in Appendix A.2. For KK-modes with $\tau_n \ll 1$, it is a good approximation to set $A_q^h(\tau_n) = 1$. The task is now to sum up the tower, at least up to the IR cut-off. Naively, one would expect the whole sum to be logarithmically divergent, as the single contributions to the $g \to hh$ amplitude is proportional to y_n/m_n^q. However, as we will see in a moment, there is a cancellation taking place between the contributions of the various KK modes within each KK level, leading to a finite result. Nevertheless, one should remember the hard IR cut-off and truncate the sum over KK modes. This is also necessary in few of the solution of the hierarchy problem. Any KK fermion which couples to the Higgs gives rise to a term $\Lambda_{\rm IR}^2$ in the Higgs boson self-energy [90]. Thus, the sum over the whole quark tower will force the self-energy to diverge for finite $\Lambda_{\rm IR}^2$. Though it may be done analytically, a summation over n up to infinity[1] will be meaningless, as long

[1]For one generation this has been achieved in [88] for a perturbative treatment of EWSB.

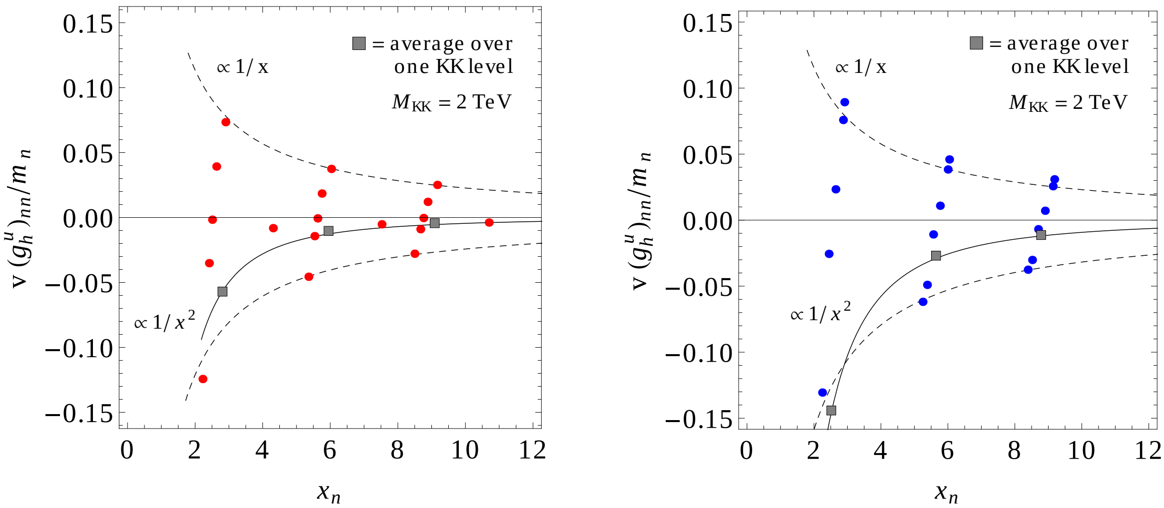

Figure 8.2: Numerical results for the summands in $\nu_{u,d}$ corresponding to our default parameter set. The red (blue) dots in the left (right) panel display the first 18 terms in the KK sum of up(down)-type quarks, while the gray boxes indicate the sums over a complete KK level. See text for details.

as the required UV completion is not known. At this point, one may complain that we have performed analytical summations over KK gauge boson towers for scattering amplitudes featuring strong and electroweak gauge interactions. However, the rejection of the cut-off does not lead to conceptional problems for that case. Moreover, the KK sum is dominated by the lowest modes, such that a truncated evaluation gives a similar result compared to the complete sum. As it turns out, this is not the case for brane-localized Higgs couplings to Z_2-odd fermions. Without going into details here, we refer the interested reader to an upcoming paper [90].

Coming back to the zero-mode exchange, we observe that also the Higgs-boson couplings to heavy quarks need to be corrected due to the misalignment (8.6) between the masses and Yukawa couplings. Therefore, we have introduced

$$\kappa_t = 1 - \frac{v}{m_t}\,(\Delta g_h^u)_{33}\,, \qquad \kappa_b = 1 - \frac{v}{m_b}\,(\Delta g_h^d)_{33} \tag{8.21}$$

in the relation (8.20). The corrections from the KK-tower can be written as

$$\sum\nolimits_n \kappa_n^{\rm KK} A_q^h(\tau_n) = \sum\nolimits_{q=u,d,(\lambda)} \nu_q\,, \tag{8.22}$$

where

$$\begin{aligned} \nu_u &= v \sum_{n=4} \frac{\mathrm{Re}[(g_h^u)_{nn}]}{m_n^u}\, A_q^h(\tau_n^u) \\ &= \frac{2\pi}{\epsilon L} \sum_{n=4} \mathrm{Re}\left[\vec{a}_n^{U\dagger}\, \boldsymbol{C}_n^U(\pi^-) \left(\mathbf{1} - \frac{v^2}{3M_{\rm KK}^2}\, \tilde{\boldsymbol{Y}}_u \bar{\boldsymbol{Y}}_u^\dagger\right) \boldsymbol{S}_n^U(\pi^-)\, \vec{a}_n^U\right] (x_n^u)^{-1}\, A_q^h(\tau_n^u)\,, \end{aligned} \tag{8.23}$$

and similar for $q = d, (\lambda)$. The sum should be truncated at low n. For instance, if we include the first two KK-levels, we have to up to $n = 15$ in the minimal RS model. Note that, due to the IR BCs (6.16), we could replace the $SU(2)_L$-doublet profiles and vectors by those corresponding to $SU(2)_L$ singlets in the above expression, if in addition we changed the order $\tilde{\boldsymbol{Y}}_u \bar{\boldsymbol{Y}}_u^\dagger \to \bar{\boldsymbol{Y}}_u^\dagger \tilde{\boldsymbol{Y}}_u$ and added an overall sign factor.

In Figure 8.2, we show the individual summands of the first three KK levels within the minimal model for our reference parameter set (A.2, A.3), using $M_{\rm KK} = 2\,\text{TeV}$. The plots show clearly the bunches belonging to a single level. In the up sector, the $SU(2)_L$-singlet top-quark turns out to be an outlier due to its strong IR localization. The dashed lines mark $1/x_n$ fits for single fermion species and recover the naive y_n/m_n behavior. Note especially that the various Higgs couplings contribute with different signs. Therefore a cancellation takes place within each KK level. The gray boxes mark the average values of the masses and Higgs couplings of each KK level. As indicated by the continuous lines, they fit to a $1/x_l^2$ behavior, and therefore guarantee the convergence of the sum (8.23).

In analogy to (8.21), we define the correction factors

$$\kappa_W = 1 - \Delta g_h^W \,, \qquad \kappa_Z = 1 - \Delta g_h^Z \tag{8.24}$$

for the exchange of $W^\pm$ and Z^0 bosons. These are needed for computing the RS corrections to the Higgs production cross section of vector-boson fusion $qq^{(\prime)} \to qq^{(\prime)}V^*V^* \to qq^{(\prime)}h$ ($V = W, Z$), which is another important possibility at the LHC. Note that contributions from KK gauge bosons can be neglected to excellent approximation in these channels: Either the respective couplings to light quarks are RS GIM suppressed, or, in the case of top-quarks in the initial state, they are negligible due to the parton distribution function (PDF) of the proton. Moreover, the flavor non-universal corrections of the $W^\pm$ and Z^0 couplings to light quarks are also RS GIM suppressed, whereas the universal modifications are absorbed into a redefinition of G_F (3.38). Thus, we are left with the corrections to the VVh couplings (8.24), as indicated by the black square in the Feynman diagram on the right-hand side of Figure 8.1.

In [53], we have performed an analysis of the Higgs-boson production cross sections at the LHC for a center-of-mass energy $\sqrt{s} = 10\,\text{TeV}$. The calculation of $\sigma(gg \to h)_{\rm SM}$ is based on [91]. Furthermore, `MRST2006NNLO` parton distribution functions [92] and the associated normalization $\alpha_s(m_Z) = 0.1191$ for the strong coupling constant have been used. Considering the RS corrections, we have computed the quantities (8.21) and (8.24) for 10000 appropriate parameter sets. Average values have been extracted by fitting the results to $\kappa_i = 1 - a_i\, v^2/M_{\rm KK}^2$ and taking the mean values of the coefficients ν_i. The results are shown in Figure 8.3 (solid lines) for $M_{\rm KK} = 2\,\text{TeV}$ and $M_{\rm KK} = 3\,\text{TeV}$ respectively, where the dashed lines indicate the SM expectation. For the gluon fusion, the dependence on the Higgs mass enters through the loop function $A_q^h(\tau_i)$ ($i = t, b$), and therefore solely comes from RS corrections to the zero-modes to first approximation. As we see, we observe sizable reductions of the Higgs production cross section via gluon fusion compared to the SM. For $M_{\rm KK} = 2\,\text{TeV}$ and $m_h \approx 2m_t$, we find an almost perfect destructive interference between corrections to the zero-modes and KK-quarks in the triangle loop. Raising the

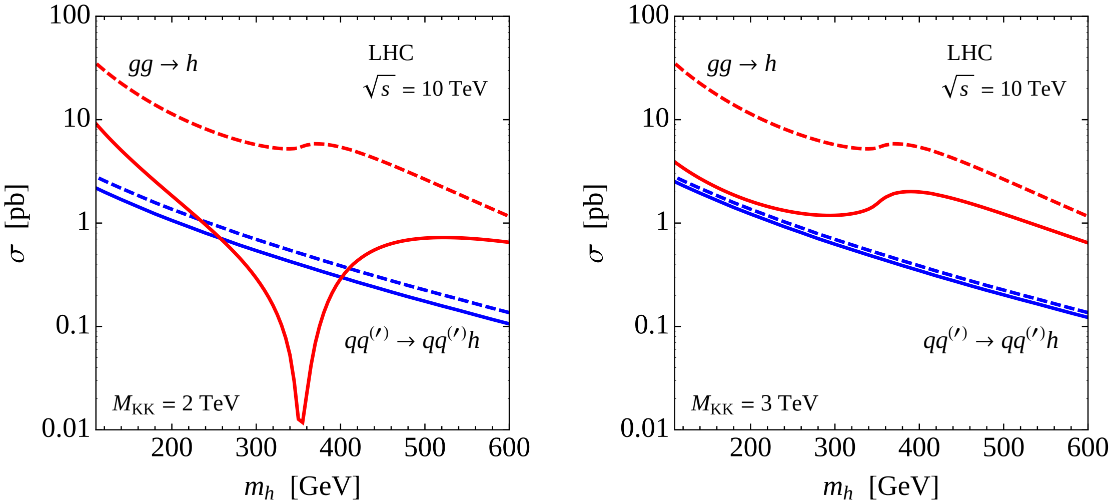

Figure 8.3: Main Higgs-boson production cross sections via gluon-(red) and vector-boson fusion (blue) at the LHC for a center-of-mass energy of $\sqrt{s} = 10\,\text{TeV}$, and $M_{\text{KK}} = 2$ TeV (left) and $M_{\text{KK}} = 3$ TeV (right). The figures are taken from [53]. See text for details.

Higgs mass flips the sign of the real part of the amplitude in the threshold region. For higher KK scales, the corrections to the zero-modes always dominate, and the real part of the amplitude is positive for all values of the Higgs mass. As a consequence, there is no dip of the cross esection in the plot for $M_{\text{KK}} = 3\,\text{TeV}$. On the other hand, a reduction of the gluon-fusion cross section by a factor of ≈ 10 is still present for light Higgs masses. The RS corrections to vector-boson fusion are rather moderate, not exceeding -20% (-10%) for $M_{\text{KK}} = 2\,\text{TeV}$ ($M_{\text{KK}} = 3\,\text{TeV}$).

We have further performed a numerical analysis of the modification of the various Higgs decay branching fractions. Details of the calculations can be found in [53]. At this point, we just quote the most important results. For $m_h \gtrsim 180\,\text{GeV}$ the experimentally cleanest signature for the Higgs discovery at the LHC is the "golden" decay to four leptons, $h \to Z^{(*)}Z^{(*)} \to l^+l^-l^+l^-$. As it turns out, the $h \to ZZ$ branching fraction is essential SM-like. Thus, the reduction in the $gg \to h$ production cross section will make an observation of the Higgs boson in the golden channel more difficult. The most pronounced effects are found for the decays $h \to gg$ and $h \to \gamma\gamma$. For Higgs masses below the WW threshold, the branching fraction of the former is reduced by a factor of almost 4 (8) for $M_{\text{KK}} = 2$ (3) TeV, while the branching ratio of the latter transition is enhanced by a factor of around 4 (2). It follows that the statistical significance for a LHC discovery of the Higgs boson in $h \to \gamma\gamma$ can be enhanced in the custodial RS model for low KK scales.

9 Forward-backward asymmetry in $t\bar{t}$ production

As we have learned above, the top-quark is exceptional in RS scenarios, as its couplings to KK gauge bosons are not suppressed by the RS GIM mechanism. As a consequence, we may expect sizable RS corrections within observables related to top production and decay. One of these is the forward-backward asymmetry observed in $t\bar{t}$ production at the Tevatron. The CDF and DØ experiments have collected thousands of top-quark pair events, which allowed to measure the top-quark mass, m_t, and its total inclusive cross section, $\sigma_{t\bar{t}}$, with an accuracy of below 1% [93] and 10% [94, 95], respectively. The forward-backward asymmetry, $A_{\rm FB}^t$, which is closely related to the charge-symmetric and asymmetric cross sections, has been measured [96, 97, 98, 99, 100] and consistently found to be larger than expected. In the laboratory ($p\bar{p}$) frame, the CDF result reads

$$\left(A_{\rm FB}^t\right)_{\rm exp}^{p\bar{p}} = (15.0 \pm 5.0_{\,\rm stat.} \pm 2.4_{\,\rm syst.})\,\%\,, \tag{9.1}$$

where the quoted uncertainties are of statistical and systematical origin, respectively. Recently, CDF presented measurements of $A_{\rm FB}^t$ in the dilepton decay channel with $5.1\,{\rm fb}^{-1}$ of collected data [101]. After correcting for background, detector acceptance and resolution effects, the asymmetry has been found to be $(A_{\rm FB}^t)_{\rm dilep}^{p\bar{p}} = (42.0 \pm 15.0_{\,\rm stat.} \pm 5.0_{\,\rm syst.})\,\%$.

The DØ collaboration reported a measurement of $(A_{\rm FB}^t)_{\rm exp}^{\rm obs.} = (8 \pm 4_{\rm stat.} \pm 1_{\rm syst.})\%$ for $t\bar{t}$ events that satisfy the experimental acceptance cuts [102]. The corresponding SM prediction reads $(A_{\rm FB}^t)_{\rm SM}^{\rm obs.} = \left(1^{+2}_{-1}\right)\%$ and is similarly below the observed value.

In order to get into the subject, we first explain how the asymmetry arises within the SM. Then, we will extend our considerations to general NP models. Here, we will work in a general EFT language and give results for the RS Wilson coefficients of the respective four-fermion operators. A numerical analysis of possible NP corrections within the RS scenario is presented in the last subsection. All these results have been published in [103].

9.1 Production cross section and asymmetry in the SM

The Tevatron produces $t\bar{t}$ pairs in collisions of protons and anti-protons, $p\bar{p} \to t\bar{t}X$ at a center-of-mass energy of 1.96 TeV. At the Born-level, the process is mediated by quark-anti-quark annihilation and gluon fusion

$$\begin{aligned} q(p_1) + \bar{q}(p_2) &\to t(p_3) + \bar{t}(p_4)\,,\\ g(p_1) + g(p_2) &\to t(p_3) + \bar{t}(p_4)\,. \end{aligned} \tag{9.2}$$

The four-momenta $p_{1,2}$ of the initial state partons are given by the fractions $x_{1,2}$ of the momenta $P_{1,2}$ of the colliding hadrons, $p_{1,2} = x_{1,2} P_{1,2}$. As usual, $s = (P_1 + P_2)^2$ denotes the hadronic center-of-mass (CM) energy squared. The partonic cross section can be expressed as a function of the kinematic invariants

$$\hat{s} = (p_1 + p_2)^2 \,, \qquad t_1 = (p_1 - p_3)^2 - m_t^2 \,, \qquad u_1 = (p_2 - p_3)^2 - m_t^2 \,, \tag{9.3}$$

where momentum conservation implies that $\hat{s} + t_1 + u_1 = 0$.

Important observables are the differential cross section with respect to the invariant mass $M_{t\bar{t}} = \sqrt{(p_3 + p_4)^2}$ of the $t\bar{t}$ pair and the angle θ between $\vec{p}_1$ and $\vec{p}_3$ in the partonic CM frame. Therefore, we express t_1 and u_1 in terms of θ and the top-quark velocity β,

$$t_1 = -\frac{\hat{s}}{2}(1 - \beta\cos\theta) \,, \qquad u_1 = -\frac{\hat{s}}{2}(1 + \beta\cos\theta) \,, \qquad \beta = \sqrt{1-\rho} \,, \qquad \rho = \frac{4m_t^2}{\hat{s}} \,. \tag{9.4}$$

The hadronic differential cross section may then be written as

$$\frac{d\sigma^{p\bar{p}\to t\bar{t}X}}{d\cos\theta} = \frac{\alpha_s}{m_t^2} \sum_{i,j} \int_{4m_t^2}^{s} \frac{d\hat{s}}{s}\, ff_{ij}\left(\hat{s}/s, \mu_f\right) K_{ij}\left(\frac{4m_t^2}{\hat{s}}, \cos\theta, \mu_f\right) \,, \tag{9.5}$$

where μ_f denotes the factorization scale and we have introduced the parton luminosity functions

$$ff_{ij}(y, \mu_f) = \int_y^1 \frac{dx}{x}\, f_{i/p}(x, \mu_f)\, f_{j/\bar{p}}(y/x, \mu_f) \,. \tag{9.6}$$

The luminosities for $ij = q\bar{q}, \bar{q}q$ are understood to be summed over all species of light quarks, and the functions $f_{i/p}(x, \mu_f)$ ($f_{i/\bar{p}}(x, \mu_f)$) are the universal non-perturbative PDFs, which describe the probability of finding the parton i in the proton (anti-proton) with longitudinal momentum fraction x. The hard-scattering kernels $K_{ij}(\rho, \cos\theta, \mu_f)$ can be expanded in α_s and thus be written in the form

$$K_{ij}(\rho, \cos\theta, \mu_f) = \sum_{n=0}^{\infty} \left(\frac{\alpha_s}{4\pi}\right)^n K_{ij}^{(n)}(\rho, \cos\theta, \mu_f) \,. \tag{9.7}$$

Calculating the LO amplitudes of s-channel gluon exchange yields

$$\begin{aligned} K_{q\bar{q}}^{(0)} &= \alpha_s \frac{\pi\beta\rho}{8} \frac{C_F}{N_c} \left(\frac{t_1^2 + u_1^2}{\hat{s}^2} + \frac{2m_t^2}{\hat{s}}\right) \,, \\ K_{gg}^{(0)} &= \alpha_s \frac{\pi\beta\rho}{8(N_c^2 - 1)} \left(C_F \frac{\hat{s}^2}{t_1 u_1} - N_c\right) \left[\frac{t_1^2 + u_1^2}{\hat{s}^2} + \frac{4m_t^2}{\hat{s}} - \frac{4m_t^4}{t_1 u_1}\right] . \end{aligned} \tag{9.8}$$

The coefficient $K_{\bar{q}q}^{(0)}$ is obtained from $K_{q\bar{q}}^{(0)}$ by replacing $\cos\theta$ with $-\cos\theta$. The factors $N_c = 3$ and $C_F = 4/3$ are the usual color factors of $SU(3)_c$.

Next we introduce charge-asymmetric (a) and -symmetric (s) differential cross sections

$$\frac{d\sigma_{a,s}}{d\cos\theta} \equiv \frac{1}{2}\left[\frac{d\sigma^{p\bar{p}\to t\bar{t}X}}{d\cos\theta} \mp \frac{d\sigma^{p\bar{p}\to \bar{t}tX}}{d\cos\theta}\right] \,. \tag{9.9}$$

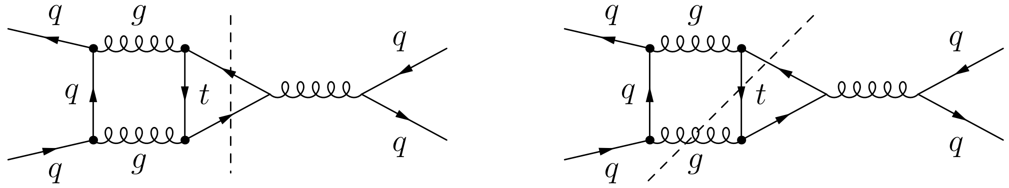

Figure 9.1: Feynman diagrams contributing to $A_{\rm FB}^t$ in $t\bar{t}$ production at NLO QCD. The two-particle (three-particle) cut corresponds to the interference of $q\bar{q} \to t\bar{t}$ ($q\bar{q} \to t\bar{t}g$) amplitudes.

The superscripts $p\bar{p} \to t\bar{t}X$ and $p\bar{p} \to \bar{t}tX$ indicate that the angle θ corresponds to the scattering angles of the top and anti-top in the partonic CM frame, respectively. Obviously, the total hadronic cross section is given by

$$\sigma_{t\bar{t}} = \int_{-1}^{1} d\cos\theta \, \frac{d\sigma_s}{d\cos\theta} \,. \tag{9.10}$$

Since QCD is symmetric under charge conjugation, we can replace

$$\left. \frac{d\sigma^{p\bar{p}\to\bar{t}tX}}{d\cos\theta} \right|_{\cos\theta = c} = \left. \frac{d\sigma^{p\bar{p}\to t\bar{t}X}}{d\cos\theta} \right|_{\cos\theta = -c} \tag{9.11}$$

for any fixed value c. The forward-backward asymmetry is defined as

$$A_{\rm FB}^t \equiv \frac{\displaystyle\int_0^1 d\cos\theta \, \frac{d\sigma^{p\bar{p}\to t\bar{t}X}}{d\cos\theta} - \int_{-1}^0 d\cos\theta \, \frac{d\sigma^{p\bar{p}\to t\bar{t}X}}{d\cos\theta}}{\displaystyle\int_0^1 d\cos\theta \, \frac{d\sigma^{p\bar{p}\to t\bar{t}X}}{d\cos\theta} + \int_{-1}^0 d\cos\theta \, \frac{d\sigma^{p\bar{p}\to t\bar{t}X}}{d\cos\theta}} = \frac{\sigma_a}{\sigma_s} \equiv A_c^t \,, \tag{9.12}$$

and compares the number of top quarks scattered along the direction of the incoming proton with the respective number of the opposite hemisphere. Due to the relation (9.11), its definition is equivalent to that of a charge asymmetry A_c^t, which is given by the ratio of the charge-asymmetric and -symmetric cross sections (9.9). In the following, we will denote the respective hard-scattering kernels by A_{ij} and S_{ij}.

In the SM the LO coefficients of the symmetric part read

$$\begin{aligned} S_{q\bar{q}}^{(0)} &= \alpha_s \, \frac{\pi\beta\rho}{27} \, (2+\rho) \,, \\ S_{gg}^{(0)} &= \alpha_s \, \frac{\pi\beta\rho}{192} \left[\frac{1}{\beta} \ln\left(\frac{1+\beta}{1-\beta}\right) \left(16 + 16\rho + \rho^2\right) - 28 - 31\rho \right] , \end{aligned} \tag{9.13}$$

while the asymmetric contributions $A_{q\bar{q}}^{(0)}$ and $A_{gg}^{(0)}$ both vanish identically.

At next-to-leading order (NLO) a non-zero coefficient $A_{q\bar{q}}^{(1)}$ is generated from the interference of tree-level gluon exchange with one-loop QCD box diagrams and the interference of initial- and final-state radiation (see Figure 9.1). Including QCD NLO as well as electroweak corrections [104, 105], the SM prediction in the $p\bar{p}$ frame for the inclusive asymmetry is [106]

$$\left(A_{\rm FB}^t\right)_{\rm SM}^{p\bar{p}} = (5.1 \pm 0.6)\,\%\,, \tag{9.14}$$

where the total error includes the individual uncertainties due to different choices of the parton distribution functions (PDFs), the factorization and renormalization scales, and a variation of m_t within its experimental error. Recent theoretical determinations of $(A_{\rm FB}^t)_{\rm SM}$, that include the resummation of logarithmically enhanced threshold effects at NLO [107] and NNLO [108, 109], are in agreement with the latter number. If we compare this result to (9.1), we see that the SM prediction is about 2σ away from the experimental value (9.1). Recently, an evidence for a mass dependent forward-backward asymmetry has been presented in [110] for $5.3\,{\rm fb}^{-1}$ of $p\bar{p}$ collisions. It has been found that for an invariant mass of $M_{t\bar{t}} \geq 450\,{\rm Gev}$, the tension in the $t\bar{t}$-rest frame exceeds 3σ.

9.2 NP corrections at LO

In general, it turns out to be difficult to explain the large central experimental value, since any viable NP model must simultaneously avoid giving rise to unacceptably large deviations in $\sigma_{t\bar{t}}$ and/or $d\sigma_{t\bar{t}}/dM_{t\bar{t}}$, which both show no evidence of non-SM physics. In [103] we have listed a bunch of publications, which propose NP in the s-channel through the exchange of new vector bosons, or contributions to the $t(u)$-channel by the exchange of either vector bosons W' and Z', or color singlet, triplet and sextet scalars. Concerning the s-channel exchange, color octets are preferred as they directly interfere with LO QCD diagrams. They should exhibit sizable axial-vector couplings to both the light quarks, g_A^q, and the top quark, g_A^t. In order to induce a positive shift in $A_{\rm FB}^t$, the new vectors have to couple to the first and the third generation of quarks with axial-vector couplings [111] of opposite sign[1].

As noted in [112], the RS scenario of a warped extra dimension offers the possibility to fulfill the latter requirement, as gauge couplings of quarks to KK gluons depend on flavor. Further corrections to $A_{\rm FB}^t$ arise from the neutral current sector, where KK excitations of the photon and the Z boson give rise to flavor-violating couplings. At the order $v^4/M_{\rm KK}^4$, there are also contributions from the Z^0 and the Higgs boson. The LO diagrams are shown in Figure 9.2. The gluon-fusion channel $gg \to t\bar{t}$ does not receive a correction at the Born level, since the coupling of two gluons to a KK gluon is zero due to the orthonormality of the gauge-boson wave functions.

[1] The sign is needed as to first approximation the interference term is proportional to $g_A^q g_A^t/(-M_{\rm NP}^2)$, where $M_{\rm NP}$ is the mass of the new exchange particle.

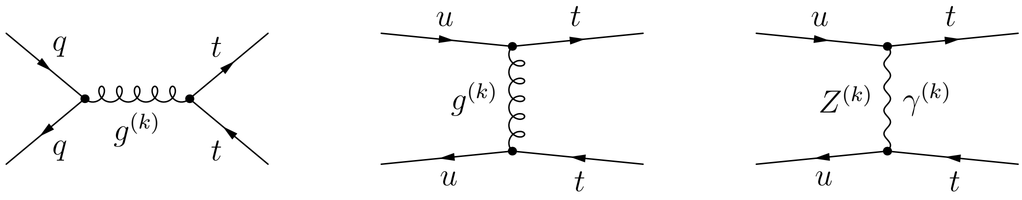

Figure 9.2: Tree-level contributions to the $q\bar{q} \to t\bar{t}$ (left) and the $u\bar{u} \to t\bar{t}$ (right) transition arising from s- and t-channel exchange of KK gauge bosons.

The effective Lagrangian, needed to account for the effects of the order $v^2/M_{\rm KK}^2$, reads

$$\mathcal{L}_{\rm eff} = \sum_{q,u} \sum_{A,B=L,R} \left[C_{q\bar{q},AB}^{(V,8)} Q_{q\bar{q},AB}^{(V,8)} + C_{t\bar{u},AB}^{(V,8)} Q_{t\bar{u},AB}^{(V,8)} + C_{t\bar{u},AB}^{(V,1)} Q_{t\bar{u},AB}^{(V,1)} \right], \tag{9.15}$$

where

$$\begin{aligned} Q_{q\bar{q},AB}^{(V,8)} &= (\bar{q}\gamma_\mu T^a P_A q)(\bar{t}\gamma^\mu T^a P_B t)\,, \\ Q_{t\bar{u},AB}^{(V,8)} &= (\bar{u}\gamma_\mu T^a P_A t)(\bar{t}\gamma^\mu T^a P_B u)\,, \\ Q_{t\bar{u},AB}^{(V,1)} &= (\bar{u}\gamma_\mu P_A t)(\bar{t}\gamma^\mu P_B u)\,. \end{aligned} \tag{9.16}$$

The sum over q (u) involves all light (up-type) quark flavors, and the superscripts $(V,1)$ and $(V,8)$ label color-octet and singlet vector currents, respectively. The chiral projectors $P_{L,R}$ have been introduced in (1.18). Starting from (9.15), we calculate the interference between the matrix elements of the s-channel SM gluon exchange and the s- and t-channel NP contributions, which arise from the Feynman graphs displayed in Figure 9.2. In terms of the linear combinations

$$C_{ij,\parallel}^{(P,a)} = {\rm Re}\left[C_{ij,LL}^{(P,a)} + C_{ij,RR}^{(P,a)} \right], \qquad C_{ij,\perp}^{(P,a)} = {\rm Re}\left[C_{ij,LR}^{(P,a)} + C_{ij,RL}^{(P,a)} \right], \tag{9.17}$$

the resulting hard-scattering kernels take the form

$$\begin{aligned} K_{q\bar{q},{\rm RS}}^{(0)} &= \frac{\beta\rho}{32}\,\frac{C_F}{N_c} \left[\frac{t_1^2}{\hat{s}}\, C_{q\bar{q},\perp}^{(V,8)} + \frac{u_1^2}{\hat{s}}\, C_{q\bar{q},\parallel}^{(V,8)} + m_t^2 \left(C_{q\bar{q},\parallel}^{(V,8)} + C_{q\bar{q},\perp}^{(V,8)} \right) \right], \\ K_{t\bar{u},{\rm RS}}^{(0)} &= \frac{\beta\rho}{32}\,\frac{C_F}{N_c} \left[\left(\frac{u_1^2}{\hat{s}} + m_t^2 \right) \left(\frac{1}{N_c} C_{t\bar{u},\parallel}^{(V,8)} - 2 C_{t\bar{u},\parallel}^{(V,1)} \right) \right]. \end{aligned} \tag{9.18}$$

Here, N_c is the number of colors and C_F has been introduced in (1.35).

After integrating over $\cos\theta$, one obtains the LO corrections to the symmetric and asymmetric parts of the cross section in the partonic CM frame

$$\begin{aligned} S_{u\bar{u},{\rm RS}}^{(0)} &= \frac{\beta\rho}{216}\,(2+\rho)\,\hat{s} \left[C_{u\bar{u},\parallel}^{(V,8)} + C_{u\bar{u},\perp}^{(V,8)} + \frac{1}{3} C_{t\bar{u},\parallel}^{(V,8)} - 2 C_{t\bar{u},\parallel}^{(V,1)} \right], \\ S_{d\bar{d},{\rm RS}}^{(0)} &= \frac{\beta\rho}{216}\,(2+\rho)\,\hat{s} \left[C_{d\bar{d},\parallel}^{(V,8)} + C_{d\bar{d},\perp}^{(V,8)} \right], \end{aligned} \tag{9.19}$$

and

$$
\begin{aligned}
A^{(0)}_{u\bar{u},\mathrm{RS}} &= \frac{\beta^2\rho}{144}\,\hat{s}\,\left[C^{(V,8)}_{u\bar{u},\parallel} - C^{(V,8)}_{u\bar{u},\perp} + \frac{1}{3}C^{(V,8)}_{t\bar{u},\parallel} - 2C^{(V,1)}_{t\bar{u},\parallel}\right] \\
A^{(0)}_{d\bar{d},\mathrm{RS}} &= \frac{\beta^2\rho}{144}\,\hat{s}\,\left[C^{(V,8)}_{d\bar{d},\parallel} - C^{(V,8)}_{d\bar{d},\perp}\right]\,.
\end{aligned}
\tag{9.20}
$$

Obviously, the coefficients involving down-type quarks do not receive corrections from flavor-changing t-channel transitions. Note that in (9.19) the coefficients $C^{(V,8)}_{q\bar{q},\parallel}$ and $C^{(V,8)}_{q\bar{q},\perp}$ enter in the combination $C^{V}_{q\bar{q}} \equiv \big(C^{(V,8)}_{q\bar{q},\parallel} + C^{(V,8)}_{q\bar{q},\perp}\big)$, while in (9.20) they contribute as the difference $C^{A}_{q\bar{q}} \equiv \big(C^{(V,8)}_{q\bar{q},\parallel} - C^{(V,8)}_{q\bar{q},\perp}\big)$. This feature is related to the fact that the symmetric (asymmetric) LO cross section σ_s (σ_a) measures the product $g^q_V g^t_V$ $\big(g^q_A g^t_A\big)$ of the vector (axial-vector) parts of the respective gauge couplings.

The expressions (9.19) and (9.20) hold for any NP model, which goes along with tree-level exchange of new color-octet vectors in the s- and t-channel, as well as t-channel transitions due to flavor changing color-singlet vectors. Whithin the minimal RS model, the coefficients are explicitly given by [103]

$$
\begin{aligned}
C^{(V,8)}_{q\bar{q},\parallel} &= -\frac{2\pi\alpha_s}{M^2_{\mathrm{KK}}}\left\{\frac{1}{L} - \sum_{a=Q,q}\left[(\Delta'_a)_{11} + (\Delta'_a)_{33} - 2L\,(\widetilde{\Delta}_a)_{11}\otimes(\widetilde{\Delta}_a)_{33}\right]\right\}, \\
C^{(V,8)}_{q\bar{q},\perp} &= -\frac{2\pi\alpha_s}{M^2_{\mathrm{KK}}}\left\{\frac{1}{L} - \sum_{a=Q,q}\left[(\Delta'_a)_{11} + (\Delta'_a)_{33}\right]\right. \\
&\qquad\left. + 2L\left[(\widetilde{\Delta}_Q)_{11}\otimes(\widetilde{\Delta}_q)_{33} + (\widetilde{\Delta}_q)_{11}\otimes(\widetilde{\Delta}_Q)_{33}\right]\right\},
\end{aligned}
\tag{9.21}
$$

$$
\begin{aligned}
C^{(V,8)}_{t\bar{u},\parallel} &= -\frac{4\pi\alpha_s}{M^2_{\mathrm{KK}}}\,L\sum_{a=U,u}\left[(\widetilde{\Delta}_a)_{13}\otimes(\widetilde{\Delta}_a)_{31}\right], \\
C^{(V,1)}_{t\bar{u},\parallel} &= -\frac{4\pi\alpha_e}{M^2_{\mathrm{KK}}}\,\frac{L}{s^2_w c^2_w}\left[\left(T^u_3 - s^2_w Q_u\right)^2(\widetilde{\Delta}_U)_{13}\otimes(\widetilde{\Delta}_U)_{31} + \left(s^2_w Q_u\right)^2(\widetilde{\Delta}_u)_{13}\otimes(\widetilde{\Delta}_u)_{31}\right] \\
&\quad - \frac{4\pi\alpha_e}{M^2_{\mathrm{KK}}}\,L\,Q^2_u\sum_{a=U,u}\left[(\widetilde{\Delta}_a)_{13}\otimes(\widetilde{\Delta}_a)_{31}\right],
\end{aligned}
\tag{9.22}
$$

for $q = u, d$ and $Q = U, D$. Analogous expressions with the index 1 replaced by 2 hold if the quarks in the initial state belong to the second generation. As in the charge-current sector, the tensor products indicate that the respective terms do not factorize into single vertex corrections. The definition of these terms have been given in [38, 84]. The overlap integrals $(\Delta_{Q,q})_{ij}$ have been introduced in (7.16). Here, they stem from the non-universal (t-dependent) terms in our expression for the sum over the KK-gluon tower (3.36). In Appendix B.1, we collect ZMA expressions and give the results of the RG evaluation at leading logarithmic accuracy, which are used for our numerical analysis. As it turns out, the dominant RS corrections stem from the vector couplings of KK gluons, which are collected into $C^V_{q\bar{q}}$. This is also true for the custodial scenario.

Coming to the subleading corrections we observe that the left-handed part of the KK Z-boson contribution to $C^{(V,1)}_{t\bar{u},\parallel}$ is enhanced by a factor of around 3 within the custodial RS model compared to the minimal one. On the other hand, the right-handed contribution is protected by the custodial symmetry and thus smaller by a factor of roughly $1/L \approx 1/37$. In contrast, the KK-gluon contributions remain unchanged at the order $(v^2/M^2_{\rm KK})$. Higher order corrections arise from the admixture of KK fermions to the light quarks. We conclude that the predictions for the $t\bar{t}$ observables are rather model-independent. However, as we will see later, the constraints from the $Z^0 b\bar{b}$-pseudo observables restrict the possible range of RS corrections within the minimal model compared to the custodial one.

In order to get a feeling about the size of the RS hard-scattering kernels for $t\bar{t}$ production, we just consider corrections proportional to α_s and suppress relative $\mathcal{O}(1)$ factors as well as numerically sub-leading terms for the moment. Thus, we can simplify the ZMA results (B.1) and find that the coefficient functions $S^{(0)}_{ij,\rm RS}$ and $A^{(0)}_{ij,\rm RS}$ scale like

$$
\begin{aligned}
S^{(0)}_{u\bar{u},\rm RS} &\sim \frac{4\pi\alpha_s}{M^2_{\rm KK}} \sum_{A=L,R} F^2(c_{t_A})\,, \\
A^{(0)}_{u\bar{u},\rm RS} &\sim -\frac{4\pi\alpha_s}{M^2_{\rm KK}}\, L \left\{ \prod_{q=t,u} \Big[F^2(c_{q_R}) - F^2(c_{q_L})\Big] + \frac{1}{3} \sum_{A=L,R} F^2(c_{t_A}) F^2(c_{u_A}) \right\},
\end{aligned}
\tag{9.23}
$$

for the case of up-type quarks. Here, we have again used the notation $c_{t_L} \equiv c_{Q_3}$, $c_{t_R} \equiv c_{u_3}$, $c_{u_L} \equiv c_{Q_1}$, and $c_{u_R} \equiv c_{u_1}$.

Under the natural assumptions that the bulk mass parameters of the top and up quarks satisfy $c_{t_A} > -1/2$ and $c_{u_A} < -1/2$, we can use the approximate scaling behavior (6.34) of the zero-mode profiles, and expand the above result in the small number $(c_{u_L} - c_{u_R})$. Thus, we find

$$
\begin{aligned}
S^{(0)}_{u\bar{u},\rm RS} &\sim \frac{4\pi\alpha_s}{M^2_{\rm KK}}\, 2\left(1 + c_{t_L} + c_{t_R}\right)\,, \\
A^{(0)}_{u\bar{u},\rm RS} &\sim \frac{4\pi\alpha_s}{M^2_{\rm KK}}\, 2L\, e^{L(1+c_{u_L}+c_{u_R})} \left(1 + c_{u_L} + c_{u_R}\right) \\
&\quad \times \left\{ \left(2 + \frac{1}{3}\right) L \left(c_{t_L} - c_{t_R}\right)\left(c_{u_L} - c_{u_R}\right) + \frac{1}{3}\left(1 + c_{t_L} + c_{t_R}\right) \right\}.
\end{aligned}
\tag{9.24}
$$

The symmetric function entirely arises from s-channel KK-gluon exchange, while the asymmetric one collects contributions from the s-channel (proportional to the term multiplied by 2 in the curly bracket) and the t-channel (terms $\propto 1/3$). The relations (9.24) reveal a couple of interesting features. We first observe that the hard-scattering kernel $S^{(0)}_{u\bar{u},\rm RS}$ of the charge-symmetric cross section is independent of the localization of the up-quark to first approximation. Furthermore, it is strictly positive, as long as $c_{t_A} > -1/2$. This implies that the inclusive $t\bar{t}$ production cross section gets enhanced with increasing IR localization of the left- and right-handed top quarks.

In contrast to $S^{(0)}_{u\bar{u},\mathrm{RS}}$, both terms in $A^{(0)}_{u\bar{u},\mathrm{RS}}$ are exponentially suppressed for UV-localized up quarks, *i.e.*, $c_{u_A} < -1/2$. For typical values of the bulk mass parameters, one finds that the magnitude of the first term in the curly bracket of (9.24) is larger than the second term by a factor of almost 10. This implies that, to first approximation, the asymmetric cross section can be described by including only the effects from s-channel KK-gluon exchange. Note that the difference of the bulk mass parameters for light quarks $(c_{u_L} - c_{u_R})$ is typically small and positive. It follows that the product $(1 + c_{u_L} + c_{u_R})(c_{u_L} - c_{u_R}) < 0$ is generically negative. In order to find a positive LO contribution to $A^{(0)}_{u\bar{u},\mathrm{RS}}$, one requires $(c_{t_L} - c_{t_R})$ to be negative as well. Fortunately, this is the natural assumption in warped models which satisfy bounds from the $Z^0 b_L \bar{b}_L$ vertex and generate the hierarchies in the flavor sector by means of the warped-space Froggatt-Nielsen mechanism. Applying the latter, we can deduce the condition $c_{t_R} \gtrsim m_t/(\sqrt{2}v\,|Y_t|) - 1/2$, where the top-quark mass is understood to be normalized at the KK scale and $Y_t \equiv (Y_u)_{33}$. For $m_t(1\,\mathrm{TeV}) = 144\,\mathrm{GeV}$ and $|Y_t| = 1$, this implies that positive values of c_{t_R} lead to $A^{(0)}_{u\bar{u},\mathrm{RS}} > 0$, and thus to a positive shift in σ_a. However, we want to stress that the latter bound is only a crude approximation of the leading QCD corrections. The inclusion of electroweak corrections does not change this picture qualitatively.

At this point, remember that at LO QCD in the presence of NP the symmetric (asymmetric) piece is generated from vector (axial vector) currents. The important message here is that at tree-level the axial-vector current is RS GIM suppressed due to the IR localization of the light quarks in the initial state. Therefore it is tiny for a natural choice of bulk masses. On the other hand, the RS corrections to the vector current can be sizable. Therefore, it is worth to go to NLO in the $\alpha_s/(4\pi)$ expansion, where an asymmetric contribution is generated by the vector current.

9.3 Calculation of NLO effects

Since QCD is a pure vector theory, the lowest-order processes $q\bar{q} \to t\bar{t}$ and $gg \to t\bar{t}$ of the $\mathcal{O}(\alpha_s^2)$ do not contribute to A^t_{FB} within the SM. However, at $\mathcal{O}(\alpha_s^3)$ there is an charge-asymmetric piece arising in quark- anti-quark-annihilation $q\bar{q} \to t\bar{t}(g)$ and flavor excitation $qg \to qt\bar{t}$ processes [104, 105]. The Feynman diagrams are given in Figure 9.1, where one still has to add their counterparts with crossed gluon lines in the box. Note that the crossing of gluons is equivalent of changing the direction of the arrows in the fermion loop, that is replacing top by anti-top. The charge or forward-backward asymmetry arises from interference terms that are odd under the exchange of $t \leftrightarrow \bar{t}$. Since the axial-vector current is even under this exchange, it does not contribute to the asymmetry at NLO. The vector-current on the other hand will generate asymmetric terms proportional to the color structure $d^2_{abc} = \left(2\mathrm{Tr}\left(\{T^a, T^b\}T^c\right)\right)^2$ [104, 105]. Gluon-fusion processes $gg \to t\bar{t}(g)$, on the other hand, remain symmetric to all orders in perturbation theory. Explicit formulas for the asymmetric contributions to the $t\bar{t}$ production cross section in QCD are given in [105]. Contributions from flavor excitation are negligibly small at the Tevatron and will not be taken into account in the following.

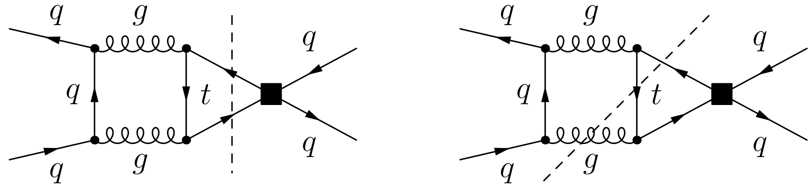

Figure 9.3: Interference of SM and NP diagrams contributing to the forward-backward asymmetry in $t\bar{t}$ production at NLO. The insertion of the effective operator is indicated by a black square.

If order to compute the NLO corrections due to NP at leading order in $v^2/\Lambda_{\rm NP}^2$, one considers the interference between SM and NP diagrams. Examples are shown in Figure 9.3, where we replace the tree-level SM amplitude by an effective four-fermion operator. Of course, NP can also arise within the loop. We will however not consider this possibility.

For the case of the RS model, one concludes from (9.19), (9.20), and (9.24) that the NLO corrections to σ_a should dominate over the LO ones, if the condition

$$\frac{\alpha_s}{4\pi}\left(1+c_{t_L}+c_{t_R}\right) \gtrsim L\, e^{L(1+c_{u_L}+c_{u_R})} \tag{9.25}$$

is fulfilled. Note that this inequality should be considered only as a crude approximation valid up to a factor of $\mathcal{O}(1)$. Due to the rather strong UV localization of light quarks, it can easily be satisfied. Note that in contrast to the SM, in the RS framework the Feynman graphs displayed in Figure 9.3 are not the only sources of charge-asymmetric contributions. Self-energy, vertex, and counter-term diagrams will also lead to an asymmetry. However, these corrections turn out to be RS GIM suppressed, just as the tree-level RS correction. Compared to the latter, these contributions are accompanied by an additional factor of $\alpha_s/(4\pi)$, and can therefore be ignored for all practical purposes.

In the partonic CM frame ($q\bar{q}=u\bar{u}, d\bar{d}$) the leading RS NLO asymmetric hard-scattering kernel is related to that of the SM model by

$$A^{(1)}_{q\bar{q},\rm RS} = \frac{\hat{s}}{16\pi\alpha_s}\, C^V_{q\bar{q}}\, A^{(1)}_{q\bar{q}}\,. \tag{9.26}$$

Note that the Wilson coefficient $C^V_{q\bar{q}}$ contains a factor $4\pi\alpha_s/M^2_{\rm KK}$ (B.1). The SM result $A^{(1)}_{q\bar{q}}$ is normalized according to (9.7), and can be described through a parametrization which is accurate to the permille level. The explicit expression is given in Appendix A.3. A numerical integration of the asymmetric differential cross section given in [105] over the relevant phase has been performed in [103]. As the forward-backward asymmetry $A^t_{\rm FB}$ is measured in the $p\bar{p}$ laboratory frame, we have to transform the results of the partonic CM frame by a change of the integration boundaries within the integration over $\cos\theta$. The resulting reduction factors are collected in Appendix A.3.

The Wilson coefficients appearing in the effective Lagrangian (9.15) do not only give rise to corrections of the forward-backward asymmetry $A_{\rm FB}^t$, but also to the theoretical prediction of the total cross section $\sigma_{t\bar{t}}$, and the invariant mass spectrum $d\sigma_{t\bar{t}}/dM_{t\bar{t}}$. In SM the latter quantities agree with the recent Tevatron results ($\sqrt{s} = 1.96\,\text{TeV}$) [94, 113, 114]

$$
\begin{aligned}
(\sigma_{t\bar{t}})_{\rm exp} &= (7.50 \pm 0.31_{\rm stat.} \pm 0.34_{\rm syst.} \pm 0.15_{\rm lumi.})\,\text{pb}\,, \\
\left(\frac{d\sigma_{t\bar{t}}}{dM_{t\bar{t}}}\right)_{\rm exp}^{M_{t\bar{t}}\,\in\,[800,1400]\,\text{GeV}} &= (0.068 \pm 0.032_{\rm stat.} \pm 0.012_{\rm syst.} \pm 0.004_{\rm lumi.})\,\frac{\text{fb}}{\text{GeV}}\,,
\end{aligned}
\tag{9.27}
$$

within the theoretical and experimental errors. In the case of the $t\bar{t}$ invariant mass spectrum, we have restricted our attention to the last bin of the available CDF measurement, $M_{t\bar{t}} \in [800, 1400]\,\text{GeV}$, which is most sensitive to the presence of new DOFs with masses in the TeV range. In terms of the dimensionless coefficients $\widetilde{C}_{q\bar{q}}^V \equiv 1\,\text{TeV}^2\, C_{q\bar{q}}^V$ and $\widetilde{C}_{t\bar{u}}^V \equiv 1\,\text{TeV}^2\,\big(1/3\, C_{t\bar{u},\|}^{(V,8)} - 2C_{t\bar{u},\|}^{(V,1)}\big)$, we find the theoretical predictions[2]

$$
\begin{aligned}
(\sigma_{t\bar{t}})_{\rm RS} &= \Big[1 + 0.053\,\big(\widetilde{C}_{u\bar{u}}^V + \widetilde{C}_{t\bar{u}}^V\big) + 0.008\,\widetilde{C}_{d\bar{d}}^V\Big]\,\big(6.73^{+0.52}_{-0.80}\big)\,\text{pb}\,, \\
\left(\frac{d\sigma_{t\bar{t}}}{dM_{t\bar{t}}}\right)_{\rm RS}^{M_{t\bar{t}}\,\in\,[800,1400]\,\text{GeV}} &= \Big[1 + 0.33\,\big(\widetilde{C}_{u\bar{u}}^V + \widetilde{C}_{t\bar{u}}^V\big) + 0.02\,\widetilde{C}_{d\bar{d}}^V\Big]\,\big(0.061^{+0.012}_{-0.006}\big)\,\frac{\text{fb}}{\text{GeV}}\,.
\end{aligned}
\tag{9.28}
$$

All Wilson coefficients are understood to be evaluated at $\mu = m_t$. The RG evolution of the Wilson coefficients can be found in Appendix B.1. Details concerning the numerical evaluation are given in [103]. The latter results constrain the size of the Wilson coefficients appearing in the effective Lagrangian (9.15).

From (A.6) and (9.28), we obtain the forward-backward asymmetry in the laboratory frame

$$
(A_{\rm FB}^t)_{\rm RS}^{p\bar{p}} = \left[\frac{1 + 0.22\,\big(\widetilde{C}_{u\bar{u}}^A + \widetilde{C}_{t\bar{u}}^V\big) + 0.03\widetilde{C}_{d\bar{d}}^A + 0.034\widetilde{C}_{u\bar{u}}^V + 0.005\widetilde{C}_{d\bar{d}}^V}{1 + 0.053\,\big(\widetilde{C}_{u\bar{u}}^V + \widetilde{C}_{t\bar{u}}^V\big) + 0.008\widetilde{C}_{d\bar{d}}^V}\right]\big(5.6^{+0.8}_{-1.0}\big)\,\%\,. \tag{9.29}
$$

The central value of the SM prediction has been obtained by integrating the formulas given in [105] over the relevant phase space (A.6), weighted with `MSTW2008LO` PDFs [115] with the unphysical scales fixed to m_t. The above result (9.29) is in good agreement with (9.14) as well as the findings of [107, 108]. Electroweak corrections have not been included within the calculation of the central value (9.29). Such effects have been found to enhance the $t\bar{t}$ forward-backward asymmetry by around 4% to 9% [106, 116]. Therefore, we have added in quadrature an error of 5% to the combined scale and PDF uncertainties.

In Table 9.1 we show the results for the various Wilson coefficient functions for appropriate parameter sets. The bulk mases and (anarchic) Yukawa couplings used for the calculation of the first three rows are given in [103]. The last row corresponds to our default

[2] Here, we have ignored the tiny contributions from the (anti-)strange-, (anti-)charm-, and (anti-)bottom quark content of the proton (anti-proton).

c_{t_L}	c_{t_R}	$\widetilde{C}^V_{u\bar{u}}/\alpha_s$	$\widetilde{C}^A_{u\bar{u}}/\alpha_s$	$\widetilde{C}^V_{d\bar{d}}/\alpha_s$	$\widetilde{C}^A_{d\bar{d}}/\alpha_s$	$\widetilde{C}^V_{t\bar{u}}/\alpha_s$
-0.41	0.09	4.496	$0.71 \cdot 10^{-2}$	0.680	$-1.40 \cdot 10^{-3}$	$-1.3 \cdot 10^{-4}$
-0.47	0.48	4.950	$0.22 \cdot 10^{-2}$	0.268	$-0.03 \cdot 10^{-3}$	$-0.7 \cdot 10^{-4}$
-0.49	0.90	5.309	$1.79 \cdot 10^{-2}$	0.084	$-0.64 \cdot 10^{-3}$	$-2.5 \cdot 10^{-4}$
-0.47	0.87	5.263	$2.82 \cdot 10^{-2}$	0.035	$-3.71 \cdot 10^{-3}$	$-0.2 \cdot 10^{-4}$

Table 9.1: Results for the Wilson coefficients corresponding to three different parameter points in the minimal RS model. The coefficients scale as $(1\,\text{TeV}/M_{\text{KK}})^2$.

parameter set given in Appendix A.1. The values of the left- and right-handed top-quark bulk mass parameters c_{t_L} and c_{t_R} are given in the first two columns, as these are of special importance for the size of the LO cross sections (see (9.24)). From the numbers it is evident that the Wilson coefficients of the axial-vector current contributions are suppressed against those of the vector current by at least two orders of magnitude. Thus, the relative $\alpha_s/(4\pi)$ factor gets (over)compensated, and the NLO vector current gives the dominant contribution to σ_a. Explicitly, this can be seen by inserting the above numbers into the numerator of (9.29). The RS contributions from t-channel transitions (last column) turn out to be negligible. Restricting ourselves on the corrections arising from s-channel KK-gluon exchange, we conclude that one can also neglect the contributions from down quarks in the initial state. First, the respective Wilson coefficients are smaller than those belonging to up quarks by about one order of magnitude. Second, they are suppressed in the total cross section (last bin of the $t\bar{t}$ invariant mass spectrum) by the small ratio of quark luminosities $f\!f_{d\bar{d}}\,(0.04)\,/\,f\!f_{u\bar{u}}\,(0.04) \approx 1/5$ $(f\!f_{d\bar{d}}\,(0.17)\,/\,f\!f_{u\bar{u}}\,(0.17) \approx 1/15)$. We further observe that $\widetilde{C}^V_{u\bar{u}}$ grows with increasing values of $(c_{t_L} + c_{t_R})$, as expected from (9.24).

As we have now identified the dominant RS corrections to A^t_{FB}, we want to find out which corrections are allowed by the RS parameter space, and whether they decrease or increase the SM prediction. As the dominant contributions arise from the exchange of KK-gluons, there is no difference between the minimal and the custodial model at LO in v^2/M^2_{KK}. Dropping all numerical irrelevant terms in (9.29), we obtain

$$(A^t_{\text{FB}})^{p\bar{p}}_{\text{RS}} \approx \left[\frac{1 + 0.22\,\widetilde{C}^A_{u\bar{u}} + 0.034\,\widetilde{C}^V_{u\bar{u}}}{1 + 0.053\,\widetilde{C}^V_{u\bar{u}}}\right] \left(5.6^{+0.8}_{-1.0}\right)\%\,. \tag{9.30}$$

Looking at the numerator, we observe that the correction due to the axial-vector current plays a minor role, being just a few percent compared to the one of the vector current. On the other hand, the corrections to the symmetric cross section in the denominator have a stronger sensitivity to $\widetilde{C}^V_{u\bar{u}}$, and are also positive. It follows that the ratio $(A^t_{\text{FB}})^{p\bar{p}}_{\text{RS}}/(A^t_{\text{FB}})^{p\bar{p}}_{\text{SM}}$ is smaller than one. In other words, for a natural choice of input parameters, the RS corrections to the SM prediction of the forward-backward asymmetry A^t_{FB} turn out to be negative due to the normalization with respect to the symmetric cross section. This feature is illustrated in Figure 9.4, where we show the (approximate) results for the absolute RS corrections to A^t_{FB} in the $p\bar{p}$ frame as a function of c_{t_L} and c_{t_R}. The figures have been

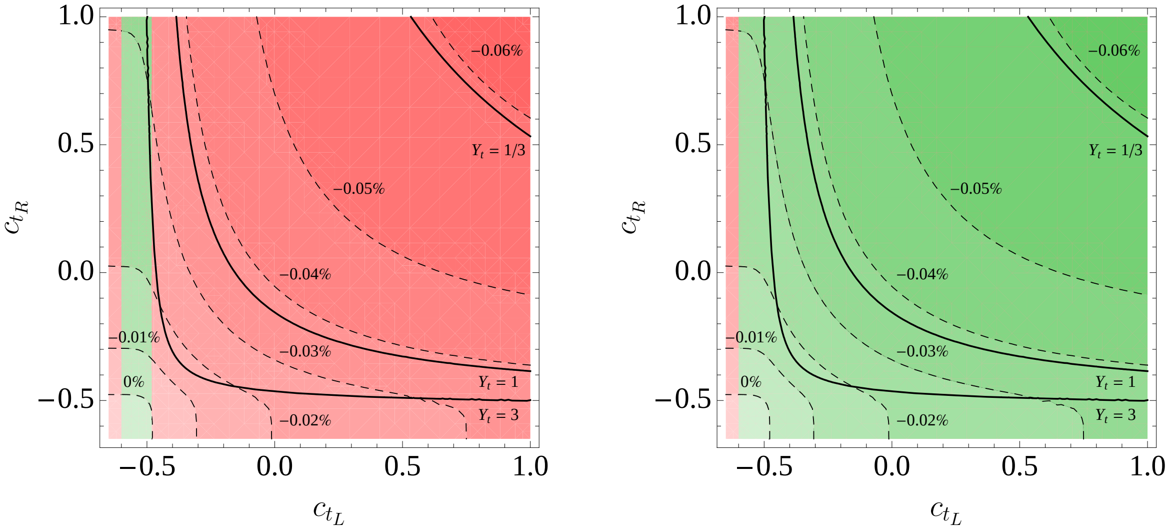

Figure 9.4: Absolute correction to $(A_{\rm FB}^t)^{p\bar{p}}_{\rm RS}$ in the c_{t_L}-c_{t_R} plane for a KK scale of 1 TeV. The parameter region which is in agreement with the $Z^0 b\bar{b}$ "pseudo observables" is colored in green (light gray). Figure taken from [103].

obtained by including only the KK-gluon corrections to $\widetilde{C}^{V,A}_{u\bar{u}}$. Here, we have employed $M_{\rm KK} = 1\,\text{TeV}$, $c_{u_L} = c_{d_L} = -0.63$, $c_{u_R} = -0.68$, $c_{d_R} = -0.66$, $c_{c_L} = c_{s_L} = -0.56$, $c_{c_R} = -0.53$, $c_{s_R} = -0.63$, and assumed the minors of the Yukawa matrices $Y_{u,d}$ to be equal for simplicity. Furthermore, we imposed constraints from the $Z^0 b_L \bar{b}_L$ vertex and the top mass, which restrict the value of $c_{t_L} = c_{Q_3}$. The allowed parameter region is colored in green (light gray). For the custodial model only the bound from the top mass survives, whereas in the minimal version only the thin stripe with $c_{t_L} \in [-0.60, -0.49]$ is allowed. The solid lines indicate the required value of the top-Yukawa coupling $Y_t = (Y_u)_{33}$ for the given bulk masses.

Both panels in Figure 9.4 show that the corrections to $(A_{\rm FB}^t)^{p\bar{p}}_{\rm RS}$ interfere destructively with the SM in the whole c_{t_L}-c_{t_R} plane. However, even for a low KK scale of $M_{\rm KK} = 1\,\text{TeV}$ (which is rather unrealistic in view of the constraints from the electroweak precision observables and various flavor-changing interactions [38]), the maximal attainable effects do not exceed -0.03% (-0.06%) in the minimal (custodial) RS model. Since the RS corrections decouple as $1/M_{\rm KK}^2$, it follows that for $M_{\rm KK} = 2\,\text{TeV}$ the maximal absolute corrections are about -0.02%. Thus, we conclude that the RS prediction for the forward-backward asymmetry in $t\bar{t}$ production, $A_{\rm FB}^t$, is essentially SM-like within an anarchic approach to flavor.

This result should be contrasted with the analysis [112], which finds positive corrections to the $t\bar{t}$ forward-backward asymmetry of up to 5.6% (7%) arising from KK gluons (Z'-boson exchange) at LO. Here, the authors obtain sizable values for $\widetilde{C}^{A}_{q\bar{q}}$ by assuming an IR-localized quark field u_L and a strongly UV-localized u_R. This choice, however, reintroduces hierarchies in the Yukawa matrices in order to reproduce the correct light quark masses simultaneously with the desired CKM structure. Moreover, the RS GIM suppression for the gauge couplings of left-handed up and down quarks vanishes, giving rise to possible conflicts with the flavor phenomenology. Positive corrections to the asymmetry have also been found in [117] in the context of a warped Higgsless model.

We close this section by noting that, due to the universal result (9.29), a sizable positive correction to $(A_{\rm FB}^t)_{\rm SM}$ from s-channel NP exchange requires at least an $\mathcal{O}(1)$ tree level axial-vector current with a different sign for heavy and light quarks, which in addition interferes with the tree-level QCD diagram of quark-anti-quark annihilation [111]. On the other hand, there should not be vast corrections to the top-quark vector couplings, as otherwise the good agreement for the total cross section and the invariant mass spectrum would be spoiled (see (9.3) and (9.3)). A viable model should therefore involve a massive color octet, which possesses a sizable axial-vector coupling to fermions. A possible candidate an axigluon within the chiral color model [118], where quarks of opposite chirality but same flavor are charged under different $SU(3)$ groups.

10 CP Violation in B_s-meson decays

As a final project, we want to study RS corrections in the decay of B_s^0-mesons. An important observable is the width difference $\Delta\Gamma_s \equiv \Gamma_L^s - \Gamma_H^s$ between the light and the heavy meson state, which involves a CP-violating phase. According to the above definition, $\Delta\Gamma_s$ happens to be positive in the SM. It can be computed from the dispersive and absorptive part of the $\bar{B}_s^0$-B_s^0 mixing amplitude, M_{12}^s and Γ_{12}^s. For $|\Gamma_{12}^s| \ll |M_{12}^s|$, one can derive the simple relation [119, 120]

$$\Delta\Gamma_s \approx -\frac{2\,\mathrm{Re}(M_{12}^s \Gamma_{12}^{s*})}{|M_{12}^s|} = 2\,|\Gamma_{12}^s|\,\cos\phi_s\,. \tag{10.1}$$

We define the relative phase ϕ_s between the mixing and the decay amplitude according to the convention

$$\frac{M_{12}^s}{\Gamma_{12}^s} = -\frac{|M_{12}^s|}{|\Gamma_{12}^s|}\,e^{i\phi_s}\,, \qquad \phi_s = \arg(-M_{12}^s \Gamma_{12}^{s*})\,, \tag{10.2}$$

for which the SM value is positive and explicitly given by $\phi_s^{\mathrm{SM}} = (4.2 \pm 1.4)\cdot 10^{-3}$ [121]. The combined experimental results of CDF and DØ differ from the SM prediction in the $(\beta_s^{J/\psi\phi}, \Delta\Gamma_s)$-plane by about 2σ [122], whereas the latest CDF results disagree by 1σ only [123]. Here, $\beta_s^{J/\psi\phi} \in [-\pi/2, \pi/2]$ is the CP-violating phase in the interference of mixing and decay, obtained from the time-dependent angular analysis of flavor-tagged $B_s^0 \to J/\psi\phi$ decays. In the SM it is given by [121, 124]

$$\beta_s^{J/\psi\phi} = -\arg\left(-\frac{\lambda_t^{bs}}{\lambda_c^{bs}}\right) = 0.020 \pm 0.005\,, \tag{10.3}$$

with $\lambda_q^{bs} = V_{qb}V_{qs}^*$. In the presence of NP, the prediction of $\Delta\Gamma_s$ is modified [125, 126] . Adopting the notation of [127], we extend the SM relations according to

$$\begin{aligned} M_{12}^s &= M_{12}^{s\,\mathrm{SM}} + M_{12}^{s\,\mathrm{NP}} = M_{12}^{s\,\mathrm{SM}} R_M\, e^{i\phi_M}\,,\\ \Gamma_{12}^s &= \Gamma_{12}^{s\,\mathrm{SM}} + \Gamma_{12}^{s\,\mathrm{NP}} = \Gamma_{12}^{s\,\mathrm{SM}} R_\Gamma\, e^{i\phi_\Gamma}\,. \end{aligned} \tag{10.4}$$

Inserting the latter definitions into (10.1) it follows that

$$\Delta\Gamma_s = 2\,|\Gamma_{12}^{s\,\mathrm{SM}}|\,R_\Gamma\,\cos(\phi_s^{\mathrm{SM}} + \phi_M - \phi_\Gamma)\,, \tag{10.5}$$

where $\Delta\Gamma_s^{\mathrm{SM}} = (0.087 \pm 0.021)\,\mathrm{ps}^{-1}$ [128]. A further important observable is the CP asymmetry in semileptonic decays

$$A_{\mathrm{SL}}^s = \frac{\Gamma(\bar{B}_s^0 \to l^+X) - \Gamma(B_s^0 \to l^-X)}{\Gamma(\bar{B}_s^0 \to l^+X) + \Gamma(B_s^0 \to l^-X)} = \mathrm{Im}\left(\frac{\Gamma_{12}^s}{M_{12}^s}\right)\,. \tag{10.6}$$

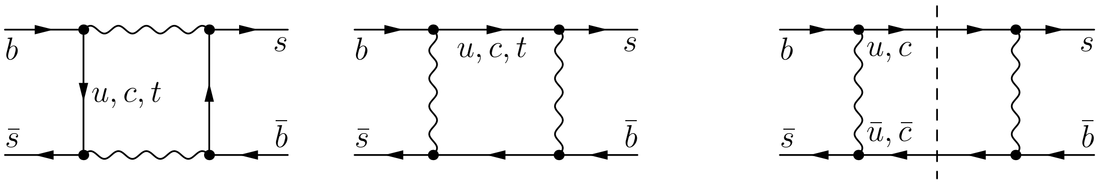

Figure 10.1: Feynman diagrams that contribute to the dispersive and absorptive part of the $\bar{B}_s^0$-B_s^0 mixing amplitude, M_{12}^s and Γ_{12}^s, at LO in the SM.

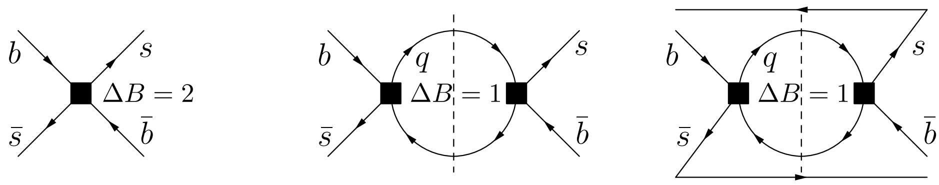

Figure 10.2: Feynman diagrams for generic NP contributions to M_{12}^s and Γ_{12}^s through insertion of effective $\Delta B = 2$ and $\Delta B = 1$ operators, respectively.

Including NP corrections, we find

$$A_{\rm SL}^s = \frac{|\Gamma_{12}^{s\,\rm SM}|}{|M_{12}^{s\,\rm SM}|}\,\frac{R_\Gamma}{R_M}\,\sin(\phi_s^{\rm SM} + \phi_M - \phi_\Gamma)\,. \tag{10.7}$$

Within the SM, the leading contribution to the dispersive part of the $\bar{B}_s^0$-B_s^0 mixing amplitude M_{12}^s appears at the one-loop level. The respective Feynman diagrams are shown on the left-hand side of Figure 10.1. If NP involves FCNCs at tree level, these give rise to sizable corrections to the mass difference $\Delta m_{B_s} \equiv M_H^s - M_L^s = 2\,|M_{12}^s|$ [119]. The generic m_W^2/Λ^2 suppression compared to the SM amplitude is (over)compensated by the inverse loop factor $4\pi/\alpha$ in the ratio $M_{12}^{s\,\rm NP}/M_{12}^{s\,\rm SM}$. Here, Λ denotes the NP mass scale. For the case of the minimal and custodial RS model, the corrections have been calculated in [38] and [74], respectively. On the other hand, the presence of tree level FCNCs and right-handed charged current interactions give rise to new decay diagrams. However, NP corrections to the absorptive part of the amplitude Γ_{12}^s do not gain an inverse loop factor compared to the leading SM diagrams, which can be seen in Figure 10.2. Therefore, the m_W^2/Λ^2 (here $m_W^2/M_{\rm KK}^2$) suppression does not get attenuated and the effects are expected to be small. Thus, they are neglected in many NP studies.

Recently, model-independent estimates on $A_{\rm SL}^s$ in the presence of heavy gluons have been presented in [129], taking into account modifications in Γ_{12}. NP contributions from EW penguin operators as well as right-handed charged currents have not been considered. We will see below that the former can compete with or even dominate contributions from

QCD penguins within the minimal RS model [34, 38], where part of the latter tend to give the dominant contribution to $\Gamma_{12}^{s\,\mathrm{RS}}$ for the most natural choice of input parameters. The results presented in the following can also be found in our recent article [75].

10.1 Calculation of Γ_{12}^s

Within the SM, Γ_{12}^s is known to NLO in QCD [130, 131, 132, 133, 134, 135, 121]. In this section, we (re-)calculate the leading contribution to Γ_{12}^s in the presence of NP. Formally, one has to evaluate the hadronic matrix element of the transition amplitude, which converts $\bar{B}_s^0$ into B_s^0

$$\begin{aligned}\Gamma_{12}^s &= \frac{1}{2m_{B_s}} \langle B_s^0|\mathcal{T}|\bar{B}_s^0\rangle \,, \\ \mathcal{T} &= \mathrm{Disc} \int d^4x \, \frac{i}{2} \, T \, \left[\mathcal{H}_{\mathrm{eff}}^{\Delta B=1}(x)\mathcal{H}_{\mathrm{eff}}^{\Delta B=1}(0)\right] \,.\end{aligned} \tag{10.8}$$

Here, T stands for "time-ordered", and the effective Hamiltonian collects all $\Delta B = 1$ operators which can be inserted into the Feynman diagrams of the right-hand side in Figure 10.2. Taking the discontinuity in the expression above projects out on-shell intermediate states. Explicitly, this is done by cutting the diagram and allowing only for light quarks (leptons) as decay products. The leading correction to the SM result is given by the interference between SM and NP insertions. The framework of heavy-quark expansion (HQE) allows for a systematic evaluation of the matrix element in powers of $1/m_b$. At the zeroth order, the momentum of the B-meson p in its rest frame corresponds to the momentum of the bottom quark ($p^2 = m_b^2$), while the strange-quark momentum is set to zero. Therefore, we make use of the EOMs $\not{p}u_b(p) = -\not{p}v_b(p) = m_b u_b(p)$ and $\not{p}u_s(p) = \not{p}v_s(p) = 0$. At typical hadronic distances $x > 1/m_b$, the transition of $\bar{B}_s^0$ into B_s^0 is a local process. Thus, the matrix element can be expanded in terms of local $\Delta B = 2$ operators. QCD corrections are implemented by running the $\Delta B = 1$ operators from the matching scale down to the mass of the bottom quark. The leading SM contributions can be collected into matrix elements of the $\Delta B = 2$ operators

$$\begin{aligned}\mathcal{Q}_1 &= (\bar{s}_i b_i)_{V-A}(\bar{s}_j b_j)_{V-A} \,, \\ \mathcal{Q}_2 &= (\bar{s}_i b_i)_{S+P}(\bar{s}_j b_j)_{S+P} \,,\end{aligned} \tag{10.9}$$

where i and j denote color indices, and a summation over repeated indices is understood. The shorthand notation $V \pm A$ indicates the Dirac structure $\gamma^\mu(1 \pm \gamma^5)$ in between the spinors, whereas $S \pm P$ denotes $(1 \pm \gamma^5)$. The possibility of having right-handed charged currents within the RS model asks for further $\Delta B = 2$ operators, caused by interference of SM with NP insertions. We introduce

$$\begin{aligned}\mathcal{Q}_3 &= (\bar{s}_i b_j)_{S+P}(\bar{s}_j b_i)_{S+P} \,, \\ \mathcal{Q}_4 &= (\bar{s}_i b_i)_{S-P}(\bar{s}_j b_j)_{S+P} \,, \\ \mathcal{Q}_5 &= (\bar{s}_i b_j)_{S-P}(\bar{s}_j b_i)_{S+P} \,.\end{aligned} \tag{10.10}$$

The appropriate $\Delta B = 1$ Hamiltonian, allowing for new right-handed charged currents as well as tree-level FCNCs, is given by

$$\begin{aligned}\mathcal{H}_{\text{eff}}^{\Delta B=1} = \frac{G_F}{\sqrt{2}} \lambda_c^{bs} \Big[\sum_{i=1,2} \Big(C_i Q_i + C_i^{LL} Q_i + C_i^{LR} Q_i^{LR} + C_i^{RL} Q_i^{RL} \Big) + \sum_{i=3}^{10} C_i Q_i \Big] \\ + \sum_{i=3}^{10} \Big(C_i^{\text{NP}} Q_i + \widetilde{C}_i^{\text{NP}} \widetilde{Q}_i \Big) .\end{aligned} \tag{10.11}$$

In the RS model the operators $Q_{1,2}$ arise from (KK) $W^{\pm}$-boson exchange, and the LR/RL operators involve right-handed charged currents. They are defined as

$$\begin{aligned} Q_1 &= (\bar{s}_i c_j)_{V-A} (\bar{c}_j b_i)_{V-A} , & Q_2 &= (\bar{s}_i c_i)_{V-A} (\bar{c}_j b_j)_{V-A} , \\ Q_1^{LR} &= (\bar{s}_i c_j)_{V-A} (\bar{c}_j b_i)_{V+A} , & Q_2^{LR} &= (\bar{s}_i c_i)_{V-A} (\bar{c}_j b_j)_{V+A} , \end{aligned} \tag{10.12}$$

and the Q_i^{RL} are chirality flipped with respect to Q_i^{LR}. Operators of the type RR are not included into our analysis as their coefficients scale like v^4/M_{KK}^4 in the models at hand. We also do not consider the small contributions from electromagnetic and chromomagnetic dipole operators Q_7^{γ} and Q_8^{g}. Due to the hierarchies in the CKM matrix and the RS-GIM mechanism, it is sufficient to restrict ourselves on c quarks as intermediate states, when we calculate the RS corrections related to W-boson exchange. For the SM contribution however, we include the combinations uc, cu, and uu in addition to the operators given above. Concerning the NP corrections encoded in the coefficients with superscripts LL, LR, RL, we pull out the CKM factor λ_c^{bs} for convenience. As discussed at the end of Section 7, the measured values for V_{cb} and V_{cs} (extracted from semileptonic B and D decays) should be identified with the exchange of all $(SU(2)_L)$ W-type bosons. As a consequence, the NP coefficients $C_{1,2}^{LL}$ arise only due to non-factorizable corrections (7.36), which can not be absorbed into λ_c^{bs}. As we will discuss later, the dominant RS corrections however arise from the chirality-mixed operators Q_i^{LR}. Explicit ZMA expressions for the Wilson coefficients are collected in Appendix B.2. Besides the charged-curent operators (10.12), we take into account contributions from QCD penguin operators

$$\begin{aligned} Q_3 &= (\bar{s}_i b_i)_{V-A} \sum\nolimits_q (\bar{q}_j q_j)_{V-A} , & Q_4 &= (\bar{s}_i b_j)_{V-A} \sum\nolimits_q (\bar{q}_j q_i)_{V-A} , \\ Q_5 &= (\bar{s}_i b_i)_{V-A} \sum\nolimits_q (\bar{q}_j q_j)_{V+A} , & Q_6 &= (\bar{s}_i b_j)_{V-A} \sum\nolimits_q (\bar{q}_j q_i)_{V+A} , \end{aligned} \tag{10.13}$$

as well as EW penguin operators

$$\begin{aligned} Q_7 &= \frac{3}{2} (\bar{s}_i b_i)_{V-A} \sum\nolimits_q Q_q (\bar{q}_j q_j)_{V+A} , & Q_8 &= \frac{3}{2} (\bar{s}_i b_j)_{V-A} \sum\nolimits_q Q_q (\bar{q}_j q_i)_{V+A} , \\ Q_9 &= \frac{3}{2} (\bar{s}_i b_i)_{V-A} \sum\nolimits_q Q_q (\bar{q}_j q_j)_{V-A} , & Q_{10} &= \frac{3}{2} (\bar{s}_i b_j)_{V-A} \sum\nolimits_q Q_q (\bar{q}_j q_i)_{V-A} , \end{aligned} \tag{10.14}$$

where $q = u, c, d, s$, and Q_q is the electric charge. Here, no CKM suppression factors are involved. Thus, one should keep all light quarks as intermediate states, if one considers double neutral-current insertions. The operators $\widetilde{Q}_{3..10}$ are chirality-flipped with respect to (10.13) and (10.14). In principle, there is the possibility of a flavor change on both vertices for NP penguins. Furthermore, the interaction is not universal with respect to the quark flavor q. However, these non-universal effects and internal flavor changes suffer from an additional RS-GIM suppression and can be neglected for all practical purposes. For the same reason, the chirality flipped penguins $\widetilde{C}_{3-10}^{\rm RS}$ can be neglected compared to $C_{3-10}^{\rm RS}$ for bs transitions [38]. Within the minimal RS model it turns out that, despite of the relative α/α_s-suppression, the EW penguin operators can dominate over the gluon penguins [38]. This is explained by the extra factor L, which shows up in the leading correction to the left-handed Z^0-coupling (7.15). Remember that this factor vanishes in the custodial model. The RS Wilson coefficients of the penguin operators can be found in [38] and are collected in Appendix B.3 for completeness. There further is the possibility of a flavor-changing Higgs coupling which, however, can be neglected against the contributions of the flavor-changing heavy gauge bosons in RS models.

Concerning double-penguin insertions, we include all light quarks with masses set to zero (besides m_c). For $q = c$ and penguin-operator insertions that contain $V - A$ structures only, the calculation resembles that of the charged-current sector by applying a Fierz transformation. The double-penguin insertion moreover allows for leptons within the cut-diagram. However, as the related SM coefficient is suppressed by α/α_s, there is no chance to obtain big effects from $\bar{s}b \to \bar{\tau}\tau$ transitions, which are less constrained by experiment [136]. Note that this is not a general statement about NP models. If there is a tree-level transition $\bar{s}b \to \bar{\tau}\tau$ mediated by light NP particles in the range of $\sim 100\,\mathrm{GeV}$, the double NP insertion becomes comparable to the SM diagrams. Possible candidates are scalar leptoquarks [127, 137].

In order to determine Γ_{12}^s, one has to evaluate integrals of the form

$$\begin{aligned}
&\int d^4k\, \delta\left(\left(k+\tfrac{p}{2}\right)^2 - m_q^2\right)\, \delta\left(\left(k-\tfrac{p}{2}\right)^2 - m_q^2\right) \left\{1,\, k^2,\, k^\mu k^\nu\right\} \\
&= \int d\Omega \int_0^\infty d|\vec{k}|\, |\vec{k}|\, \frac{1}{4m_b}\, \delta\big(|\vec{k}| - \sqrt{m_b^2/4 - m_q^2}\big) \left\{1,\, k^2,\, \frac{k^2}{3}\left(g^{\mu\nu} - \frac{p^\mu p^\mu}{m_b^2}\right)\right\} \\
&= \frac{\pi}{2}\sqrt{1 - 4\frac{m_q^2}{m_b^2}} \left\{1,\, m_b^2\left(\frac{m_q^2}{m_b^2} - \frac{1}{4}\right),\, \frac{m_b^2}{3}\left(\frac{m_q^2}{m_b^2} - \frac{1}{4}\right)\left(g^{\mu\nu} - \frac{p^\mu p^\mu}{m_b^2}\right)\right\}.
\end{aligned} \tag{10.15}$$

The δ-functions stem from the two-particle cut, p is the outer momentum associated to the b quark, and k is the loop momentum. In the first step, we have applied Passarino-Veltman reduction to the term $\propto k^\mu k^\nu$. The cut fixes k^2 and the absolute value of $\vec{k}$. The residual integration over the solid angle can easily be performed, as the problem is 4π-symmetric.

Within the calculation of the amplitude it is often required to perform Fierz re-arrangements of the spinors. Therefore, it is convenient to use the master formula [5], which directly applies to the chiral basis (1.28) (i, j, k, l denote Dirac indices),

$$(\Gamma^A)_{ij}(\Gamma^B)_{kl} = \frac{1}{4}\,\mathrm{Tr}\,[\Gamma^A\Gamma_C\Gamma^B\Gamma_D]\,(\Gamma^D)_{il}(\Gamma^C)_{kj}\,. \tag{10.16}$$

At the end, the results of the various $\Delta B = 1$ operator insertions are matched on the B_s^0-meson matrix elements of the $\Delta B = 2$ operators (10.9) and (10.10). In other words, performing the evaluation of the cut shrinks the diagrams on the right-hand side of Figure 10.2 to a local $\Delta B = 2$ four-fermion transition, as depicted on the left-hand side. Note that the twisted diagram on the very right of Figure 10.2 picks up a minus sign due to the interchanged order of fermionic field operators. Neglecting intermediate leptons, we find to LO in $1/m_b$

$$
\begin{aligned}
\Gamma_{12}^s = & -\frac{m_b^2}{12\pi(2M_{B_s})}\, G_F^2 (\lambda_c^{bs})^2 \sqrt{1-4z} \\
& \Bigg\{ \bigg[(1-z)\big(\Sigma_1 + \Sigma_1^{LL}\big) + \frac{1}{2}(1-4z)\big(\Sigma_2 + \Sigma_2^{LL}\big) + 3z\left(\Sigma_3 + K_3^{\prime LL}\right) \\
& \quad - \frac{3}{2}\sqrt{z}\left(\Sigma_1^{LR} + \Sigma_2^{LR} + K_3^{\prime LR} + K_4^{\prime LR}\right) \\
& \quad + \frac{1}{\sqrt{1-4z}}\big(3\bar{K}_1'' + K_{s1}'' + \frac{3}{2}\bar{K}_2'' + \frac{1}{2}K_{s2}''\big) \\
& \quad + \frac{1}{\sqrt{1-4z}}\Big(\frac{\lambda_u^{bs}}{\lambda_c^{bs}}\,(1-z)^2\big((2+z)K_1 + (1-z)K_2\big) + \frac{1}{2}\frac{(\lambda_u^{bs})^2}{(\lambda_c^{bs})^2}\,(2K_1 + K_2)\Big)\bigg]\,\langle\mathcal{Q}_1\rangle \\
& + \bigg[(1+2z)\big(\Sigma_1 + \Sigma_1^{LL} - \Sigma_2 - \Sigma_2^{LL}\big) - 3\sqrt{z}\left(2\Sigma_1^{LR} + \Sigma_2^{LR} - K_4^{\prime LR}\right) \\
& \quad + \frac{1}{\sqrt{1-4z}}\big(3\bar{K}_1'' + K_{s1}'' - 3\bar{K}_2'' - K_{s2}''\big) \\
& \quad + \frac{1}{\sqrt{1-4z}}\Big(2\,\frac{\lambda_u^{bs}}{\lambda_c^{bs}}\,(1-z)^2(1+2z)(K_1 - K_2) + \frac{(\lambda_u^{bs})^2}{(\lambda_c^{bs})^2}(K_1 - K_2)\Big)\bigg]\,\langle\mathcal{Q}_2\rangle \\
& - 3\sqrt{z}\left(\Sigma_1^{LR} + 2\Sigma_2^{LR} + K_3^{\prime LR}\right)\langle\mathcal{Q}_3\rangle \\
& + 3\sqrt{z}\left(\Sigma_1^{RL} - K_3^{\prime RL}\right)\langle\mathcal{Q}_4\rangle + 3\sqrt{z}\,(\Sigma_2^{RL} - K_4^{\prime RL})\,\langle\mathcal{Q}_5\rangle \Bigg\} \\
& - \frac{m_b^2}{12\pi(2M_{B_s})}\,\sqrt{2}\,G_F \lambda_c^{bs}\sqrt{1-4z} \\
& \Bigg\{ \bigg[(1-z)\,\Sigma_1^{\rm NP} + \frac{1}{2}(1-4z)\,\Sigma_2^{\rm NP} + 3z\,\Sigma_3^{\rm NP} \\
& \quad + \frac{1}{\sqrt{1-4z}}\big(3\bar{K}_1^{\prime\prime\rm NP} + K_{s1}^{\prime\prime\rm NP} + \frac{3}{2}\bar{K}_2^{\prime\prime\rm NP} + \frac{1}{2}K_{s2}^{\prime\prime\rm NP}\big)\bigg]\,\langle\mathcal{Q}_1\rangle \\
& + \bigg[(1+2z)\big(\Sigma_1^{\rm NP} - \Sigma_2^{\rm NP}\big) \\
& \quad + \frac{1}{\sqrt{1-4z}}\big(3\bar{K}_1^{\prime\prime\rm NP} + K_{s1}^{\prime\prime\rm NP} - 3\bar{K}_2^{\prime\prime\rm NP} - K_{s2}^{\prime\prime\rm NP}\big)\bigg]\,\langle\mathcal{Q}_2\rangle + \mathcal{O}\left(\frac{1}{m_b}\right)\Bigg\},
\end{aligned}
\tag{10.17}
$$

where $z = m_c^2/m_b^2$ and $\langle\mathcal{Q}_i\rangle \equiv \langle B_s^0|\,\mathcal{Q}_i\,|\bar{B}_s^0\rangle$. The meaning of all the coefficients will be explained in a moment. At this point, note that our result (10.17) holds for any NP model, which gives rise to the operators collected in (10.11). Remember that we have neglected contributions from the chirality flipped penguins $\widetilde{Q}_{3..10}$, as they turn out to be unimportant for the model at hand. In order to get a (more or less) compact expression for Γ_{12}^s, we have introduced the linear combinations $(A, B \in \{L, R\})$

$$\begin{aligned} \Sigma_i &= K_i + K_i' + K_i'' \qquad & \Sigma_i^{AB} &= K_i^{AB} + K_i'^{AB}, \quad i = 1,2, \\ \Sigma_3 &= K_3' + K_3''\,, \qquad & \Sigma_i^{\rm NP} &= K_i'^{\rm NP} + K_i''^{\rm NP} \quad i = 1,2,3\,, \end{aligned} \tag{10.18}$$

where the coefficients on the right-hand side of (10.18) are themselves linear combinations of Wilson coefficients. In agreement with [130] we obtain

$$\begin{aligned} K_1 &= N_c C_1^2 + 2\, C_1 C_2\,, \qquad K_2 = \; C_2^2\,, \\ K_1' &= 2\,(N_c C_1 C_{3+9} + C_1 C_{4+10} + C_2 C_{3+9})\,, \qquad K_2' = \; 2\, C_2 C_{4+10}\,, \\ K_3' &= 2\,(N_c C_1 C_{5+7} + C_1 C_{6+8} + C_2 C_{5+7} + C_2 C_{6+8})\,, \\ K_1'' &= N_c C_{3+9}^2 + 2\, C_{3+9} C_{4+10} \; + N_c C_{5+7}^2 + 2\, C_{5+7} C_{6+8}\,, \\ K_2'' &= C_{4+10}^2 + C_{6+8}^2\,, \\ K_3'' &= 2(N_c C_{3+9} C_{5+7} + C_{3+9} C_{6+8} \; + C_{4+10} C_{5+7} + C_{4+10} C_{6+8})\,, \end{aligned} \tag{10.19}$$

with $C_{i+j} \equiv C_i + C_j$. The combinations K_i stem from the insertion of charged-current operators and give the dominant contribution in the SM. The coefficients K_i' and K_i'' correspond to the interference of charged-current with penguin operators and penguin-penguin insertions, respectively. As we consider light quarks $(q = u, d, s\,)$ in the limit $m_q = 0$, there is a cancellation in the EW penguin sector due to the electric charges. The coefficients $\bar{K}_i''$ therefore resemble the K_i'', with $C_{7..10}$ set to zero. For strange quarks as intermediate states, there is a second possibility for the penguin insertion. In the limit $m_s = 0$ we find additional contributions from

$$\begin{aligned} K_{s1}'' &= (2 + N_c)(C_4 - C_{10}/2)^2 \; + 2\,(N_c + 1)(C_3 - C_9/2)(C_4 - C_{10}/2) \; + 2\,(C_3 - C_9/2)^2\,, \\ K_{s2}'' &= 2\,(C_3 - C_9/2)(C_4 - C_{10}/2) + (C_3 - C_9/2)^2\,. \end{aligned} \tag{10.20}$$

At $\mathcal{O}(v^2/M_{\rm KK}^2)$, we have to consider interference of SM diagrams with NP penguins, which give rise to

$$\begin{aligned} K_1'^{\rm NP} &= 2\,(N_c C_1 C_{3+9}^{\rm NP} + C_1 C_{4+10}^{\rm NP} + C_2 C_{3+9}^{\rm NP})\,, \qquad K_2'^{\rm NP} = \; 2\, C_2 C_{4+10}^{\rm NP}\,, \\ K_3'^{\rm NP} &= 2\,(N_c C_1 C_{5+7}^{\rm NP} + C_1 C_{6+8}^{\rm NP} + C_2 C_{5+7}^{\rm NP} + C_2 C_{6+8}^{\rm NP})\,, \\ K_{s1}''^{\rm NP} &= 2\,\big((N_c + 2) C_4 (C_4^{\rm NP} - C_{10}^{\rm NP}/2) \; + (N_c + 1) C_4 (C_3^{\rm NP} - C_9^{\rm NP}/2) \\ &\qquad + (N_c + 1) C_3 (C_4^{\rm NP} - C_{10}^{\rm NP}/2) \; + 2 C_3 (C_3^{\rm NP} - C_9^{\rm NP}/2)\big)\,, \\ K_{s2}''^{\rm NP} &= 2\,\big(C_3 (C_3^{\rm NP} - C_9^{\rm NP}/2) + C_3 (C_4^{\rm NP} - C_{10}^{\rm NP}/2) \; + C_4 (C_3^{\rm NP} - C_9^{\rm NP}/2)\big)\,, \end{aligned} \tag{10.21}$$

and

$$\begin{aligned}
K_1^{\prime\prime\mathrm{NP}} &= 2\,(N_c C_3 C_{3+9}^{\mathrm{NP}} + C_3 C_{4+10}^{\mathrm{NP}} + C_4 C_{3+9}^{\mathrm{NP}} + N_c C_5 C_{5+7}^{\mathrm{NP}} + C_5 C_{6+8}^{\mathrm{NP}} + C_6 C_{5+7}^{\mathrm{NP}})\,,\\
K_2^{\prime\prime\mathrm{NP}} &= 2\,(C_4 C_{4+10}^{\mathrm{NP}} + C_6 C_{6+8}^{\mathrm{NP}})\,,\\
K_3^{\prime\prime\mathrm{NP}} &= 2\,(N_c C_3 C_{5+7}^{\mathrm{NP}} + C_3 C_{6+8}^{\mathrm{NP}} + C_4 C_{5+7}^{\mathrm{NP}} + C_4 C_{6+8}^{\mathrm{NP}}\\
&\quad + N_c C_5 C_{3+9}^{\mathrm{NP}} + C_5 C_{4+10}^{\mathrm{NP}} + C_6 C_{3+9}^{\mathrm{NP}} + C_6 C_{4+10}^{\mathrm{NP}})\,.
\end{aligned} \tag{10.22}$$

Here, we have neglected the tiny contributions from the interference of SM EW penguins with NP graphs. There further is interference between NP charged currents and SM penguins

$$\begin{aligned}
K_1^{\prime LL} &= 2\,(N_c C_3 C_1^{LL} + C_3 C_2^{LL} + C_4 C_1^{LL})\,, & K_2^{\prime LL} &= 2\,C_4 C_2^{LL}\,,\\
K_3^{\prime LL} &= 2\,(N_c C_5 C_1^{LL} + C_5 C_2^{LL} + C_6 C_1^{LL} + C_6 C_2^{LL})\,, & &\\
K_1^{\prime LR} &= 2\,(N_c C_3 C_1^{LR} + C_3 C_2^{LR} + C_4 C_1^{LR})\,, & K_2^{\prime LR} &= 2\,C_4 C_2^{LR}\\
K_3^{\prime LR} &= 2\,(N_c C_5 C_1^{LR} + C_5 C_2^{LR} + C_6 C_1^{LR})\,, & K_4^{\prime LR} &= 2\,C_6 C_2^{LR}\,.
\end{aligned} \tag{10.23}$$

The double charged-current insertions that contribute at $\mathcal{O}(v^2/M_{\mathrm{KK}}^2)$ are collected into

$$\begin{aligned}
K_1^{LL} &= 2\left(N_c C_1 C_1^{LL} + C_1 C_2^{LL} + C_2 C_1^{LL}\right), & K_2^{LL} &= 2\,C_2 C_2^{LL}\,,\\
K_1^{LR} &= 2\,(N_c C_1 C_1^{LR} + C_1 C_2^{LR} + C_2 C_1^{LR})\,, & K_2^{LR} &= 2\,C_2 C_2^{LR}\,.
\end{aligned} \tag{10.24}$$

The coefficients $K_i^{(\prime)RL}$ resemble $K_i^{(\prime)LR}$, with C_i^{LR} replaced by C_i^{RL}. All NP coefficients should by evaluated at the NP mass scale and then be evolved down to m_b. For the RS model, explicit ZMA expressions are given in the Appendices B.2 and B.3.

Finally, one has to compute the B_s^0-meson matrix elements $\langle B_s^0|\,\mathcal{Q}_i\,|\bar{B}_s^0\rangle$. Here, we use existing results from the lattice. In terms of

$$R(\mu) \equiv \left(\frac{M_{B_s}}{\bar{m}_b(\mu) + \bar{m}_s(\mu)}\right)^2, \tag{10.25}$$

the matrix elements are given by

$$\begin{aligned}
\langle \mathcal{Q}_1\rangle &= \frac{8}{3}\,M_{B_s}^2 f_{B_s}^2 B_1(\mu)\,, & \langle \mathcal{Q}_2\rangle &= -\frac{5}{3}\,M_{B_s}^2 f_{B_s}^2\,R(\mu)\,B_2(\mu)\,,\\
\langle \mathcal{Q}_3\rangle &= \frac{1}{3}\,M_{B_s}^2 f_{B_s}^2 R(\mu) B_3(\mu)\,, & \langle \mathcal{Q}_4\rangle &= 2\,M_{B_s}^2 f_{B_s}^2 R(\mu) B_4(\mu)\,,\\
\langle \mathcal{Q}_5\rangle &= \frac{2}{3}\,M_{B_s}^2 f_{B_s}^2 R(\mu) B_5(\mu)\,.
\end{aligned} \tag{10.26}$$

We take the bag parameters B_i from [138], which are given in Appendix A.4 for completeness. In order to resum large logarithms we employ $\bar{z} = \bar{m}_c^2(\bar{m}_b)/\bar{m}_b^2(\bar{m}_b) = 0.048(4)$ [121] in our numerical analysis. We further use $\bar{m}_b(\bar{m}_b) = (4.22 \pm 0.08)\,\mathrm{GeV}$ and $\bar{m}_s(\bar{m}_b) = (0.085 \pm 0.017)\,\mathrm{GeV}$.

For the sake of completeness, we quote the known results for the mixing amplitude. The general effective $\Delta B = 2$ Hamiltonian is given by

$$\mathcal{H}_{\text{eff}}^{\Delta B=2} = \sum_{i=1}^{5} C_i \mathcal{Q}_i + \sum_{i=1}^{3} \widetilde{C}_i \widetilde{\mathcal{Q}}_i \,, \tag{10.27}$$

where there are no tree-level contributions to $C_{2,3}$ and $\widetilde{C}_{2,3}$ in the RS model. The mixing amplitude

$$2\, m_{B_s} M_{12}^s = \langle B_s^0 |\, \mathcal{H}_{\text{eff}}^{\Delta B=2} \,| \bar{B}_s^0 \rangle \tag{10.28}$$

has been calculated in [74, 38], and found to be

$$M_{12}^{s\,\text{RS}} = \frac{4}{3}\, m_{B_s} f_{B_s}^2 \Big[\Big(C_1^{\text{RS}} + \widetilde{C}_1^{\text{RS}} \Big) B_1 + \frac{3}{4}\, R(\bar{m}_b)\, C_4^{\text{RS}} B_4 + \frac{1}{4}\, R(\bar{m}_b)\, C_5^{\text{RS}} B_5 \Big] \,. \tag{10.29}$$

The bag parameters $B_{1,4,5}$ are listed in (A.8), and the $\Delta B = 2$ coefficients evaluated at the KK scale can be found in Appendix B.4. These should be evolved down to $\bar{m}_b$. As it turns out, the coefficient C_4^{RS} is suppressed compared to C_1^{RS} by about two orders of magnitude, because of a stronger RS-GIM mechanism. The coefficients $\widetilde{C}_1^{\text{RS}}(m_b)$ and C_5^{RS} are even further suppressed. The SM mixing amplitude can be taken from [10, 121, 139]

$$M_{12}^{s\,\text{SM}} = \frac{G_F^2}{12\,\pi^2}\, (\lambda_t^{bs})^2 m_W^2 m_{B_s} \eta_B f_{B_s}^2 B_1 S_0(x_t) \,, \tag{10.30}$$

where $\eta_B = 0.837$ involves NLO QCD corrections in naive dimensional reduction (NDR). $S_0(x_t)$ is the Inami-Lim function stemming from the evaluation of the box-diagram, and $x_t = \bar{m}_t(\bar{m}_t)^2/m_W^2$ with $\bar{m}_t(\bar{m}_t) = (163.8 \pm 2.0)\,\text{GeV}$. The meson mass and decay constant are given by $m_{B_s} = 5.366(1)\,\text{GeV}$ [140] and $f_{B_s} = (238.8 \pm 9.5)\,\text{MeV}$ [141], respectively. If not stated otherwise, all other experimental input is taken from [140].

10.2 Numerical analysis

In our analysis, we use 10000 randomly generated parameter sets with $|(Y_{u,d})_{ij}| \in [0.1, 3]$. The bulk masses are chosen such that in the ZMA, the correct zero-mode masses, CKM mixing angles and phase are obtained within the 1σ range. We summarize the results for some individual ingredients of Γ_{12}^s (10.17) in Table 10.1. The SM coefficients are taken from [142]. For the sake of comparison, we rescale the RS penguin coefficients, for instance $\widetilde{K}_2^{\prime\text{RS}} \equiv \sqrt{2}\,(G_F \lambda_c^{bs})^{-1} K_2^{\prime\text{RS}}$ (SM: $\widetilde{K}_2' = K_2'$), as they are not supplemented with a CKM factor in (10.11). The numbers in the table have to be multiplied by the factors given in the last column. The maximum values of the RS contributions exceed the respective mean results by at least one order of magnitude, as suggested by the large standard deviations. The KK scale is set to $M_{\text{KK}} = 2\,\text{TeV}$ and we discard all points which are in conflict with the $Z^0 \to b\bar{b}$ "pseudo observables". Therefore, the number of points is reduced by a factor of about five in the minimal RS model.

Model/Coef.	$\lvert\widetilde{K}_2'\rvert$	$\lvert\widetilde{K}_2''\rvert$	$\lvert K_2^{(LL)}\rvert$	$\lvert K_2^{LR}\rvert$	$\lvert K_2^{RL}\rvert$	$\times$
SM	0.543	0.016	12.656	-	-	10^{-1}
mean(min RS)	0.16	0.03	0.01	4.40	0.04	10^{-3}
stand. dev.	0.17	0.03	0.05	7.41	0.06	10^{-3}
mean(cust)	0.94	0.06	0.23	2.22	0.03	10^{-3}
stand. dev.	1.39	0.09	1.38	4.98	0.05	10^{-3}

Table 10.1: Selected SM penguin and charged-current coefficients contributing to Γ_{12}^s compared to the mean absolute values of the corresponding RS coefficients for $M_{\rm KK} = 2\,{\rm TeV}$ and $\mu = \bar{m}_b$. See text for details.

Concerning the contributions from the charged-current sector, there is no difference between the prediction of the minimal and the custodial RS model at LO in $v^2/M_{\rm KK}^2$. The different average numbers arise due to the $Z^0 b\bar{b}$ selection. For the natural assumption $c_{Q_2} < -1/2$ the biggest correction comes from the operator Q_2^{LR}. This is easy to understand if we apply the warped-space Froggatt-Nielsen analysis to the charged-current Wilson coefficients (B.4). Setting all Yukawa factors to one, we can derive simplified expressions by performing an expansion in the Wolfenstein parameter λ, which is related to the ratios of IR zero-mode profiles (6.47). Thus, we find the scaling behavior

$$\begin{aligned}
C_2^{LL} &\propto \frac{m_W^2}{2M_{\rm KK}^2}\, L\, F(c_{Q_2})^2 F(c_{Q_3})^2\,,\\
C_2^{LR} &\propto \frac{v^2}{2M_{\rm KK}^2}\,\frac{F(c_{Q_3})}{F(c_{Q_2})}\, F(c_{u_2})F(c_{d_3}) \propto \frac{m_c m_b}{M_{\rm KK}^2}\,\frac{1}{F(c_{Q_2})^2}\,,\\
C_2^{RL} &\propto \frac{v^2}{M_{\rm KK}^2}\, F(c_{u_2})F(c_{d_2}) \propto \frac{2\,m_c m_s}{M_{\rm KK}^2}\,\frac{1}{F(c_{Q_2})^2}\,.
\end{aligned} \tag{10.31}$$

Note that the importance of C_2^{LR} grows with increasing UV-localization of the $(c,s)_L$ doublet. The coefficients C_1^{AB} with $A,B \in \{L,R\}$ are zero at the matching scale, but generated through operator mixing when running down to $\mu = \bar{m}_b$. As it turns out, the values of $|K_1^{AB}|$ are about a third of the respective values of $|K_2^{AB}|$ at $\mu = \bar{m}_b$. From the result (10.31) and the numbers in Table 10.1 we conclude that one can neglect contributions from the coefficients C_i^{LL} and C_i^{RL} in the RS model.

Turning our attention to the contributions of RS penguins, we observe that the coefficients $K_i'^{\rm RS}$ and $K_i''^{\rm RS}$ grow with an increasing value of $c_{b_L} \equiv c_{Q_3}$ and $c_{s_L} \equiv c_{Q_2}$. The reason is that the latter are dominated by overlap integrals of left-handed fermions with intermediate KK-gauge bosons and mixing effects of the latter with Z^0. The relevant expressions are given in (B.6). As KK modes are peaked towards the IR brane, overlap integrals with UV-localized fermions are exponentially suppressed (RS-GIM). The leading correction due to Z^0 exchange is enhanced by a factor L within the minimal RS variant. Nevertheless, due to the stringent bounds from the $Z^0 b_L \bar{b}_L$ vertex, the total penguin contributions typically remain smaller than in the custodial model. Furthermore, we note that it is sufficient to

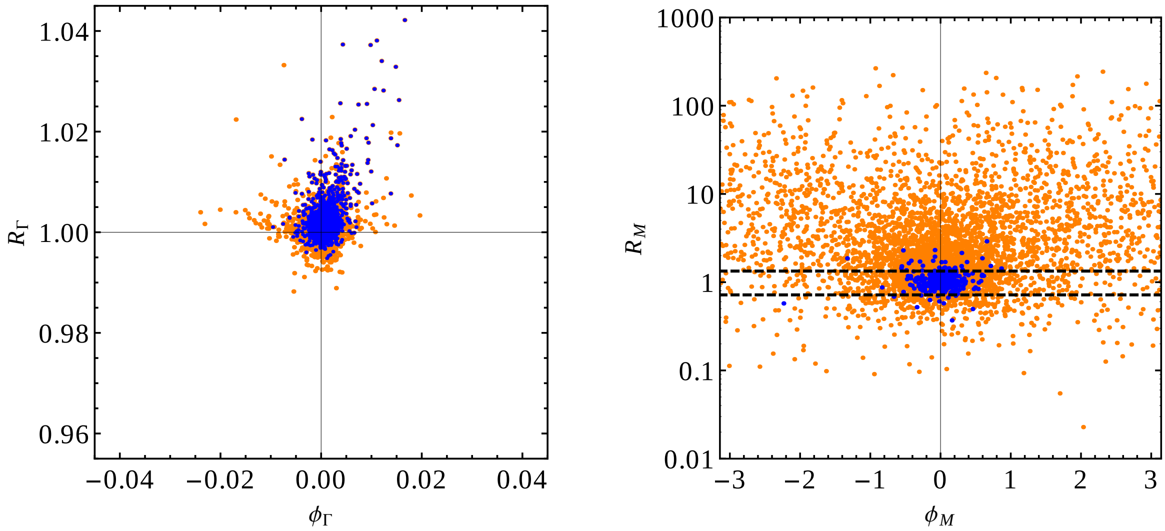

Figure 10.3: RS corrections to the magnitude and CP-violating phase of the $\bar{B}_s^0$-B_s^0 decay amplitude, R_Γ and ϕ_Γ, as well as of the mixing amplitude, R_M and ϕ_M. Blue (dark gray) points correspond to the minimal, orange (light gray) to the custodial RS model. The dashed lines mark the 95% confidence region with respect to the measurement of Δm_{B_s}. See text for details.

consider just the contributions stemming from the coefficients $K_i^{\prime\mathrm{NP}}$ in the neutral-current sector, as the impact of double-penguin insertions is typically about 1% of the leading correction due to charged currents.

In the first panel of Figure 10.3 we show the RS corrections to the magnitude and CP-violating phase of Γ_{12}^s, R_Γ and ϕ_Γ, for our set of 10000 parameter points at $M_{\mathrm{KK}} = 2\,\mathrm{TeV}$. The blue (dark gray) points correspond to the minimal RS model, where we plot only those that satisfy the bounds from the $Z^0 b_L \bar{b}_L$ vertex. The orange (light gray) points correspond to the custodial extension, where the latter requirement is always fulfilled. As we are just interested in the approximate size of RS corrections, we work with the LO SM expressions contained in (10.17) and (10.30). For precise predictions of a certain parameter point, one should include the full NLO corrections to Γ_{12}^s and M_{12}^s. As expected, the RS corrections to $|\Gamma_{12}^s|$ are rather small, typically not exceeding $\pm 4\%$. As already found in [38] and [74], there are sizable corrections to the magnitude and phase of the dispersive part of the mixing amplitude, R_M and ϕ_M, which are plotted in the second panel of Figure 10.3. At this point, one should keep in mind the experimental result from the time-dependent measurement of the $\bar{B}_s^0$-B_s^0 oscillation frequency [143]

$$\Delta m_{B_s}^{\mathrm{exp}} = (17.77 \pm 0.10\,(\mathrm{stat}) \pm 0.07\,(\mathrm{syst}))\,\mathrm{ps}^{-1}\,, \tag{10.32}$$

which is in good agreement with the SM prediction $(17.3{\pm}2.6)\,\mathrm{ps}^{-1}$ [128]. As a consequence, all points with $R_M \notin [0.718, 1.336]$ are excluded at 95% confidence level, as we have indicated by the dashed lines. We observe that for a sufficient amount of scatter points, the phase correction ϕ_M can take any value of $[-\pi, \pi]$ within the custodial RS model. Compared to ϕ_M, the new phase ϕ_Γ can be neglected (what we will do from now on).

Further important constraints to the bulk masses stem from the RS prediction of the observable $\epsilon_K = \epsilon_K^{\rm SM} + \epsilon_K^{\rm RS}$ [38, 74, 84]. Explicitly, one needs to satisfy $|\epsilon_K| \in [1.2, 3.2] \cdot 10^{-3}$, where

$$\epsilon_K = \frac{\kappa_\epsilon \, e^{i\varphi_\epsilon}}{\sqrt{2}\,(\Delta m_K)_{\rm exp}} \, {\rm Im}(M_{12}^{K{\rm SM}} + M_{12}^{K{\rm RS}}) \,, \tag{10.33}$$

with $\varphi_\epsilon = (43.51 \pm 0.05)^\circ$ [140] and $\kappa_\epsilon = 0.92 \pm 0.02$ [144]. The mixing amplitude of the neutral kaon is defined in analogy to (10.28). The input data needed for the calculation is given in Appendix B of [38]. As it turns out, without some tuning of the parameters, the prediction for ϵ_K is generically too large. Within the $\bar{K}^0$-K^0 mixing, the contributions from the operators $Q_{4,5}^{sd}$ can become comparable to those of Q_1^{sd} because of the large value $R_K(2\,{\rm GeV}) \approx 20$ in the matrix-element, and a more pronounced RG running. A protection can however be achieved by imposing a $U(3)$ flavor symmetry in the right-handed down-quark sector [145]. This symmetry is broken by the Yukawa couplings to obtain the correct zero-mode masses. On the other hand, if all bulk masses are equal, there are no tree-level FCNCs in the ZMA. The latter statement is evident from the expression (B.9), where $(\boldsymbol{W}_d^\dagger)_{mj} (\boldsymbol{W}_d)_{jn} = 0$ for $m \neq n$ due to the unitarity of $\boldsymbol{W}_d$. Non-vanishing contributions arise at $\mathcal{O}(v^4/M_{\rm KK}^4)$ from mixing with KK-modes. For $M_{\rm KK} = 2\,{\rm TeV}$, we can reduce $C_{4,5}^{sd}$ by a factor of about 100. The same suppression factor applies to the B-meson sector. For the coefficient $C_1^{\rm RS}$ however, there is no protection. In our analysis, we will not impose the proposed $U(3)$ flavor symmetry in the down sector, but rather use the bound from ϵ_K as a filter. As we will see below, this still allows for sizable corrections to the observables introduced at the beginning of this section.

10.3 Predictions for $\Delta\Gamma^s$, ϕ_s, and $A_{\rm SL}^s$

Neglecting the small SM phases, the width difference (10.5) can be written as

$$\Delta\Gamma_s = \Delta\Gamma_s^{\rm SM} \, R_\Gamma \, \cos 2\beta_s \,, \tag{10.34}$$

where $2\beta_s \approx -\phi_M^{\rm RS}$ [122][1]. The preliminary CDF analysis [123] uses the older SM prediction $\Delta\Gamma_s^{\rm SM} = (0.096 \pm 0.039){\rm ps}^{-1}$ [121], which we will take as central value for our calculation. Taking the more recent value will not change our conclusions. Comparing the latest CDF results in the $\Delta\Gamma_s/\phi_s$-plane (Figure 10.4) to the RS predictions shown in the left panel of Figure 10.5, we conclude that the RS model can enter the 68% confidence region and come close to the best fit value. It stays below the desired value of $\Delta\Gamma_s$, as there are no sizable positive corrections to $|\Gamma_{12}^s|$.

The SM prediction $(A_{\rm SL}^s)_{\rm SM} = (1.9 \pm 0.3) \cdot 10^{-5}$ [128], which is often named $a_{\rm sl}^s$ or $a_{\rm fs}^s$ in the literature, agrees with the direct measurement $(A_{\rm SL}^s)_{\rm exp} = -0.0017 \pm 0.0092$

[1] Be careful to discriminate between β_s and $\beta_s^{J/\psi\phi}$.

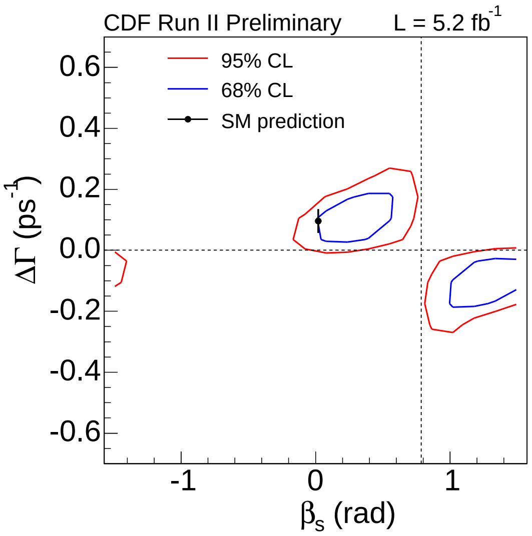

Figure 10.4: Experimental constraints from flavor-tagged $B \rightarrow^0_s J/\psi\phi$ decays in the $\Delta\Gamma_s^{\rm SM}/\beta_s$-plane. Figure taken from [123].

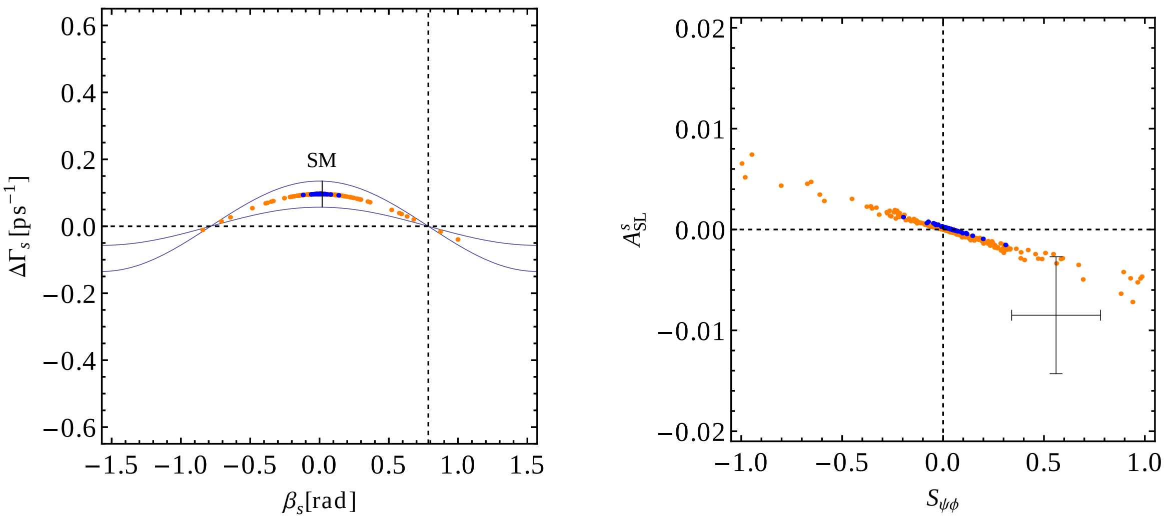

Figure 10.5: Left panel: Corrections within the $\Delta\Gamma_s^{\rm SM}/\beta_s$-plane for the minimal (blue/dark gray) and the custodial (orange/light gray) RS model. Bounds from $Z^0 b_L \bar{b}_L$, Δm_{B_s}, and ϵ_K are satisfied. Right panel: Corrections within the $A^s_{\rm SL}/S_{\psi\phi}$-plane for the minimal (blue/dark gray) and the custodial (orange/light gray) RS model, and the same set of scatter points .

[146] within the (large) error. However, recent measurements of the like-sign dimuon charge asymmetry $A^b_{\rm SL}$ [147], which connects $A^s_{\rm SL}$ to its counterpart $A^d_{\rm SL}$ of the B^0_d-meson sector [148], imply a deviation of almost 2σ. If one neglects the tiny SM phases and the NP phase corrections related to decay, $A^s_{\rm SL}$ is proportional to the quantity $S_{\psi\phi}$ [124], which is given by the amplitude of the time-dependent asymmetry in $B^0_s \to J/\psi\phi$ decays, $A^s_{\rm CP}(t) = S_{\psi\phi}\sin(\Delta m_{B_s} t)$. Setting just the NP phase in decay to zero, one obtains the well known expression $S_{\psi\phi} = \sin(2\beta_s^{J/\psi\phi} - \phi_M)$ [149], and thus

$$A^s_{\rm SL} \approx -\frac{|\Gamma^{s\,\rm SM}_{12}|}{|M^{s\,\rm SM}_{12}|}\,\frac{R_\Gamma}{R_M}\,S_{\psi\phi}\,. \tag{10.35}$$

The RS result is shown in the right panel of Figure 10.5, where we have sketched the experimental favored values $S_{\psi\phi} = 0.56 \pm 0.22$ [150] and $A^s_{\rm SL} = -0.0085 \pm 0.0058$ [146]. The latter number combines the direct measurement with the results derived from the measurement of $A^b_{\rm SL}$ in semileptonic B-decays in combination with the average value $A^d_{\rm SL} = -0.0047 \pm 0.0046$ from B-factories. It is evident from the plot that the best fit value of $S_{\psi\phi}$ can be reproduced (with some tuning in the minimal RS variant). This has already been noted in [38]. Furthermore, the custodial RS model can enter the 1σ range of the measured value of $A^s_{\rm SL}$. The same conclusion has been drawn in [129] recently, using a different approach. Here, the authors did not produce any concrete sets of input parameters, but scanned FCNC vertices across the allowed range subject to bounds from $\Delta\Gamma_s$ and Δm_{B_s}.

From $S_{\psi\phi} \approx \sin(2\beta_s)$ it follows that the corrections in the $\Delta\Gamma^{\rm SM}_s/\beta_s$-plane and $A^s_{\rm SL}/S_{\psi\phi}$-plane are aligned. An improvement in the former also leads to an improvement in the latter. We conclude that in the RS model, the current experimental results of all observables introduced in this section can be simultaneously reproduced within the range of 1σ. In the minimal RS model, this requires some moderate tuning of the parameters due to the combined constraints from the $Z^0 b_L \bar{b}_L$ vertex, the $\bar{B}^0_s$-B^0_s oscillation frequency Δm_{B_s}, and ϵ^K. In the custodial model, the first bound vanishes and generically allows for bigger corrections to the CP violating phase ϕ_s. This can be understood by noting that the coefficient $C^{\rm RS}_1$, which gives the dominant contribution of the mixing amplitude M^s_{12}, scales like $F(c_{Q_2})^2 F(c_{Q_3})^2$. In the custodial model we could choose a positive value of about one for $c_{Q_3} = c_{b_L}$ (which in turn would imply a strong UV localization of the right-handed bottom quark). As we have learned above, this is not possible in the minimal model, as the analysis of Section 7.3 has given the bound $c_{b_L} \lesssim -0.43$. In order to maximize the RS corrections to ϕ_s, one has to localize the second generation $SU(2)_L$ doublet as close to the IR brane as possible. This maximizes the value of $F(c_{Q_2})^2$. On the other hand, due to the scaling behavior of the charged-current $\Delta B = 1$ coefficients (10.31), this choice would minimize the leading correction to Γ^s_{12}, and therefore excludes the possibility of having a moderate positive correction to the width difference $\Delta\Gamma^s$ by some tuning of the parameters. However, due to the latest CDF results, an enhancement of $\Delta\Gamma^s$ is no longer mandatory.

11 Summary and conclusions

In this thesis we have studied important observables of current hadron collider experiments in the context of Randall-Sundrum scenarios, where gauge and matter fields are assumed to propagate in the bulk, and the Higgs is localized on the IR brane. After the introduction of a useful parametrization of the extra dimension, we have generalized the gauge-sector of the SM to a gauge theory in five dimensions. The Kaluza-Klein decomposition has been performed in the mass basis after applying a covariant R_ξ-gauge fixing, which is needed if one intends to perform higher order calculations involving KK vector bosons. We presented compact expressions for the sum over KK propagators, which at tree level give rise to corrections of the order $v^2/M_{\rm KK}^2$ compared to the SM for any scattering process.

As a first application, we calculated the universal corrections which modify the theoretical prediction of Fermi's constant. We emphasized that such a universal correction is non-observable, as it appears in any process mediated by the exchange of charged $W^{\pm(n)}$ bosons. We further determined the corrections to the zero-mode masses and couplings, which give rise to sizable modifications of the Peskin-Takeuchi parameters compared to their SM value. As it turned out, the (positive) corrections to T-parameter are enhanced with the "volume" L of the extra dimension. Agreement with the electroweak precision data can be achieved by rising the Higgs mass for instance.

On the other hand, the L-enhanced term can be eliminated by imposing a gauged custodial symmetry in the bulk. Therefore, we extended the discussion to the custodial Randall-Sundrum model and introduced a formalism which allowed for a straightforward generalization of our findings within the minimal scenario. Therefore, it can be used for any choice of the local gauge symmetry. For instance, the treatment of a GUT scenario within the 5D bulk would be an easy exercise. We furthermore presented exact results for the couplings among (KK) gauge bosons, which are needed in the study of Higgs branching fractions. After all, we re-derived the (leading) expressions for the Peskin-Takeuchi parameters using the holographic approximation. Though the latter approach is not the method of choice if one assumes the fifth dimension to be physical, it offers new ways in the treatment of strongly coupled four dimensional conformal field theories, which is a promising topic on its own.

In order to derive the RS corrections to gauge couplings of SM-like quarks, we have performed a KK decomposition also for 5D fermions. Here, the choice of the exact treatment, which includes the symmetry breaking effects due to the Higgs sector within the solution of the bulk EOMs, asks for a proper regularization. We have derived exact solutions of the fermion profiles in the vicinity of the IR brane, which for the case of the brane-Higgs scenario hold for any finite KK mass. Hierarchies in the Yukawa sector have been eliminated with the help of the warped space Froggatt-Nielsen mechanism, and expressions for the quark masses in the zero-mode approximation have been derived. We have investigated the flavor mixing of KK quarks and found $\mathcal{O}(1)$ mixing effects caused by the near degeneracy of the bulk masses. We shortly discussed how a generalization to more evolved fermion embeddings into the given gauge group is achieved. Again, we benefit from our vector notation, which collects 5D quantum fields that are supposed to be decomposed into the same 4D basis.

Concerning the neutral gauge interactions, we presented a detailed discussion of the couplings to zero-mode gauge bosons. While the universality of the photon and gluon couplings is guaranteed by the flatness of their profiles, the massive $W^\pm$ and Z^0 bosons go along with a vertex correction. For the case of the $Z^0 b_L \bar{b}_L$ vertex, we discussed how a custodial protection can be achieved by an appropriate embedding of the fermions into the extended gauge group. Here, we distinguished between protection through the admixture of heavy Z' bosons, and suppression of quark-mixing effects. We emphasized that the protection mechanism is broken by UV BCs and identified all terms that escape custodial protection. We have calculated the RS predictions for the left- and right-handed couplings of the Z^0 boson and found that in the minimal RS model the constraints from the $Z^0 \to b\bar{b}$ "pseudo observables" can be satisfied with moderate tuning. The overall fit can moreover significantly be improved by choosing a heavy Higgs mass of about 500 GeV. In the custodial model, the latter possibility seems to be excluded by the T-parameter. However, due to the chosen fermion embedding, all scatter points are safely localized within the 2σ confidence ellipse in the g_L^b-g_R^b plane.

Concerning weak decay processes mediated by the exchange of charged gauge bosons, we have written down the effective Hamiltonian and identified the expressions for the quark-mixing matrices. Here, we distinguished between factorizable RS corrections which can be observed through unitarity violations of the CKM matrix, and those that explicitly depend on the decay under consideration. We pointed out that right-handed charged currents already arise in the minimal model due to the admixture off right-handed KK $SU(2)_L$ doublets into the right-handed zero-mode singlets.

As another important topic, we have investigated how the RS model modifies the main Higgs production channels. A significant reduction of the gluon-fusion cross section is predicted, which can be about one order of magnitude or even more, depending on the value of the Higgs mass and the KK scale. Against the naive expectation, the sum over the KK tower in the fermion triangle loop is finite due to a cancellation within the doubled KK fermion spectrum. However, the presence of an IR cut-off asks for a truncation at low KK number, as the triangle loops are coupled to the brane-localized Higgs. For vector-boson fusion we observe a moderate suppression with respect to the SM prediction.

Motivated by the latest Tevatron results, we have studied the forward-backward asymmetry in $t\bar{t}$ production, where the SM prediction is about 2σ below the experimental favored value. Although the RS model looks as a promising candidate for closing the gap at first sight, it turns out that the outcome resembles the SM prediction. At LO, this is explained by the RS-GIM suppression of the tree level axial-vector currents for light quarks in the initial state. At NLO, RS corrections of the vector currents of the top quark cancel in the ratio of the charge-asymmetric and symmetric differential cross section. A sizable enhancement of the SM prediction therefore seems to be excluded for a setup with anarchic $\mathcal{O}(1)$ Yukawa couplings.

Furthermore, we have studied observables related to CP violation in B_s^0-meson decays. Therefore, we have calculated the NP corrections to the absorptive part of the $\bar{B}_s^0$-B_s^0 mixing amplitude Γ_{12}^s in the framework of an effective field theory based on operator product expansion. Taking existing results for the absorptive part M_{12}^s, we observe that the RS model gives rise to a sizable new CP violating phase. Taking care of the constraints from the $Z^0 b_L \bar{b}_L$ vertex, the $\bar{B}_s^0$-B_s^0-oscillation frequency Δm_{B_s}, and the RS prediction of ϵ_K, we conclude that an improvement within the $\Delta\Gamma_s/\beta_s$-plane and the $A_{\rm SL}^s/S_{\psi\phi}$-plane can be obtained simultaneously.

Finally, we conclude that the RS model of warped extra dimensions, regarded as an EFT, is an interesting alternative to SUSY (where is does not exclude the latter). Apart from solving the gauge-hierarchy problem of the SM, it also offers an explanation for the hierarchies in the flavor sector. It possesses a build-in Froggatt-Nielsen-mechanism, as well as a natural suppression of dangerous four-fermion operators involving light quarks. A direct hint for extra dimensions would be the discovery of Kaluza-Klein excitations, which, contrary to SUSY partners, possess the same spin as the related SM particles. However, for realistic choices of the KK scale, the masses of the lightest KK fermions (gauge bosons) are at least about 4 (5) TeV. Thus, a direct evidence seems to be impossible even at LHC energies. As a consequence, the search for NP within precision measurements is of special interest. Precise measurements of various weak decay cross sections may give hints for unitarity violations of the CKM matrix. The observation of right-handed charged currents would be a striking signal for either a mixing of SM fermions with non-SM fermions, or the realization of a gauged $SU(2)_R$ symmetry, which is broken at LHC energies. Even if not realized in nature, warped extra dimensions provide a new way of treating strongly coupled conformal field theories in the ordinary 4D space-time. However, if there is an evidence for extra dimensions, the next theoretical step has to be the construction of an appropriate UV completion.

Acknowledgments

I wish to thank some people who accompanied my way in the past years. First of all, I want to mention some (former) members of our working group THEP, who helped me with good advice. These are

Valentin Ahrens, Martin Bauer, Michael Benzke, Stefan Berge, Sandro Casagrande, Rainer Häußling, Tobias Hurth, Florian Jung, Alim Kadeer, Elen Lugert, Jeniffer Mutschall, Florian Scheck, Christoph Schmell, Hubert Spiesberger, Heidi Stein, Stefan Weinzierl, and Susanne Westhoff.

Special thanks are dedicated to Marc Vanderhaeghen, Florian Goertz, Uli Haisch, and Matthias Neubert.

Of course I want to thank all of my friends, which I do not list explicitly. You know who you are!

Finally, I want to thank my family, especially Nadja, Markus, Ute, and Heribert.

A Input data and formulas

A.1 Reference values for SM parameters

The central values and errors of the quark masses used for the generation of scatter points

$$
\begin{aligned}
m_u &= (1.5 \pm 1.0)\,\text{MeV}\,, & m_c &= (520 \pm 40)\,\text{MeV}\,, & m_t &= (144 \pm 5)\,\text{GeV}\,,\\
m_d &= (3.0 \pm 2.0)\,\text{MeV}\,, & m_s &= (50 \pm 15)\,\text{MeV}\,, & m_b &= (2.4 \pm 0.1)\,\text{GeV}\,.
\end{aligned}
\tag{A.1}
$$

They correspond to $\overline{\text{MS}}$ masses evaluated at the scale $M_{\text{KK}} = 1\,\text{TeV}$, obtained by using the low-energy values as compiled in [151].

A possible set of RS input parameters is given by

$$
\begin{aligned}
c_{Q_1} &= -0.597\,, & c_{Q_2} &= -0.531\,, & c_{Q_3} &= -0.473\,,\\
c_{u_1} &= -0.706\,, & c_{u_2} &= -0.575\,, & c_{u_3} &= +0.874\,,\\
c_{d_1} &= -0.691\,, & c_{d_2} &= -0.660\,, & c_{d_3} &= -0.583\,,
\end{aligned}
\tag{A.2}
$$

and

$$
\begin{aligned}
\widetilde{\boldsymbol{Y}}_u &= \begin{pmatrix} -1.101 - 1.692\,i & -0.298 + 0.695\,i & 0.908 - 1.513\,i \\ 0.386 - 1.330\,i & 0.564 + 1.399\,i & -0.048 + 0.105\,i \\ 0.316 + 2.211\,i & 0.098 - 1.176\,i & 0.788 + 1.776\,i \end{pmatrix},\\
\widetilde{\boldsymbol{Y}}_d &= \begin{pmatrix} 0.465 + 1.430\,i & 0.017 - 2.261\,i & -0.652 + 2.376\,i \\ 0.710 - 0.074\,i & -0.665 + 2.183\,i & -0.255 + 0.016\,i \\ 0.313 + 2.397\,i & -0.563 + 1.544\,i & -1.783 - 1.898\,i \end{pmatrix}.
\end{aligned}
\tag{A.3}
$$

A.2 Form factors for Higgs-boson production

The form factor $A^h_{q,W}(\tau)$ describing the effects of quark loops in the production of the Higgs boson is given by [152]

$$
A^h_q(\tau) = \frac{3\tau}{2}\left[1 + (1-\tau)\,f(\tau)\right], \tag{A.4}
$$

where

$$
f(\tau) = \begin{cases} -\dfrac{1}{4}\left[\ln\left(\dfrac{1+\sqrt{1-\tau}}{1-\sqrt{1-\tau}}\right) - i\pi\right]^2, & \tau \le 1\,,\\[2ex] \arcsin^2\left(\dfrac{1}{\sqrt{\tau}}\right), & \tau > 1\,. \end{cases} \tag{A.5}
$$

A.3 Reduction factors for $t\bar{t}$-production cross sections

In order to transform expressions for the $t\bar{t}$-production cross sections valid in the partonic CM frame to the laboratory frame, we employ

$$\sigma_a^{p\bar{p}} = \frac{\alpha_s}{m_t^2} \sum_{i,j} \int_{4m_t^2/s}^{1} d\tau \int_{\tau}^{1} \frac{dx}{x} \, f_{i/p}(x, \mu_f) \, f_{j/\bar{p}}(\tau/x, \mu_f) \, A_{ij}^{p\bar{p}}(x, \tau, \mu_f) \,, \tag{A.6}$$

where $\tau \equiv \hat{s}/s$, and

$$A_{ij}^{p\bar{p}}(x, \tau, \mu_f) \equiv \int_{c(x,\tau)}^{1} d\cos\theta \, K_{ij}(\rho, \cos\theta, \mu_f) - \int_{-1}^{c(x,\tau)} d\cos\theta \, K_{ij}(\rho, \cos\theta, \mu_f) \tag{A.7}$$

with $c(x, \tau) \equiv 1/\beta \, (x^2 - \tau)/(x^2 + \tau)$. The latter formula (A.6) applies at the Born level. Beyond LO the phase-space integration is more involved. The respective corrections can be parametrized by the reduction factors $R \equiv \sigma_a^{p\bar{p}}/\sigma_a$ that convert the SM as well as the EFT results from the partonic CM to the laboratory frame at NLO. In the SM we find $R_{\rm SM} = 0.64$, while the reduction factors of the effective operators are given by $R^V_{u\bar{u}} = 0.73$, $R^V_{d\bar{d}} = 0.72$, $R^S_{t\bar{u}} = -1.78$, $R^A_{u\bar{u}} = 0.58$, and $R^A_{d\bar{d}} = 0.56$ [103].

A.4 Bag parameters for B_s-meson matrix elements

In the following we quote bag parameters of the matrix elements (10.26) as given [138]. These have been renormalized in the NDR-$\overline{\rm MS}$ scheme of [131] at $\mu = m_b = 4.6\,$GeV, and read

$$\begin{aligned} &B_1 = 0.87(2)\left(^{+5}_{-4}\right), \quad B_2 = 0.84(2)(4), \\ &B_3 = 0.91(3)(8), \qquad B_4 = 1.16(2)\left(^{+5}_{-7}\right), \quad B_5 = 1.75(3)\left(^{+21}_{-6}\right), \end{aligned} \tag{A.8}$$

The first (second) number in brackets corresponds to the statistical (systematic) error.

B Wilson coefficients

B.1 Wilson coefficients for $t\bar{t}$ production

In the following, we present the ZMA results for the Wilson coefficients (9.21). If we have up quarks in the initial state ($q = u$), we obtain for the KK gluon s-channel exchange

$$
\begin{aligned}
C_{u\bar{u},\parallel}^{(V,8)} = -\frac{4\pi\alpha_s}{M_{\mathrm{KK}}^2}\Bigg[& \frac{1}{2L} - \frac{F^2(c_{t_R})\,(2c_{t_R}+5)}{4(2c_{t_R}+3)^2} - \frac{F^2(c_{t_L})\,(2c_{t_L}+5)}{4(2c_{t_L}+3)^2} \\
& - \frac{F^2(c_{u_R})}{4\,|(M_u)_{11}|^2}\sum_{i=1,2,3}\frac{(2c_{u_i}+5)\,|(M_u)_{1i}|^2}{(2c_{u_i}+3)^2} - \frac{F^2(c_{u_L})}{4\,|(M_u)_{11}|^2}\sum_{i=1,2,3}\frac{(2c_{Q_i}+5)\,|(M_u)_{i1}|^2}{(2c_{Q_i}+3)^2} \\
& + \frac{L}{2}\,\frac{F^2(c_{t_R})F^2(c_{u_R})}{(2c_{t_R}+3)\,|(M_u)_{11}|^2}\sum_{i=1,2,3}\frac{(c_{u_i}+c_{t_R}+3)\,|(M_u)_{1i}|^2}{(2c_{u_i}+3)(c_{u_i}+c_{t_R}+2)} \\
& + \frac{L}{2}\,\frac{F^2(c_{t_L})F^2(c_{u_L})}{(2c_{t_L}+3)\,|(M_u)_{11}|^2}\sum_{i=1,2,3}\frac{(c_{Q_i}+c_{t_L}+3)\,|(M_u)_{i1}|^2}{(2c_{Q_i}+3)(c_{Q_i}+c_{t_L}+2)}\Bigg],
\end{aligned}
$$

$$
\begin{aligned}
C_{u\bar{u},\perp}^{(V,8)} = -\frac{4\pi\alpha_s}{M_{\mathrm{KK}}^2}\Bigg[& \frac{1}{2L} - \frac{F^2(c_{t_R})\,(2c_{t_R}+5)}{4(2c_{t_R}+3)^2} - \frac{F^2(c_{t_L})\,(2c_{t_L}+5)}{4(2c_{t_L}+3)^2} \\
& - \frac{F^2(c_{u_R})}{4\,|(M_u)_{11}|^2}\sum_{i=1,2,3}\frac{(2c_{u_i}+5)\,|(M_u)_{1i}|^2}{(2c_{u_i}+3)^2} - \frac{F^2(c_{u_L})}{4\,|(M_u)_{11}|^2}\sum_{i=1,2,3}\frac{(2c_{Q_i}+5)\,|(M_u)_{i1}|^2}{(2c_{Q_i}+3)^2} \\
& + \frac{L}{2}\,\frac{F^2(c_{t_L})F^2(c_{u_R})}{(2c_{t_L}+3)\,|(M_u)_{11}|^2}\sum_{i=1,2,3}\frac{(c_{u_i}+c_{t_L}+3)\,|(M_u)_{1i}|^2}{(2c_{u_i}+3)(c_{u_i}+c_{t_L}+2)} \\
& + \frac{L}{2}\,\frac{F^2(c_{t_R})F^2(c_{u_L})}{(2c_{t_R}+3)\,|(M_u)_{11}|^2}\sum_{i=1,2,3}\frac{(c_{Q_i}+c_{t_R}+3)\,|(M_u)_{i1}|^2}{(2c_{Q_i}+3)(c_{Q_i}+c_{t_R}+2)}\Bigg].
\end{aligned}
\tag{B.1}
$$

Similar relations hold for the case of the light quarks $q = d, s, c$. Here, $(M_u)_{ij}$ denote the minors of the up-type Yukawa matrix $\tilde{\boldsymbol{Y}}_u$. The coefficients for the t-channel exchange are given by

$$\begin{aligned}
C_{t\bar{u},\parallel}^{(V,8)} &= -\frac{\pi\alpha_s}{M_{\rm KK}^2}\, L\left[\frac{F^2(c_{t_R})F^2(c_{u_R})\,|(M_u)_{13}|^2}{(2c_{t_R}+3)(c_{t_R}+1)\,|(M_u)_{11}|^2} + \frac{F^2(c_{t_L})F^2(c_{u_L})\,|(M_u)_{31}|^2}{(2c_{t_L}+3)(c_{t_L}+1)\,|(M_u)_{11}|^2}\right], \\
C_{t\bar{u},\parallel}^{(V,1)} &= -\frac{\pi\alpha_e}{M_{\rm KK}^2}\,\frac{L}{s_w^2c_w^2}\left[(T_3^u - Q_u s_w^2)^2\,\frac{F^2(c_{t_L})F^2(c_{u_L})\,|(M_u)_{31}|^2}{(2c_{t_L}+3)(c_{t_L}+1)\,|(M_u)_{11}|^2}\right. \\
&\qquad\left. + \left(s_w^2Q_u\right)^2\,\frac{F^2(c_{t_R})F^2(c_{u_R})\,|(M_u)_{13}|^2}{(2c_{t_R}+3)(c_{t_R}+1)\,|(M_u)_{11}|^2}\right] \\
&\quad - \frac{\pi\alpha_e Q_u^2}{M_{\rm KK}^2}\, L\left[\frac{F^2(c_{t_R})F^2(c_{u_R})\,|(M_u)_{13}|^2}{(2c_{t_R}+3)(c_{t_R}+1)\,|(M_u)_{11}|^2} + \frac{F^2(c_{t_L})F^2(c_{u_L})\,|(M_u)_{31}|^2}{(2c_{t_L}+3)(c_{t_L}+1)\,|(M_u)_{11}|^2}\right].
\end{aligned} \tag{B.2}$$

All coefficients have to be matched at the KK scale and evolved down to the top-quark mass m_t. We perform the RG evolution at leading-logarithmic accuracy, *i.e.*, at one-loop order, neglecting tiny effects that arise from the mixing with QCD penguin operators. For the s-channel Wilson coefficients entering the formulas (9.28) and (9.29), we find

$$\widetilde{C}_{q\bar{q}}^P(m_t) = \left(\frac{2}{3\eta^{4/7}} + \frac{\eta^{2/7}}{3}\right)\widetilde{C}_{q\bar{q}}^P(M_{\rm KK})\,, \tag{B.3}$$

where $P = V, A$, and $\eta \equiv \alpha_s(M_{\rm KK})/\alpha_s(m_t)$ is the ratio of strong coupling constants evaluated at the relevant scales $M_{\rm KK}$ and m_t. Since in the RS model the t-channel Wilson coefficients $\widetilde{C}_{t\bar{u}}^V$ and $\widetilde{C}_{t\bar{u}}^S$ turn out to be numerically irrelevant, we do not consider their running.

B.2 Wilson coefficients of $\Delta B = 1$ charged-current operators

According to the definition (10.11), we find at LO in $v^2/M_{\rm KK}^2$ for the Wilson coefficients of charged-current $\Delta B = 1$ operators

$$\begin{aligned}
C_2^{LL} &= \frac{m_W^2}{2M_{\rm KK}^2}\, L\,\frac{(\boldsymbol{U}_d^\dagger)_{2i}(\boldsymbol{U}_u)_{i2}}{(\boldsymbol{U}_d^\dagger\boldsymbol{U}_u)_{22}}\,(\widetilde{\boldsymbol{\Delta}}_{QQ})_{ij}\,\frac{(\boldsymbol{U}_u^\dagger)_{2j}(\boldsymbol{U}_d)_{j3}}{(\boldsymbol{U}_u^\dagger\boldsymbol{U}_d)_{23}}\,, \\
C_2^{LR} &= \frac{1}{M_{\rm KK}^2}\,\frac{(\boldsymbol{m}_u\boldsymbol{U}_u^\dagger)_{2i}\,f(c_{Q_i})\,(\boldsymbol{U}_d\,\boldsymbol{m}_d)_{i3}}{(\boldsymbol{U}_u^\dagger\boldsymbol{U}_d)_{23}}\,, \\
C_2^{RL} &= \frac{1}{M_{\rm KK}^2}\,\frac{(\boldsymbol{m}_d\boldsymbol{U}_d^\dagger)_{2i}\,f(c_{Q_i})\,(\boldsymbol{U}_u\,\boldsymbol{m}_u)_{i2}}{(\boldsymbol{U}_d^\dagger\boldsymbol{U}_u)_{22}}\,,
\end{aligned} \tag{B.4}$$

and $C_1^{LL}(M_{\rm KK}) = C_1^{LR}(M_{\rm KK}) = C_1^{RL}(M_{\rm KK}) = 0$ for both the minimal and the custodial model. All coefficients have to be evolved down to the bottom mass. The coefficients

$C_1^{LL/LR/RL}(m_b)$ are non-zero as the operators Q_1^{AB} $(A, B = L, R)$ mix with the operators Q_2^{AB} within the renormalization procedure. Note that there is no mixing between operators of different chirality assignments. The LO QCD anomalous dimension matrix (1.80) for all three cases is given by

$$\hat{\gamma}_0 = \begin{pmatrix} -\frac{6}{N_c} & 6 \\ 6 & -\frac{6}{N_c} \end{pmatrix} . \tag{B.5}$$

We fix the running of $\alpha_s(\mu)$ at $\mu = m_t = 171.2\,\text{GeV}$ and $\mu = M_{\text{KK}} = 2\,\text{TeV}$, and apply the general formula (1.85) with $n_{f1} = 5,\ n_{f2} = 6$.

B.3 Wilson coefficients of $\Delta B = 1$ penguin operators

At $\mathcal{O}(v^2/M_{\text{KK}}^2)$ the Wilson coefficients of the penguin operators in equation (10.11) are explicitly given by [38]

$$\begin{aligned}
C_3^{\text{RS}} &= \frac{\pi\alpha_s}{M_{\text{KK}}^2}\,\frac{(\boldsymbol{\Delta}'_D)_{23}}{2N_c} - \frac{\pi\alpha}{6s_w^2c_w^2\,M_{\text{KK}}^2}(\,\boldsymbol{\Sigma}_D)_{23}\,,\\
C_4^{\text{RS}} &= C_6^{\text{RS}} = -\frac{\pi\alpha_s}{2M_{\text{KK}}^2}\,(\boldsymbol{\Delta}'_D)_{23}\,,\\
C_5^{\text{RS}} &= \frac{\pi\alpha_s}{M_{\text{KK}}^2}\,\frac{(\boldsymbol{\Delta}'_D)_{23}}{2N_c}\,,\\
C_7^{\text{RS}} &= \frac{2\pi\alpha}{9M_{\text{KK}}^2}\,(\boldsymbol{\Delta}'_D)_{23} - \frac{2\pi\alpha}{3c_w^2\,M_{\text{KK}}^2}(\,\boldsymbol{\Sigma}_D)_{23}\,,\\
C_8^{\text{RS}} &= C_{10}^{\text{RS}} = 0\,,\\
C_9^{\text{RS}} &= \frac{2\pi\alpha}{9M_{\text{KK}}^2}\,(\boldsymbol{\Delta}'_D)_{23} + \frac{2\pi\alpha}{3s_w^2\,M_{\text{KK}}^2}(\,\boldsymbol{\Sigma}_D)_{23}\,,
\end{aligned} \tag{B.6}$$

where

$$\boldsymbol{\Sigma}_D \equiv \omega_Z^{d_L}\,L\left(\frac{1}{2} - \frac{s_w^2}{3}\right)\boldsymbol{\Delta}_D + \frac{M_{\text{KK}}^2}{m_Z^2}\,\boldsymbol{\delta}_D\,. \tag{B.7}$$

These results are to be evaluated at the KK scale with $\omega_Z^{d_L} = 1$ in the minimal RS model, and $\omega_Z^{d_L} = 0$ in the custodial one. The exact analytic expressions for $\boldsymbol{\Delta}_D$, $\boldsymbol{\Delta}'_D$, and $\boldsymbol{\delta}_D$ are given in (7.16), (7.17), and (7.18). However, as we only deal with light SM quarks in the initial and final state, it is convenient to insert the ZMA expressions (7.20), (7.21), and (7.22) into the above defintions of Wilson coefficients.

Within the RG running, the penguin operators mix with each other. Furthermore, there is a small admixture from charged-currents. For the operator basis $\vec{Q} = (Q_1, Q_2, Q_{3,..,10})$, the anomalous dimension matrix $\gamma^{(0)}$ is a function of N_c, n_f, n_u, and n_d (number of colors, flavors, up- and down-type quarks), and can be found in [153, 154]. The upper left 2×2 sub-matrix is just the anomalous dimensions matrix (B.5) given above. Note that while the charged-current operators mix into the penguin operators, the former evolve independent from the latter.

B.4 Wilson coefficients for $\Delta B = 2$ operators

The $\Delta B = 2$ operators that contribute to the $\bar{B}_s^0$-B_s^0 mixing amplitude at tree-level are given by $\mathcal{Q}_1$, $\widetilde{\mathcal{Q}}_1$, $\mathcal{Q}_4$, and $\mathcal{Q}_5$. There is no mixing between $\mathcal{Q}_1$ and $\widetilde{\mathcal{Q}}_1$ under renormalization. The anomalous dimension for both cases is given by $\gamma_0^{\rm VLL} = 6 - 6/N_c$ [155]. The operators $\mathcal{Q}_{4,5}$ mix under renormalization and the anomalous dimension matrix of the vector $(C_5, C_4)^T$ explicitly reads [155, 156]

$$\hat{\gamma}_0 = \begin{pmatrix} \frac{6}{N_c} & 12 \\ 0 & -6N_c + \frac{6}{N_c} \end{pmatrix} . \tag{B.8}$$

Defining $\widetilde{\boldsymbol{\Delta}}_{dd}$ and $\widetilde{\boldsymbol{\Delta}}_{Qd}$ in analogy to (7.36), the RS coefficients evaluated at the KK scale are given by [38]

$$\begin{aligned} C_1^{\rm RS} &= \frac{\pi L}{M_{\rm KK}^2}\, (\boldsymbol{U}_d^\dagger)_{2i} (\boldsymbol{U}_d)_{i3} (\widetilde{\boldsymbol{\Delta}}_{QQ})_{ij} (\boldsymbol{U}_d^\dagger)_{2j} (\boldsymbol{U}_d)_{j3} \\ &\quad \times \left[\frac{\alpha_s}{2} \left(1 - \frac{1}{N_c} \right) + Q_d^2\, \alpha + (\omega_Z^{d_L d_L}) \frac{(T_L^{3d_L} - s_w^2\, Q_d)^2\, \alpha}{s_w^2 c_w^2} \right] , \\ \widetilde{C}_1^{\rm RS} &= \frac{\pi L}{M_{\rm KK}^2}\, (\boldsymbol{W}_d^\dagger)_{2i} (\boldsymbol{W}_d)_{i3} (\widetilde{\boldsymbol{\Delta}}_{dd})_{ij} (\boldsymbol{W}_d^\dagger)_{2j} (\boldsymbol{W}_d)_{j3} \\ &\quad \times \left[\frac{\alpha_s}{2} \left(1 - \frac{1}{N_c} \right) + Q_d^2\, \alpha + (\omega_Z^{d_R d_R}) \frac{(s_w^2\, Q_d)^2\, \alpha}{s_w^2 c_w^2} \right] , \\ C_4^{\rm RS} &= \frac{\pi L}{M_{\rm KK}^2}\, (\boldsymbol{U}_d^\dagger)_{2i} (\boldsymbol{U}_d)_{i3} (\widetilde{\boldsymbol{\Delta}}_{Qd})_{ij} (\boldsymbol{W}_d^\dagger)_{2j} (\boldsymbol{W}_d)_{j3}\, [-2\alpha_s] , \\ C_5^{\rm RS} &= \frac{\pi L}{M_{\rm KK}^2}\, (\boldsymbol{U}_d^\dagger)_{2i} (\boldsymbol{U}_d)_{i3} (\widetilde{\boldsymbol{\Delta}}_{Qd})_{ij} (\boldsymbol{W}_d^\dagger)_{2j} (\boldsymbol{W}_d)_{j3} \\ &\quad \times \left[\frac{2\alpha_s}{N_c} - 4Q_d^2\, \alpha + \omega_Z^{d_L d_R} \frac{4s_w^2\, Q_d\, (T_L^{3d_L} - s_w^2\, Q_d)\, \alpha}{s_w^2 c_w^2} \right] . \end{aligned} \tag{B.9}$$

Here we have introduced the correction factors $\omega_Z^{qq'}$, which are equal to 1 in the minimal RS model, and given by

$$\omega_Z^{qq'} = 1 + \frac{1}{c_w^2 - s_w^2} \left(\frac{s_w^2 (T_L^{3q} - Q^q) - c_w^2 T_R^{3q}}{T_L^{3q} - s_w^2 Q^q} \right) \left(\frac{s_w^2 (T_L^{3q'} - Q^{q'}) - c_w^2 T_R^{3q'}}{T_L^{3q'} - s_w^2 Q^{q'}} \right) \tag{B.10}$$

in the custodial one [75]. Numerically we find $\omega_Z^{d_L d_L} \approx 2.9$, $\omega_Z^{d_R d_R} \approx 150.9$, and $\omega_Z^{d_L d_R} \approx -15.7$. The quantum numbers $T_{L,R}^{3q}$ of the (+) type fields $q = d_{L,R}$ are listed in Table 6.2.

Bibliography

[1] F. Scheck, *Theoretische Physik 4 Quantisierte Felder*, Springer 2007

[2] M. E. Peskin, D. V. Schroeder, *An Introduction to Quantum Field Theory*, Westview Press 1995

[3] T. C. Cheng, L. F. Lee, *Gauge theory of elementary particle physics*, Oxford University Press 2006

[4] L. D. Faddeev and V. N. Popov, Phys. Lett. B **25** (1967) 29.

[5] C. C. Nishi, Am. J. Phys. **73** (2005) 1160

[6] M. E. Peskin and T. Takeuchi, Phys. Rev. Lett. **65** (1990) 964.

[7] M. E. Peskin and T. Takeuchi, Phys. Rev. D **46** (1992) 381.

[8] B. W. Lee, C. Quigg and H. B. Thacker, Phys. Rev. D **16** (1977) 1519.

[9] M. Kobayashi and T. Maskawa, Prog. Theor. Phys. **49** (1973) 652.

[10] A. J. Buras, arXiv:hep-ph/9806471.

[11] M. Neubert, arXiv:hep-ph/0512222.

[12] H. Georgi and S. L. Glashow, Phys. Rev. Lett. **32** (1974) 438.

[13] S. Dodelson and L. M. Widrow, Phys. Rev. Lett. **72** (1994) 17 [arXiv:hep-ph/9303287].

[14] M. Loewenstein and A. Kusenko, Astrophys. J. **714** (2010) 652 [arXiv:0912.0552 [astro-ph.HE]].

[15] N. Arkani-Hamed, S. Dimopoulos and G. R. Dvali, Phys. Lett. B **429** (1998) 263

[16] D. J. Kapner, T. S. Cook, E. G. Adelberger, J. H. Gundlach, B. R. Heckel, C. D. Hoyle and H. E. Swanson, Phys. Rev. Lett. **98** (2007) 021101 [arXiv:hep-ph/0611184].

[17] E. A. Mirabelli, M. Perelstein and M. E. Peskin, Phys. Rev. Lett. **82** (1999) 2236

[18] S. Cullen and M. Perelstein, Phys. Rev. Lett. **83** (1999) 268

[19] L. Randall and R. Sundrum, Phys. Rev. Lett. **83** (1999) 3370

[20] K. Agashe, A. Delgado, M. J. May and R. Sundrum, JHEP **0308** (2003) 050

[21] S. S. Gubser, I. R. Klebanov and A. M. Polyakov, Phys. Lett. B **428** (1998) 105

[22] E. Witten, Adv. Theor. Math. Phys. **2** (1998) 253

[23] R. Barbieri, A. Pomarol and R. Rattazzi, Phys. Lett. B **591** (2004) 141

[24] K. Agashe, R. Contino, L. Da Rold and A. Pomarol, Phys. Lett. B **641** (2006) 62

[25] W. D. Goldberger and M. B. Wise, Phys. Rev. Lett. **83** (1999) 4922

[26] H. Davoudiasl, J. L. Hewett and T. G. Rizzo, Phys. Rev. Lett. **84** (2000) 2080

[27] T. Gherghetta and A. Pomarol, Nucl. Phys. B **586** (2000) 141

[28] Y. Grossman and M. Neubert, Phys. Lett. B **474** (2000) 361

[29] C. Csaki, J. Erlich and J. Terning, Phys. Rev. D **66** (2002) 064021

[30] H. Davoudiasl, J. L. Hewett and T. G. Rizzo, Phys. Lett. B **473** (2000) 43

[31] A. Pomarol, Phys. Lett. B **486** (2000) 153

[32] F. Goertz and T. Pfoh, JHEP **0810** (2008) 035

[33] S. J. Huber and Q. Shafi, Phys. Rev. D **63** (2001) 045010

[34] S. Casagrande, F. Goertz, U. Haisch, M. Neubert and T. Pfoh, JHEP **0810** (2008) 094

[35] C. Csaki, J. Hubisz and P. Meade, arXiv:hep-ph/0510275.

[36] L. Randall and M. D. Schwartz, JHEP **0111** (2001) 003

[37] J. Hirn and V. Sanz, Phys. Rev. D **76** (2007) 044022

[38] M. Bauer, S. Casagrande, U. Haisch and M. Neubert, JHEP **1009** (2010) 017

[39] A. Delgado and A. Falkowski, JHEP **0705** (2007) 097

[40] M. S. Carena, E. Ponton, T. M. P. Tait and C. E. M. Wagner, Phys. Rev. D **67**, 096006 (2003)

[41] The Tevatron Electroweak Working Group, arXiv:0803.1683 [hep-ex].

[42] B. A. Dobrescu and C. T. Hill, Phys. Rev. Lett. **81**, 2634 (1998)

[43] R. S. Chivukula and N. J. Evans, Phys. Lett. B **464**, 244 (1999)

[44] M. E. Peskin and J. D. Wells, Phys. Rev. D **64**, 093003 (2001)

[45] D. Choudhury, T. M. P. Tait and C. E. M. Wagner, Phys. Rev. D **65**, 053002 (2002)

[46] R. Barbieri, L. J. Hall and V. S. Rychkov, Phys. Rev. D **74**, 015007 (2006)

[47] B. Grzadkowski and J. F. Gunion, arXiv:hep-ph/0610105.

[48] H. Davoudiasl, G. Perez and A. Soni, Phys. Lett. B **665** (2008) 67

[49] H. Davoudiasl, J. L. Hewett and T. G. Rizzo, Phys. Rev. D **68**, 045002 (2003)

[50] M. S. Carena, A. Delgado, E. Ponton, T. M. P. Tait and C. E. M. Wagner, Phys. Rev. D **68**, 035010 (2003)

[51] H. Georgi, A. K. Grant and G. Hailu, Phys. Lett. B **506** (2001) 207

[52] H. C. Cheng, K. T. Matchev and M. Schmaltz, Phys. Rev. D **66**, 036005 (2002)

[53] S. Casagrande, F. Goertz, U. Haisch, M. Neubert and T. Pfoh, JHEP **1009** (2010) 014

[54] M. E. Albrecht, M. Blanke, A. J. Buras, B. Duling and K. Gemmler, JHEP **0909** (2009) 064

[55] G. Burdman and L. Da Rold, JHEP **0811** (2008) 025

[56] M. S. Carena, E. Ponton, J. Santiago and C. E. M. Wagner, Nucl. Phys. B **759** (2006) 202

[57] M. S. Carena, E. Ponton, J. Santiago and C. E. M. Wagner, Phys. Rev. D **76** (2007) 035006

[58] J. M. Maldacena, Adv. Theor. Math. Phys. **2** (1998) 231 [Int. J. Theor. Phys. **38** (1999) 1113]

[59] K. Agashe, C. Csaki, C. Grojean and M. Reece, JHEP **0712** (2007) 003

[60] R. Contino and A. Pomarol, JHEP **0411** (2004) 058

[61] K. Agashe, R. Contino and A. Pomarol, Nucl. Phys. B **719** (2005) 165

[62] K. Agashe and R. Contino, Nucl. Phys. B **742** (2006) 59

[63] T. Gherghetta, arXiv:1008.2570 [hep-ph].

[64] N. Arkani-Hamed, M. Porrati and L. Randall, JHEP **0108** (2001) 017

[65] R. Rattazzi and A. Zaffaroni, JHEP **0104** (2001) 021

[66] M. Perez-Victoria, JHEP **0105** (2001) 064

[67] A. Azatov, M. Toharia and L. Zhu, Phys. Rev. D **80** (2009) 035016

[68] J. A. Bagger, F. Feruglio and F. Zwirner, Phys. Rev. Lett. **88** (2002) 101601

[69] K. Agashe, G. Perez and A. Soni, Phys. Rev. Lett. **93** (2004) 201804

[70] K. Agashe, G. Perez and A. Soni, Phys. Rev. D **71** (2005) 016002

[71] S. J. Huber and Q. Shafi, Phys. Lett. B **498** (2001) 256

[72] C. D. Froggatt and H. B. Nielsen, Nucl. Phys. B **147** (1979) 277.

[73] S. J. Huber, Nucl. Phys. B **666** (2003) 269

[74] M. Blanke, A. J. Buras, B. Duling, S. Gori and A. Weiler, JHEP **0903** (2009) 001

[75] F. Goertz and T. Pfoh, arXiv:1105.1507 [hep-ph].

[76] F. del Aguila and J. Santiago, Phys. Lett. B **493** (2000) 175

[77] J. L. Hewett, F. J. Petriello and T. G. Rizzo, JHEP **0209** (2002) 030

[78] A. J. Buras, B. Duling and S. Gori, JHEP **0909** (2009) 076

[79] G. Burdman, Phys. Rev. D **66** (2002) 076003

[80] J. H. Field, Mod. Phys. Lett. A **13**, 1937 (1998)

[81] S. Schael *et al.* [ALEPH Collaboration], Phys. Rept. **427**, 257 (2006)

[82] D. Y. Bardin, P. Christova, M. Jack, L. Kalinovskaya, A. Olchevski, S. Riemann and T. Riemann, Comput. Phys. Commun. **133**, 229 (2001)

[83] A. B. Arbuzov *et al.*, Comput. Phys. Commun. **174**, 728 (2006)

[84] M. Bauer, S. Casagrande, L. Grunder, U. Haisch and M. Neubert, Phys. Rev. D **79** (2009) 076001

[85] K. Agashe, G. Perez and A. Soni, Phys. Rev. D **75** (2007) 015002

[86] K. Agashe and R. Contino, Phys. Rev. D **80**, 075016 (2009)

[87] C. Bouchart and G. Moreau, Phys. Rev. D **80** (2009) 095022

[88] A. Azatov, M. Toharia and L. Zhu, Phys. Rev. D **82** (2010) 056004

[89] I. Low, R. Rattazzi and A. Vichi, JHEP **1004**, 126 (2010)

[90] Matthias Neubert *et al.* in preparation

[91] V. Ahrens, T. Becher, M. Neubert and L. L. Yang, Eur. Phys. J. C **62**, 333 (2009)

[92] A. D. Martin, W. J. Stirling, R. S. Thorne and G. Watt, Phys. Lett. B **652**, 292 (2007)

[93] The Tevatron Electroweak Working Group for the CDF and DØ Collaborations, arXiv:0903.2503 [hep-ex].

[94] E. Thomson *et al.* [CDF Collaboration], Conference Note 9913, October 19, 2009,

[95] DØ Collaboration, Conference Note 5907-CONF, March 12, 2009,

[96] T. A. Schwarz, FERMILAB-THESIS-2006-51, UMI-32-38081.

[97] V. M. Abazov *et al.* [DØ Collaboration], Phys. Rev. Lett. **100**, 142002 (2008)

[98] T. Aaltonen *et al.* [CDF Collaboration], Phys. Rev. Lett. **101**, 202001 (2008)

[99] G. Strycker *et al.* [CDF Collaboration], CDF/ANAL/TOP/PUBLIC/9724 Note, March 17, 2009,

[100] G. Strycker *et al.* [CDF Collaboration], CDF/ANAL/TOP/PUBLIC/10224 Note, July 14, 2010,

[101] CDF Note 10398, March 10, 2011, http://www-cdf.fnal.gov/physics/new/top/2011/DilAfb/

[102] DØ Collaboration, Conference Note 6062-CONF, July 23, 2010,

[103] M. Bauer, F. Goertz, U. Haisch, T. Pfoh and S. Westhoff, JHEP **1011** (2010) 039

[104] J. H. Kühn and G. Rodrigo, Phys. Rev. Lett. **81**, 49 (1998)

[105] J. H. Kühn and G. Rodrigo, Phys. Rev. D **59**, 054017 (1999)

[106] O. Antunano, J. H. Kühn, and G. Rodrigo, Phys. Rev. D **77**, 014003 (2008),

[107] L. G. Almeida, G. Sterman and W. Vogelsang, Phys. Rev. D **78**, 014008 (2008)

[108] V. Ahrens, A. Ferroglia, M. Neubert, B. D. Pecjak and L. L. Yang, JHEP **1009** (2010) 097

[109] V. Ahrens, A. Ferroglia, M. Neubert, B. D. Pecjak and L. L. Yang, arXiv:1103.0550 [hep-ph].

[110] T. Aaltonen *et al.* [CDF Collaboration], arXiv:1101.0034 [hep-ex].

[111] P. Ferrario and G. Rodrigo, Phys. Rev. D **78**, 094018 (2008)

[112] A. Djouadi, G. Moreau, F. Richard and R. K. Singh, Phys. Rev. D **82** (2010) 071702

[113] A. Bridgeman, FERMILAB-THESIS-2008-50.

[114] T. Aaltonen *et al.* [CDF Collaboration], Phys. Rev. Lett. **102**, 222003 (2009)

[115] A. D. Martin, W. J. Stirling, R. S. Thorne and G. Watt, Eur. Phys. J. C **63**, 189 (2009)

[116] W. Bernreuther and Z. G. Si, Nucl. Phys. B **837**, 90 (2010)

[117] R. Barcelo, A. Carmona, M. Masip and J. Santiago, arXiv:1105.3333 [hep-ph].

[118] P. H. Frampton, J. Shu and K. Wang, Phys. Lett. B **683** (2010) 294

[119] A. J. Buras, W. Slominski and H. Steger, Nucl. Phys. B **245** (1984) 369.

[120] I. Dunietz, Annals Phys. **184** (1988) 350.

[121] A. Lenz and U. Nierste, JHEP **0706** (2007) 072

[122] T. Aaltonen *et al.*, CDF public note CDF/PHYS/BOTTOM/CDFR/9787, June, 2009.

[123] CDF public note CDF/ANAL/BOTTOM/PUBLIC/10206, November, 2010.

[124] Z. Ligeti, M. Papucci and G. Perez, Phys. Rev. Lett. **97** (2006) 101801

[125] Y. Grossman, Phys. Lett. B **380** (1996) 99

[126] I. Dunietz, R. Fleischer and U. Nierste, Phys. Rev. D **63**, 114015 (2001)

[127] A. Dighe, A. Kundu and S. Nandi, Phys. Rev. D **82** (2010) 031502

[128] A. Lenz and U. Nierste, arXiv:1102.4274 [hep-ph].

[129] A. Datta, M. Duraisamy and S. Khalil, Phys. Rev. D **83** (2011) 094501

[130] M. Beneke, G. Buchalla and I. Dunietz, Phys. Rev. D **54**, 4419 (1996)

[131] M. Beneke, G. Buchalla, C. Greub, A. Lenz and U. Nierste, Phys. Lett. B **459** (1999) 631

[132] A. S. Dighe, T. Hurth, C. S. Kim and T. Yoshikawa, Nucl. Phys. B **624** (2002) 377

[133] M. Beneke, G. Buchalla, A. Lenz and U. Nierste, Phys. Lett. B **576**, 173 (2003)

[134] M. Ciuchini, E. Franco, V. Lubicz, F. Mescia and C. Tarantino, JHEP **0308** (2003) 031

[135] A. Badin, F. Gabbiani and A. A. Petrov, Phys. Lett. B **653** (2007) 230

[136] C. W. Bauer and N. D. Dunn, Phys. Lett. B **696** (2011) 362

[137] A. Dighe, A. Kundu and S. Nandi, Phys. Rev. D **76** (2007) 054005

[138] D. Becirevic, V. Gimenez, G. Martinelli, M. Papinutto and J. Reyes, JHEP **0204** (2002) 025

[139] A. J. Buras, M. Jamin and P. H. Weisz, Nucl. Phys. B **347**, 491 (1990).

[140] K. Nakamura *et al.* [Particle Data Group], J. Phys. G **37** (2010) 075021.

[141] J. Laiho, E. Lunghi and R. S. Van de Water, Phys. Rev. D **81** (2010) 034503

[142] G. Buchalla, A. J. Buras and M. E. Lautenbacher, Rev. Mod. Phys. **68** (1996) 1125

[143] A. Abulencia *et al.* [CDF Collaboration], Phys. Rev. Lett. **97** (2006) 242003

[144] A. J. Buras and D. Guadagnoli, Phys. Rev. D **78** (2008) 033005

[145] J. Santiago, JHEP **0812** (2008) 046

[146] D. Asner *et al.* [Heavy Flavor Averaging Group], arXiv:1010.1589 [hep-ex].

[147] V. M. Abazov *et al.* [D0 Collaboration], Phys. Rev. D **82** (2010) 032001

[148] Y. Grossman, Y. Nir and G. Raz, Phys. Rev. Lett. **97** (2006) 151801

[149] M. Blanke, A. J. Buras, D. Guadagnoli and C. Tarantino, JHEP **0610** (2006) 003

[150] M. Bona *et al.* [UTfit Collaboration], PMC Phys. A **3** (2009) 6

[151] C. Amsler *et al.* [Particle Data Group], Phys. Lett. B **667**, 1 (2008) and updated results available at: `http://pdglive.lbl.gov/`

[152] A. Djouadi, Phys. Rept. **457**, 1 (2008) and references therein.

[153] A. J. Buras, M. Jamin, M. E. Lautenbacher and P. H. Weisz, Nucl. Phys. B **400** (1993) 37

[154] M. Ciuchini, E. Franco, G. Martinelli and L. Reina, Nucl. Phys. B **415** (1994) 403

[155] A. J. Buras, M. Misiak and J. Urban, Nucl. Phys. B **586** (2000) 397

[156] J. A. Bagger, K. T. Matchev and R. J. Zhang, Phys. Lett. B **412** (1997) 77